

The
University
Of
Sheffield.

**Polymersome mediated intracellular
delivery: A tool for research and
treatment of infectious and
inflammatory diseases**

James David Robertson

Submitted for the degree of Doctor of Philosophy

Faculty of Science, Department of Biomedical Science

**The University of Sheffield
September 2014**

Abstract:

Neutrophils contain a destructive arsenal of toxic molecules that are used to kill invading microorganisms, but inappropriate neutrophil responses can lead to excessive tissue damage, or inefficient destruction of infectious pathogens. Controlling this balance is crucial to prevent chronic disease. Neutrophil apoptosis and clearance by macrophages is a key step in the resolution of inflammation, but excessive production of pro-inflammatory cytokines can prolong neutrophil survival and lead to inflammatory disease. In contrast, inefficient destruction of the bacterium *Staphylococcus aureus* is thought to play an important role in the progression and dissemination of *Staphylococcus aureus* bacteraemia. Neutrophil dysfunction in infectious or inflammatory diseases might be correctable using synthetic vectors to deliver anti-inflammatory or antibacterial molecules intracellularly, but neutrophils have proven notoriously difficult cells to manipulate.

In this thesis I explore the potential of PMPC-PDPA polymersomes as intracellular vectors for neutrophils. I investigate how the physical properties of polymersomes influence their internalisation and reveal that the size and shape of polymersomes has a big impact on the efficiency of cargo delivery. I go on to show that these vectors do not affect neutrophil viability and can successfully deliver a range of cargo into these cells. Finally I show that polymersomes can deliver antibiotics and anti-inflammatory compounds intracellularly to help promote inflammation resolution and clear *Staphylococcus aureus* infection.

Publications

James D. Robertson, Guy Yealland, Milagros Avila-Olias, Luca Chierico, Oliver Bandmann, Stephen A. Renshaw, Giuseppe Battaglia
pH-Sensitive Tubular Polymersomes: Formation and Applications in Cellular Delivery
ACS nano. **2014** 27(5): 4650-61.

James D. Robertson, Nisa Patikarnmonthon, Adrian S. Joseph, Giuseppe Battaglia.
Block Copolymer Micelles and Vesicles for Drug Delivery.
John Wiley & Sons, **2014** p 163-183

Irene Canton, Marzia Massignani, Nia Patikarnmonthon, Luca Chierico, **James D. Robertson**, Stephen A. Renshaw, Nicolas J. Warren, Jeppe P. Madsen, Steven P. Armes, Andrew L. Lewis Giuseppe Battaglia
Fully synthetic polymer vesicles for intracellular delivery of antibodies in live cells.
Faseb Journal. **2013** 27(1): 98-108.

Acknowledgements

My PhD has been funded by the Medical Research Council and I am very grateful to them for giving me the opportunity to carry out the research. I would like to thank my supervisors Prof. Stephen Renshaw and Prof. Giuseppe Battaglia for welcoming me into their labs and providing me with support and guidance during my PhD.

I would also like to thank Dr. Nicholas Warren and Dr Jeppe Madsen from Prof. Steve Armes group, and Dr. Jens Gaitzch from the Battaglia lab for the synthesis of the polymer, without which none of this thesis would be possible. Another huge thanks goes to Dr. Tomasz Prajsnar and Prof. Simon Foster, for their help, training and discussion with the zebrafish infection experiments. Thanks to Jamil Jubrail and his supervisors Prof. David Dockrell and Dr. Helen Marriott for his training and assistance with the macrophage infection experiments. For initial training in the labs I would like to thank Dr. Irene Canton and Dr. Jon Ward for teaching me various techniques. Additionally I would like to thank Pranvera Sadiku for training in RNA extraction and PCR. Many thanks to all of the blood donors and phlebotomists who have kindly donated their time so that I could conduct my neutrophil experiments.

I am very grateful to everyone in the Renshaw and Battaglia labs for their friendship and help. Particularly Guy Yealland, Maria Milagros Avila Olias, Anne Robertson, Gavin Fullstone, Russell Pearson and Joseph Burgon, who have all

made my PhD very enjoyable. Finally I would like to thank the rest of my friends and family for all their love and support.

Table of Contents

Publications	4
Acknowledgements	5
Table of Contents	7
List of Figures	13
List of Tables	16
Abbreviations	17
Chapter 1: Introduction	21
1.1 The Immune System	21
1.1.1 Inflammation	21
1.1.2 Initiation of Inflammation.....	22
1.1.3 Neutrophils.....	24
1.1.4 Neutrophil Priming and Recruitment	24
1.1.5 Neutrophil Chemotaxis.....	25
1.1.6 Neutrophil Antimicrobial Functions.....	26
1.1.7 Neutrophil Killing Mechanisms	27
1.1.8 Neutrophil Production and Clearance	29
1.1.9 Inflammation Resolution	30
1.1.10 Neutrophil Survival Factors and Mcl-1	32
1.1.11 Neutrophil Tissue Damage and Role in Disease	34
1.1.12 Genetic Manipulation of Neutrophils.....	36
1.1.13 Targeting Neutrophil Apoptosis by Pharmacological Intervention	36
1.1.14 Cyclin Dependent Kinase Inhibitors.....	39
1.2 <i>Staphylococcus aureus</i>	41
1.2.1 Treatment of <i>S. aureus</i> Infection and Antibiotic Resistance.....	41
1.2.2 Development of a <i>S. aureus</i> Vaccine	43

1.2.3 Virulence Factors and the Pathogenesis of <i>S. aureus</i>	44
1.2.4 Intracellular Survival of <i>S. aureus</i>	46
1.3 Nanomedicine.....	52
1.3.1 Soft Nanotechnology in Drug Delivery	52
1.3.2 Block Copolymer Amphiphiles.....	53
1.3.3 Nanoparticle Biodistribution	57
1.3.4 Endocytosis.....	58
1.3.5 Nanoparticle Endocytosis.....	62
1.3.6 “Stealth” Nanotechnology.....	66
1.3.7 Block Copolymer Nanoparticles for the Treatment of Infectious and Inflammatory Diseases	68
1.3.8 PMPC-PDPA Polymersomes for Treating Infectious and Inflammatory Diseases	71
Chapter 2: Aims and Objectives	77
Chapter 3: Materials and Methods.....	79
3.1 Reagents	79
3.2 PMPC-PDPA	80
3.3 Polymersome Formation.....	81
3.3.1 Film Rehydration.....	81
3.3.2 pH Switch.....	81
3.4 Polymersome purification techniques.....	82
3.4.1 Removal of Non-Encapsulated Molecules	82
3.4.2 Polymersome Size Purification Methods	82
3.4.3 Tubular Polymersome Purification.....	83
3.5 Polymersome size and shape characterisation	84
3.5.1 Dynamic Light Scattering.....	84
3.5.2 Transmission Electron Microscopy.....	84

3.6 Quantification of Polymer and Encapsulated Cargo.....	85
3.6.1 UV-Vis spectroscopy and Fluorescence Spectroscopy Calibration Curves.....	85
3.6.2 RP-HPLC Chromatograms and Calibration Curves.....	88
3.7 <i>In vitro</i> Biological Analysis.....	91
3.7.1 Neutrophil Purification	91
3.7.2 Ultrapure Neutrophil Purification using Magnetic Selection.....	93
3.7.3 Flow Cytometry	93
3.7.4 Cytospin Analysis of Neutrophil Apoptosis Rates	95
3.7.5 Enzyme-Linked Immunosorbent Assay (ELISA).....	98
3.7.6 Fluorescence Microscopy	99
3.7.7 siRNA Knockdown Experiments	101
3.7.8 <i>Staphylococcus aureus</i> Experiments	104
3.8 Zebrafish Embryo Experiments	106
3.8.1 Zebrafish Husbandry	106
3.8.2 Zebrafish Inflammation Resolution Assay	107
3.8.3 Zebrafish Microinjections.....	108
3.8.4 Zebrafish Microscopy Experiments	109
3.8.5 Zebrafish <i>S. aureus</i> Infection Experiments.....	111
3.9 Statistical Analysis.....	111
Chapter 4: Optimisation of Polymersome Size for Intracellular Delivery into Human Neutrophils	113
4.1 Introduction.....	113
4.2 Results	116
4.2.1 Polymersome Formation by pH Switch.....	116
4.2.2 Polymersome Internalisation by Human Neutrophils.....	116
4.2.3 Polymersome Purification Using Cross Flow Filtration.....	118
4.2.4 Purification Using Size Exclusion Chromatography	118

4.2.5 Separation of Polymersome Sizes by Differential Centrifugation.....	120
4.2.6 The Influence of Polymersome Size on Uptake by Human Neutrophils	123
4.3 Discussion.....	128
4.3.1 Purification of Polymersomes into Different Sizes.....	128
4.3.2 Comparison of Polymersome Size on the Rate of Internalisation and the Efficiency of Cargo Delivery.....	129
 Chapter 5: Tubular polymersomes: Formation, Purification and	
Internalisation by Neutrophils	133
5.1 Introduction.....	133
5.2 Results.....	135
5.2.1 Polymersome Rehydration Morphological Analysis	135
5.2.2 The Mechanism of Tubular Polymersome Formation	136
5.2.3 Separation of Tubular Polymersomes.....	140
5.2.4 Tubular Polymersome Internalisation	143
5.2.5 Delivery of BSA into Neutrophils by Tubular Polymersomes.....	145
5.3 Discussion.....	149
5.3.1 Non-Spherical Nanoparticles	149
5.3.2 Internalisation of Tubular Polymersomes	149
 Chapter 6: Polymersomes as Intracellular Delivery Vectors for Human	
Neutrophils.....	153
6.1 Introduction.....	153
6.2 Results.....	156
6.2.1 Neutrophil Viability and Cytokine Release are not Altered by PMPC-PDPA Polymersomes	156
6.2.2 Polymersome Mediated Delivery of Rhodamine B Octadecyl ester Perchlorate	158
6.2.3 Polymersome Mediated Delivery of Alexa-647-Labelled siRNA	160

6.2.4 Polymersome Mediated Delivery of Antibodies	163
6.2.5 Encapsulation of (R)-Roscovitine to Promote Neutrophil Apoptosis	166
6.2.6 Encapsulated (R)-Roscovitine Promotes Inflammation Resolution in an <i>in vivo</i> Zebrafish Model	170
6.3 Discussion.....	173
6.3.1 Polymersomes do not Alter Neutrophil Viability or Induce Cellular Activation	173
6.3.2 Polymersome Delivery of Fluorescent Cargo into Neutrophils.....	174
6.3.3 Polymersome Mediated Delivery of siRNA and Antibodies into Human Neutrophils.....	175
6.3.4 Polymersome Delivery of Roscovitine Drives Neutrophil Apoptosis.....	178
6.3.5 Roscovitine Polymersomes Enhance Inflammation Resolution in an <i>in vivo</i> Zebrafish Model	179
 Chapter 7: Treating Intracellular <i>Staphylococcus aureus</i> Infection with Encapsulated Antibiotics	 181
7.1 Introduction.....	181
7.2 Results	184
7.2.1 Encapsulation of Antibiotics within Polymersomes.....	184
7.2.2 Polymersome Mediated Intracellular Delivery of Antibiotics to Treat Intracellular <i>S. aureus</i> infection in THP-1 Macrophages.....	187
7.2.3 Polymersome Mediated Intracellular Delivery into Zebrafish Phagocytes	190
7.3 Discussion.....	207
7.3.1 Polymersome Mediated Delivery of Antibiotics to Kill Intracellular <i>S. aureus</i> in THP-1 Monocyte Derived Macrophages.....	208
7.3.2 Intracellular Delivery into Phagocytes <i>in vivo</i>	210
7.3.3 Polymersome Mediated Intracellular Delivery of Antibiotics in an <i>in vivo S.</i> <i>aureus</i> Infection Model	211

Chapter 8: Final Discussion and Future Perspectives.....	215
8.1 Optimisation of Polymersome Size	215
8.2 Tubular Polymersomes.....	216
8.3 Polymersome as Intracellular Delivery Vectors for Neutrophils	218
8.4 Polymersome Mediated Delivery of Antibiotics to Treat Intracellular <i>S. aureus</i> Infection	219
8.5 Limitations	221
8.6 Conclusions	224
References	226

List of Figures

Figure 1.1 Survival of <i>S. aureus</i> within blood stream neutrophils may facilitate bacterial dissemination.	49
Figure 1.2 Geometries formed from block copolymer amphiphiles with different packing parameters	55
Figure 1.3 A summary of endocytic mechanisms in eukaryotic cells.....	61
Figure 1.4 Accumulation of nanoparticles in inflamed joint.....	70
Figure 1.5 pH sensitive PMPC-PDPA.....	74
Figure 1.6 pH sensitive PMPC-PDPA polymersome endosomal escape	75
Figure 3.1 UV-Vis spectroscopy and fluorescence spectroscopy calibration curves.....	87
Figure 3.2 HPLC chromatograms and calibration curves for encapsulated antibiotics.....	89
Figure 3.3 HPLC chromatograms and calibration curves for PC and (R)-roscovitine	90
Figure 3.4 Annexin V Pi staining.....	96
Figure 3.5 Human neutrophil cytopins	97
Figure 3.6. Site of tail injury in a 3dpf <i>Tg(mpx:GFP)i114</i> zebrafish embryo.....	108
Figure 3.7 Microinjection site in 30hpf zebrafish embryo	109
Figure 4.1 Uptake of spherical polymersomes by human neutrophils.....	117
Figure 4.2 Purification of polymersomes from micelles using the KrosFlo Research Ili System	119
Figure 4.3 Size separations using recycling size exclusion chromatography.	121
Figure 4.4 Size separations using differential centrifugation.....	122
Figure 4.5 Uptake of rhodamine-labelled polymersomes encapsulating cascade blue in human neutrophils.....	125

Figure 4.6 Quantified neutrophil rMFI over time after incubation with rhodamine labelled polymersomes encapsulating cascade blue.....	127
Figure 5.1 Morphology of nanoparticles formed through pH switch or film rehydration.....	135
Figure 5.2 Swelling and detachment of a thin film of Rhodamine labelled PMPC-PDPA.....	137
Figure 5.3 Release of components of the polymer film into the solution.....	139
Figure 5.4 Formation of tubular polymersomes and spherical polymersomes from larger structures.....	140
Figure 5.5 Separation of self-assembled structures by centrifugation.....	141
Figure 5.6 Formation of structures over time.....	142
Figure 5.7 Internalisation of tubular polymersomes into neutrophils.....	144
Figure 5.8 Delayed internalisation of tubular polymersomes.....	146
Figure 5.9 Analysis of confocal z-stacks on single neutrophils.....	147
Figure 5.10 Tubular polymersomes encapsulating Alexa-647 labelled BSA.....	148
Figure 6.1. Polymersomes have no effect on neutrophil activation or viability ..	157
Figure 6.2. Uptake of polymersomes encapsulating Rhodamine B by human neutrophils.....	159
Figure 6.3. Delivery of siRNA into live human neutrophils.....	162
Figure 6.4. Intracellular delivery of alexa-647 labelled alpha-tubulin targeting antibodies into human neutrophils.....	165
Figure 6.5 Polymersome delivery of brilliant violet gamma tubulin targeting antibody into neutrophils.....	166
Figure 6.6 Purification of (R)-roscovitine polymersomes by shape.....	168
Figure 6.7 roscovitine encapsulated within polymersomes promotes neutrophil apoptosis <i>in vitro</i>	169

Figure 6.8. Encapsulation of roscovitine within polymersomes improves inflammation resolution <i>in vivo</i>	172
Figure 7.1. Purification of polymersomes to the optimum size range.....	185
Figure 7.2. Intracellular delivery of antibiotics into THP-1 macrophages	188
Figure 7.3. Encapsulated Gentamicin reduces intracellular <i>S. aureus</i> burden in a dose dependent manner.....	189
Figure 7.4. Internalisation of rhodamine-labelled polymersomes by circulating cells in the zebrafish embryo	191
Figure 7.5 <i>In vivo</i> imaging of polymersome internalisation by zebrafish neutrophils and macrophages.....	193
Figure 7.6 <i>In vivo</i> imaging of zebrafish phagocytes after injection of CFP-labelled <i>S. aureus</i> and rhodamine-labelled polymersomes.....	194
Figure 7.7 Polymersome cargo co-localises with <i>S. aureus</i> in infected phagocytes	196
Figure 7.8. Intracellular delivery of Gentamicin in an <i>in vivo S. aureus</i> infection model	198
Figure 7.9 Optimisation of polymer concentration for uptake into circulating phagocytes.....	200
Figure 7.10 Intracellular delivery of gentamicin in an <i>in vivo S. aureus</i> infection model at a polymer concentration of 1mg/ml	202
Figure 7.11. Intracellular delivery of lysostaphin and vancomycin in an <i>in vivo S. aureus</i> infection model at a polymer concentration of 1mg/ml.....	203
Figure 7.12. Polymersome mediated intracellular delivery of rifampicin <i>in vivo</i> in infected zebrafish embryos	205
Figure 7.13. Zebrafish survival after <i>S. aureus</i> infection and treatment with encapsulated rifampicin.....	206

List of Tables

Table 3.1. Chemical structure and molecular weight of PMPC-PDPA and Rho-PMPC-PDPA used in this thesis	80
Table 3.2. List of reagents in the wash buffer and coating buffer	99
Table 3.3 Mcl-1 primers for PCR.....	103
Table 3.4 50x TAE buffer constituents.....	104
Table 3.5. The reagents for making a 60x E3 stock solution.....	107
Table 4.1 Cascade blue encapsulation after purification of 6 polymersome size fractions.....	124
Table 6.1 Polymer and roscovitine concentrations for tubular polymersomes and spherical polymersomes as measured by HPLC	168
Table 7.1. Concentration of encapsulated antibiotics in 10mg/ml of polymersomes after encapsulation by pH switch or film rehydration.....	187

Abbreviations

• A1	Bcl-2-related protein A1
• ANOVA	Analysis of Variance
• ARDS	Acute Respiratory Distress Syndrome
• ATRP	Atom Transfer Radical Polymerisation
• BAD	Bcl-2-associated death promoter
• BAK	Bcl-2 homologous antagonist killer
• BAX	Bcl-2 Associated X protein
• Bcl-2	B-cell lymphoma 2
• BHI	Brain Heart Infusion
• Bik	Bcl-2-interacting killer
• BSA	bovine serum albumin
• C5a	Complement Component 5a
• CAC	Critical Aggregation Concentration
• CaCl ₂	Calcium Chloride
• CD	Cluster of Differentiation
• CDK	Cyclin Dependent Kinases
• CDKi	Cyclin Dependent Kinase Inhibitor
• cDNA	Complementary DNA
• CFP	Cyan Fluorescent Protein
• CFU	Colony Forming Units
• CME	Clathrin-Mediated Endocytosis
• COPD	Chronic Obstructive Pulmonary Disease
• CsA	Cyclosporine A
• CXCR	CX Chemokine Receptor
• DAMP	Damage-Associated Molecular Pattern
• DISC	Death-Inducing Signalling Complex
• DLS	Dynamic Light Scattering
• DMSO	Dimethyl Sulfoxide
• DNA	Deoxyribonucleic acid
• dNTP	deoxynucleotide triphosphates
• dPBS	Dulbecco's Phosphate Buffered Saline buffer
• dpf	days post fertilisation
• EC ₅₀	Half maximal Effective Concentration
• ELISA	Enzyme-Linked Immunosorbent Assay
• ERK	Extracellular-Signal-Regulated Kinases
• FADD	Fas-Associated Death Domain
• FCS	Fetal Calf Serum
• FMLP	Formyl-Methionyl-Leucyl-Phenylalanine

• G-CSF	Granulocyte-Colony Stimulating Factor
• GFP	Green Fluorescent Protein
• GM-CSF	Granulocyte Macrophage-Colony Stimulating Factor
• GPCR	G-protein coupled receptors
• H ₂ O ₂	Hydrogen Peroxide
• HBSS	Hanks Buffered Saline Solution
• HCl	Hydrogen Chloride
• hpij	Hours post injury
• hpif	hours post infection
• ICAM	Intracellular Adhesion Molecules
• IFN- γ	Interferon - γ
• Ig	Immunoglobulin
• IL-	Interleukin
• ISG20	Interferon Stimulated Exonuclease Gene 20kDa
• KCl	Potassium Chloride
• LBP	Lipopolysaccharide-binding protein
• LPS	lipopolysaccharide
• LukAB/LukGH	Leukocidin A/B
• LWT	London Wild Type
• MAC-1	Macrophage-1 Antigen
• MAPK	Mitogen-Activated Protein Kinase
• MBC	Minimum Bactericidal Concentration
• Mcl-1	Myeloid cell leukemia 1
• MDA5	Melanoma Differentiation-Associated protein 5
• MgCl ₂	Magnesium Chloride
• MgSO ₄	Magnesium Sulphate
• MMLV	Murine Leukemia Virus Reverse Transcriptase
• MMP	Matrix Metalloprotease
• MOI	Multiplicity Of Infection
• MPO	myeloperoxidase
• MRSA	Methicillin-Resistant <i>Staphylococcus aureus</i>
• MSCRAMM	microbial surface component recognizing adhesivematrix molecule
• MULE	Mcl-1 Ubiquitin Ligase E2
• NaCl	Sodium Chloride
• NADPH oxidase	Nicotinamide Adenine Dinucleotide Phosphate- Oxidase
• NaOH	Sodium Hydroxide
• NET	Neutrophil Extracellular Trap

- NF- κ B nuclear factor kappa-light-chain-enhancer of activated B cells
- OPA o-Phthaldialdehyde
- PAF Platelet-activating factor
- PAMP pathogen-associated molecular pattern
- PBG Poly(Butylene Glycol)
- PBMC Peripheral Blood Mononuclear Cell
- PCL poly(ϵ -caprolactone)
- PDMA poly(2-(dimethylamino) ethyl methacrylate)
- PDPA poly(2-(diisopropylamino)ethyl methacrylate)
- PDPA poly(2-(diisopropylamino) ethyl methacrylate)
- PEE Poly(ethylethylene)
- PEG polyethylene glycol
- PEO polyethylene oxide
- PI Propidium Iodide
- PI3K Phosphatidylinositol-4,5-bisphosphate 3-kinase
- PLGA poly(lactic-co-glycolic acid)
- PMA phorbol 12-myristate 13-acetate
- PMPC poly(2-(methacryloyloxy)ethyl phosphorylcholine)
- PPP Platelet Poor Plasma
- PRP Platelet Rich Plasma
- PRR Pattern recognition receptor
- PTA Phosphotungstic acid
- PtdIns(3,4,5)P₃ Phosphatidylinositol (3,4,5)-trisphosphate
- PVL Panton Valentine leukocidin
- RAFT Reversible Addition-Fragmentation Chain Transfer
- RES Reticuloendothelial System
- RhoA Ras homolog gene family, member A
- RIG-I Retinoic acid-Inducible Gene 1
- rMFI relative Median Fluorescence Intensity
- RNA Ribonucleic acid
- RNAi RNA interference
- ROS Reactive Oxygen Species
- RP-HPLC Reverse Phase-High Performance Liquid Chromatography
- RPMI-1640 Roswell Park Memorial Institute-1640
- RT-PCR Reverse Transcription Polymerase Chain Reaction
- *S. aureus* *Staphylococcus aureus*
- SAA Serum Amyloid A
- SDF-1 stromal-derived factor-1

- SEC Size Exclusion Chromatography
- siRNA Small interfering RNA
- SLPI Secretory Leukocyte Protease Inhibitor
- SR-B1 Scavenger Receptor B1
- TEM Transmission Electron Microscope
- TFA Trifluoroacetic acid
- TGF β Transforming Growth Factor- β
- TLR Toll Like Receptors
- TNF- α Tumor necrosis factor- α
- TRAIL TNF-Related Apoptosis-Inducing Ligand
- UV-Vis Ultraviolet-Visible
- VEGF Vascular endothelial growth factor
- VISA Vancomycin Intermediate Staphylococcus aureus
- VRSA Vancomycin Resistant Staphylococcus aureus
- WT Wild Type
- α -toxin α -haemolysin

Chapter 1: Introduction

1.1 The Immune System

The main function of the immune system is to protect our bodies from invading organisms. Physical barriers such as the skin constitute the first line of defence, but if these barriers are penetrated, we are protected by a complex network of small molecules, proteins and cells that can be subdivided into two major parts; the innate and adaptive immune systems.

The cellular adaptive immune system is only found in vertebrates, whereas, the innate immune system evolved much earlier and is found in all multicellular organisms (Cooper and Alder, 2006). The adaptive immune system allows animals to maintain an “immunological memory” upon infection, which results in an improved immune response in subsequent exposures to that specific organism. In contrast, the innate immune system provides less specific protection by identifying conserved residues on pathogens, which are not found on the body’s own cells (Kawai and Akira, 2010). Once recognised, pathogens can be cleared through the inflammatory response.

1.1.1 Inflammation

The inflammatory response is an essential part of immunity that is initiated following tissue injury or infection. The hallmarks of inflammation were initially described by Aulus Cornelius Celsus a Roman encyclopaedist; he described

cardinal signs of inflammation as pain, heat, redness and swelling (Celsus and Broca, 1876). We now know that these symptoms are consequences of the physical processes that occur during inflammation. Vasodilators such as Nitric oxide released from the endothelium result in an increased blood flow and the accumulation of fluid, leading to redness, heat and swelling. In parallel, the production of inflammatory mediators such as prostaglandin E2 and bradykinin sensitise nerve terminals to pain (Davies et al., 1984). A fifth cardinal sign, loss of function, otherwise known as disturbance of function, was added later by Rudolph Virchow, which has numerous causes depending on the location and strength of the inflammatory response (Majno, 1991).

1.1.2 Initiation of Inflammation

The inflammatory response is classically initiated by microbial infection. During infection the immune system senses foreign organisms through highly conserved motifs that are not present on eukaryotic cells; these are known as pathogen-associated molecular patterns (PAMPs). Pattern recognition receptors (PRRs) are located both on the surface of immune cells and on intracellular membranes. Toll Like Receptors (TLR) are one of the most well studied PRR and are highly expressed on tissue resident macrophages and neutrophils (Kawai and Akira, 2010). TLRs recognise a range of PAMPs, for instance TLR4 binds to the bacterial residue lipopolysaccharide (LPS), TLR2 binds to fungal chitin and TLR3 recognises viral double stranded RNA (Nurnberger and Brunner, 2002). The PRRs can also be activated by endogenous molecules released from damaged cells, known as damage-

associated molecular patterns (DAMPs) (Hirsiger et al., 2012). Examples of endogenous DAMPS include heat shock proteins, hyaluronan, uric acid and mitochondrial DNA (Zhang et al., 2010, Bianchi, 2007). These provide further signals to alert immune cells of tissue injury during infection.

The engagement of PRRs by pathogenic residues results in the induction of specific gene profiles tailored to coordinate an appropriate immune response (Moynagh, 2005). For instance, cytosolic viral RNA is recognised by PRRs of the RIG-I-like receptor family, RIG-I and MDA5 (Yoneyama et al., 2004). Activation of these receptors results in the production of type 1 interferons that initiate an antiviral response (Medzhitov, 2007). Whereas, detection of bacterial LPS through TLR4 leads to the activation of transcription factors such as NF- κ B (Chow et al., 1999) and the expression of NF- κ B controlled genes for pro-inflammatory cytokines such as IL-1, IL-6, TNF- α and IL-8 (Kempe et al., 2005, Medzhitov et al., 1997).

Sentinel cells such as tissue resident mast cells and macrophages are the first cells to detect injury or infection. Activated sentinels release pro-inflammatory mediators such as TNF- α , IL-7, histamine and PAF that activate nearby endothelial cells and leukocytes. In parallel, extracellular macromolecules such as lipopolysaccharide-binding protein (LBP) and complement provide further signals, which together, promote transmigration and recruitment of new immune cells (Nathan, 2002).

1.1.3 Neutrophils

Neutrophils are the most abundant leukocyte in mammals and are the first cells recruited to sites of infection. Neutrophils belong to a class of white blood cells called granulocytes, which are characterised by the presence of granules within their cytoplasm. Granulocytes consist of neutrophils, basophils and eosinophils, which were named based on their staining patterns with haematoxylin and eosin. Neutrophils make up over 95% of the granulocyte population and 40-60% of the total leukocyte population in humans (Wright et al., 2010).

1.1.4 Neutrophil Priming and Recruitment

In the circulation neutrophils are in a resting state, which prevents the release of their destructive intracellular contents. Once exposed to pro-inflammatory cytokines neutrophils become primed and this facilitates their recruitment to inflammatory sites (Hallett and Lloyds, 1995). Neutrophil priming enables these cells to upregulate effector functions by mobilising additional receptors to the plasma membrane and by activating NADPH oxidase (Wright et al., 2010, Summers et al., 2010).

Neutrophil contact with an activated endothelium facilitates their interaction with attached chemokines that can also lead to neutrophil priming (Kolaczowska and Kubes, 2013). Primed neutrophils upregulate adhesion molecules including L-selectin and CD44 (Borregaard, 2010). These adhesion ligands bind to the P and E selectins and intracellular adhesion molecules

(ICAMs) on endothelial cells, leading to tethering, rolling and firm attachment (Kolaczkowska and Kubes, 2013).

1.1.5 Neutrophil Chemotaxis

Adhered neutrophils transmigrate across the endothelial wall through endothelial cell junctions or by transcellular migration (Yang et al., 2005). Once neutrophils have passed through the endothelium they travel towards the inflammatory site by a process called chemotaxis, which directs neutrophils through a chemical gradient of chemoattractants such as the complement fragment C5a, formylated bacterial peptides like fMLP or various chemokines released by immune cells.

Chemoattractants are detected by neutrophils through G-protein coupled receptors (GPCRs) such as CXCR1 and CXCR2 (White et al., 1998). One important downstream target of these GPCRs is phosphatidylinositol (3,4,5)-triphosphate (PtdIns(3,4,5)P₃), a signalling molecule that promotes actin polymerisation (Wang et al., 2011). Driven by PtdIns(3,4,5)P₃ and other signalling molecules, chemokines trigger the polarisation of chemoreceptors and actin polymerisation to the leading edge of the cell (Servant et al., 2000). Actin polymerisation drives the extension of pseudopods at the “front” of the cell that attach to the extracellular matrix. As the cells moves, pseudopods detach from the matrix proteins and receptors are endocytosed and recycled back to the leading edge of the cell (Lawson and Maxfield, 1995).

1.1.6 Neutrophil Antimicrobial Functions

Neutrophils play an essential role in the elimination of invading pathogens. Deficiencies in neutrophil number or function, such as mutations in the NADPH oxidase genes (chronic granulomatous disease), lead to severe and recurrent life-threatening infections (Winkelstein et al., 2000). Neutrophils can kill microorganisms by a number of mechanisms including phagocytosis, degranulation, or the formation of neutrophil extracellular traps (NETs), which all utilise antimicrobial molecules from cytoplasmic granules to degrade pathogens intracellularly or extracellularly.

Neutrophil intracellular granules are subdivided based on their function and contents into primary, secondary or tertiary granules. These granules contain proteins, enzymes and receptors that are involved in a number of functions including chemotaxis, adhesion and the destruction of microorganisms. Granules are formed throughout neutrophil differentiation in the bone marrow and the contents of the granules are regulated by the gene expression profile during maturation. The primary granules, otherwise known as azurophilic granules, are produced during the promyelocytic stage and are the first granules formed during maturation (Amulic et al., 2012). Primary granules contain a number of antimicrobial proteins and proteases including elastase and cathepsin G. They are characterised by the presence of myeloperoxidase (MPO), a peroxidase enzyme that converts H_2O_2 from NADPH oxidase into the potent antimicrobial hypochlorous acid (Weiss et al., 1982).

As the cells mature from promyelocytes to myelocytes the production of MPO stops and the production of peroxidase negative secondary and tertiary granules begins (Faurischou and Borregaard, 2003). Secondary, otherwise known as specific granules, are produced in myelocytes and metamyelocytes and contain high concentrations of antimicrobial proteins such as defensins and lactoferrin (Hager et al., 2010). Tertiary granules, or gelatinase granules, have relatively low concentrations of antimicrobials, but have high amounts of matrix degrading enzymes such as matrix metalloprotease-8 (MMP-8) and gelatinase (MMP-9), which aid neutrophils during migration by degrading the extracellular matrix (Owen and Campbell, 1999).

1.1.7 Neutrophil Killing Mechanisms

Neutrophils recruited to an inflammatory site bind to pathogens through direct recognition with PRRs, or through binding to opsonised microorganisms with complement or antibody receptors. Once bound to its target, cytoskeletal rearrangements enable the membrane to wrap around and internalise the microorganism (Nordenfelt and Tapper, 2011). This process is referred to as phagocytosis. After internalisation, the resulting phagosome fuses with lysosomes and preformed granules. The NADPH oxidase, assembled after neutrophil priming or following phagocytosis, enables the production of reactive oxygen species (ROS) such as superoxide that enhance microbial killing.

Phagocytosis allows neutrophils to eliminate microorganisms intracellularly without damaging the host. However, inevitably some pathogens may escape

contact with neutrophils and thus extracellular killing mechanisms are essential. If neutrophils are exposed to certain cytokines, or sense infection but do not contact a pathogen, they degranulate. Intracellular granules fuse with the plasma membrane and their contents are released by exocytosis. These include numerous antimicrobials, degradative proteases and components of NADPH oxidase (Amulic et al., 2012). Release of these molecules helps in the destruction of extracellular pathogens, but can also cause damage to host tissues. This, however, may also aid in complete sterilisation, by collapsing nearby capillaries and lymph vessels to prevent bacteria and other microorganisms from escaping (Nathan, 2006).

A new mechanism of neutrophil killing by the formation of neutrophil extracellular traps (NETs) was first described by the Zychlinsky group in 2004 (Brinkmann et al., 2004). NETs are produced by a form of cell death called NETosis, where nuclear chromatin, granule proteins and antimicrobial peptides are expelled from the cell as a NET (Brinkmann and Zychlinsky, 2007). NETosis can be initiated by certain pro-inflammatory cytokines, antibodies or pathogens (Yipp et al., 2012), and following activation the nucleus begins to lose its multi-lobed structure and the chromatin decondenses. After approximately one hour the intracellular granules release their contents into the cytoplasm and the nuclear membrane disintegrates. Finally, the cell membrane ruptures and the NETs are released into the extracellular environment (Brinkmann and Zychlinsky, 2012).

NETs are now believed to play an important role in immunity against a range of pathogens, including bacteria, fungi and even viruses (Brinkmann et al., 2004, Urban et al., 2006, Saitoh et al., 2012). By trapping pathogens NETs prevent their dissemination and expose them to a high concentration of antimicrobial peptides. Attached histones, in particular, are believed to be highly toxic to bacteria and have a number of antimicrobial functions including membrane permeabilisation, binding to intracellular bacterial DNA and binding to LPS (Saitoh et al., 2012).

1.1.8 Neutrophil Production and Clearance

Neutrophils are formed within haematopoietic cords of the bone marrow from myeloid cells in a differentiation process known as granulopoiesis. Neutrophil granulopoiesis is primarily controlled by granulocyte-colony stimulating factor (G-CSF), which controls myeloid cell commitment, differentiation, proliferation and release from the bone marrow (Lord et al., 1989, Richards et al., 2003). G-CSF acts on the neutrophil G-CSF receptor that is expressed very early in neutrophil development. Another important neutrophil receptor is CXCR4, which recruits neutrophils towards stromal-derived factor 1 (SDF-1) produced by bone marrow derived stromal cells. This interaction retains neutrophils in the bone marrow until maturation (Summers et al., 2010).

Neutrophils are released into the bloodstream as terminally differentiated cells at a rate of 10^{11} cells per day under normal conditions (Furze and Rankin, 2008). To compensate for this rapid production, neutrophils have a short life span and

undergo constitutive apoptosis. *Ex vivo* labelling of neutrophils estimate their circulating half-life at 6-8 hours (Dancey et al., 1976). This view was recently challenged by Pillay and colleagues, who calculated an average life span of 5.4 days using orally administered deuterium-labelled water (Pillay et al., 2010). However, this technique has received criticism as the approach may also label bone marrow neutrophils, resulting in an overestimation of the life span in the blood (Tofts et al., 2011).

The exact mechanisms by which neutrophils are cleared from the body are not completely understood. Aged neutrophils are removed from the blood through uptake in the liver, bone marrow and spleen (Saverymuttu et al., 1985, Shi et al., 2001, Suratt et al., 2001). It is believed that damaged or apoptotic neutrophils are predominantly removed by Kupffer cells in the liver (Shi et al., 2001) and in parallel, aged neutrophils upregulate CXCR4, which directs them back to the bone marrow where they undergo apoptosis (Martin et al., 2003).

1.1.9 Inflammation Resolution

During inflammation neutrophils are recruited into tissues to help fight infection. Once an infection is cleared, it is important that inflammation resolves with minimal damage to the host. Apoptosis ensures that neutrophils cease pro-inflammatory functions and packages their toxic contents within apoptotic bodies for safe clearance by macrophages. At inflammatory sites neutrophils can undergo constitutive apoptosis or apoptosis can be induced by ligation of death receptors initiating the extrinsic cell death pathway.

Neutrophils express a number of death receptors including the TNF- α receptor 1 and 2, the Fas receptor and TRAIL receptors (Liles et al., 1996, Murray et al., 1997, Renshaw et al., 2003). Death receptor ligation leads to the formation of the death-inducing signalling complex (DISC) that signals through intracellular adaptor proteins such as the Fas-associated death domain (FADD) to activate cysteine proteases called caspases (Thorburn, 2004). Caspases cleave aspartate residues on intracellular proteins dismantling the cells into apoptotic bodies (Witko-Sarsat et al., 2011).

During apoptosis neutrophils upregulate “eat me” signals such as phosphatidylserine, which allow them to be recognised and phagocytosed by macrophages, a process known as efferocytosis (Bratton and Henson, 2011, Savill et al., 1989). This polarises macrophages towards a pro-resolution phenotype, inhibiting the production of inflammatory cytokines such as IL-1 β , IL-8 and TNF- α , and initiating the production of IL-10, TGF β , VEGF and SLPI, which are involved in inflammation resolution and tissue repair (Fadok et al., 1998b, Golpon et al., 2004, Ashcroft et al., 2000).

Lipid mediators also play an important role in inflammation resolution. During the course of inflammation the production of pro-inflammatory eicosanoids of the leukotriene and prostaglandin families are reduced and pro-resolution lipoxins, resolvins and protectins are upregulated, predominantly through transcellular biosynthesis (Serhan and Savill, 2005). These mediators have a

wide range of pro-resolving effects; they inhibit neutrophil recruitment (Colgan et al., 1993, Lee et al., 1989), cytokine release (Hachicha et al., 1999), leukocyte activation (Takano et al., 1997, Levy et al., 2002) and promote neutrophil apoptosis and uptake by macrophages (El Kebir et al., 2009, Godson et al., 2000).

1.1.10 Neutrophil Survival Factors and Mcl-1

Inflammation resolution can be delayed if neutrophil apoptosis is postponed by certain survival factors. Neutrophil apoptosis is regulated by a number of complex signalling pathways that control the expression of pro-apoptotic and anti-apoptotic proteins. Neutrophil longevity is augmented by physical conditions such as the local oxygen concentration (Walmsley et al., 2005), host derived survival factors including Granulocyte Macrophage-Colony Stimulating Factor (GM-CSF), G-CSF and Interferon- γ (IFN- γ) (Cox et al., 1992, Lopez et al., 1986, Ellis and Beaman, 2004), or pathogenic PAMPs such as LPS and lipoteichoic acid (Lotz et al., 2004, Lee et al., 1993). These survival factors activate intracellular signalling cascades, most notably the MAPK/ERK and PI3K pathways, which influence the expression of the Bcl-2 family of proteins (Filep and El Kebir, 2009).

The Bcl-2 family of proteins are essential regulators of apoptosis. There are more than 20 proteins in the Bcl-2 family and they are characterised by the presence of one or more of the Bcl-2 homology domains. The Bcl-2 family

contains both pro-apoptotic and anti-apoptotic proteins, and the balance of these proteins within the cell is important in regulating cell life span.

Insertion of the pro-apoptotic Bcl-2 proteins Bax and Bak into the mitochondrial membrane leads to the formation of pores and mitochondrial outer membrane permeabilisation (Wei et al., 2001). This results in the release of pro-apoptotic proteins into the cytosol including cytochrome-c. Cytochrome-c activates a NOD family protein called Apoptotic Peptidase Activating Factor-1 (APAF-1). Seven activated APAF-1 proteins assemble to form a large wheel shaped complex called the apoptosome (Yu et al., 2005). The assembled apoptosome then binds and activates caspase-9 leading to apoptosis.

The anti-apoptotic members of the Bcl-2 family are thought to predominantly act by dimerising with pro-apoptotic members and inhibiting their function. Bcl-2 and Bcl-XL bind to Bax through their BH1 and BH2 domains and inhibit Bax induced mitochondrial membrane permeabilisation. Whereas, the anti-apoptotic Bcl-2 family protein Mcl-1 binds and sequesters Bak, and keeps it in an inactive protein complex (Cuconati et al., 2003). Mcl-1 is also thought to delay apoptosis by binding and inactivating truncated Bid (Clohessy et al., 2006). Bid acts as a pro-apoptotic Bcl-2 protein by promoting the translocation of Bax to the mitochondria. Thus by inactivating Bid and Bak Mcl-1 prevents mitochondrial permeabilisation and delays apoptosis.

Neutrophils constitutively express a number of pro-apoptotic Bcl-2 family members including Bad, Bax, Bak, and Bik, which are very stable and have long half-lives (Moulding et al., 2001). For survival, neutrophils predominantly rely on the unstable expression of the anti-apoptotic Bcl-2 members Mcl-1 and A1, with half-lives of only 2-3 hours. The expression of Mcl-1, in particular, closely correlates with neutrophil survival (Moulding et al., 1998) and is known to be upregulated by survival factors such as GM-CSF and a variety of TLR agonists (Derouet et al., 2004, Francois et al., 2005).

The importance of Mcl-1 in neutrophil survival is highlighted by Mcl-1 knockout mice, which show severe neutropenia and 2-3 times higher rates of neutrophil apoptosis (Dzhagalov et al., 2007). The fast turnover of Mcl-1 is attributed to rapid polyubiquitination and subsequent degradation by the proteasome. This is predominantly driven by the E3 ubiquitin ligase called Mcl-1 Ubiquitin Ligase E2 (MULE), although other ubiquitin ligases are also involved (Ding et al., 2007). Mcl-1 can also be degraded by proteases such as granzyme or certain caspases (Clohessy et al., 2004, Han et al., 2004).

1.1.11 Neutrophil Tissue Damage and Role in Disease

Disruption of neutrophil apoptosis, deficiencies in inflammation resolution or persistent stimulation with survival factors can lead to non-resolving inflammation (Nathan and Ding, 2010). Under these circumstances, neutrophil degranulation can cause excessive tissue damage leading to chronic inflammatory disease or even acute organ dysfunction. In patients with rheumatoid arthritis, the accumulation of neutrophils correlates with the extent

of joint inflammation at early stages (Wright et al., 2010). Within the joints neutrophils can become activated by autoantibody complexes such as rheumatoid factor, leading to the release of ROS and degradative proteases into the synovial fluid or directly onto the joint (Wright et al., 2014),

Numerous other inflammatory diseases are associated with delayed neutrophil apoptosis and local neutrophilia, including acute respiratory distress syndrome (ARDS), graft versus host disease, sepsis, inflammatory bowel disease and chronic obstructive pulmonary disease (COPD) (Schwab et al., 2014, MatuteBello et al., 1997, Gernez et al., 2010). In chronic lung diseases such as COPD, the extent of neutrophilic inflammation is closely associated with the clinical severity and frequency of exacerbations (Di Stefano et al., 1998, Bhowmik et al., 2000). Neutrophil derived MPO, ROS, elastase and matrix metalloproteases promote epithelial and lung parenchymal damage and the destruction of elastic lung tissue, which can lead to emphysema (Beeh and Beier, 2006).

Despite the high prevalence, morbidity and mortality associated with neutrophil dominated inflammatory diseases, many of these diseases remain poorly treated. Chronic lung diseases are primarily treated with inhaled corticosteroids, but these are often ineffective at stopping neutrophilic inflammation and disease progression, and can have serious long-term side effects (Fardet et al., 2007, Morjaria et al., 2010). Therefore, the development of new medicines targeting neutrophils has become a clear therapeutic goal.

1.1.12 Genetic Manipulation of Neutrophils

The importance of Mcl-1 in neutrophil survival indicates that neutrophil apoptosis may be effectively driven by selective genetic knockdown of Mcl-1. However, the short half-life of neutrophils prevent techniques that require long incubation periods, and they are often sensitive to the harsh reagents used in mainstream techniques, which can induce activation or cell death. To date, no techniques have become established and the few reports of success have failed to be reproduced by other groups (Leuenroth et al., 2000, Sivertson et al., 2007). This has not only limited manipulation of neutrophils for therapeutic intervention, but also restricts the understanding of their molecular functions.

1.1.13 Targeting Neutrophil Apoptosis by Pharmacological Intervention

Not only does apoptosis prevent neutrophils from responding to pro-inflammatory stimuli, but apoptotic cells can actively promote inflammation resolution through sequestering cytokines (Ariel et al., 2006) and by converting macrophages to a pro-resolution phenotype following efferocytosis (Bratton and Henson, 2011). In fact, in one study a single injection of endogenous apoptotic neutrophils into mice with LPS-induced sepsis significantly reduced the levels of pro-inflammatory cytokine release, decreased the severity and duration of symptoms and increased survival rates (Ren et al., 2008).

Induction of neutrophil apoptosis may be achieved by actively targeting pro-apoptotic machinery, or through blocking the actions of survival factors and

downstream signalling pathways. As mentioned previously, the MAPK/ERK and PI3K pathways are activated by survival factors and are involved in the upregulation of anti-apoptotic proteins such as Mcl-1. In one study a selective ERK1/2 inhibitor improved the outcome of a rat carrageenan-induced pleurisy model, which was attributed to its ability to increase the rate of neutrophil apoptosis (Sawatzky et al., 2006). Similarly, inhibitors of the PI3K γ and PI3K δ isoforms of PI3Kinase reduce joint damage in mouse models of rheumatoid arthritis (Camps et al., 2005, Randis et al., 2008). Finally rolipram, a phosphodiesterase 4 inhibitor, has also been shown to drive neutrophil apoptosis through inhibition of the PI3k pathway and resulted in the resolution of neutrophilic inflammation in a mouse model of pleurisy (Sousa et al., 2010).

A target for promoting neutrophil apoptosis through an active mechanism is the extrinsic cell death pathway. This is particularly relevant in patients with severe injuries or trauma, where an abundance of survival factors and pro-inflammatory cytokines can result in resistance to apoptosis through the intrinsic cell death pathways. Paunel-Goerguelue and colleagues demonstrated that neutrophils from critically ill trauma patients remain susceptible to apoptosis by agonist Fas ligand antibodies (Paunel-Goerguelue et al., 2009), which demonstrates the potential of targeting this pathway. However, Fas ligand apoptosis is not specific to neutrophils and so would be detrimental *in vivo*.

When targeting neutrophil apoptosis it is important that macrophages maintain their ability to clear apoptotic neutrophils. If neutrophils are not cleared

efficiently they can undergo secondary necrosis, resulting in the release of their destructive contents into the extracellular environment and exacerbation of inflammation. Unlike Fas ligand, the extrinsic cell death pathway agonist TNF-related apoptosis inducing ligand (TRAIL) has shown specificity for neutrophil apoptosis over other cell types (McGrath et al., 2011). This is thought to be a result of the expression of cell surface decoy receptors on many primary cells (Sheridan et al., 1997). *In vivo*, treatment of wild type mice with recombinant TRAIL resulted in an increase in neutrophil apoptosis, without a reduction in the number of macrophages, and enhanced the resolution of neutrophilic inflammation in LPS-induced acute lung injury and zymosan-induced peritonitis (McGrath et al., 2011). More recently, TRAIL has also proven efficacious in treating mouse models of sepsis and allergic airway inflammation (Faustino et al., 2014, Beyer et al., 2014).

Treatment with endogenous anti-inflammatory molecules can promote neutrophil apoptosis and enhance inflammation resolution. On its own, the anti-inflammatory cytokine IL-10 does not promote neutrophil apoptosis, but it can inhibit neutrophil survival from other pro-inflammatory molecules and reduce further pro-inflammatory cytokine release from immune cells. In mice challenged with intratracheal LPS, administration of IL-10 resulted in reduced neutrophilia and faster neutrophil clearance (Cox, 1996).

As mentioned previously, lipid mediators such as the lipoxins have a number of dual anti-inflammatory and pro-resolution properties (Serhan and Chiang,

2013). *In vitro*, aspirin derived lipoxinA₄ eliminates the pro-survival effect of serum amyloid A (SAA) on neutrophils and enables them to undergo constitutive apoptosis (El Kebir et al., 2007). LipoxinA₄ can reduce further neutrophil recruitment through downregulation of the β_2 integrin Mac-1, which has an important role in neutrophil adhesion and transmigration. Additionally, Mac-1 also plays a role in neutrophil survival; binding of MPO to MAC-1 results in neutrophil activation and upregulation of anti-apoptotic Mcl-1 through activation of the ERK pathways (El Kebir et al., 2008). *In vivo* studies have demonstrated that aspirin derived lipoxinA₄ can override neutrophil survival through Mac-1 and promote inflammation resolution in MPO-mediated acute lung injury (El Kebir et al., 2009).

1.1.14 Cyclin Dependent Kinase Inhibitors

Cyclin dependent kinases (CDKs) are a family of serine/threonine kinases that regulate the progression through the cell cycle. Neutrophils are terminally differentiated cells and remain at rest within the G₀ phase of the cell cycle and for a long time CDKs were believed to be redundant in these cells. But this view was challenged by the Haslett group, which demonstrated that a range of CDK inhibitors (CDKis) could promote neutrophil apoptosis (Rossi et al., 2006).

Neutrophils show varying levels of gene expression for all CDKs, with the greatest expression seen for CDK7 and CDK9 (Leitch et al., 2012). At the protein level, significant expression is thought to be mainly restricted to CDK5, CDK7 and CDK9 (Leitch et al., 2012). The roles of CDKs in neutrophils are yet to be

fully elucidated, but recently it was shown that CDK9 declines as neutrophils age and undergo apoptosis, suggesting this kinase plays an important role in constitutive neutrophil apoptosis (Pinho et al., 2007).

It has now been demonstrated that a number of CDKs can promote neutrophil apoptosis, but (R)-roscovitine is the most widely studied. Roscovitine is an inhibitor of CDK2, CDK5, CDK7 and CDK9 (McClue et al., 2002) and has entered clinical trials for a number of cancers (Benson et al., 2007, Le Tourneau et al., 2010). *In vitro*, roscovitine is a potent inducer of neutrophil apoptosis and can override survival factors such as GM-CSF and LPS (Rossi et al., 2006, Leitch et al., 2010). In a pioneering study by Rossi and colleagues it was demonstrated that roscovitine could enhance the resolution of inflammation in three mouse models of neutrophil dependent inflammation; bleomycin-induced lung injury, passively induced arthritis and carrageenan-induced pleurisy (Rossi et al., 2006).

Roscovitine mediated apoptosis is due to downregulation of Mcl-1 at the mRNA level and this is thought to occur independently of the major survival signalling pathways such as the ERK pathway (Leitch et al., 2010). The exact mechanisms by which CKDs promote neutrophil apoptosis have not been fully elucidated. One possibility is that the CDKs increase the rate of Mcl-1 proteasomal degradation (Leitch et al., 2009). Recently it has been suggested that roscovitine may inhibit Mcl-1 transcription by blocking CDK7 and CDK9 mediated phosphorylation and activation of RNA polymerase II (Leitch et al., 2012).

1.2 *Staphylococcus aureus*

Staphylococcus aureus (*S. aureus*) is a Gram-positive spherical cocci with a diameter of approximately 0.5-1.5µm. The bacterium is an opportunistic human pathogen that permanently colonises mucosal surfaces of 20% of the population and transiently colonises a further 60% (Kluytmans et al., 1997). At any one time, approximately 30% of the population is colonised, which enables *S. aureus* to maintain its ubiquity within our environment and predisposes colonised individuals to infection (Weidenmaier et al., 2004).

Within hospitals, nasal colonisation with *S. aureus* can reach as high as 70% of patients (Wenzel and Perl, 1995) and *S. aureus* is the most frequent bacterial pathogen identified in hospital-associated infections (Otto, 2010). The bacterium can cause a wide range of diseases including superficial skin lesions and boils, toxin diseases such as enterotoxin mediated food poisoning and toxic shock syndrome, and systemic infections by bacteraemia, which can cause life-threatening diseases such as sepsis, endocarditis or osteomyelitis.

1.2.1 Treatment of *S. aureus* Infection and Antibiotic Resistance

Treatment of bacterial infections was revolutionised by the introduction of the first antibiotic penicillin in the 1940s. Resistance to penicillin through the production of penicillinase, an enzyme that degrades penicillin by hydrolysing the β-lactam ring, was reported in 1940, before penicillin was even given to humans for the first time (Abraham and Chain, 1940, Abraham et al., 1941). As the

production and use of penicillin increased, non-resistant *S. aureus* strains rapidly acquired the gene for penicillinase (Kirby, 1944). To overcome this resistance, the first semi-synthetic penicillin that was insensitive to penicillinase was produced in 1959, called methicillin. But in less than two years methicillin-resistant *S. aureus* (MRSA) strains began to arise and by 1963 over one hundred strains of MRSA had been identified (Jevons et al., 1963, Jevons et al., 1961).

Throughout the 20th Century a number of new antibiotic classes active against *S. aureus* were discovered including aminoglycosides, tetracyclines and more recently the oxazolidinones (DeLeo and Chambers, 2009). But *S. aureus* rapidly gained resistance to all of these classes of antibiotics. For a long time it was thought that *S. aureus* may not be able to develop resistance to the glycopeptide antibiotic vancomycin. Vancomycin binds to the bacterial cell wall and inhibits the synthesis of important structural polymers called acetylmuramic acid and N-acetylglucosamine. It was believed that developing resistance to vancomycin would be challenging as it might require large alterations in the structure of the *S. aureus* cell wall, and indeed intentional development of resistance to vancomycin *in vitro* was very difficult (Moellering, 1998). However, slowly resistance started to develop and by the 1990s a number of partially resistant strains had appeared, known as vancomycin intermediate *Staphylococcus aureus* (VISA) (Hiramatsu et al., 1997, Smith et al., 1999). In 2002 the first report of vancomycin-resistant *Staphylococcus aureus* (VRSA) emerged (Goldrick, 2002).

1.2.2 Development of a *S. aureus* Vaccine

The rapid development of resistance towards antibiotics has motivated researchers to explore the development of *S. aureus* vaccines. To date a number of bacterial vaccines have been approved, including vaccines for *Streptococcus pneumoniae* and *Neisseria meningitidis*. These vaccines tend to target single components of the bacterium such as the outer capsule and immunisation results in the production of antibodies that protect the host in subsequent infections.

Clinical trials for *S. aureus* vaccines have targeted extracellular components of biofilms, the polysaccharide capsule, components of the cell wall and ATP-binding cassette transporters, which are transmembrane proteins involved in the transport of essential nutrients and lipids (Salgado-Pabon and Schlievert, 2014). But despite these efforts, vaccines have failed to provide significant protection, even where they have demonstrated large antibody titers in humans (Proctor, 2012). The reason for this is unclear, but many researchers have suggested that the heterogeneity of *S. aureus* virulence mechanisms allows *S. aureus* to defy vaccines targeting a narrow range of antigens.

The most recent failure was the V710 vaccine developed by Merck that targeted the iron surface determinant B, a highly conserved cell wall anchored iron-sequestering protein (Fowler et al., 2013). After successful phase I clinical trials demonstrating that the V710 vaccine was well tolerated in humans (Harro et al., 2012), the vaccine proceeded into a randomised, double blind phase 2b/3

clinical trial to assess the safety and efficacy of the vaccine in preventing *S. aureus* infections after cardiothoracic surgery (Fowler et al., 2013). Astonishingly, not only did the vaccine fail to reduce the rate of postoperative *S. aureus* infections, but those vaccinated patients who developed an infection were five times more likely to die than unvaccinated individuals (Fowler et al., 2013).

In all of these trials a key goal was to produce antibodies to opsonise *S. aureus* for subsequent destruction by phagocytosis or through complement binding, but there is no evidence that antibodies provide additional protection against *S. aureus* in humans and clearance by non-opsonic methods such as pattern recognition receptors (PRRs) may be sufficient. One possible explanation for the failure of vaccines, which will be discussed in more detail later, is that *S. aureus* infection has an important intracellular component and thus extracellular targeting of the bacteria through antibodies is insufficient. If this is true, future vaccines targeting cell mediated immunity may be more efficacious in preventing *S. aureus* disease (Proctor, 2012). A clearer understanding of the complex mechanisms that control *S. aureus* infection should help produce new therapies to overcome bacterial resistance, build new classes of antibiotics and help guide the production of a successful vaccine.

1.2.3 Virulence Factors and the Pathogenesis of *S. aureus*

Bacterial genes and effector molecules that control pathogenicity are called virulence factors. Virulence factors are controlled by virulence regulators, which

alter the expression of the encoding genes. Virulence regulators enable virulence factors to be switched on in environments where their expression is favourable and turned off to limit the metabolic burden when they are not required. A range of *S. aureus* virulence factors have been described which can be separated into three categories based on their function: adhesins, toxins and evasins (Priest et al., 2012).

During the early stages of infection the synthesis of adhesins is upregulated. Adhesins control *S. aureus* attachment to the host, which is essential for the bacterium to colonise and then disseminate. Perhaps the most crucial and prevalent group of adhesins is the family of cell wall anchored proteins called microbial surface component recognizing adhesive matrix molecules (MSCRAMMs) (Foster et al., 2014). These enable *S. aureus* to bind and adhere to extracellular matrix components including fibrinogen and collagen. The expression of MSCRAMM and other adhesion proteins have been linked to the formation of abscesses, endocarditis and other diseases where *S. aureus* colonisation plays an important role (Que et al., 2005, Edwards et al., 2010).

As the infection progresses the expression of the surface adhesins is reduced and toxins and evasins are upregulated. Toxins are thought to benefit the organism by facilitating their dissemination through the blood and tissues. For instance α -haemolysin (α -toxin), a well-studied toxin secreted by *S. aureus*, binds to mammalian cells and forms β -barrel pores that lead to apoptosis or necrosis. Lysis of erythrocytes may be beneficial for *S. aureus* by allowing the

bacteria to sequester iron, which is essential for a number of functions. Similarly, proteases such as the V8 protease enable *S. aureus* to degrade tissues and penetrate into organs (Cheung et al., 2004).

The evasins regulate genes that enable *S. aureus* to resist destruction by the immune system. *S. aureus* can secrete numerous effector molecules including: inhibitors of neutrophil chemotaxis (de Haas et al., 2004) and complement (Rooijackers et al., 2005), and molecules that neutralise antimicrobials (Peschel, 2002). The haemolysins also act as evasins by lysing leukocytes, which will be discussed in more detail later. Another role of evasins is to reduce opsonisation and recognition of the bacterium by the immune system. For instance, protein A interacts with IgG to promote binding of the antibodies at unusual orientations which inhibits its recognition by neutrophil IgG receptors, thereby inhibiting phagocytosis (Foster, 2005).

1.2.4 Intracellular Survival of *S. aureus*

Despite the presence of virulence factors to reduce recognition and clearance by phagocytes, these mechanisms appear to be insufficient to guarantee escape from phagocytosis. Neutrophil phagocytosis of *S. aureus* leads to the fusion of intracellular granules and lysosomes with the phagosome, delivering antimicrobials that help to degrade *S. aureus*. The enzyme called lysozyme attacks peptidoglycan on the bacterial cell wall by hydrolysing glycosidic bonds, and cationic cathepsin G disrupts the *S. aureus* membrane and increases its permeability (Spaan et al., 2013). Neutrophil activation also leads to NADPH

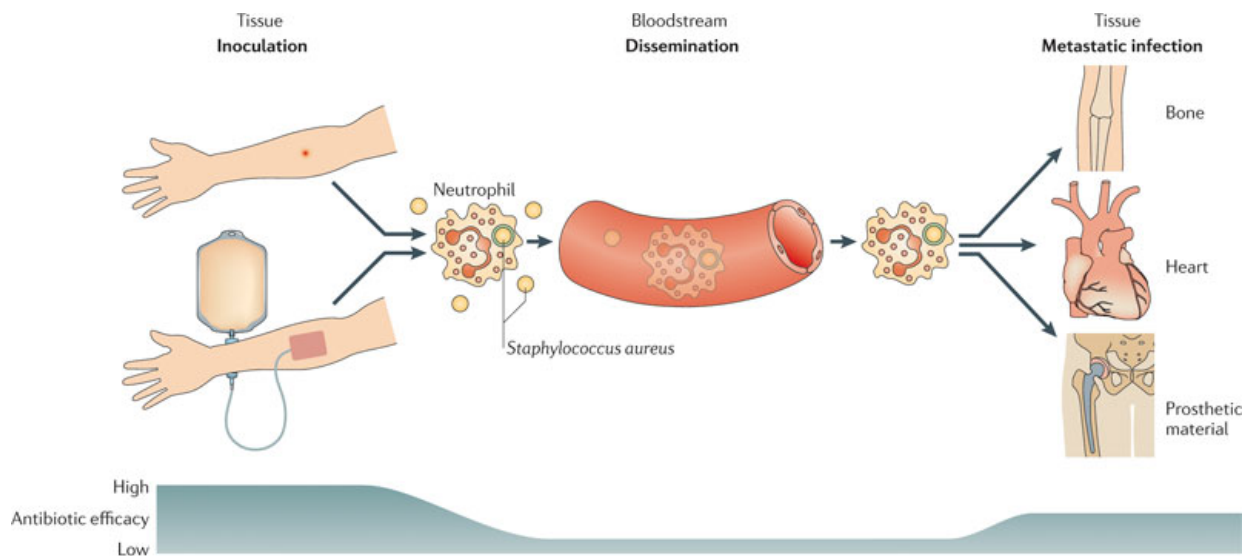
oxidase assembly and the production of ROS. Within the neutrophil phagosome, hydrogen peroxide and myeloperoxidase form hypochlorous acid, which react with the *S. aureus* amino acids, proteins, lipids and nucleic acids (Davies, 2011).

Despite the abundance of intracellular antimicrobials, phagocytosis of *S. aureus* may not be entirely detrimental to the bacterium, and while *S. aureus* is traditionally considered an extracellular pathogen, there is accumulating evidence that the bacteria can survive for prolonged periods within host cells (Garzoni and Kelley, 2009). In fact, *S. aureus* has evolved numerous mechanisms to survive within the neutrophil phagosome (Anwar et al., 2009), despite the presence of destructive reactive oxygen species and degradative proteases.

Voyich and colleagues demonstrated that upon phagocytosis virulent strains of *S. aureus* upregulate genes involved in overcoming oxidative stress, synthesis of the protective polysaccharide capsule and numerous other genes that reduce the ability of neutrophils to degrade the bacterium (Voyich et al., 2005). The Voyich group later demonstrated that *saeR/S*, a 2 component gene regulatory system is essential for the regulation of a wide range of virulence factors involved in the intracellular survival of *S. aureus* (Voyich et al., 2009). Deletion of *saeR/S* in mice resulted in an impairment of intracellular *S. aureus* survival and reduced bacterial dissemination. Interestingly, deletion of *saeR/S* did not influence the formation of skin abscesses after subcutaneous injection, but it almost completely eliminated the pathogenicity of the bacterium in a sepsis model where the mutant caused far fewer fatalities (Voyich et al., 2009).

Following phagocytosis *S. aureus* may escape the phagosome by secreting certain leukocytic toxins known as leukocidins (Alonzo and Torres, 2013, Vandenesch et al., 2012). A number of leukocidins have been identified which have varying potency in causing cell lysis depending on the target cell. For instance, α -haemolysin mediates cell death of lymphocytes, eosinophils and monocytes (Bantel et al., 2001, Prince et al., 2012), but does not appear to cause neutrophil apoptosis even at very high concentrations (Valeva et al., 1997, Loeffler et al., 2010). Whereas, a number of other *S. aureus* leukocidins, such as Pantone Valentine leukocidin (PVL) and leukocidin A/B (LukAB (also known as LukGH), are known to lyse human neutrophils *in vitro* (Loeffler et al., 2010, DuMont et al., 2011).

Survival within phagocytes and subsequent escape may enable *S. aureus* to disseminate throughout the body and form abscess within the tissue (Figure 1.1) (Thwaites and Gant, 2011). The importance of intracellular *S. aureus* was highlighted in a study by Gresham and colleagues, who showed that the transfer of *S. aureus* infected neutrophils into naïve mice was sufficient for the bacterium to establish infection (Gresham et al., 2000). Similarly, other studies in mice demonstrate that high concentrations of neutrophil chemokines at sites of *S. aureus* infection are associated with a greater accumulation of neutrophils, enhanced intracellular survival of *S. aureus* and a more detrimental infection (McLoughlin et al., 2008, McLoughlin et al., 2006).



Nature Reviews | Microbiology

Figure 1.1 Survival of *S. aureus* within blood stream neutrophils may facilitate bacterial dissemination.

Once *S. aureus* is engulfed by a circulating neutrophil the bacterium upregulates virulence factors that allow it to survive intracellularly. Neutrophils may then act as a Trojan horse to facilitate dissemination of the bacteria throughout the body. The bacteria may then escape from the phagocyte and form metastatic infections in organs such as the heart. Intracellular bacteria are also partially protected from antibiotics by the phagocyte membrane, which reduce the efficacy of circulating antibiotics. Figure taken from (Thwaites and Gant, 2011).

Recently the zebrafish has emerged as a powerful model for studying *S. aureus* infection. Zebrafish embryos are transparent, which allows live *in vivo* imaging. The organism contains a competent immune system with neutrophils and macrophages that can be fluorescently labelled by transgenesis. Together this enables the host-pathogen interaction to be studied in ways that are impossible in other organisms. When *S. aureus* is injected into the circulation of zebrafish embryos it is rapidly internalised by neutrophils and macrophages (Prajsnar et al., 2008). Over time the infection either resolves or escalates and overwhelms the fish. Perhaps most significantly, this model reveals that zebrafish infected with a mixed inoculum of two *S. aureus* strains differing only in their resistance marker or fluorescence marker have an output population of bacteria that is often asymmetrically distributed, with one of the two strains predominating (Prajsnar et al., 2012). Confocal analysis revealed that abscesses frequently contained just one of the two strains injected. Importantly, this result was dependent on the presence of phagocytes; when phagocytes were depleted overwhelming infections occurred much more rapidly and the output of bacteria was symmetrical. Taken together this data provides strong evidence that *S. aureus* infection can be dispersed and then seeded by host phagocytes (Prajsnar et al., 2012).

The clinical importance of intracellular *S. aureus* has remained somewhat controversial, which may be due to the difficulties in demonstrating its role in humans. But human reports are starting to highlight a role for neutrophils in *S. aureus* dissemination. Large clinical studies have shown that neutropenic

patients are less likely to develop blood stream *S. aureus* infections, and where bacteraemia does occur, patients have a greater chance of survival, fewer symptoms of sepsis and are less likely to develop metastatic infections (Venditti et al., 2003, Velasco et al., 2006).

Intracellular survival and dissemination may explain the high occurrence of relapsing and persistent *S. aureus* infections. In fact, recurrent infections are particularly common following bacteraemia and are associated with significant morbidity and mortality (Chang et al., 2003). Dissemination by phagocytes also explains how *S. aureus* is capable of infecting almost any organ in the human body (Khatib et al., 2006). Furthermore, intracellular survival reveals why *S. aureus* can persist even after treatment with active antibiotics. Indeed, numerous studies have demonstrated that the intracellular bactericidal effects of antibiotics against *S. aureus* is always lower than that observed extracellularly (Barcia-Macay et al., 2006b, Barcia-Macay et al., 2006a, Lemaire et al., 2005, Carryn et al., 2003).

Together these studies suggest that effective treatment of *S. aureus* infection may benefit from antibiotics that can efficiently pass through the plasma membrane to target intracellular bacteria. An alternative approach is to selectively deliver antibiotics intracellularly using drug delivery vectors. This may allow us to use our current antibiotics more effectively, eliminate *S. aureus* bacteraemia more rapidly and reduce the risk of patients developing disseminated or relapsing infections.

1.3 Nanomedicine

1.3.1 Soft Nanotechnology in Drug Delivery

Nanoparticles can be broadly categorised into two types depending on the chemical bonds that hold them together. “Hard” nanotechnology such as gold nanoparticles and carbon nanotubes, are held together by strong covalent, ionic or metallic bonds; this makes the nanoparticles stiff and inflexible. Whereas, “soft” nanotechnology such as lipid or polymeric nanoparticles, are held together by a combination of weak interactions, including hydrogen bonding, Coulombic forces and the hydrophobic effect. These nanoparticles are less rigid and have a much greater flexibility.

While soft nanoparticles are more fragile, their surface energies are similar to biological membranes and their components can be more easily integrated (Nel et al., 2009). Soft nanoparticles have been utilised to improve drug solubility and biodistribution, to target drugs to specific tissues, or to deliver cell impermeable molecules intracellularly. Liposomes are one of the most common soft nanoparticles used in drug delivery. Liposomes are spherical vesicles formed from phospholipids; they can encapsulate a range of molecules and are biocompatible and biodegradable. However, liposomes have a relatively short shelf life and can have low circulation times and limited mechanical stability. Many of these shortfalls may be overcome by using synthetic vesicles made from polymers. One major advantage of synthetic polymeric vesicles is that their properties, such as their surface chemistry, can be tuned to fit the desired application.

1.3.2 Block Copolymer Amphiphiles

Polymers are molecules composed of chains of repeating units created through covalent bonding of monomers in a process known as polymerisation. When two or more polymers are made from different monomers which are covalently joined end to end, the polymer is referred to as a block copolymer. A block copolymer composed of at least one hydrophobic block and at least one hydrophilic block is an amphiphilic block copolymer.

Synthetic block copolymers are formed using controlled polymerisation techniques that enable the production of polymer chains with a defined length and molecular weight. When mixed with water, amphiphiles assemble into a range of structures depending on the balance of forces from the hydrophilic and hydrophobic blocks. While hydrophilic blocks interact well with water the hydrophobic blocks do not. Therefore the strong hydrogen bonding between water molecules leads to a clustering of the hydrophobic molecules in order to minimise the interaction between water and the nonpolar hydrophobic groups; this is known as the hydrophobic effect (Tanford, 1980).

At low concentrations amphiphiles can remain as single chains molecularly dissolved within a solution, but once this rises above a certain concentration, referred to as the critical aggregation concentration (CAC), the hydrophobic effect drives the chains together forming an aggregate. With block copolymer amphiphiles, the CAC is essentially zero, which means it is rare for chains to be

freely dissolved in solution and for them to be exchanged between assembled aggregates (Jain and Bates, 2004).

Aggregation of block copolymer amphiphiles limits the favourable interaction of the hydrophilic block with water, so to compensate for the requirements of both the hydrophilic and hydrophobic sections, amphiphiles orient themselves into ordered structures; a process known as self-assembly. For a diblock copolymer amphiphile, the structure that forms through self-assembly is predominantly dictated by the curvature of the interface between the hydrophobic and hydrophilic blocks. The dimensionless packing parameter P describes the molecular curvature that the amphiphile would ideally adopt in an aggregate:

$$P = \frac{v}{a_0 l}$$

Where v is the volume of the hydrophobic block, l is the length of the hydrophobic block normal to the interface and a_0 is the optimal area of the interface between the hydrophilic block and hydrophobic block. As shown in Figure 1.2, aggregates formed with low packing parameters ($\leq 1/3$) have high interface curvatures, which favour the formation of solid spherical structures called micelles. Intermediate packing parameters (between $1/3$ and $1/2$) favour the formation of cylindrical micelles, and high packing parameters ($\geq 1/2$) with low curvatures result in the formation of bilayers, which wrap into vesicles. Vesicles made from block copolymer amphiphiles are also known as polymersomes.

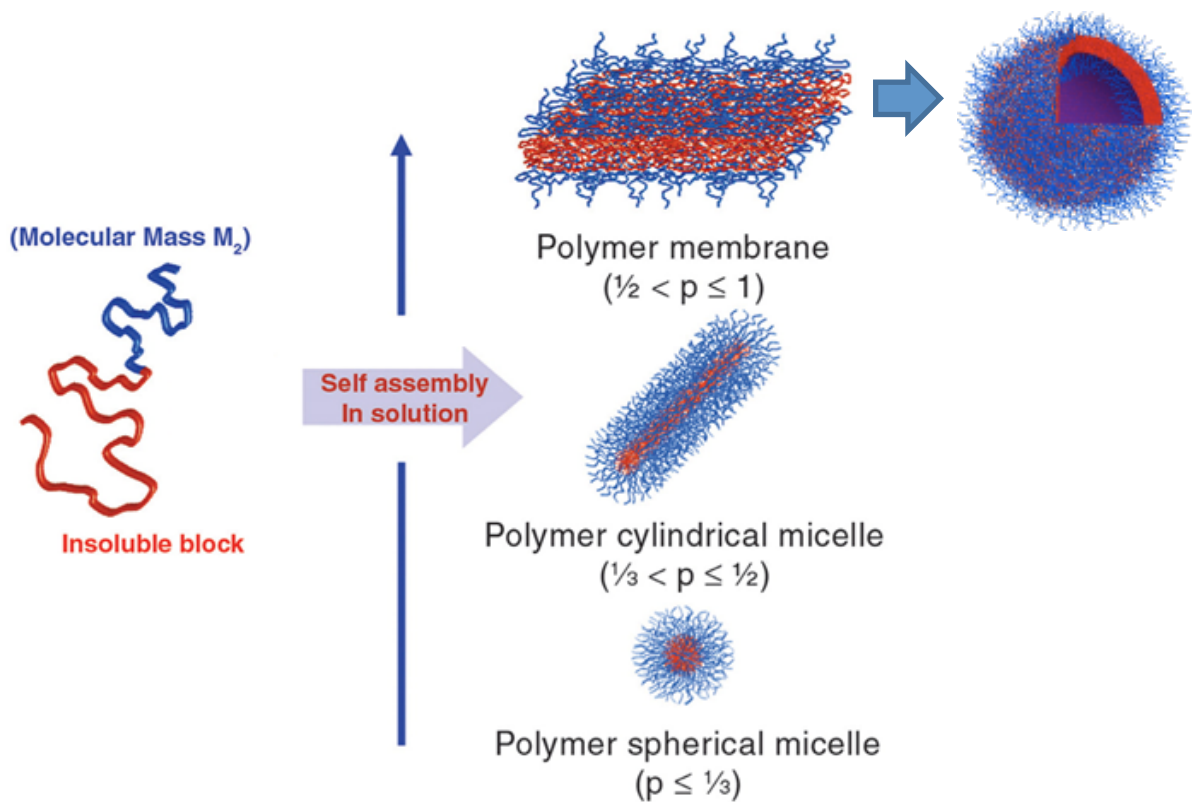


Figure 1.2 Geometries formed from block copolymer amphiphiles with different packing parameters.

For a diblock copolymer amphiphile the structure that forms through self-assembly is dictated by the curvature of the interface between the hydrophobic and hydrophilic blocks, which is described by the molecular packing parameter. High packing parameters have low interface curvatures which favours the formation of membranes. These membranes wrap and enclose into vesicles. Medium packing parameters have slightly higher interface curvatures that favour the formation of cylindrical micelles. And finally low packing parameters have high interface curvature which favours the formation of spherical micelles. Picture adapted from (Smart et al., 2008).

In aqueous solutions micelles and cylindrical micelles assemble with the hydrophilic block on the outside and the hydrophobic block forming the inner core. The diameter of spherical micelles ranges from approximately 5-100nm in diameter and these aggregates can encapsulate hydrophobic drugs within their core. In comparison, spherical polymersomes have a larger range of sizes from approximately 30nm to hundreds of micrometres. One major advantage of polymersomes over micelles is they are able to encapsulate both hydrophobic molecules within their hydrophobic membrane and hydrophilic molecules within their aqueous core.

Compared to liposomes, polymersomes have a thicker more robust membrane with a greater elastic strength and mechanical stability. While liposomes have a membrane thickness of approximately 3-5nm, the polymersome membrane can range from 2-50nm in diameter depending on the copolymer chain length. The high mechanical stability of polymersomes is in part due to the chain entanglement and interdigitation of the hydrophobic blocks (Battaglia and Ryan, 2005a). When the membrane of liposomes and poly(ethyleneoxide)–poly(ethylene) (PEO-PEE) polymersomes were compared, the polymersome membrane required a force ten times greater for membrane rupture and was ten times less permeable to water than the liposome membrane (Discher et al., 1999).

1.3.3 Nanoparticle Biodistribution

Size, shape and surface chemistry are important parameters when designing block-copolymer nanoparticles for drug delivery. Size is probably the best-studied property and is known to have an important role in numerous *in vivo* functions including: the rate of tissue extravasation, circulation time, internalisation speed, and biodistribution (Mitragotri and Lahann, 2009, Akinc and Battaglia, 2013).

Nanoparticle biodistribution depends on the rate of extravasation into tissues and the rate of clearance by the immune system or the kidneys. In the circulation, nanoparticles with diameters below 6nm tend to exhibit rapid urinary excretion (Choi et al., 2007), while nanoparticles above 200nm rapidly accumulate in the liver and spleen (Sengupta, 2014). However, clearance from the reticuloendothelial system (RES) is not only dependent on the nanoparticle size, but can also vary widely depending on the nanoparticle flexibility and surface chemistry. Indeed the membrane flexibility and surface proteins on erythrocytes enable them to pass through the RES when healthy, but these cells lose flexibility as they age and are subsequently removed.

As the zeta potential (or surface charge) of a nanoparticle increases the interaction with the RES rises, resulting in a more rapid clearance from the blood stream. A higher zeta potential also correlates with a greater rate of opsonisation and adhesion to serum proteins (Jain and Stylianopoulos, 2010). To avoid rapid opsonisation and clearance of nanoparticles many groups employ

highly solvated hydrophilic blocks such as Poly (ethylene oxide) (PEO), commonly known as Poly (ethylene glycol) (PEG), which reduces non-selective adhesion and protein adsorption of block copolymer nanoparticles, this will be discussed in more detail in due course.

Extravasation of nanoparticles into tissues requires a size below approximately 100nm; nanoparticles smaller than this can leave the blood through vessel fenestrations in the endothelial cell lining. However, the leaky vasculature surrounding tumours or inflamed tissue enable an enhanced accumulation of nanoparticles in these regions (Bader, 2012). Particle size also influences the biodistribution of the nanoparticles within tissues. Reddy and colleagues demonstrated that intradermal 25nm polymeric nanoparticles were transported efficiently to lymph nodes, whereas 100nm nanoparticles displayed less movement through the tissue and accumulated 10 times less in the lymph nodes (Reddy et al., 2007).

1.3.4 Endocytosis

Physical properties such as size, shape and surface chemistry can also influence particle biodistribution by altering the rate of cellular internalisation. Block copolymer nanoparticles are internalised through an energy dependent process called endocytosis, where particles bound to the cell membrane are wrapped, internalised and trafficked intracellularly. Endocytosis is broadly separated into two categories; phagocytosis (cell eating) and pinocytosis (cell drinking). While phagocytosis is limited to phagocytes, pinocytosis occurs in almost all

eukaryotic cells. Pinocytosis can be further divided into a number of sub-categories depending on the mechanisms of internalisation, and the lipids and proteins involved.

Macropinocytosis was one of the first endocytosis mechanisms discovered; this can facilitate the uptake of relatively large macromolecules of up to 1 μ m in diameter. Unlike other forms of endocytosis, macropinocytosis is not directly initiated by ligand binding but is thought to occur from rearrangements in the actin cytoskeleton that cause membrane ruffling in response to certain growth factors, which can form cups in the membrane that close and then contract towards the cell (Swanson, 2008).

Clathrin-mediated endocytosis (CME) and caveolae-mediated endocytosis are the most well studied internalisation mechanisms. CME has been implicated in the internalisation of a wide range of materials with sizes up to approximately 200nm in diameter. It is characterised by the formation of a polyhedral lattice from the triskelion protein clathrin. Clathrin function is coordinated by adaptor proteins and surrounds the internalising vesicle to form a clathrin-coated pit (McMahon and Boucrot, 2011). Caveolae-mediated endocytosis is initiated by the formation of 50-80nm caveolae, flask shaped invaginations in the cell membrane formed primarily from the protein caveolin (Pelkmans and Helenius, 2002). These caveolae are thought to be involved in the internalisation of a variety of materials, but caveolae are also known to play a role in transcytosis and as sensors of membrane tension (Parton and del Pozo, 2013).

A number of new mechanisms of endocytosis have been discovered in the last few decades including RhoA-mediated and flotillin mediated endocytosis, but the exact mechanisms of these new routes remain relatively undefined. It is clear that endocytosis is a complex process that involves numerous sensors and adaptors that are often overlapping between the separate pathways.

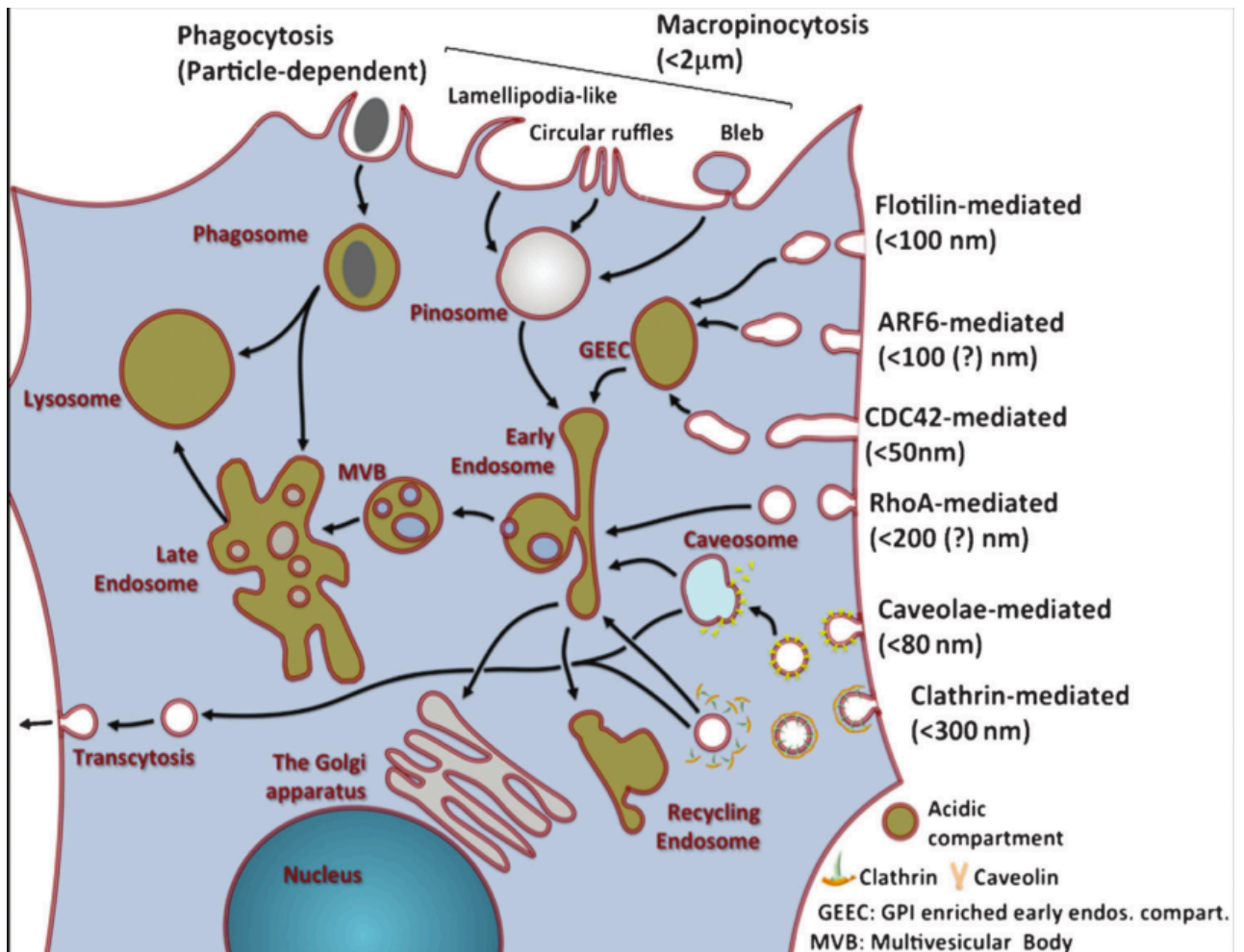


Figure 1.3 A summary of endocytic mechanisms in eukaryotic cells.

Endocytosis can be separated into phagocytosis or pinocytosis. Pinocytosis can be further subcategorised depending on the specific proteins and lipids involved in the internalisation process. Pinocytosis is typically initiated by receptor-mediated internalisation followed by intracellular trafficking to an early endosome, maturation into a late endosome and finally fusion with a lysosome. Phagocytosis is performed in specialised phagocytic cells and is primarily associated with the uptake of larger (>500nm) solid materials including pathogens and dead cells. It is typically triggered by specific receptor binding, followed by the energy dependent formation of a cup-shaped membrane that encloses the target and internalises it into a phagosome. The phagosome then fuses with lysosomes and intracellular granules which allow the phagocyte to degrade its contents. Image taken from (Canton and Battaglia, 2012).

1.3.5 Nanoparticle Endocytosis

It has been recognised for some time that pathogenic organisms, particularly viruses, can utilise eukaryotic endocytosis mechanisms to transport themselves into host cells (McMahon and Boucrot, 2011, Dimitrov, 2004). We now know that many synthetic nanoparticles are also internalised by endocytosis, but the exact mechanisms used by nanoparticles are poorly understood. It is likely that the combination of pathways that are used and the efficiency to which each pathway is exploited could determine the rate of internalisation. Gratton and colleagues showed that macropinocytosis, clathrin-mediated endocytosis and caveolae-mediated endocytosis were all involved in the internalisation of nanometre and micrometre sized hydrogels to varying extents depending on their size and shape (Gratton et al., 2008b). They found the nanoparticles that were most readily internalised utilised all 3 internalisation pathways to a high degree (Gratton et al., 2008b).

Strong interactions between nanoparticles and the plasma membrane can be sufficient to drive membrane wrapping around nanoparticles (Zhao et al., 2011). Ligands on the nanoparticle surface can bind to membrane receptors to temporarily adhere to the cell. Over time more membrane receptors diffuse to the contact area and bind to the particle. This is driven by the favourable interaction energy from receptor-ligand formation. As receptors continue to be recruited and the contact area between the nanoparticle and the cell increases, the membrane wraps around the particle and eventually engulfs it completely (Gao et al., 2005).

Using theoretical calculations Gao and colleagues demonstrated that there was an optimal size of 50-60nm in diameter that facilitates membrane wrapping in the shortest time period (Gao et al., 2005). For particles below this optimal size the high bending requirement of the membrane causes a decreased overall driving force for membrane wrapping, leading to an increased wrapping time, or preventing wrapping from occurring altogether. Particles above the optimal size require diffusion of receptors over a greater distance, which takes a longer period of time.

Most experimental studies agree that smaller nanoparticles (<100nm) tend to be internalised more readily than larger particles (Desai et al., 1997, Rejman et al., 2004, Lu et al., 2009, Prabha et al., 2002, Nakai et al., 2003), and several studies have found that a diameter of 40-60nm is optimal for efficient internalisation (Nakai et al., 2003, Osaki et al., 2004, Chithrani et al., 2006, Jiang et al., 2008). However, these experimental studies and other theoretical models highlight that the rate of internalisation also depends on the receptor ligand affinity, the cell membrane bending modulus, the receptor-ligand density ratio and the nanoparticle surface topology (Yuan and Zhang, 2010, Massignani et al., 2009, Gao et al., 2005). This means that the optimum size of a nanoparticle will depend on its surface chemistry and on the properties of the target cell.

Altering the surface charge of nanoparticles can increase the speed of endocytosis by improving their interaction with the plasma membrane. Cationic

nanoparticles interact strongly with the plasma membrane and are internalised more readily than neutral ones. This has driven a lot of research into cationic block copolymer nanoparticles for the intracellular delivery of nucleic acids (Kakizawa and Kataoka, 2002). However, cationic nanoparticles have also been associated with high levels of cytotoxicity and can cause mitochondrial damage, activation of inflammatory cascades and even cell death (Xia et al., 2008, Hunter and Moghimi, 2010, Nel et al., 2006). To investigate the effect of charge on the rate of internalisation of polymersomes, Blanazs and colleagues used the triblock copolymer poly(ethylene oxide)- poly(2-(diisopropylamino) ethyl methacrylate)- poly(2-(dimethylamino) ethyl methacrylate) (PEO-PDPA-PDMA). By varying the proportion of the cationic PDMA block they showed that the highly cationic polymersomes were more rapidly internalised than the neutral polymersomes, but caused a rapid drop in cell viability (Blanazs et al., 2009b).

Shape is another physical property of nanoparticles that will influence their rate of internalisation. The angle at the point of contact between a nanoparticle and cell will influence the bending requirement of the membrane for wrapping and internalisation to occur. The Mitragotri group investigated the ability of macrophages to internalise a range of polystyrene particles with different shapes. When the macrophage attached to highly curved regions on the particles they were rapidly internalised, whereas, when the contact angle was “flat” internalisation was either delayed, or stopped altogether (Champion and Mitragotri, 2009, Champion and Mitragotri, 2006). Likewise, by modelling the receptor mediated internalisation of cylindrical nanoparticles, Decuzzi and

Ferrari showed that the rate of internalisation was highly dependent on the aspect ratio when the particle was lying parallel to the cell. As the aspect ratios were raised, the time required for membrane wrapping significantly increased (Decuzzi and Ferrari, 2008) and at very high aspect ratios the particle was only partially wrapped, which was referred to as “frustrated endocytosis” (Decuzzi and Ferrari, 2008).

Under flow, particles with high aspect ratios are more easily detached from the membrane by shear forces (Decuzzi and Ferrari, 2006, Lee et al., 2009). The Discher group demonstrated that the circulation time of PEG-poly(ϵ -caprolactone) (PEG-PCL) cylindrical micelles improved with increasing length, with a maximum circulating half-life of approximately 5 days; almost an order of magnitude higher than circulation times recorded for spherical nanoparticles (Geng et al., 2007). Another interesting property of rod shaped particles is their high adhesive binding strength. Compared with spherical particles of the same volume, rod-shaped particles form more receptor-ligand interactions on the cell surface leading to an increased binding avidity (Decuzzi and Ferrari, 2006, Lee et al., 2009). The combination of increased shear induced detachment and improved adhesive strength for rod shaped particles means the ability of these particles to attach to a cell in the blood stream will depend strongly on the affinity of the receptor ligand interaction and the density of receptors on the target cell. In practice, this means that rod shaped objects decorated with targeting ligands are more likely to bind to cells that can form high affinity

interactions and less likely to bind unspecifically to cells with only low affinity interactions (Kolhar et al., 2013).

1.3.6 “Stealth” Nanotechnology

In drug delivery, the immune system is both a target and an obstacle. The human immune system has evolved a vast array of machinery that allows it to recognise and eliminate almost any foreign body whilst maintaining tolerance to “self” antigens. For this reason, many nanoparticles that have proven effective *in vitro* are rapidly cleared *in vivo* by the immune system. Even when leukocytes or inflammatory tissues are targets in drug delivery, recognition and clearance of the nanoparticles by the immune system is undesirable, because nanoparticles recognised as foreign are quickly removed by the reticuloendothelial system (RES) and hence may not reach their target tissue. Additionally the identification of foreign bodies can initiate an immune response that may in itself be detrimental to the host. This has motivated the development of “stealth” nanoparticles that can circumvent these defence mechanisms in order to reach their target.

When particles are injected into the circulation, they are opsonised by complement proteins and antibodies, which leads to rapid clearance by circulating phagocytes and the RES. As mentioned earlier, PEG is a common choice of hydrophilic block as it has proven to be highly resistant to protein adhesion. As the grafting density of the PEG block increases it becomes more spread and aligned, changing from a “mushroom” to a “brush” configuration, this

produces a steric hydrophilic barrier reducing the accessibility of proteins to the nanoparticle. However, even PEGylated nanoparticles are not completely resistant to opsonisation, anti-PEG IgM antibodies have been found in patients injected with liposomes coated in PEG (PEGylated liposomes) (Dufort et al., 2011). PEGylated liposomes have higher circulation times than normal liposomes, but it is still reduced in subsequent doses. This process is referred to as the accelerated blood clearance phenomenon (Ishida et al., 2004).

In comparison to PEG, the biocompatibility and immunogenicity of other hydrophilic blocks have been relatively unexplored. Examples of other hydrophilic polymers with proposed steric hindrance include the poly(2-oxazoline)s and poly(2-(methacryloyloxy)ethyl phosphorylcholine) (PMPC). The phosphorylcholine polymer PMPC stemmed from an observation that the phospholipids composing the inner membrane of erythrocytes were thrombolytic, while the phosphatidylcholine and sphingomyelin dominated outer membrane were non-thrombolytic (Zwaal et al., 1977). We now know that the non-thrombolytic nature of the outer leaflet is attributed to phosphorylcholine; the head group of phosphatidylcholine and sphingomyelin (Hayward and Chapman, 1984).

Although the mechanism by which phosphorylcholine based polymers prevent protein adhesion is not completely understood, a great deal of research has demonstrated that they are very resistant to interactions with blood proteins such as fibrinogen, albumin and immunoglobulins (reviewed in (Lewis, 2000)).

The highly hydrophilic zwitterionic head group associates with a large quantity of water, which allows proteins to bind transiently without undergoing any conformational changes (Ishihara et al., 1998). In addition, MPC has a strong affinity for plasma phospholipid, which builds up on the MPC surface (Ueda et al., 1992). Resistance to protein adhesion *in vivo* is most likely the result of a combination of these mechanisms.

1.3.7 Block Copolymer Nanoparticles for the Treatment of Infectious and Inflammatory Diseases

As mentioned previously, one of the hallmarks of inflammation is swelling and the accumulation of fluid. This is because pro-inflammatory mediators released at the inflammatory site increase the permeability of local blood vessels to enable leukocytes to move into the tissue. This results in nanoparticles accumulating in the inflamed region. The selective accumulation of radiolabelled nanoparticles in the joints of patients with rheumatoid arthritis has even been used for imaging the joints of humans (Williams et al., 1987). By exploiting this passive accumulation of nanoparticles at inflamed joints, nanoparticles may be able to deliver drugs more specifically to the diseased areas (Figure 1.4). Ishihara and colleagues showed that micelles encapsulating Cy7-dodecylamine accumulated within the inflamed joints of mice with adjuvant arthritis (Ishihara et al., 2009). Subsequently, the glucocorticoid betamethasone was encapsulated within these micelles and injected intravenously. A single injection resulted in a 35% decrease in inflammation after one day, which was maintained for nine

days. This response was superior to an injection of free betamethasone even with a dose three times greater (Ishihara et al., 2009).

Another drug that may benefit from encapsulation within block copolymer nanoparticles is cyclosporine A (CsA). CsA is an immunosuppressant commonly used in the treatment of graft versus host disease and other autoimmune diseases. However, CsA has a number of clinical drawbacks including poor solubility, low permeability and some serious long-term side effects such as nephrotoxicity. *In vivo*, CsA loaded PEG-PCL micelles gave comparable immunosuppressive potency to the commercial formulation of CsA but were able to give controlled release of the drug and reduce the accumulation of CsA in the kidneys, which the authors suggest may reduce nephrotoxicity (Hamdy et al., 2011).

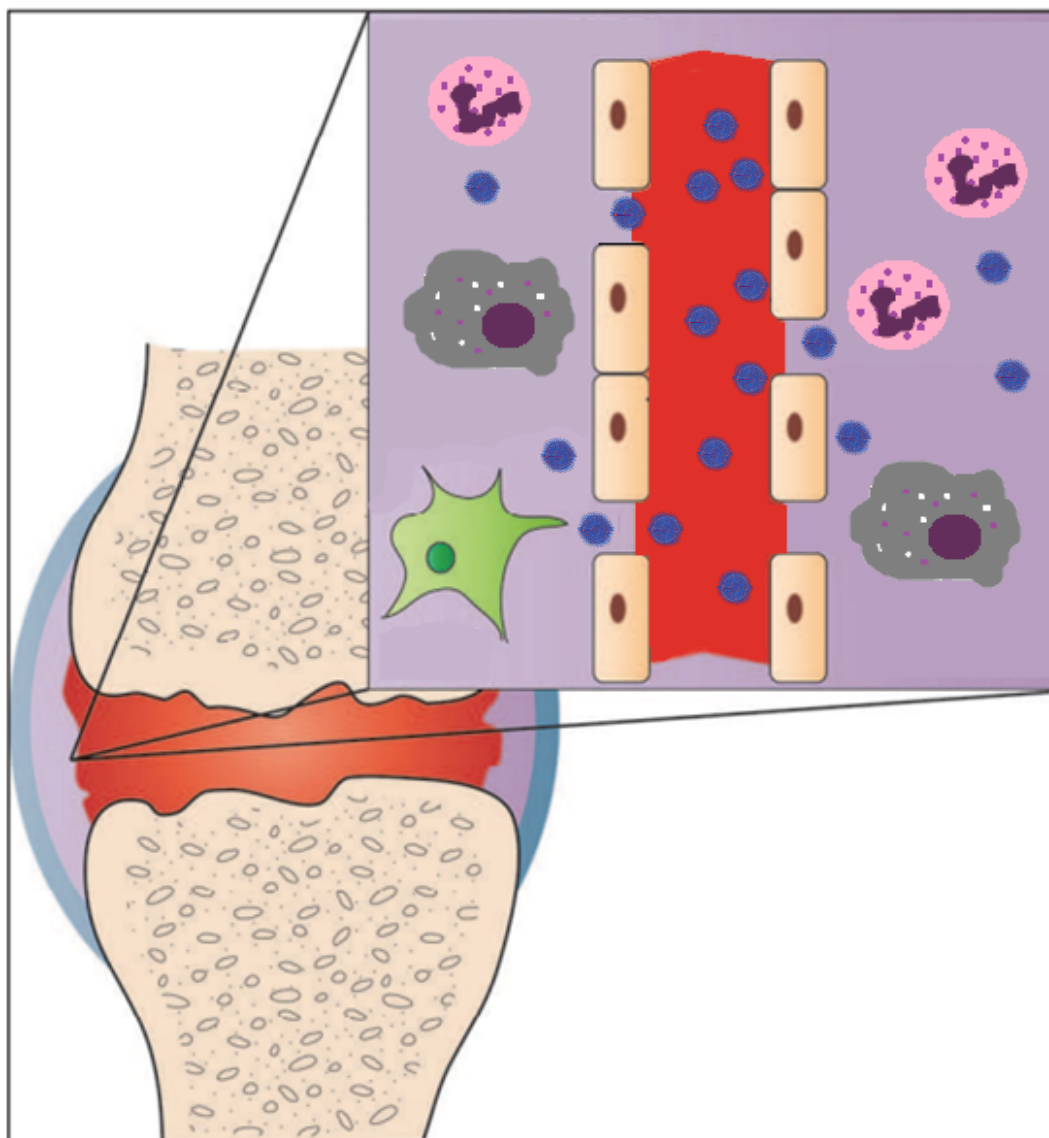


Figure 1.4 Accumulation of nanoparticles in inflamed joint.

Proinflammatory mediators released at sites of inflammation result in a more leaky vasculature. This leaky vasculature around inflamed joints allows nanoparticles to move into the joint and accumulate. This enables arthritic joints to be passively targeted by nanoparticles. Picture adapted from (Bader, 2012).

The ability of some nanoparticles to deliver drugs intracellularly may be beneficial in the treatment of infectious diseases where pathogens are able to survive within the cell. Examples of intracellular microorganisms include the bacteria *Mycobacterium tuberculosis*, *Staphylococcus aureus*, *Salmonella* species and *Brucella* species, fungi such as *Aspergillus fumigatus* and *Candida albicans*, and protozoa including *Leishmania donovani* and *Toxoplasma gondii*. These diseases can be difficult to treat despite the availability of effective antibiotics, which may be due to the poor penetration of the antibiotics across the host cell membrane. This has led to the development of encapsulated antibiotic formulations to deliver the antibiotics intracellularly (reviewed in (Briones et al., 2008)).

Despite the accumulating evidence that *Staphylococcus aureus* (*S. aureus*) infection has an important intracellular component, few studies have explored the use of intracellular drug delivery vectors. It has been demonstrated that antibiotics encapsulated in *poly(lactic-co-glycolic acid)* (PLGA) and chitosan nanoparticles are more effective at treating intracellular *S. aureus* infection *in vitro* (Maya et al., 2012, Imbuluzqueta et al., 2012), but *in vivo* studies are needed to determine the potential of this approach for treating human infections.

1.3.8 PMPC-PDPA Polymersomes for Treating Infectious and Inflammatory Diseases

The Battaglia group has primarily focused on polymersomes formed from the di-block copolymer Poly(2-(methacryloyloxy)ethyl phosphorylcholine)–poly (2-

(diisopropylamino) ethyl methacrylate) (PMPC-PDPA). As mentioned above, the hydrophilic PMPC block is highly biocompatible due to its resistance to protein adhesion. This is supported by its clinical use as a coating for contact lenses, coronary stents and artificial joints (Goda and Ishihara, 2006, Lewis et al., 2002, Moro et al., 2004). The PDPA block is pH-sensitive, which enables the polymersomes to assemble and disassemble depending on the local pH (Figure 1.5). At low pH DPA monomers accept a proton at the tertiary amine group, allowing PDPA to interact with water. When the pH is brought above the pKa (6.4) the DPA monomers become deprotonated and hydrophobic, allowing the polymer to self-assemble.

The pH-sensitivity of PMPC-PDPA provides a number of advantages as a drug delivery vector. By dissolving the polymer in a weakly acidic solution and slowly raising the pH above the pKa, the deprotonation of the tertiary amine group drives the assembly of the polymer into polymersomes. This method of assembly can also be used to encapsulate hydrophilic drugs in the solution. The pH-sensitivity also provides a mechanism for delivering drugs into the cytoplasm after internalisation (Figure 1.6a). Following endocytosis, polymersomes are trafficked to an early endosome where the pH begins to drop. Once the pH drops below the pKa the polymersomes disassemble and this results in a sudden increase in the number of charged species within the endosome. It has been estimated that a single polymersome with a 200nm diameter will provide over half a million ionic species (Lomas et al., 2008), which leads to a huge increase in osmotic pressure. This is thought to be sufficient to cause

temporary lysis of the endosomal membrane and release of some of the polymersome cargo into the cell cytoplasm. Importantly, when polymersomes are made with the pH-insensitive hydrophobic block poly(butylene glycol) instead of the PDPA block, endosomal escape is not observed and the polymersomes and their cargo are left entrapped within the endolysosomal compartment (Figure 1.6).

Extensive toxicity analysis on over 20 different cell types has demonstrated that PMPC-PDPA are very well tolerated even at relatively high concentrations (Massignani et al., 2009). When measuring uptake into primary human dermal fibroblasts, PMPC-PDPA and PEO-PDPA polymersomes with increasing diameters from 100nm were internalised at progressively slower rates (Massignani et al., 2009) and uptake analysis of polymersomes formed from two copolymers revealed that the surface topology also has a great impact on the rate of internalisation (Massignani et al., 2009).

PMPC-PDPA polymersome internalisation is inhibited when cells are incubated at 4°C, demonstrating that polymersomes rely on energy dependent endocytosis for their internalisation (Massignani et al., 2009). More recently the scavenger receptors, particularly SR-BI/II and CD36, were shown to be involved in mediating polymersome internalisation (Colley et al., 2014b). Blockage of these receptors using antibodies or small molecules resulted in a significant reduction in polymersome internalisation in a number of cell types (Colley et al., 2014a).

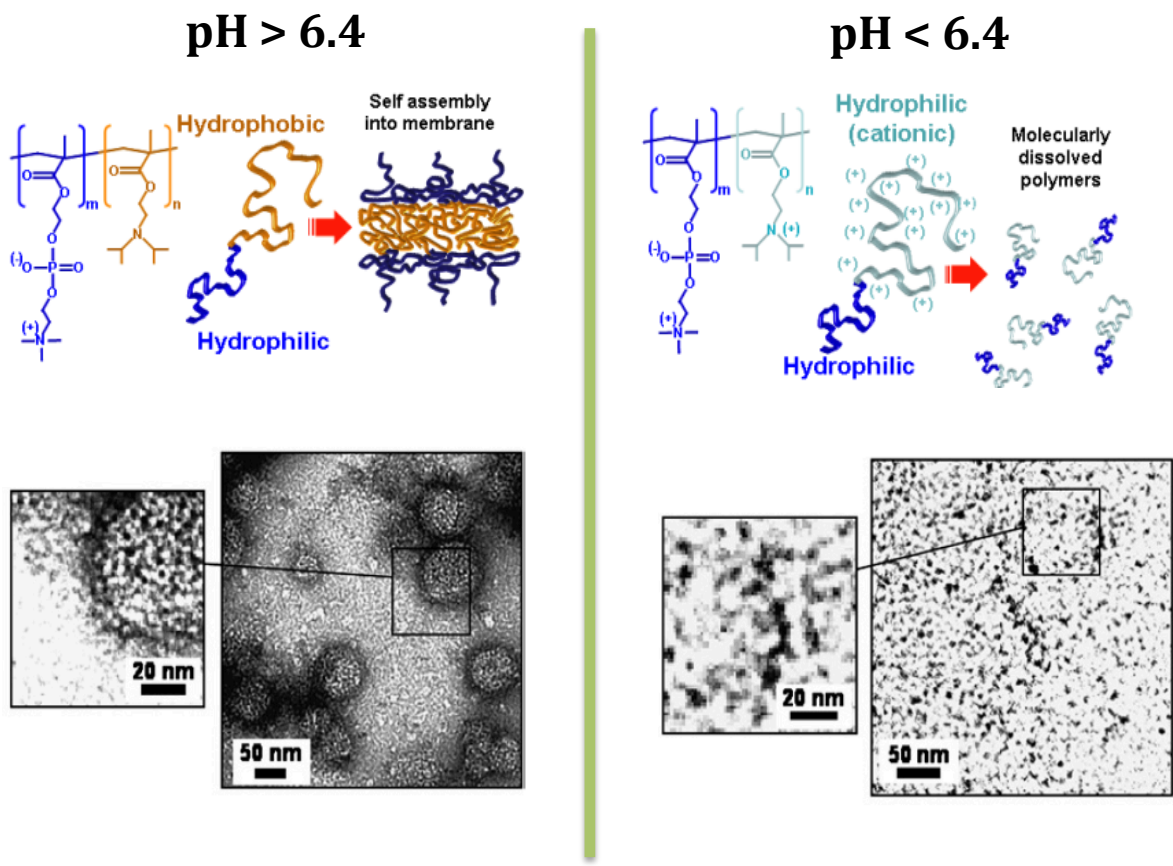
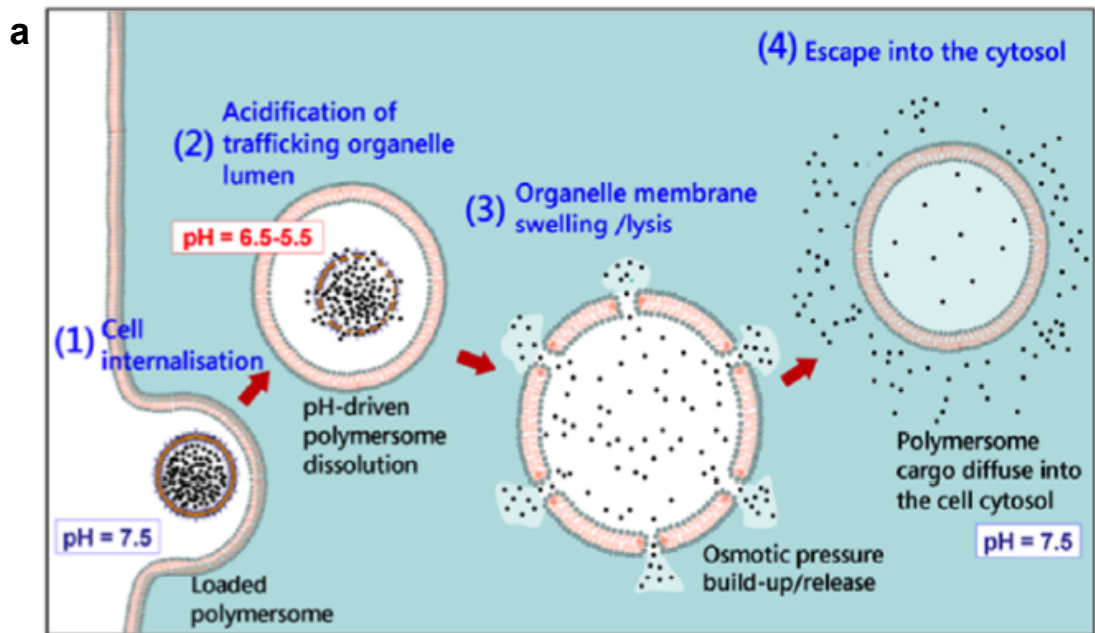


Figure 1.5 pH-sensitive PMPC-PDPA.

The PDPA block of the polymer PMPC-PDPA is pH-sensitive, with a pKa of approximately 6.4. Below pH 6.4 the DPA groups are uncharged and hydrophobic which promotes self-assembly of the polymers into a membrane bilayer. When the pH is raised above 6.4 the DPA groups accept a proton and become positively charged. This allows the PDPA block to interact with water and results in the polymer chains disassembling and dissolving within the solution. Figure adapted from (Lomas et al., 2010).



b

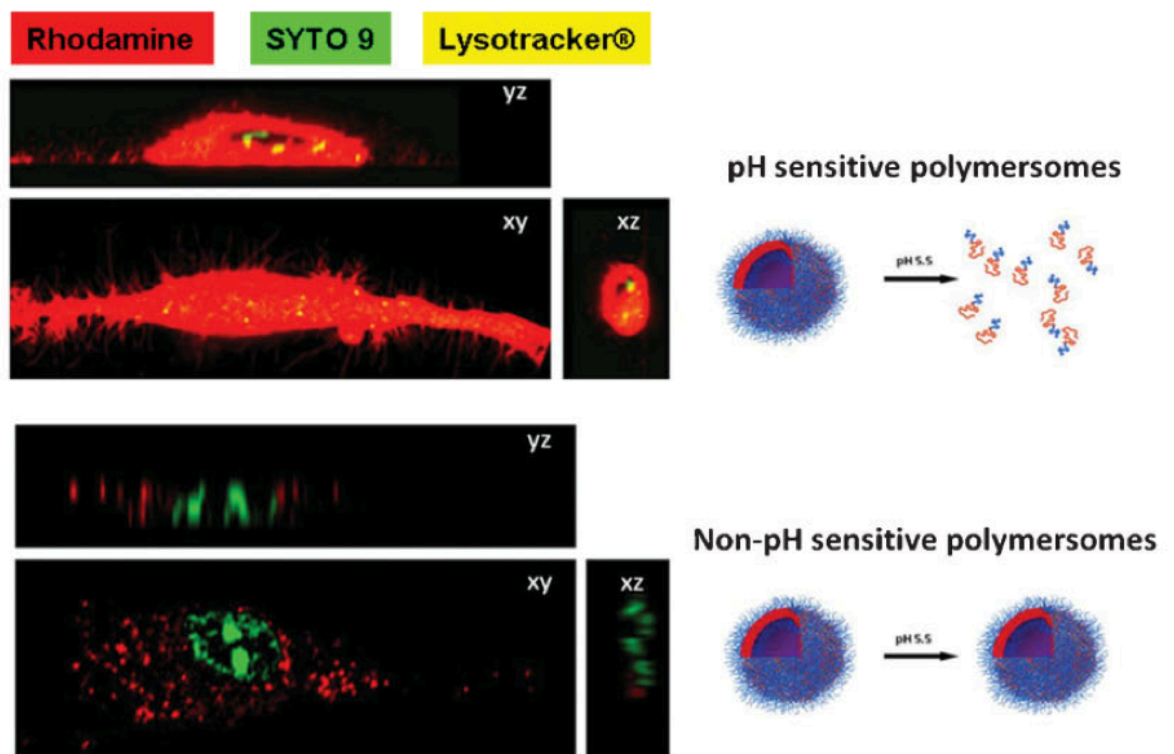


Figure 1.6 pH-sensitive PMPC-PDPA polymersome endosomal escape

a) Proposed mechanism of polymersome endocytosis and endosomal escape. b) Confocal photomicrographs of human dermal fibroblasts after incubation with pH-sensitive PMPC-PDPA polymersomes or pH insensitive PEG-PBG polymersomes encapsulating the fluorescent dye rhodamine B octadecyl ester perchlorate. Figures adapted from (Massignani et al., 2009) and (Massignani et al., 2010).

One major advantage of polymersomes over many other vectors is that they can encapsulate a range of different cargo. Hydrophobic drugs are encapsulated within the hydrophobic section of the polymersome membrane and hydrophilic cargo is retained within the aqueous core. The encapsulation efficiency varies depending on the properties of the molecule and how well they interact with the polymer. For instance, anionic DNA interacts with the cationic PDPA chain at low pH. This electrostatic binding has been demonstrated by titrating DNA-ethidium bromide complexes with aqueous PMPC-PDPA (Lomas et al., 2007) and explains the high encapsulation efficiency observed with DNA. Serum proteins, such as bovine serum albumin, are also anionic and have high encapsulation efficiencies (Wang et al., 2012). Hydrophobic molecules are also encapsulated with high efficiency because the hydrophobic effect reduces their interaction with water and promotes aggregation within the hydrophobic PDPA membrane (Massignani et al., 2010) and the hydrated PMPC brush prevents the drug from leaking into the solution. Even amphiphilic molecules can be retained within polymersomes as the hydrophobic and hydrophilic sections of the amphiphile can interact with the PDPA and PMPC chains respectively across the polymersome membrane (Pegoraro et al., 2013).

PMPC-PDPA polymersomes have been used as intracellular vectors for the delivery of nucleic acids (Lomas et al., 2007), anti-cancer drugs (Pegoraro et al., 2013), fluorescent dyes (Massignani et al., 2009) and lipids (Massignani et al., 2010). This thesis focuses on the clinical potential of PMPC-PDPA polymersomes for the treatment of neutrophil dominated infectious and inflammatory disease.

Chapter 2: Aims and Objectives

As described in the introduction, work in the Battaglia research group has demonstrated that PMPC-PDPA polymersomes can deliver a range of cargo into mammalian cells without causing adverse toxicity. Neutrophil dominated inflammatory diseases and blood stream *Staphylococcus aureus* infection are associated with high morbidity and mortality and are difficult to treat. Therefore, the overall goal of this thesis is to investigate the potential of PMPC-PDPA polymersomes as intracellular vectors for the treatment of neutrophil dominated inflammation and intracellular *Staphylococcus aureus* infection.

In order to achieve this goal the following aims and hypotheses will be addressed:

- **Aim:** Define the optimal size and shape of PMPC-PDPA polymersomes for effective cargo delivery into neutrophils.

Hypothesis: Polymersome size and shape will influence the amount of cargo that can be encapsulated and the rate of internalisation by neutrophils.

- **Aim:** Investigate the types of molecules that can be delivered into neutrophils and use this knowledge to deliver molecules that promote neutrophil apoptosis and enhance inflammation resolution.

Hypothesis: Polymersomes will be able to encapsulate and deliver both hydrophilic and hydrophobic molecules into neutrophils. Polymersome mediated delivery of cyclin-dependent kinase inhibitors or siRNA to lower the expression of Mcl-1 will drive neutrophil apoptosis.

- **Aim:** Kill intracellular *S. aureus* using polymersomes loaded with antibiotics to determine the importance of intracellular bacteria in the disease progression and to investigate the therapeutic potential of this approach.

Hypothesis: Intracellular *S. aureus* play an important role in the dissemination of the infection and the formation of tissue abscesses, the intracellular delivery of antibiotics will reduce the bacterial burden and help to reduce the occurrence of overwhelming infections.

Chapter 3: Materials and Methods

3.1 Reagents

Unless otherwise stated all reagents were purchased from Sigma-Aldrich, this includes fibrinogen, Sepharose 4b, gel permeation chromatography columns, DMSO, Bovine Serum Albumin (BSA), Dulbecco's phosphate buffered saline (dPBS), sodium hydroxide (NaOH), o-phthalaldehyde (OPA), trifluoroacetic acid (TFA), hydrochloric acid (HCL) and all of the antibiotics except for lysostaphin that was ordered from Ambi Products. Chloroform and methanol were purchased from Fisher Scientific. (R)-roscovitine was purchased from Cambridge Bioscience, GM-CSF was from PeproTech, cascade blue and the Mcl-1 silence select siRNA were purchased from Life Technologies. The AllStars Negative siRNA Alexa Fluor647 was purchased from Qiagen and the Silencer Negative Control No. 1 siRNA was from Ambion. The α -tubulin antibody [YOL1/34] was from Abcam and the Brilliant Violet γ -tubulin antibody was from BioLegend.

3.2 PMPC-PDPA

poly(2-(methacryloyloxy)ethyl phosphorylcholine)- poly(2-(diisopropylamino) ethyl methacrylate) PMPC₂₅-PDPA₇₀ and rhodamine 6G-labelled PMPC-PDPA (Rho-PMPC₂₅-PDPA₇₀) were synthesized by Dr Jeppe Madsen and Dr Nick Warren in Professor Steven Armes research group or by Dr Jens Gaitzsch in the Battaglia research group, using Reversible Addition Fragmentation chain Transfer polymerization (RAFT) or Atom-transfer radical-polymerization (ATRP) (Pearson et al., 2013, Lomas et al., 2008, Madsen et al., 2011). The copolymer chain length used in this thesis was 25 MPC monomers with 62-70 DPA monomers depending on the polymer batch (PMPC₂₅-PDPA₆₂₋₇₀). The same batch of Rho-PMPC-PDPA with 25 MPC monomers and 70 DPA monomers was used throughout. A representative example of PMPC-PDPA and Rho-PMPC-PDPA are shown in table 3.1.

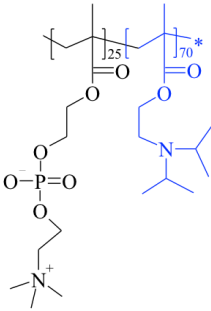
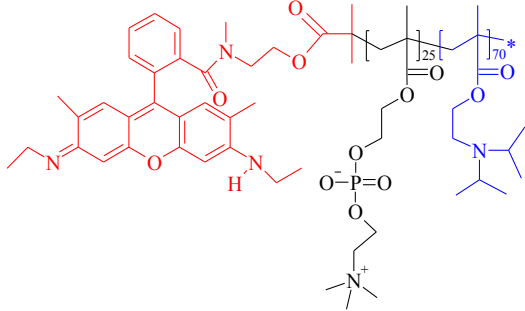
Polymer	PMPC-PDPA	Rho-PMPC-PDPA
Chemical structure		
Composition	PMPC ₂₅ -PDPA ₇₀	Rho-PMPC ₂₅ -PDPA ₇₀
Chain length		
Molecular weight (g/mol)	~22,300	~22,500

Table 3.1. Chemical structure and molecular weight of PMPC-PDPA and Rho-PMPC-PDPA used in this thesis.

3.3 Polymersome Formation

Polymersome formation was initiated by either pH switch or film-rehydration. In both methods the polymer was first weighed into a glass vial and dissolved in a 2:1 solution of chloroform: methanol at a final polymer concentration of 10mg/ml. This solution was then filtered using an autoclaved 0.2 μ m nylon filter (GE Healthcare) and the solvent was evaporated overnight in a desiccator with an autoclaved 0.2 μ m membrane filter (Millipore) placed on top of the vial. This left a thin film of polymer lining the vial.

3.3.1 Film Rehydration

For film rehydration sterile dPBS was added to the film (final concentration 10mg/ml) and the solution was left on a stirring plate with a magnetic stirrer for the specified amount of time and the solution was removed and sonicated for 20 minutes at room temperature (Sonicor Instrument Corporation). When hydrophobic molecules were encapsulated using this method, the molecules were dissolved in the organic solvent with the polymer.

3.3.2 pH Switch

For pH switch, the polymer film was dissolved in HCL acidified pH-2 dPBS. The solution was sonicated for 5 minutes and then filter sterilised using 0.2 μ m filters (Minisart, Sartorius). The pH was slowly raised by a controlled addition of 0.5M NaOH with a syringe pump (LAMBDA Laboratory Instruments), while on a stirring plate to keep the solution mixing throughout the formation process. Once the pH reached 6, materials for encapsulation were added to the solution

and then the pH was raised to 7.4 to initiate polymersome self-assembly. The polymersome solution was sonicated for 20 minutes and stored at 4°C.

3.4 Polymersome purification techniques

3.4.1 Removal of Non-Encapsulated Molecules

Following formation non-encapsulated molecules were removed using gel permeation chromatography. A size exclusion chromatography column was sterilised using 0.5M NaOH and Sepharose 4B was added to the column. The column was washed through thoroughly with dPBS and then up to 1ml of polymersome solution was added to the top of the column. The polymersome fraction was collected in a 96 well plate and the size distribution was characterised by dynamic light scattering (DLS).

3.4.2 Polymersome Size Purification Methods

3.4.2.1 Cross Flow Filtration

Cross flow filtration was achieved using the KrosFlo Research Ili Tangential Flow Filtration System at a speed of 5ml/min with a 50nm hollow fiber module (Spectrum Laboratories). Polymersomes made by pH switch were dissolved to 50ml before filtering through the machine, once the volume was lowered to 2ml, 48ml of dPBS was then added to the solution and the process was repeated.

3.4.2.2 Recycling Size Exclusion Chromatography

Purification by recycling size exclusion chromatography was performed using the drug purification technique described above, but the solution was first

concentrated with a 500kDa hollow fiber module (Spectrum Laboratories) to approximately 200 μ l before being placed on the column. The solution was collected in a 96 well plate and then added to a second column drop by drop and collected in another 96 well plate.

3.4.2.3 Differential Centrifugation

For purification by differential centrifugation small micelles and polymersomes were first removed using the cross flow filtration system with a 50nm hollow fiber module as described above. The retained solution was separated by repeated 20 minute centrifugations at increasing speeds using a 5424 micro-centrifuge (Eppendorf). The speeds used were 2000, 5000, 10000, 15000 and 20000 relative centrifugal force (RCF). After each spin the pellet was separated, resuspended in PBS and the supernatant was re-centrifuged at the higher speed. Polymersomes purified by all methods were characterised by DLS and TEM and the concentration was measured using UV-visible spectroscopy or fluorescence spectroscopy for Rho-PMPC-PDPA.

3.4.3 Tubular Polymersome Purification

Polymersomes were formed using the film rehydration method as described above and tubular polymersomes were separated by differential centrifugation. Firstly the sample was centrifuged at 2000RCF and the pellet was re-suspended in PBS; this fraction contained the large early lyotropic structures. The supernatant was re-centrifuged at 15000RCF and the pellet was resuspended; the pellet contained the tubular polymersome fraction and the supernatant

contained the predominantly spherical fraction. To measure the formation of tubular polymersomes and spherical polymersomes over time a 200 μ l aliquot of the stirring sample was taken after 1, 2, 3, 4 and 8 weeks of stirring and the sample was separated into the 3 fractions and the mass of polymer in each fraction was determined by HPLC with detection by UV absorbance.

Fluorescent BSA was encapsulated using electroporation with pre-formed empty tubular polymersomes as previously described (Wang et al., 2012). 2mm gap width electroporation cuvettes (Eppendorf) were filled with 400 μ l of polymersome solution and the BSA was encapsulated with 3 pulses at 2500 volts with the 2510 Electroporator (Eppendorf). BSA not encapsulated was removed by gel permeation chromatography as described above.

3.5 Polymersome size and shape characterisation

3.5.1 Dynamic Light Scattering

Size distribution measurements were performed on a Zetasizer Nano ZS (Malvern Ltd.) at a polymer concentration of 0.25mg/mL in a 1ml polystyrene cuvette (Fisherbrand). Polymersome size histograms were automatically calculated using a 4mW He-Ne laser at 633nm and a scattering angle of 173°. The sample was measured with 12-14 sub-cycles with a 10 second duration in each run, the average of 3 runs was plotted in a size histogram as the %number.

3.5.2 Transmission Electron Microscopy

For TEM analysis copper grids were glow discharged by exposing them to

plasma for 25-40 seconds in a vacuum chamber. The sample was adsorbed onto the glow-discharged grids by treating the grids with 5 μ l of sample at a polymer concentration of 0.5-1mg/ml for 1 minute (Agar Scientific). The sample was then stained with a 0.75wt % phosphotungstic acid (PTA) (pH 7.4) solution for 5 seconds and dried using filter paper and a drying pump. The sample was imaged with a FEI Tecnai G2 Spirit electron microscope and image analysis was performed using imageJ software.

3.6 Quantification of Polymer and Encapsulated Cargo

Following polymersome formation the concentration of polymer and its encapsulated cargo was quantified using UV-Vis spectroscopy, fluorescence spectroscopy or Reverse-Phase High Performance Liquid Chromatography (RP-HPLC) with associated UV-Vis spectroscopy. Before quantification polymersomes were disassembled into polymer chains with 1M HCL to lower the pH to between 5-6.

3.6.1 UV-Vis spectroscopy and Fluorescence Spectroscopy

Calibration Curves

UV-Visible spectroscopy was performed using a Jasco UV-Vis V-630 Spectrophotometer or a Beckman Du 520 UV-Vis spectrophotometer. To calculate the polymer concentration of empty polymersomes a calibration curve was made at 220nm after the sample was scanned between 200nm and 600nm with known concentrations of a low pH PMPC-PDPA solution. Rifampicin concentration was also determined by UV-Vis spectroscopy at 475nm. The

concentration of encapsulated cascade blue and Alexa-647 labelled BSA were measured using a Varian CaryEclipse fluorescence spectrophotometer. For cascade blue the fluorescent dye was excited at 400nm and the emission was detected at 420nm and Alexa-647 labelled BSA was excited at 650nm and detected at 668nm. Rho-PMPC-PDPA was also measured by fluorescence spectroscopy using an excitation of 540nm and an emission of 560nm. The calibration curves for these materials are shown below.

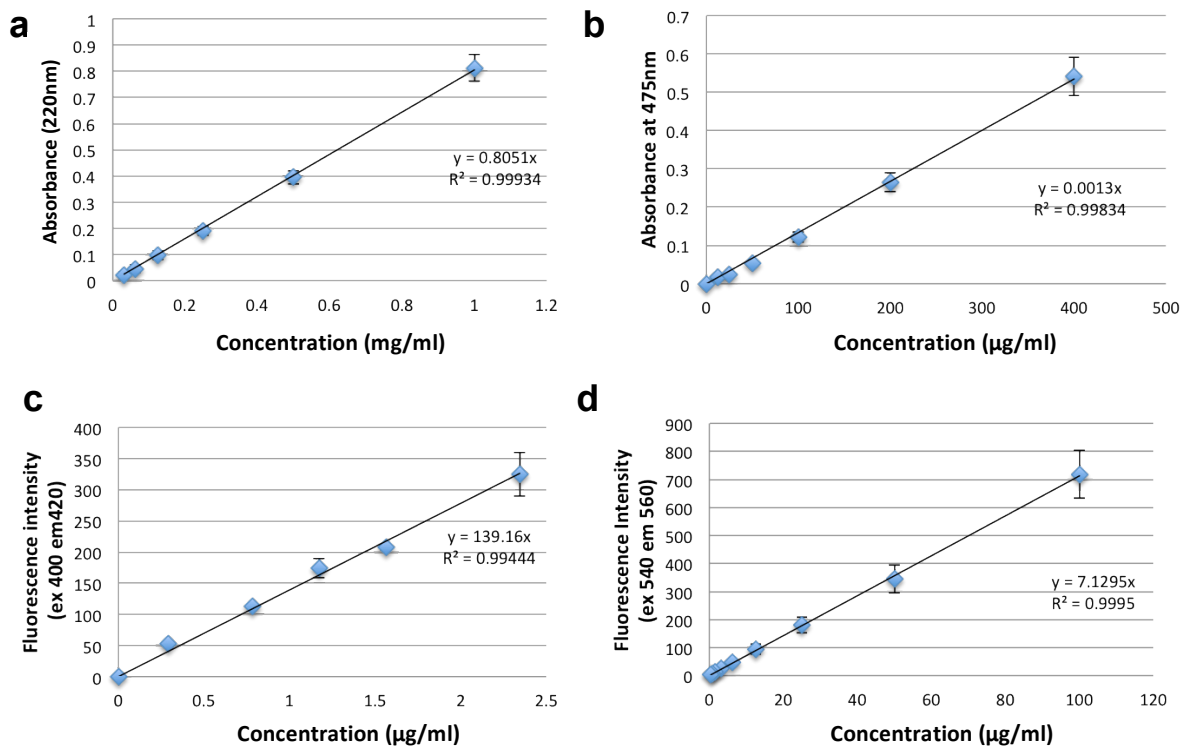


Figure 3.1. UV-Vis spectroscopy and fluorescence spectroscopy calibration curves.

Calibration curves for PMPC-PDPA (a) or Rifampicin (b) using UV-Vis spectroscopy and cascade blue (c) or Rho-PMPC-PDPA (d) using fluorescence spectroscopy.

3.6.2 RP-HPLC Chromatograms and Calibration Curves

Reverse-Phase High Performance Liquid Chromatography RP-HPLC was performed on a Dionex Ultimate 3000 system with an associated UV-Vis spectrophotometer or a Shimadzu UFLC XR system with a SPD-M20A diode array detector. In both cases the sample was passed through a C18 analytical column (Phenomenex Jupiter; 300 Å, 150x4.6mm, 5 µm). Samples were run in a multistep gradient of eluent a: methanol + 0.1% TFA and eluent b: H₂O + 0.1% TFA.

The conditions of the multistep gradient was dependent on the sample type, the concentration of polymer in chapter 5 was quantified using the following gradient, which shows the percentage of eluent B overtime: 0 min 5%, 7 min 5%, 9 min 100%, 13 min 100%, 15 min 5%, 20 min 5%. In chapter 6 the polymer and (R)-roscovitine concentrations were calculated using the following gradient: 0 min 5%, 6.5 min 5%, 12 min 100%, 14 min 100%, 15 min 5%, 20 min 5%. In chapter 7 lysostaphin was calculated using: the following gradient: 0 min 5%, 3 min 5%, 4 min 40%, 9 min 70%, 10 min 100%, 13 min 100%, 14 min 5% 17 min 5%. Vancomycin was calculated with the following gradient: 0 min 5%, 3 min 5%, 20 min 100%, 22 min 100%, 23 min 5%, 30 min 5%. Representative HPLC chromatograms are displayed in Figure 3.2 and 3.3.

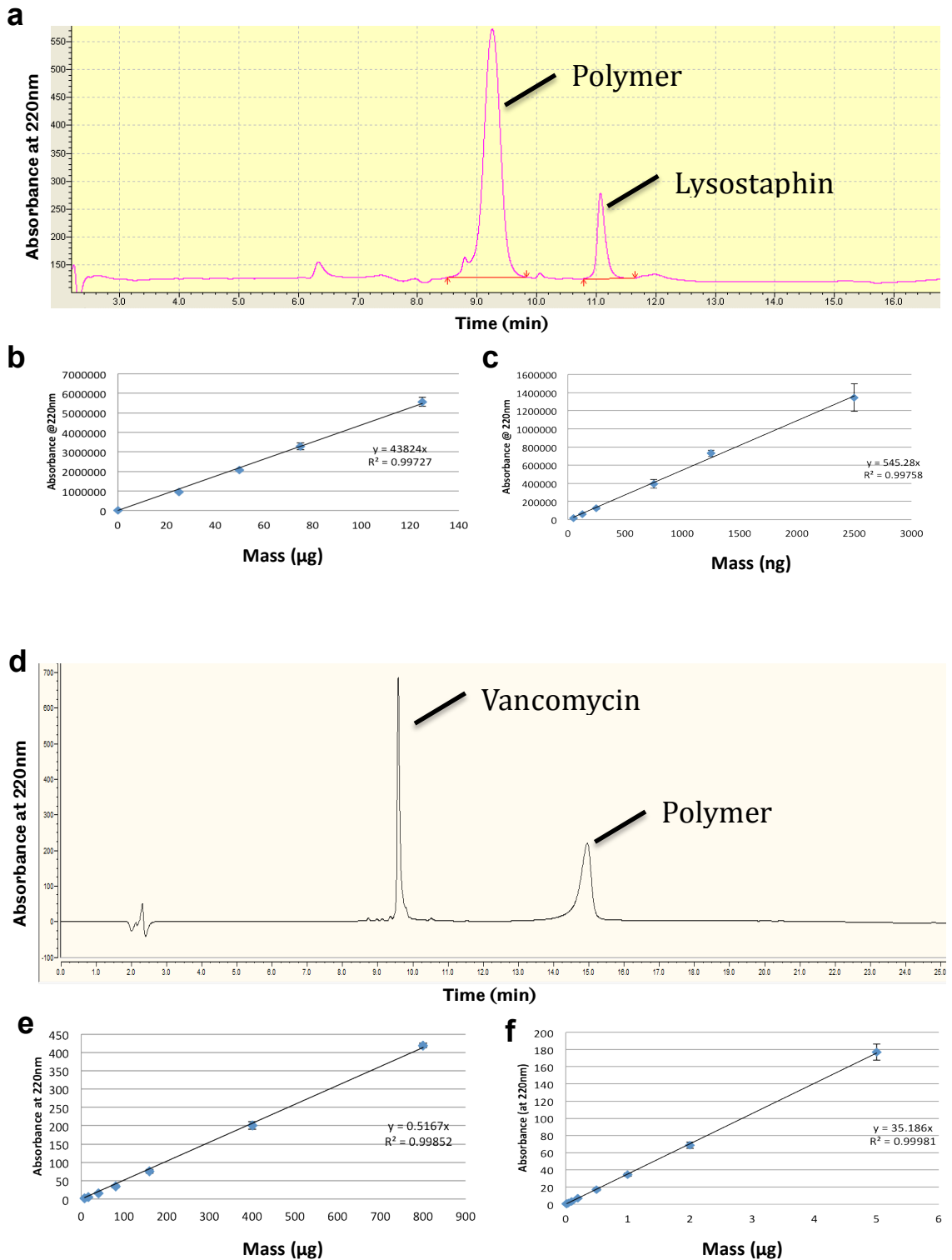


Figure 3.2 HPLC chromatograms and calibration curves for encapsulated antibiotics.

Lysostaphin HPLC chromatogram (a) with calibration curves for the polymer (b) and the encapsulated lysostaphin (c). Vancomycin HPLC chromatogram (d) with calibration curves for the polymer (e) and the encapsulated vancomycin (f).

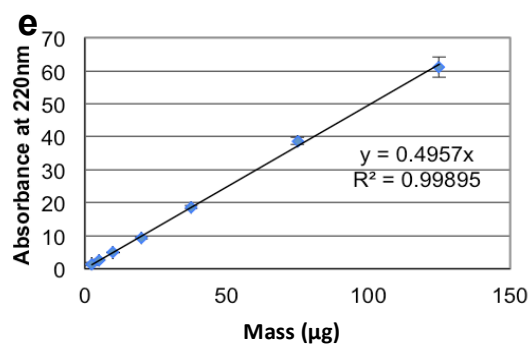
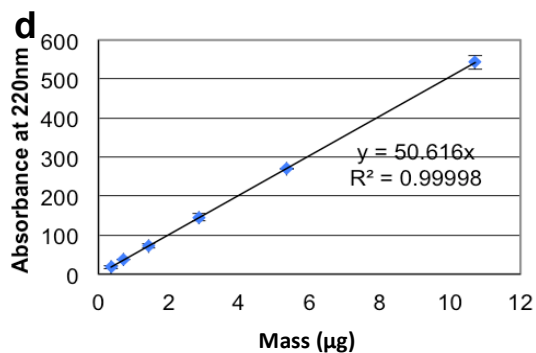
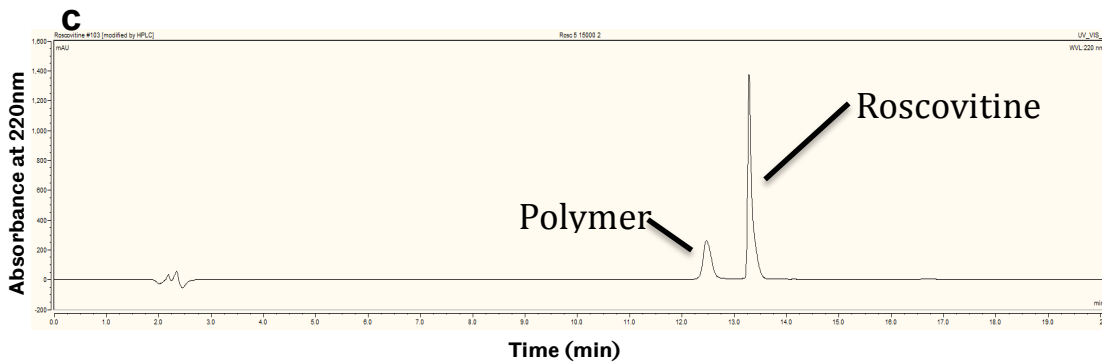
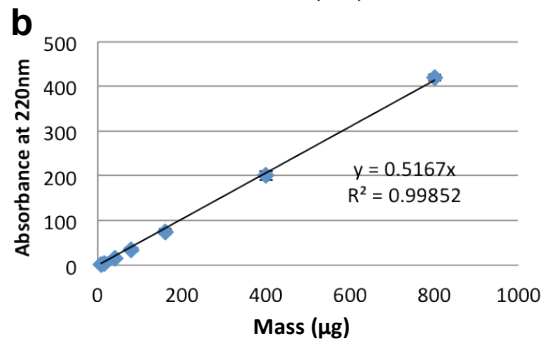
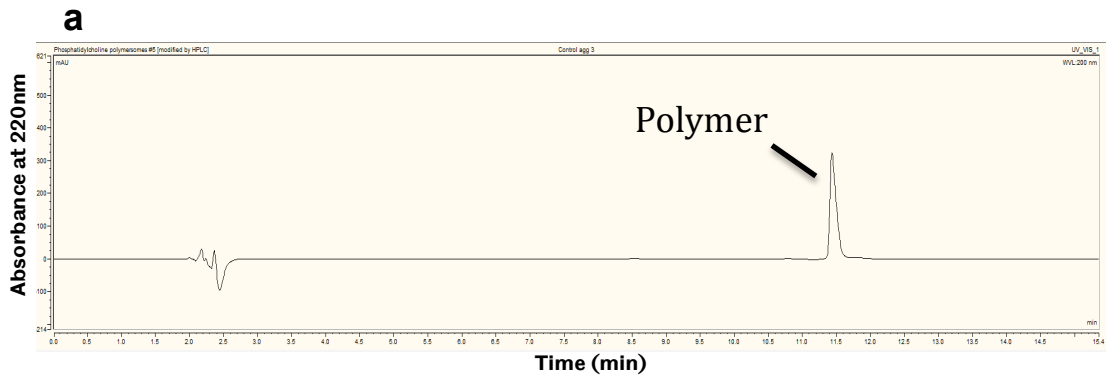


Figure 3.3. HPLC chromatograms and calibration curves for PC and (R)-roscovitine.

HPLC chromatogram for the polymer (a) and a calibration curve for the polymer (b). (R)-roscovitine HPLC chromatogram (c) with calibration curves for the polymer (d) and the encapsulated (R)-roscovitine (e).

3.6.3 siRNA and Gentamicin Quantification

Encapsulated siRNA was quantified using the Quant-iT PicoGreen assay (Invitrogen) according to the manufacturers instructions. Calibration curves were made from the original polymersome sample before un-encapsulated siRNA was removed using gel permeation chromatography. Gentamicin has a low UV-Visible absorbance and so encapsulated gentamicin was measured based on a previously described protocol for measuring gentamicin encapsulation within liposomes (Gubernator et al., 2006). The pH of gentamicin-loaded polymersomes was lowered to 6 with HCL to disassemble the polymersomes. Encapsulated gentamicin was removed from free polymer chains by filtration with a 10kDa 50nm hollow fiber module (Spectrum Laboratories) and the pH was returned to 7.4 using NaOH. 40 μ l of separated gentamicin was mixed with 58 μ l of methanol and 2 μ l of OPA. The sample was left in the dark for 10 minutes and the fluorescence intensity was measured using the fluorescence spectrophotometer (excitation 340, emission 455). A calibration curve with known concentrations of gentamicin was performed in parallel during each measurement.

3.7 *In vitro* Biological Analysis

3.7.1 Neutrophil Purification

Peripheral blood was extracted from healthy donors with a venous catheter by a trained phlebotomist (predominantly Vanessa Singleton) as approved by the South Sheffield Research Ethics Committee (STH13927). The 36ml of blood was placed into a 50ml tube containing 4ml of the anti-coagulant sodium citrate

(Martindale Pharmaceuticals). The blood was centrifuged for 20 min at 350RCF. The upper platelet-rich plasma (PRP) layer was removed. The PRP was centrifuged for 20 minutes at 800RCF to remove the platelets. The supernatant contains the platelet poor plasma (PPP), this was placed into a new 50ml tube and the pelleted platelets discarded.

The lower layer from the first centrifugation step containing the blood cells was mixed with 6ml of 6% dextran solution (Sigma-Aldrich) and the solution volume was raised to 50ml with 0.9% saline solution. The tube was left for 30 minutes to allow the red blood cells to settle and the resulting upper white blood cell layer was extracted and centrifuged at 320RCF for 6 minutes. The white blood cells were then separated using a density gradient with a solution of 90% Percoll (Sigma-Aldrich) and 10% 0.9% saline. The density layers include an upper layer of 0.84ml Percoll solution and 1.64ml PPP and a lower layer of 0.98ml Percoll solution (51%) and 1.02ml PPP.

After the white blood cells had pelleted in the previous centrifugation they were resuspended in 2ml of PPP. The upper phase was carefully pipetted onto the lower phase and the cell suspension was placed on top of the upper phase. The gradient was centrifuged for 11 minutes at 350RCF. The final gradient contained 3 layers, the lowest layer contained the red blood cells, the middle layer contained the neutrophils and the upper layer contained the peripheral blood mononuclear cells (PBMCs). The PBMCs were pipetted into a new 50ml tube containing 2ml of PPP, followed by the neutrophils in a separate 50ml tube. The

number of neutrophils was counted using a haemocytometer, centrifuged at 320RCF for 6 minutes and resuspended in RPMI 160 media (Sigma Aldrich) (containing 1% penicillin/streptomycin antibiotics (Life Technologies) and 10% Foetal Calf Serum) for a final neutrophil concentration of 5 million/ml.

3.7.2 Ultrapure Neutrophil Purification using Magnetic Selection

For experiments requiring very high neutrophil purities, the entire neutrophil pellet was instead resuspended to 100million/ml of neutrophil column buffer (1xHanks Buffered Saline Solution (HBSS) with 2% FCS). The neutrophils were incubated for 15 minutes with a cocktail of custom antibodies (Stem Cell Technologies) against contaminating blood cells (65µl/ml) (Sabroe et al., 2002). Magnetic colloid beads were then added to the solution (50µl/ml) (Stem Cell Technologies) and incubated for a further 15 minutes. Finally the cells were resuspended in an additional 10ml of column buffer and put through a magnetic MACS column (Miltenyi Biotec), this removed any contaminating cells. The column was washed through with additional column buffer and the cells were counted, pelleted and resuspended in the complete RPMI media at 5 million cells per ml.

3.7.3 Flow Cytometry

Flow cytometry was employed to determine the amount of polymer or polymersome cargo internalised by neutrophils and to determine the percentage of neutrophils that were apoptotic and necrotic through annexin V and propidium iodide (PI) staining. Polymersomes of known concentration were

added to human neutrophils and incubated at 37°C for the desired time period. The neutrophils were centrifuged at 300RCF for 3 minutes with a table-top centrifuge (Eppendorf Minispin) and the pellet was then washed with ice cold PBS and this washing step was repeated.

3.7.3.1 Polymersome Size Internalisation

Neutrophils were kept on ice before the fluorescence intensity was measured using an LSR II Flow Cytometer (BD Biosciences) with a 450nm violet laser (cascade blue) or a 575nm blue laser (Rho-PMPC-PDPA). Neutrophils incubated with polymersomes encapsulating rhodamine B octadecyl ester perchlorate (*CellLuminate*) or polymersomes loaded with the *AllStars Negative siRNA* Alexa Fluor647 were analysed using a FACSArray flow cytometer (BD Biosciences) with a 532nm laser and a 633nm laser respectively. The relative median fluorescence intensity (rMFI) was obtained by dividing the MFI of the treated neutrophils by the MFI of the untreated neutrophils and subtracting 1 so that a MFI value equal to the control has a rMFI of 0.

3.7.3.2 Annexin V Propidium Iodide Staining

Neutrophils analysed by annexin V PI staining were resuspended in annexin V Binding Buffer (Biolegend) and 1µl of Alexa Fluor 647 annexin V (Biolegend) was added to the cells, immediately followed by 5µl of PI solution (Biolegend). Cells were gently mixed by pipetting and incubated at room temperature for 15 minutes in the dark before analysis by flow cytometry using the FACSArray flow cytometer with the 532nm and 633nm lasers for PI and Alexa Fluor 647 annexin

V respectively. Cells stained with annexin V are apoptotic and cells stained with PI are cells with a permeable membrane. Neutrophils were gated based on their fluorescence intensity to determine the percentage of annexin V positive cells. Examples of dot plots generated by the flow cytometer are shown in Figure 3.4.

3.7.4 Cytospin Analysis of Neutrophil Apoptosis Rates

To determine the viability of neutrophil samples the cells were centrifuged at 300RCF for 3 minutes with a table-top centrifuge (Eppendorf Minispin), the supernatant was removed and the cells were resuspended in dPBS. The neutrophils were then centrifuged onto a glass slide using a cytocentrifuge (Shandon Cytospin 3, Thermo Scientific) for 3 minutes at 300rpm. The cells on the slide were fixed using a drop of methanol and then placed in a cytoplasmic staining solution for 1 minute (Eastain Quick-Diff Red, Gentaur) followed by a nuclear staining solution for 1 minute (Reastain Quick-Diff Blue, Gentaur). The slide was then mounted with a glass cover slip (Menzel-Glaser) with DPX mounting medium (Fisher Scientific). The slide was left to dry overnight and the percentage of viable neutrophils was determined by morphological analysis of 300 neutrophils per slide with a Zeiss Axioplan microscope at 100x magnification. Apoptotic cells are characterised by round and condensed nuclei (Figure 3.5).

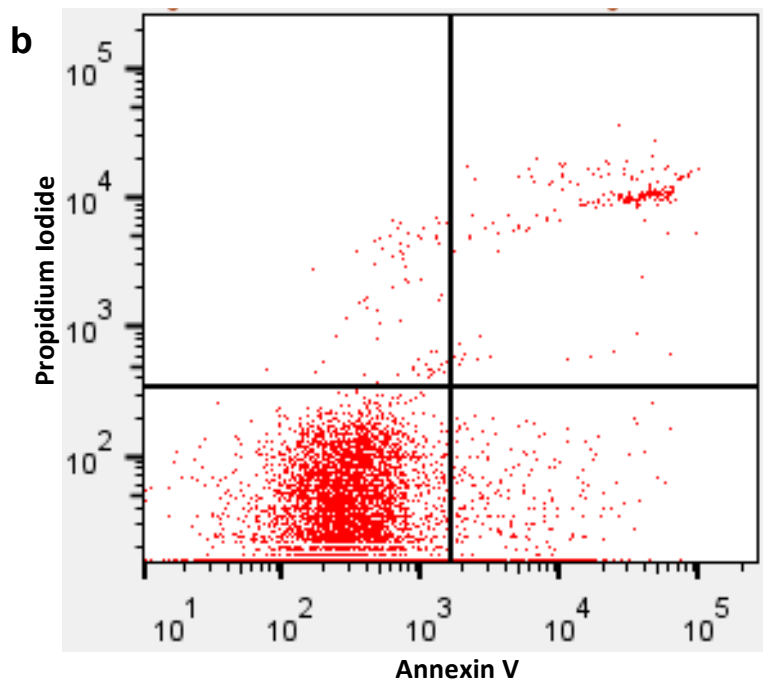
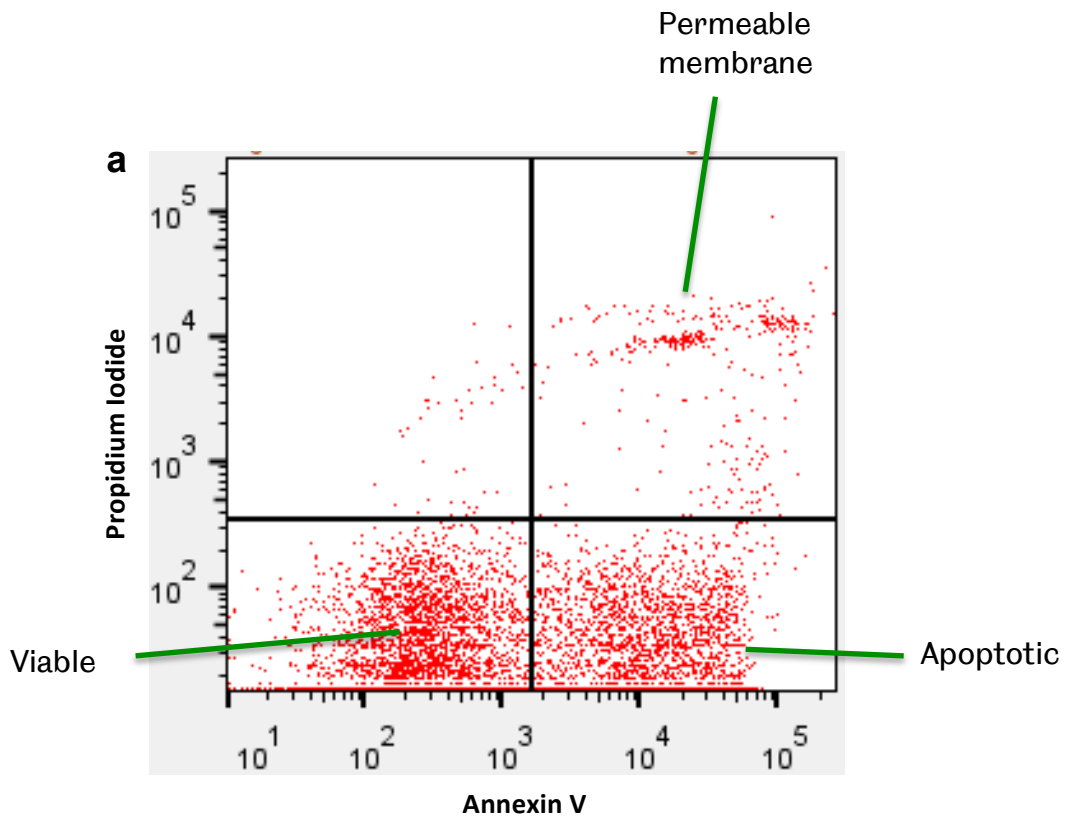


Figure 3.4 Annexin V PI staining.

Dot plots of human neutrophils after staining with annexin V and PI. (a) Neutrophils treated with empty polymersomes for 8 hours. (b) Neutrophils treated with empty polymersomes and GM-CSF for 8 hours.

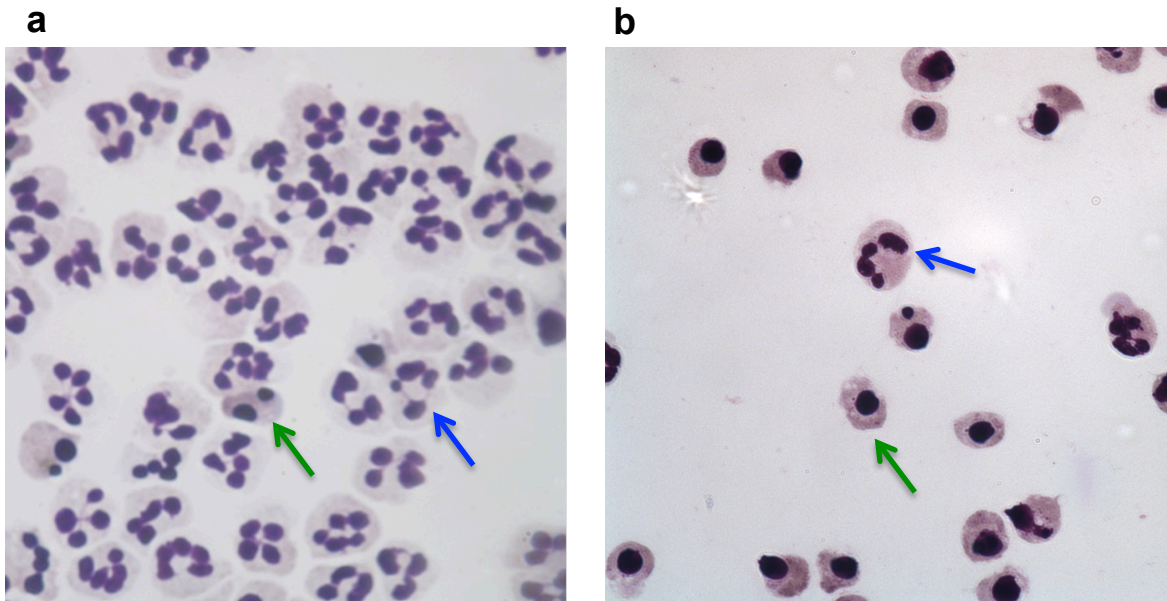


Figure 3.5 Human neutrophil cytopins

Cytopins of human neutrophils, neutrophils were marked as apoptotic (green arrow) or viable (blue arrow) based on their nuclear morphology. The figure shows two cytopins, a sample with low levels of apoptosis (a) and high levels of apoptosis (b).

3.7.5 Enzyme-Linked Immunosorbent Assay (ELISA)

Neutrophil IL-8 release was measured using an ELISA. Following incubation with polymersomes, neutrophils were centrifuged at 300RCF for 3 minutes using the table-top centrifuge. Pellets were discarded and the supernatants were frozen at -80°C until required for analysis by ELISA. The IL-8 ELISA kit was purchased from R and D systems, which includes all of the antibodies, IL-8 standards, Streptavidin-HRP solution and the substrate reagents. The wash buffer and coating buffer were made by members of Professor Ian Sabroe's research group using the composition shown in Table 3.2. The blocking buffer was composed of 0.1g of ovalbumin (Sigma Aldrich) in 10.5ml of coating buffer.

100µl of the coating antibody was added to each well of a 96 well plate (Costar 3590 polystyrene plate), except 2 wells that were left blank as a control. The plate was sealed with cling film and incubated overnight at room temperature. The following morning each well was washed four times with the wash buffer and the buffer was then removed. 100µl of blocking buffer was added to each well and incubated at room temperature for 1 hour. The IL-8 standard was prepared by serial dilutions in wash buffer for concentrations between 20-5000pg/ml. The plate was re-washed and 100µl of the sample or the IL-8 standards (for a calibration curve) was added to each well. The plates were covered and incubated for 2 hours at room temperature and then the plates were washed again, 100µl of the biotinylated antibody was added to each well and it was left to incubate for a further 2 hours. 100µl of the Streptavidin-HRP solution was added to each well and the plate was covered with aluminium foil

and incubated for 20 minutes at room temperature. The plate was washed and 100µl of the substrate solution was added to each well and left to incubate for 15-20 minutes before the reaction was stopped by adding 50µl of 1M Sulphuric acid (Sigma Aldrich). The optical density was determined immediately using a micro-plate spectrophotometer reader at 450nm.

a	Final Concentration	b	Final Concentration
NaCl	0.5M	NaCl	0.14M
NaH ₂ PO ₄	7.5mM	KCl	2.7mM
Na ₂ HPO ₄	2.5mM	Na ₂ HPO ₄	8.1 mM
Tween-20	0.1%	KH ₂ PO ₄	1.5mM
H ₂ O	Up to 10 litres	H ₂ O	Up to 1 litre

Table 3.2. List of reagents in the wash buffer (a) and coating buffer (b).

3.7.6 Fluorescence Microscopy

3.7.6.1 Protein Labelling

BSA and the α -tubulin antibody [YOL1/34] were labelled using the Alexa Fluor 647 antibody labelling kit (Molecular Probes) according to the manufacturer's instructions.

3.7.6.2 Rho-PMPC-PDPA Film Microscopy

A film of 10% Rho-PMPC-PDPA 90% PMPC-PDPA was prepared as described

above on a glass coverslip and the coverslip was placed at a 90-degree angle to an imaging dish (ibidi μ -dish). The sample was then imaged with a 561nm laser at 40x magnification with an oil immersion lens on a Zeiss LSM510 inverted laser scanning confocal microscope. At time 0 hours, PBS and a stirrer were added to the imaging dish and the sample was left stirring on a stirring plate for the indicated periods of time before imaging.

3.7.6.3 Confocal Microscopy of Rhodamine-Labelled Spherical and Tubular Polymersome Internalisation

Spherical and tubular polymersomes were made by pH switch and film rehydration respectively from 30% Rho-PMPC-PDPA and 70% PMPC-PDPA. Samples were incubated with human neutrophils for the indicated time period before the cells were centrifuged at 300RCF for 3 minutes with a table-top centrifuge and washed. This washing step was repeated and the neutrophils were placed in the imaging dish (ibidi μ -dish). Neutrophils were then visualised using a Perkin-Elmer UltraVIEW VoX spinning disk confocal microscope with a 514nm laser and a 60x oil immersion lens. Image processing and analysis was performed with Volocity software (PerkinElmer).

3.7.6.4 Confocal Microscopy of CellLuminate, Delivered Antibodies and siRNA

Fluorescent siRNA and antibodies were encapsulated using the pH switch method. Neutrophils treated with polymersomes encapsulating the α -tubulin, cellLuminate or the AllStars Negative siRNA Alexa Fluor647 antibody were prepared by the method described above and imaged on the Perkin-Elmer

UltraVIEW VoX spinning disk confocal microscope with a 514nm laser and a 60x oil immersion lens. Neutrophils treated with α -tubulin polymersomes and CellLuminate were fixed with 1x Cellfix (Becton Dickinson) after washing. All other microscopy experiments were performed on live neutrophils. To visualise neutrophils treated with polymersomes encapsulating the Brilliant Violet γ -tubulin antibody, neutrophils were incubated with the antibody at 37°C for 6 hours before the cells were washed and moved to a fibrinogen coated coverslip. The coverslip was glued to a plastic petri dish with a puncture in the centre. The cells were then imaged using a Zeiss LSM510 inverted laser scanning confocal microscope with a 405nm laser. Image processing and analysis was performed with ImageJ software.

3.7.7 siRNA Knockdown Experiments

Mcl-1 siRNA or negative control siRNA were encapsulated by pH switch as described above. Ultrapure human neutrophils were treated with GM-CSF and then incubated with the polymersomes loaded with Mcl-1 siRNA or their controls for 20 hours. Apoptosis was then measured by nuclear and cytoplasmic staining and observation of nuclear morphology as described previously, or RNA was extracted from the cells and the amount of Mcl-1 siRNA was measured by RT-PCR.

3.7.7.1 RNA extraction

RNA extraction and PCR was performed with help and training from Pranvera Sadiku. Neutrophils were pelleted by centrifugation at 300RCF for 3 minutes

and washed in PBS. The neutrophils were then re-pelleted and lysed by adding 100µl of TRI reagent (Sigma Aldrich) and incubating them for 5 minutes at room temperature. 200µl of chloroform was added, the mixture was shaken for 15 seconds and then left for 5 minutes. The mixture was centrifuged at 12000RCF; this separates it into three phases, the upper phase containing the RNA. The RNA was removed and 0.5ml per ml of isopropanol was added to the RNA. This was centrifuged at 12000RCF for 10 minutes, which forms a pellet of the RNA. The isopropanol was removed, the pellet was washed with 1ml of 75% ethanol, which was then removed and the pellet was left to dry. Finally the pellet was re-suspended in 30µl and the concentration of RNA was measured using a Nanodrop 2000 spectrophotometer (Thermo Scientific).

3.7.7.2 Reverse Transcription PCR

The RT-PCR kit components including the reverse transcriptase master mix for cDNA synthesis and the PCR master mix were purchased from Promega. 1µl of oligo dT primer was added to 1µg of extracted RNA (in 29µl) and allowed to anneal by heating to 70°C for 5 minutes. The 30µl RNA sample was then added to 20µl of the RT master mix (10µl 5x Buffer, 1.25µl 100nM dNTPs, 1.25µl RNAsin, 2 µl MMLV Reverse transcriptase and 5.5µl dH₂O). The reaction was incubated at 40°C for 1 hour to allow cDNA synthesis and then 94°C for 2 minutes to inactivate the RT enzyme. This produced the cDNA for PCR.

2µl of the cDNA sample (1µg) was added to 23µl of the PCR master mix (5µl buffer, 1.5µl MgCl₂, 1µl 10mM dNTPs, 0.7µl 10µM forward primer, 0.7µl 10µM

reverse primer, 0.25µl Taq polymerase and 13.85µl RNase free dH₂O). The sequence of the forward and reverse Mcl-1 primers is shown below in Table 3.3. As negative controls the master mix was also added to water and a reverse transcriptase product without MMLV, which highlights contaminating genomic DNA in the sample. The PCR was placed into a PCR c1000 Thermal Cycler (Bio-Rad). The sample was denatured at 94°C for 2 minutes before 30 cycles of denaturation at 94°C for 30 seconds, annealing of Mcl-1 primers for 1 minute at 60°C and strand elongation for 30 seconds at 72°C. A final extension stage was at 72°C for 2 minutes.

The agarose gel was prepared by mixing 60ml of 1xTAE buffer (see table 3.4) with 0.72g of agarose (Bioline) and heated using a microwave until the agarose melts. After the mixture has cooled 1 drop of ethidium bromide was added and the gel was poured and left to set. 7µl of hyperladder1 (Bioline) or 10µl of sample was added to each well and the gel was run at 80V for 40 minutes. The gel was then visualised under ultraviolet light using the Bio-Rad Gel Doc™ system.

Mcl-1 Forward Primer	5' ACG GCG TAA CAA ACT GGG GC 3'
Mcl-1 Reverse Primer	5' TGA TGC CAC CTT CTA GGT CCT C 3'

Table 3.3 Mcl-1 primers for PCR.

	Final Concentration
Tris Base	0.5M
Glacial Acetic Acid	7.5mM
0.5 M EDTA	2.5mM
H ₂ O	Up to 1 litre

Table 3.4 50x TAE buffer constituents

3.7.8 *Staphylococcus aureus* Experiments

Staphylococcus aureus (*S. aureus*) strains used in this thesis include the Newman strain for *in vitro* THP-1 infection experiments and the SH1000 strain for zebrafish infection experiments. SH1000 strains were inoculated from -80°C freezer laboratory stocks on Brain Heart Infusion (BHI) (Sigma Aldrich) agar plates. For short term storage plates were kept in the 4°C cold room. *S. aureus* were initially cultured by inoculating 10ml of sterile BHI media in a 25ml tube with a single colony and the bacteria were incubated overnight in a 37°C room on a shaker at 250rpm. The following morning 0.5ml of the liquid culture was added to 50ml of fresh BHI media in a sterile 250ml conical flask and this was grown in a 37°C room on a shaker at 250rpm for approximately 1 hour and 50 minutes. To measure the concentration of *S. aureus* 100µl was placed in a plastic cuvette and diluted with an additional 900µl of BHI. The optical density was measured at 600nm using a Jenway 6100 spectrophotometer. The concentration of *S. aureus* was then calculated based on an OD of 1 being equal

to 2×10^8 CFU/ml of *S. aureus*. 20ml of the culture was moved into a 25ml tube and centrifuged at maximum speed for 10 minutes; the bacterial pellet was resuspended in PBS to 1.2×10^9 CFU.

3.7.8.1 THP-1 Monocyte Derived Macrophages infection Experiment

THP-1 cells were provided, cultured and differentiated by Professor David Dockrell's lab, experimental training and technical support was provided by Jamil Jubrail. The cells were initially obtained from ATCC. They were cultured at 2×10^5 cells/ml in a 24 well plate (Costar) with RPMI 1640 medium with 10% FCS. The cells were differentiated to macrophages using 200nM phorbol 12-myristate 13-acetate (PMA) (Sigma-Aldrich). One well of cells had its media removed and was fixed with the addition of 500 μ l 2% paraformaldehyde (Sigma Aldrich) and incubated in the fridge for 10-15 minutes and then washed 3 times with PBS.

Mid-log *S. aureus* (Newman strain), also provided by David Dockrell's research group, were centrifuged at 10000rpm for 1 minute and resuspended in 1ml PBS. 1 million CFU was added to each well (multiplicity of infection (MOI) of 5). The cells were then placed on ice for 1 hour followed by a further 5 hours in a 37°C incubator (total 6 hours incubation). After incubation gentamicin was added to the media (150 μ g/ml) and the cells were left for 30 minutes in an incubator to kill the extracellular bacteria. The samples were removed from the incubator, washed twice with PBS and then replaced with RPMI media containing 15 μ g/ml of gentamicin. At each specified time point the media was removed, the cells were washed twice with PBS and then 250 μ l of 1% Saponin (Sigma Aldrich) was

added to lyse the cells. The macrophages were left in the Saponin for 12 minutes in a 37°C incubator and then an additional 750µl of PBS was added to the cells and the wells were mixed thoroughly with a pipette. 10µl of the lysed cells were taken and diluted in a 96 well plate with 6 1/10 serial dilutions. Three 10µl drops from each dilution were placed onto a labelled blood agar plate, incubated overnight at 37°C and the number of viable colonies was counted.

3.8 Zebrafish Embryo Experiments

3.8.1 Zebrafish Husbandry

Adult zebrafish were maintained at 28°C with a controlled 14:10 hour light:dark daily cycle at the University of Sheffield Zebrafish Facility in the Bateson Centre. All experiments performed in this thesis were on zebrafish embryos younger than 5.2dpf and embryos were sacrificed at the end of the experiment by immersion in bleach. Embryo maintenance and collection was achieved using standard protocols (Nusslein-Volhard and Dahm, 2002). Zebrafish embryos were cultured in E3 medium, made from the stock solution (Table 3.3) with added 1% methylene blue.

	Final Concentration
NaCl	5mM
KCL	0.27mM
CaCl ₂	0.33mM
MgSO ₄	0.33mM
dH ₂ O	Up to 1 litre

Table 3.5. The reagents for making a 60x E3 stock solution.

3.8.2 Zebrafish Inflammation Resolution Assay

The transgenic *Tg(mpx:GFP)i114* line, specifically labels neutrophils with green-fluorescent protein (GFP), which allows neutrophils to be tracked *in vivo* using a fluorescence microscope (Renshaw et al., 2006). 3-day post fertilization (dpf) transgenic *Tg(mpx:GFP)i114* zebrafish embryos were immersed in 0.02% 3-amino benzoic acid ethyl ester (tricaine) and then placed onto masking tape on a Petri dish lid. The embryos were injured by complete tail fin transection at the caudal fin with a micro-scalpel (*World Precision Instruments*). Embryos were then transferred to a petri dish containing fresh E3 media. 4 hours following injury zebrafish were visualized under a fluorescent dissecting microscope (Leica MZ10F) and embryos with 20-25 neutrophils at the injury site (posterior to the circulatory loop) were selected, transferred to a 96-well plate and treated with either roscovitine encapsulated within spherical or tubular polymersomes, free roscovitine, empty tubular, or empty spherical

polymersomes or untreated. The zebrafish were returned to the 28°C incubator for a further 8 hours before they were anaesthetised with tricaine and the number of neutrophils at the site of injury was manually counted using the dissecting microscope.

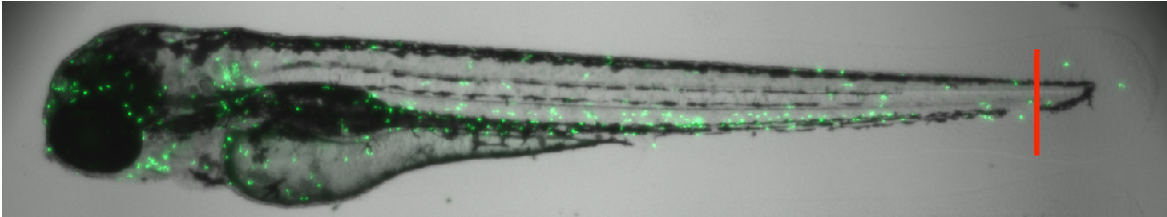


Figure 3.6. Site of tail injury in a 3dpf Tg(mpx:GFP)i114 zebrafish embryo.

3.8.3 Zebrafish Microinjections

Zebrafish injections were performed by the post-doctoral researcher Dr Tomek Prajsnar who works in Professor Steven Renshaw and Professor Simon Foster's research groups. 30 hours post fertilisation (hpf) zebrafish embryos were mechanically dechorinated and anaesthetised in tricaine. The zebrafish embryos were prepared for injection by transferring them into 3% methylcellulose on a glass microscope slide. Polymersomes were then injected into the circulation valley near the yolk sac (Figure 3.7) using glass capillary needles, pulled using an electrode puller, with a pneumatic micropump (World Precision Instruments PV820), connected to a micromanipulator (World Precision Instruments) and a dissecting microscope.

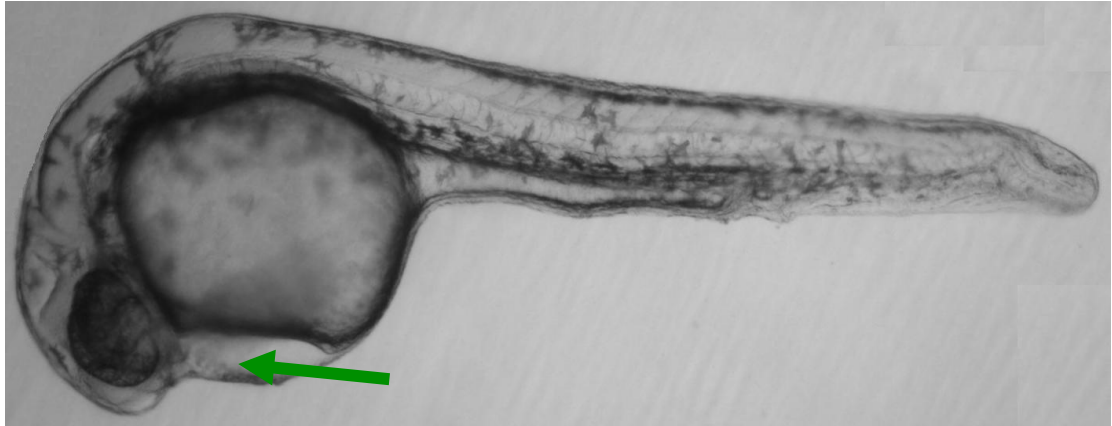


Figure 3.7 Microinjection site in 30hpf zebrafish embryo.

3.8.4 Zebrafish Microscopy Experiments

Zebrafish were prepared for imaging by immersion in tricaine followed by mounting in 1% low-melting point agarose (Sigma Aldrich) in E3 medium on an ibidi μ -dish.

3.8.4.1 Zebrafish Rhodamine-Labelled polymersome injections

10% Rho-PMPC-PDPA 90% Rho-PMPC-PDPA polymersomes made by pH switch were injected into 30hpf London Wild Type (LWT) zebrafish embryos as described above. After 2 hours incubation at 28°C zebrafish were mounted in agar and then imaged using a Nikon TE-2000 U microscope with a Hamamatsu Orca-AG camera and analysed using Volocity software (Perkin Elmer). For the dose optimisation experiment 0.1, 0.5, 1, 5 or 10mg/ml of rhodamine-labelled polymersomes were injected into zebrafish embryos. The average fluorescence intensity from six different points in the blood stream and in the blood phagocytes was measured from at least three separate zebrafish in each group

and the results were normalised by the untreated control zebrafish.

*3.8.4.2 Polymersome Injections Into *mpx:GFP; fms:mCherry* Transgenic Zebrafish*

Polymersomes encapsulating BODIPY TR Ceramide (Molecular Probes) (2mg/ml PMPC-PDPA concentration) formed using film rehydration were injected into a 2dpf transgenic zebrafish line *Tg(mpx:GFP)i114* x *Tg(fms:GAL4.VP16)i186* otherwise known as *mpx:GFP* x *fms:mCherry*, which have neutrophils labelled with GFP and macrophages labelled with mCherry (Gray et al., 2011). The zebrafish were incubated for 12 hours before they mounted in agar and imaged by confocal microscopy using the Perkin-Elmer UltraVIEW VoX spinning disk confocal microscope.

*3.8.4.3 Rhodamine-Labelled Polymersomes and CFP- *S. aureus* Injections*

10% Rho-PMPC-PDPA, 90% PMPC-PDPA polymersomes were made by pH switch. 2.dpf LWT zebrafish embryos were injected with 1200CFU of CFP-labelled *S. aureus* followed by an injection of 10mg/ml rhodamine labelled polymersomes 1 hour later. Zebrafish were incubated for 2 hours at 28°C before analysis by fluorescence microscopy using the Nikon TE-2000 U microscope.

*3.8.4.4 Polymersomes Encapsulating Fluorescent Lysostaphin and GFP- *S. aureus* Injections*

Lysostaphin was labelled using the Alexa Fluor 647 antibody labelling kit (Molecular Probes) according to the manufacturer's instructions and encapsulated by pH switch. 2dpf LWT zebrafish embryos were injected with

GFP-labelled *S. aureus* followed by polymersomes encapsulating lysostaphin 1 hour later. Zebrafish were imaged using the Perkin-Elmer UltraVIEW VoX spinning disk confocal microscope.

3.8.5 Zebrafish *S. aureus* Infection Experiments

2dpf LWT zebrafish were injected with 1200CFU of GFP-labelled *S. aureus*. 18 hours after injection zebrafish were viewed under a fluorescent dissecting microscope (Leica MZ10F) and zebrafish with visible abscesses were discarded. 20 hours post infection, zebrafish were injected with 10mg/ml or 1mg/ml (as specified) of polymersomes encapsulating an antibiotic or their subsequent controls. For survival experiments zebrafish were washed and moved to a 96 well plate. Zebrafish were checked twice a day using a dissecting microscope for survival rates; dead embryos were defined by the loss of heartbeat.

For quantification of bacterial burden zebrafish embryos were incubated at 28°C for a further 20 hours following polymersome injections. Zebrafish embryos were then homogenised using the PreCellys 24-Dual (Peqlab). The homogenates were serially diluted onto BHI agar plates, placed in a 37°C room and the number of viable colonies was manually counted the following morning.

3.9 Statistical Analysis

Experiments on human neutrophils and THP-1 macrophages were compared with either the one-way ANOVA or two-way ANOVA. Where the ANOVA was significant, Bonferroni multiple comparisons post-test was used to determine

whether the difference observed between two groups was significant. In the zebrafish infection experiments the survival comparison between the groups was made using the log rank (Mantel-Cox) test and the bacterial numbers after homogenization were compared using the Kruskal-Wallis test with Dunn's multiple comparison. All statistical analysis was performed using Prism software (Graphpad) with statistical significance represented with * $P < 0.05$, ** $P < 0.01$, *** $P < 0.001$, **** $P < 0.0001$.

Chapter 4: Optimisation of Polymersome Size for Intracellular Delivery into Human Neutrophils

4.1 Introduction

Size, shape, surface chemistry and mechanical properties are amongst the most important parameters in the design of a drug delivery vector. Size in particular has been well studied and is known to have a critical role in numerous *in vivo* functions including: circulation time, cell binding, internalisation, extravasation and biodistribution. But despite the known importance of vector size, polydispersity remains a common issue in polymersome production.

A variety of polymersome formation techniques exist such as film-rehydration, nanoprecipitation and electroformation. The average polymersome size is strongly influenced by the formation technique, but each method produces a wide distribution of sizes around their mean diameter. This polydispersity arises because the self-assembly of spherical vesicles does not have a strong size selective bias, as the energetic penalty required for an amphiphilic membrane to wrap into a spherical vesicle is not dependent on the final vesicle diameter. Once a polymersome has formed the distribution of molecules within the inner and outer monolayers is fixed, so post assembly purification steps are required for optimal control of polymersome size.

Liposomes are commonly purified by extrusion through narrow pores to break up larger structures and reduce the size range. But the force required for extrusion of polymersomes is much greater due to their higher mechanical strength, which limits the usefulness of the technique (Discher et al., 1999). Other examples of nanoparticle purification techniques include liquid chromatography (Sakai-Kato et al., 2011), filtration (Sweeney et al., 2006), size selective precipitation (Lee et al., 2006) and density gradient centrifugation (Miller et al., 2014), but these techniques remain to be fully explored in polymersome purification.

Purification of polymersomes into monodisperse size fractions is important for exploring the effect of size on the rate of internalisation. A number of groups have shown that nanoparticle size has a large influence on the rate of internalisation, but this is also dependent on surface chemistry (Massignani et al., 2009), receptor ligand density ratio (Yuan and Zhang, 2010), binding affinity (Gao et al., 2005), the mechanism(s) of receptor mediated endocytosis (Gratton et al., 2008b) and even the degree of nanoparticle clustering on the plasma membrane (Chaudhuri et al., 2011). Thus, the optimal size may depend on the specific surface properties of the nanoparticle and the target cell.

Here I explore a number of methods for purifying different sizes and morphologies of pre-assembled polymersomes from the pH-sensitive block copolymer poly(2-(methacryloyloxy) ethyl-phosphorylcholine)-co-poly(2-(diisopropylamino)ethyl methacrylate) (PMPC₂₅-PDPA₇₀). I show that these

polymersomes are internalised by human neutrophils and can be separated into different size fractions using cross flow filtration, differential centrifugation and size-exclusion chromatography. Using these purified fractions the effect of polymersome size on the rate of internalisation and the efficiency of cargo delivery into human neutrophils is explored.

4.2 Results

4.2.1 Polymersome Formation by pH Switch

The pH-sensitivity of the block copolymer PMPC-PDPA enables intracellular cargo release in the weakly acidic early endosomes (Lomas et al., 2008). Through this mechanism a range of hydrophilic and hydrophobic molecules can be delivered intracellularly (Lomas et al., 2007, Wayakanon et al., 2013, Madsen et al., 2013). Another advantage of PMPC-PDPA pH-sensitivity is that it provides a method for driving polymersome self-assembly through a controlled increase in pH. This method, referred to as pH switch, is a simple and quick procedure that facilitates the formation of spherical polymersomes in less than an hour.

4.2.2 Polymersome Internalisation by Human Neutrophils

Previous studies by Dr Jon Ward demonstrate that PMPC-PDPA polymersomes are internalised by human neutrophils (personal communication); to confirm these findings rhodamine-labelled polymersomes were formed by pH switch and incubated with human neutrophils for 5 hours. Analysis by confocal microscopy revealed that the polymersomes were internalised by neutrophils (Figure 4.1a). When the cells were incubated with different concentrations, the fluorescence intensity normalised to the untreated control, referred to as the relative median fluorescence intensity (rMFI), increased linearly with polymersome concentration (Figure 4.1b).

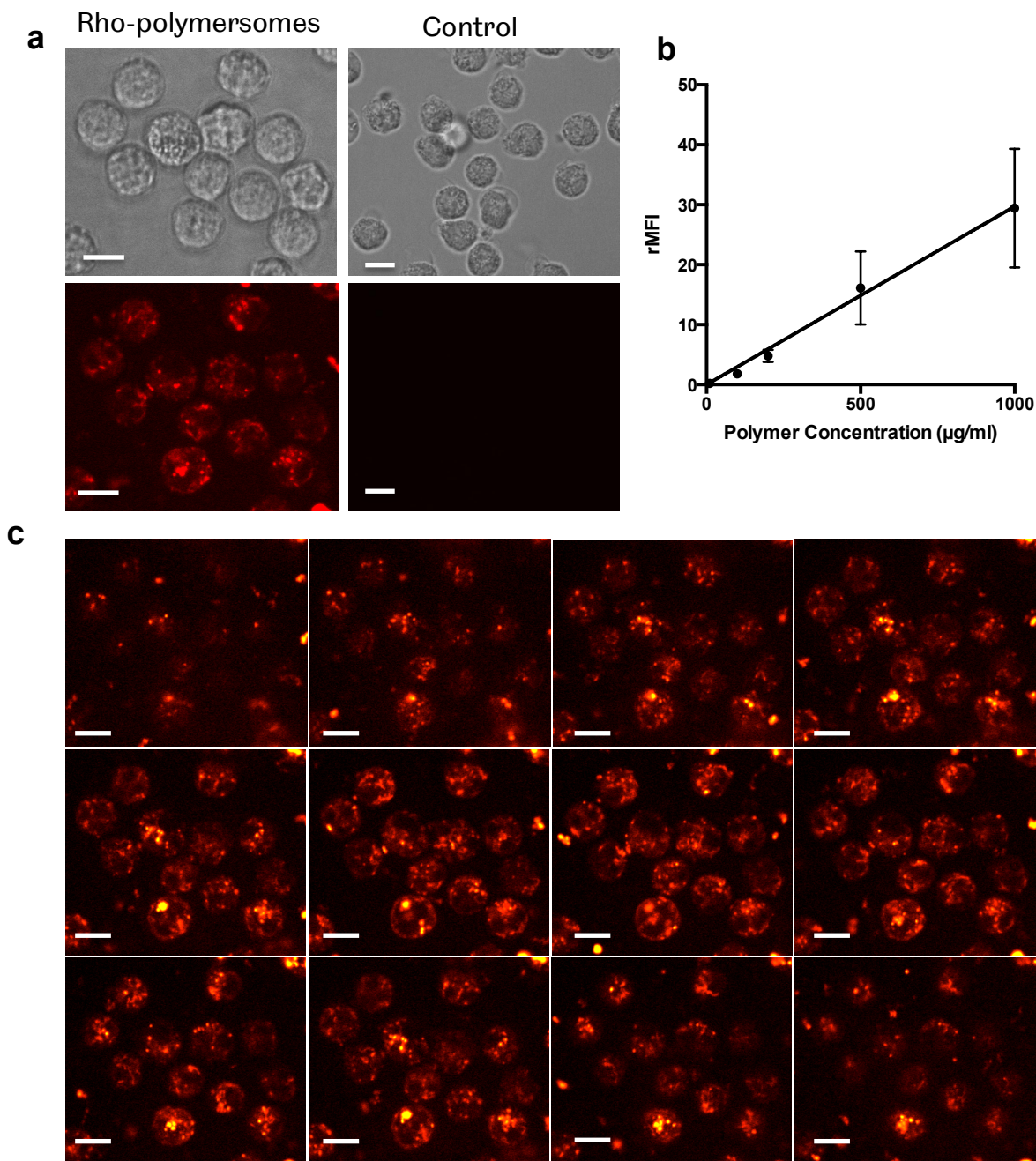


Figure 4.1 Uptake of spherical polymersomes by human neutrophils.

(a) Confocal microscopy of neutrophils incubated with rhodamine-labelled polymersomes for 5 hours at a final concentration of 0.1mg/ml, scale bar = 8µm. (b) Relative median fluorescence intensity (rMFI) of neutrophils treated with increasing concentrations of rhodamine-labelled polymersomes for 5 hours as measured by flow cytometry. (c) A montage of z-slices from a single confocal z-stack of neutrophils incubated with rhodamine-labelled polymersomes for 5 hours at a final concentration of 0.1mg/ml, scale bar = 8µm.

During pH switch, deprotonation of the PDPA block leads to fast nucleation and

aggregate assembly. While pH switch with PMPC₂₅-PDPA₇₀ favours the formation of spherical polymersomes, the fast assembly process can also lead to the formation of kinetically trapped structures such as micelles (Pearson et al., 2013). Furthermore, because the self-assembly of spherical vesicles does not have a strong size selective bias, pH switch results in nanoparticles with a range of sizes. Therefore, in order to separate the polymersomes into different size fractions post formation, a number of techniques were tested.

4.2.3 Polymersome Purification Using Cross Flow Filtration

As a method of purifying nanoparticles, dead-end filtration is generally unsuccessful because the particles accumulate at the pores resulting in a “filter cake” that blocks the filter. Cross flow-filtration overcomes this problem by providing a flow of particles at a tangent to the pores under high pressure, this allows particles smaller than the pore size to permeate the membrane while the tangential flow prevents the filter cake from forming (Figure 4.2a).

PMPC-PDPA self-assembly was driven using pH switch, resulting in a combination of spherical polymersomes and micelles (Figure 4.2b left image). Using a cross flow filtration system with 50nm pores, polymersomes were efficiently purified from the micelles as shown by dynamic light scattering (DLS) and Transmission Electron Microscopy (TEM) (Figure 4.2b).

4.2.4 Purification Using Size Exclusion Chromatography

Size exclusion chromatography (SEC) separates particles based on their

hydrodynamic volume. In SEC a column is filled with sepharose, a gel containing cross-linked agarose beads. As a mixture moves through the sepharose, otherwise known as the stationary phase of the SEC column, smaller molecules meander in and out of pores within the beads, whereas larger molecules, which cannot penetrate into all the pores, pass through the stationary phase quicker. SEC is commonly used to remove un-encapsulated small molecules, but separation of different sized polymersomes can be more challenging.

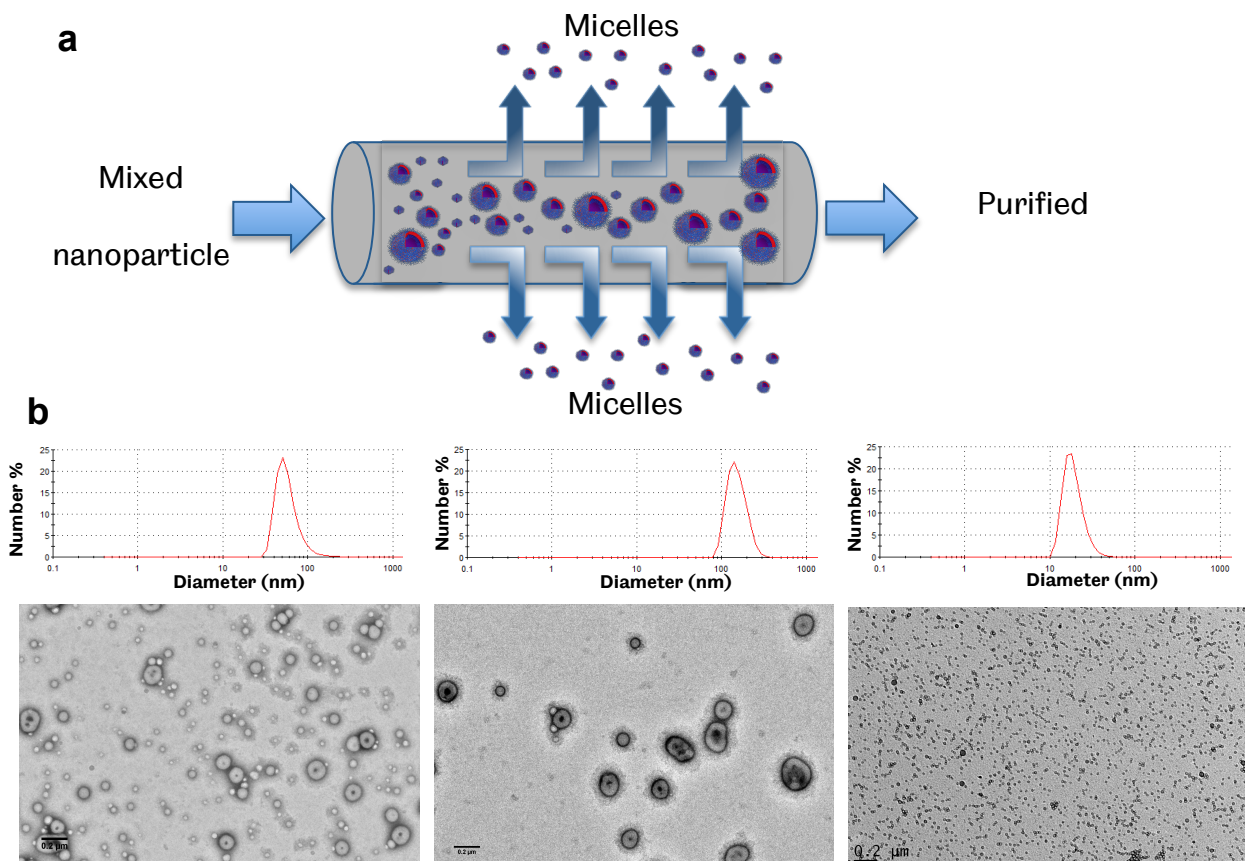


Figure 4.2 Purification of polymersomes from micelles using the KrosFlo Research Ili System.

(a) A diagram displaying the method of micelle removal by filtration through 50nm pores. (b) DLS frequency distribution and TEM photomicrographs of the polymersome solution before separation (left images), after separation (central image) and the separated micelle solution (right image), scale bar = 200nm.

To improve the resolution of SEC, 2ml of polymersomes at 10mg/ml (20mg) was concentrated into a small volume (~200 μ l) using a 10kDa hollow fiber module. Adding a lower volume to the SEC column reduces the time for all the liquid to be absorbed by the stationary phase. The eluted liquid was collected and then recycled into a new column, increasing the effective column length. The final sample was collected in a 96 well plate and the fractions were measured using DLS. As shown in Figure 4.3a, this technique was effective at separating the sample into many fractions. Figure 4.3b shows three fractions imaged by TEM, which further demonstrate the successful size purification. It is important to note that 15mg of the initial 20mg polymersome solution was recovered from the column using this technique.

4.2.5 Separation of Polymersome Sizes by Differential Centrifugation

Centrifugation is one of the most commonly used techniques in biology for separating mixtures by size and density. Differential centrifugation is a technique to separate multiple fractions in a sample. The mixture is centrifuged several times and after each run the pellet is removed and resuspended and the supernatant is re-centrifuged at a higher speed (Figure 4.4a). Polymersomes were formed by pH switch (Figure 4.4b) and the micelles were removed using the cross flow filtration system. Polymersomes were then separated into different size fractions by differential centrifugation (Figure 4.4c). TEM photomicrographs of each fraction are shown in Figure 4.4d, which demonstrate that polymersome morphology was not affected by centrifugation.

This technique was quicker and less wasteful than the SEC method and thus was employed for size purification in subsequent neutrophil experiments.

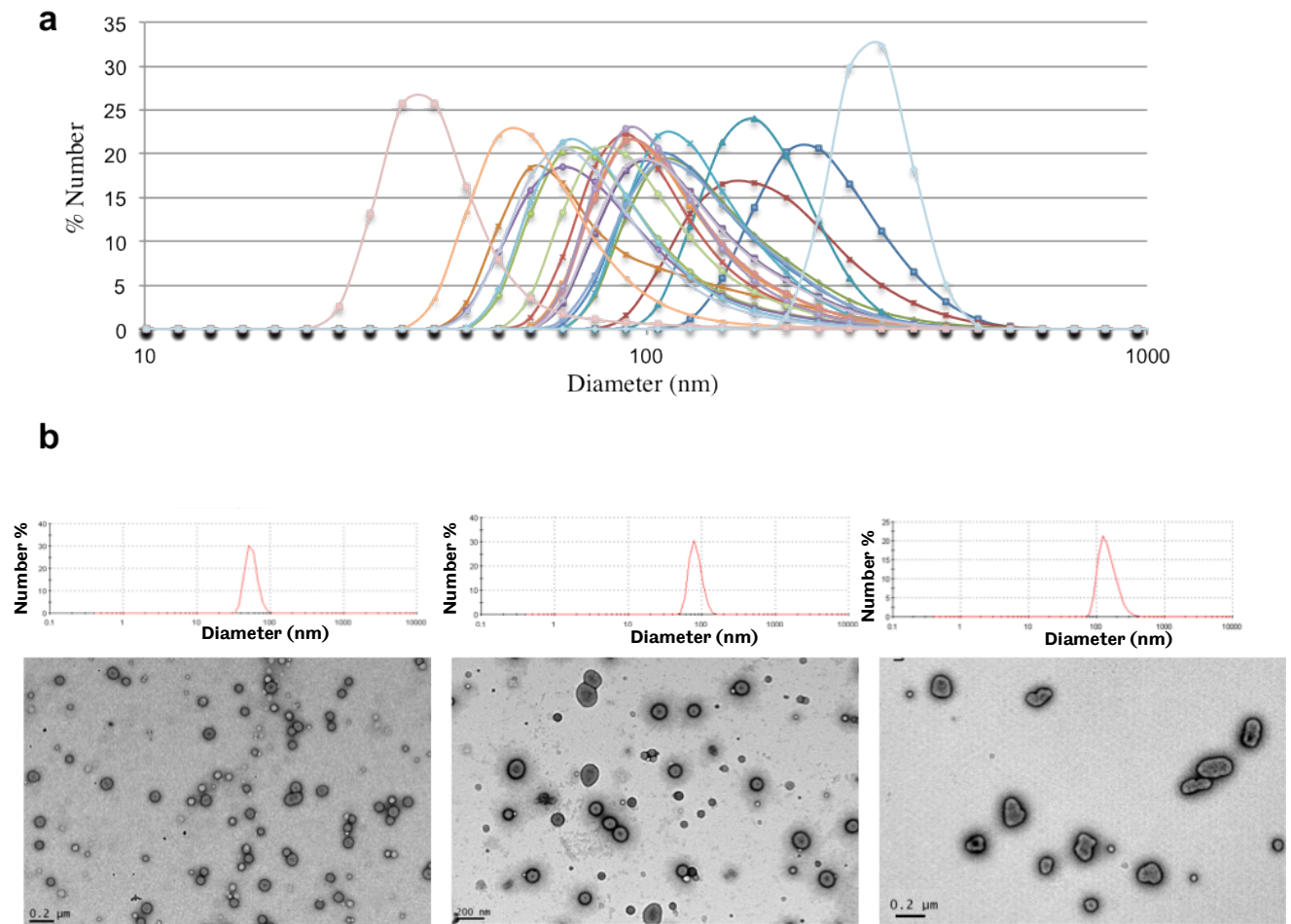


Figure 4.3 Size separation using recycling size exclusion chromatography.

(a) DLS frequency distribution of all fractions separated by size recycling chromatography. (b) DLS frequency distribution and TEM micrograph of three example fractions (Scale bar=200nm).

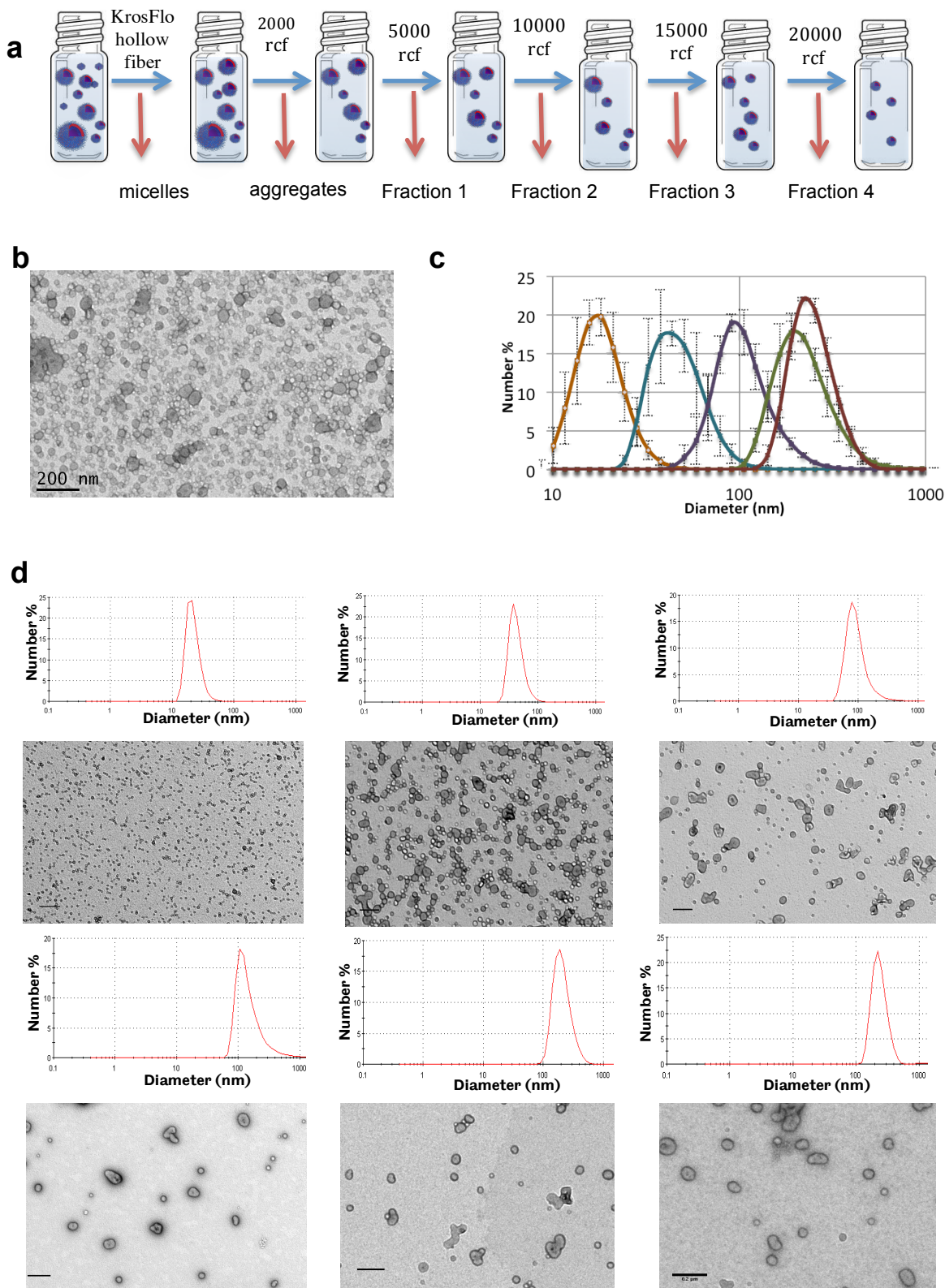


Figure 4.4 Size separations using differential centrifugation.

(a) A cartoon explaining the separation protocol. Micelles are first removed using the KrosFlo hollow fiber system. The sample is then centrifuged at 500RCF and the pellet is resuspended in PBS. The supernatant is then re-centrifuged at 2000RCF, 5000RCF, 10000RCF, 15000RCF and 20000RCF, at each centrifugation the pellet was separated and resuspended. (b) A TEM photomicrograph of the polymersome mixture before separation. (c) DLS size distribution for the 6 separated fractions (error bars = SEM, n=3). (d) DLS histograms and TEM photomicrographs displaying all the separated fractions in ascending size order, scale bar = 200nm.

4.2.6 The Influence of Polymersome Size on Uptake by Human Neutrophils

To investigate the consequence of polymersome size on internalisation by human neutrophils, rhodamine-labelled polymersomes encapsulating cascade blue were formed by pH switch. Cascade blue is a water-soluble, cell-impermeable fluorescent dye that is used to measure membrane permeability. By encapsulating cascade blue in rhodamine-labelled polymersomes it is possible to track the amount of polymer that has been internalised by the cell, as well as the amount of delivered cargo.

Cascade blue (final concentration 100 μ g/ml) was added to a pH 6 solution of 90% PMPC-PDPA and 10% rhodamine-labelled PMPC-PDPA (total polymer concentration 10mg/ml). Polymersome assembly and cascade blue encapsulation were initiated through pH switch and the formed rhodamine-labelled polymersomes encapsulating cascade blue were separated into six size fractions using cross flow filtration followed by differential centrifugation.

Following purification, the amount of cascade blue encapsulated in each size fraction was measured; polymersomes were disassembled by lowering the pH to 6 with the addition of 1M hydrochloric acid. The concentration of cascade blue and rhodamine-labelled polymer was measured using fluorescence spectroscopy. The amount of encapsulated cascade blue normalised to 10mg/ml of polymer is shown in Table 4.1 for each fraction. The encapsulation of cascade

blue increased with rising polymersome diameters, which is consistent with their greater luminal volume (Table 4.1).

Diameter (nm)	22	43	97	161	190	240
Cascade blue concentration ($\mu\text{g/ml}$)	17.2	23.3	27.0	45.1	51.1	53.5

Table 4.1 Cascade blue encapsulation after purification of six polymersome size fractions.

Cascade blue was added to a pH 6 solution of PMPC-PDPA with 10% rhodamine labelled PMPC-PDPA at a polymer concentration of 10mg/ml and a final cascade blue concentration of 100 $\mu\text{g/ml}$. The table gives the final concentration of cascade blue within each size fraction normalised to a polymer concentration of 10mg/ml.

Uptake of polymersomes into neutrophils was assessed by flow cytometry. As shown in Figure 4.5a incubation with polymersomes encapsulating cascade blue resulted in a shift in the fluorescence intensity of the neutrophils when excited with the violet laser. Incubation with rhodamine-labelled polymersomes caused a shift in the fluorescence intensity when excited with the blue laser. Neutrophils treated with rhodamine-labelled polymersomes encapsulating cascade blue showed a clear shift in both directions.

Human neutrophils were extracted from healthy donors and incubated with one of the six purified polymersome size fractions at a final polymer concentration of 0.1mg/ml. At multiple time points throughout the experiment neutrophils

were analysed by flow cytometry. Figure 4.5b shows example dot plots for each polymersome size fraction over time from one experiment.

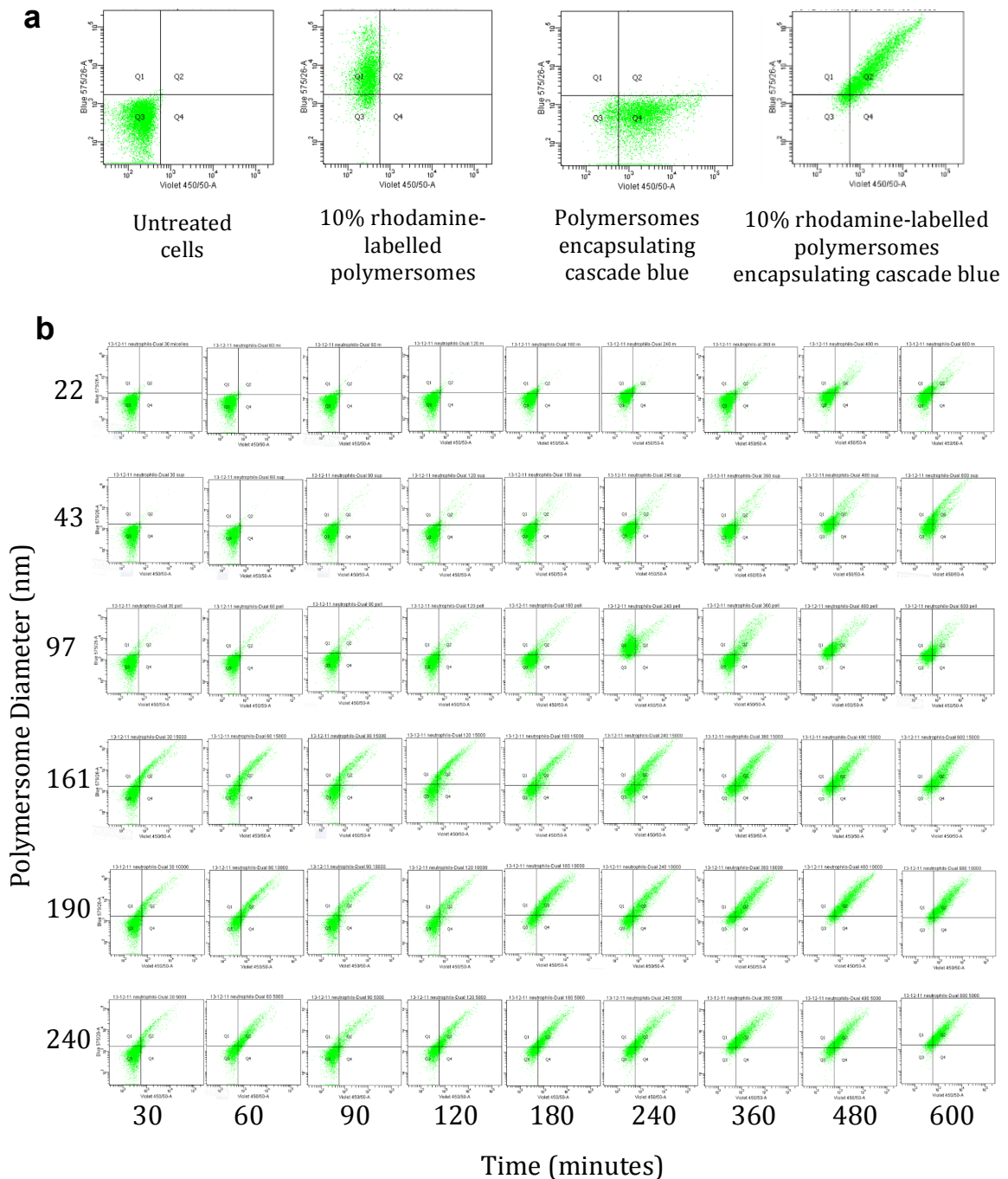


Figure 4.5 Uptake of rhodamine-labelled polymersomes encapsulating cascade blue in human neutrophils.

(a) Experiment controls showing dot plots for neutrophils without treatment, or neutrophils incubated with polymersomes encapsulating cascade blue, rhodamine labelled polymersomes or rhodamine-labelled polymersomes encapsulating cascade blue. (b) Representative dot plots for neutrophils incubated with different sized polymersomes for increasing time periods.

Neutrophil rMFI from internalised rhodamine-labelled polymer and cascade blue are shown in Figures 4.6a and 4.6b respectively. Incubation with polymersomes resulted in a rapid increase in neutrophil fluorescence, which plateaued over time. The degree of neutrophil fluorescence over time was dependent on the polymersome size. Neutrophils treated with the 190nm polymersome fraction showed the highest internalisation of rhodamine labelled polymer and cascade blue. A single graph of combined neutrophil rMFI from rhodamine and cascade blue for each size fraction are shown in Figure 4.6c and 4.6d respectively. By plotting the data from the final time point only, it can be seen that the amount of polymer internalised by neutrophils escalates with increasing diameter up to 190nm (Figure 4.6e).

To investigate the rate that polymersomes are expelled from neutrophils after internalisation, neutrophils were incubated with 190nm polymersomes using the same protocol. After 240 minutes the neutrophils were pelleted by centrifugation, washed and returned to normal media. The neutrophil rMFI was measured at three further time points to determine the rate of polymer release from the cells. Interestingly, once the extracellular polymersomes were removed, neutrophil rMFI rapidly decreased suggesting the polymer was quickly released from the cell (Figure 4.6f). This may explain the plateau in rMFI seen for neutrophils at later time periods that would correspond to the point of equilibrium between polymer release from the cell and polymersome internalisation.

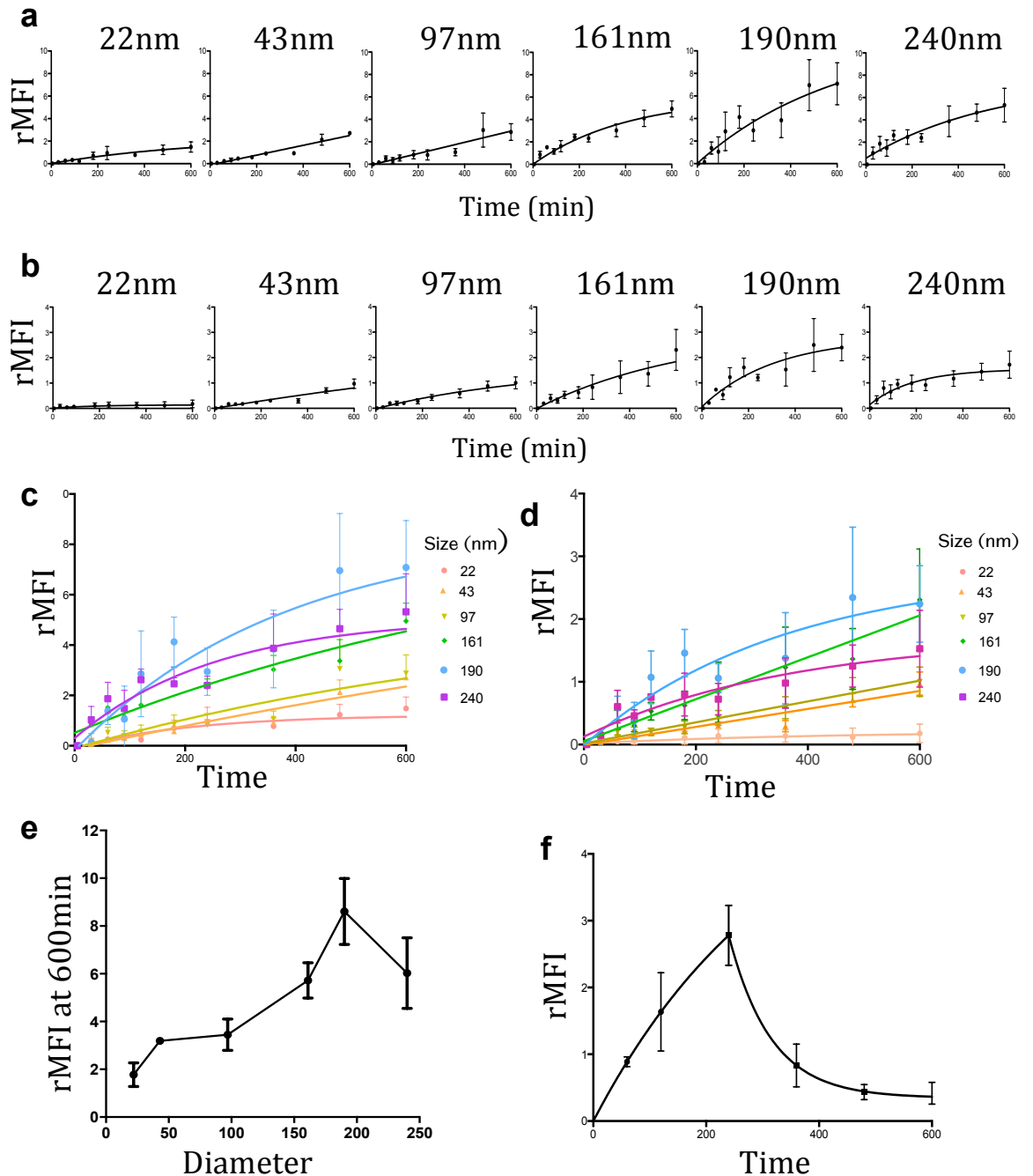


Figure 4.6 Quantified neutrophil rMFI over time after incubation with rhodamine labelled polymersomes encapsulating cascade blue.

(a) Neutrophil rMFI in the rhodamine channel showing the amount of polymer internalised over time for each of the size fractions. (B) Neutrophil rMFI in the cascade blue channel showing the amount of cascade blue delivered into neutrophils overtime for each size fraction. The sizes are combined into one graph showing the rMFI for all size fractions in the rhodamine channel (c) and the cascade blue channel (d). (e) Neutrophil rMFI after incubation with polymersomes at each size fraction for 600 minutes. (f) rMFI of neutrophils treated with rhodamine labelled polymersomes and washed after 240 minutes to determine the rate of polymer release (on all graphs error bars = SEM, n=3).

4.3 Discussion

Nanoparticle size is known to have a crucial role in numerous *in vitro* and *in vivo* functions. Self-assembly of the block-copolymer PMPC-PDPA in aqueous solutions leads to the formation of spherical polymersomes with a range of diameters. Purifying polymersomes into the desired size range is crucial when designing the vector for a specific application or to help understand the effect of size on processes such as internalisation. Nanotechnologists have consistently shown that the diameter of a vector can have a strong influence on the rate of internalisation. But the optimum size of PMPC-PDPA polymersomes for efficient internalisation is difficult to predict from data on other nanoparticles, as the rate of internalisation is dependent on other factors such as the specific endocytosis mechanism employed, the nanoparticle surface chemistry, the receptor ligand density ratio and the degree of clustering on the cell membrane.

4.3.1 Purification of Polymersomes into Different Sizes

Although a number of post assembly nanoparticle purification techniques have been developed (Sakai-Kato et al., 2011, Sweeney et al., 2006, Lee et al., 2006, Miller et al., 2014), few attempts have been made to isolate different sized polymersomes from preformed fractions. Liposomes are commonly processed using combinations of sonication and extrusion to break the membrane and reform it with the desired diameter. But the high mechanical strength of polymersomes make these methods ineffective (Discher et al., 1999). Therefore new post-assembly size purification techniques are required for polymersomes.

In this chapter polymersomes were purified from micelles using cross flow filtration. Polymersomes were then separated into distinct size fractions using differential centrifugation or recycling size exclusion chromatography. Differential centrifugation provided the fastest and simplest method of size purification, allowing similar sized fractions to be consistently produced in separate experiments. Recycling SEC provided a higher resolution of size separation and numerous fractions were recovered from the column. The TEM data shows a more monodisperse separation of the polymersomes with the SEC method, but this technique resulted in a greater sample loss during purification, with a starting mass of 20mg before addition to the column and a final mass of 15mg post purification.

4.3.2 Comparison of Polymersome Size on the Rate of Internalisation and the Efficiency of Cargo Delivery

The rate of nanoparticle internalisation is dependent on a number of factors. Internalisation can be driven in part simply from the physical interaction of a nanoparticle with the cell membrane. By modelling membrane wrapping the Freund group calculated that there is an optimal nanoparticle size of approximately 50-60nm that facilitates membrane wrapping in the shortest time period (Gao et al., 2005). However, the rate of internalisation experimentally varies depending on the specific properties of both the nanoparticle and the target cell (Desai et al., 1997, Rejman et al., 2004, Lu et al., 2009, Prabha et al., 2002, Nakai et al., 2003).

In live cells, the effect of size is influenced by the mechanism(s) of endocytosis employed for internalisation. For instance, Gratton and colleagues demonstrated that macropinocytosis, clathrin-mediated endocytosis and caveolae-mediated endocytosis were all involved in the internalisation of hydrogels to varying extents depending on the particle size and shape (Gratton et al., 2008b). They found that the nanoparticles that were most readily internalised utilized all three internalisation pathways to a high degree (Gratton et al., 2008b).

In this chapter I have shown that polymersomes with a diameter of approximately 190nm resulted in the greatest increase in neutrophil fluorescence intensity both when considering the fluorescence from the rhodamine-labelled polymer and encapsulated cascade blue. It should be emphasized that the increase in neutrophil fluorescence intensity from the rhodamine demonstrates that 190nm polymersomes are most efficient in terms of the amount of polymer delivered into the cells, but not the number of polymersomes internalised. This is because the larger polymersomes are formed from a much higher amount of polymer and hence more rhodamine is delivered into the neutrophil for every polymersome that is internalised. However, the data highlights that this size of polymersome may be optimal as a drug delivery vehicle for neutrophils because it can encapsulate more cargo than smaller polymersomes. The amount of rhodamine-labelled polymer delivered into the cell will be proportional to the amount of hydrophobic cargo

that can be encapsulated, as hydrophobic molecules are encapsulated within the polymersome membrane. Therefore, this data suggests that polymersomes with an average diameter of 190nm may be most efficient as a drug delivery vector for neutrophils *in vitro*.

After polymersomes were washed from the cell medium the neutrophil fluorescence decreased, indicating the polymer was released from the cells. Chithrani and colleagues demonstrated that gold nanoparticles were rapidly expelled after internalisation by HeLa cells (Chithrani and Chan, 2007). They showed that nanoparticles appeared to be localised in late endosomes and lysosomes that then docked on the cell membrane and released their contents into the cytoplasm along with small amounts of lipid bilayer (Chithrani and Chan, 2007). However, unlike gold nanoparticles PMPC-PDPA polymersomes disassemble into their chains within the endosome and these are subsequently released into the cell. Following release from endosomes the neutral cytoplasmic pH allows the polymer chains to become amphiphilic and this probably results in the polymer chains integrating within the membranes of intracellular organelles and the plasma membrane. It may be that the release of the polymer from the cell represents either the natural shredding of the cell membrane or the gradual release of the polymer in exosomes.

In summary, polymersomes can be purified post assembly into multiple size fractions using differential centrifugation or recycling size exclusion chromatography. After separation of polymersomes into different fractions, the

190nm polymersome fraction was most efficient at delivering cargo into neutrophils. These results emphasise the importance of polymersome size on cargo delivery and highlight that the optimal polymersome size is dependent on both the rate of internalisation and the amount of cargo that is encapsulated within each individual vector.

Chapter 5: Tubular polymersomes: Formation, Purification and Internalisation by Neutrophils

5.1 Introduction

The shape of a nanovector impacts the internalisation kinetics by influencing its interaction with the cell membrane, but controlling shape at the nanoscale can be difficult to achieve. The specific endocytosis mechanism employed by a nanoparticle is known to depend on the receptors targeted, the cell type and the vector size (Canton and Battaglia, 2012). Controlling nanoparticle shape may also enable the endocytosis machinery to be manipulated to influence the rate of binding and internalisation (Akinc and Battaglia, 2013). A number of groups have demonstrated that rod shaped nanovectors with high aspect ratios have reduced rates of internalisation in certain cell types and long cylindrical nanovectors have improved circulation times and cell targeting capability (Geng et al., 2007, Kolhar et al., 2013, Albanese et al., 2012, Chithrani et al., 2006, Gratton et al., 2008b).

Amphiphilic block copolymers with dimensionless packing parameters larger than 0.5 form membranes that are most stable when wrapped into spherical vesicles (Smart et al., 2008). The final polymersome shape is the result of the combination of forces that control the membrane wrapping and the distribution of molecules between the inner and outer monolayers. This distribution is fixed

at the time of membrane closure meaning vesicles can close into a great variety of morphologies with the spherical shape being the most stable and thus most common. In polymersomes, the high viscosity of the membrane gives it a limited lateral mobility, which can hinder molecular re-arrangements necessary to stabilise spherical vesicles (Dimova et al., 2002). This can drive the formation of meta-stable structures with long lifetimes (Battaglia et al., 2007). Without any further energy contribution to homogenise the dispersion, spherical vesicles and non-spherical vesicles can coexist (Battaglia and Ryan, 2006b, Grumelard et al., 2004).

For many applications polymersomes are a more desirable nanovector than solid micelles. In addition to encapsulating hydrophobic substances in their membrane, polymersomes can also encapsulate hydrophilic molecules within their aqueous core. However, the filamentous, or cylindrical structure, which can give micelles unique properties, is more difficult to achieve for vesicular structures. A small number of groups have reported tubular polymersomes, but these are often unstable, require complex manipulation, are formed in a non-biocompatible solvent, or have not been isolated from contaminating spherical polymersomes (Grumelard et al., 2004, Stewart and Liu, 2000, Reiner et al., 2006, Yu and Eisenberg, 1998, van Oers et al., 2013).

In this chapter I study the development and purification of tubular PMPC-PDPA polymersomes and explore the potential of these particles as a nanovector for human neutrophils.

5.2 Results

5.2.1 Polymersome Rehydration Morphological Analysis

The morphology of block copolymer assemblies varies depending on the method of formation. Figure 5.1 shows the structure of self-assembled aggregates of the diblock copolymer poly(2-(methacryloyloxy)ethyl-phosphorylcholine)-co-poly(2-(diisopropylamino) ethyl methacrylate) (PMPC-PDPA) formed using pH switch (as described in Chapter 4) or the film rehydration method. In film rehydration, the polymer is dissolved in a solvent mixture (2:1 chloroform methanol) in a glass vial. The solvent is then evaporated in a desiccator leaving a thin polymer film on the edge of the vial. PBS solution is added to the vial and left agitating with a magnetic stirrer. Over time, polymersomes bud from the interface between the film and the PBS solution. Self-assembly through pH switch resulted in the production of spherical structures only, whereas, film rehydration formed a mixture of spherical and tubular polymersomes (Figure 5.1).

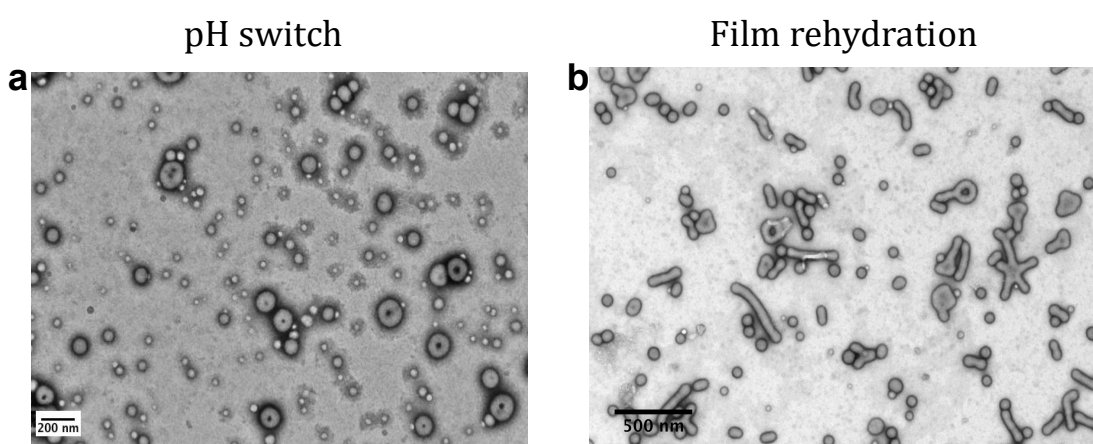


Figure 5.1 Morphology of nanoparticles formed through pH switch or film rehydration

Transmission electron photomicrographs of nanoparticles formed using the pH switch (a) or film rehydration method (b).

5.2.2 The Mechanism of Tubular Polymersome Formation

To understand why film rehydration formed tubular polymersomes as well as the energetically favourable spherical polymersomes, the formation process was monitored using confocal microscopy of a rhodamine-labelled PMPC-PDPA film. The film was formed as described above on a coverslip. The coverslip was then placed at a 90-degree angle on an imaging dish so that detachment of the particles from the film could be visualised. Figure 5.2a shows a confocal photomicrograph of the film before the addition of PBS. The initial film is consistent and smooth. At time 0 hours PBS is added to the film and a magnetic stirrer is placed in the dish. Initially the film begins to swell and its interface with water starts to become undulated and rougher through mechanical and thermal fluctuations (Limary and Green, 1999). The perturbations in film thickness cause local regions in the film with high disjoining pressures and this leads to the formation of holes. As the film continues to swell it wrinkles and diffuses towards the water, resulting in the formation of fingering instabilities (Battaglia and Ryan, 2006a) (Figure 5.2b).

As the holes in the film grow, polymer accumulates at the edges resulting in the formation of rims (Green and Limary, 2001) (Figure 5.2c). The rims continue to grow and eventually conjoin into a continuous network. Other groups studying film rehydration have found that this network breaks further into droplets, which in some instances are released from the film as spherical vesicles (Sharma and Khanna, 1998, LoPresti et al., 2009, Battaglia and Ryan, 2006b). In this study, mechanical forces from the magnetic stirrer result in the breakage

and release of parts of the network into the solution, before the film progresses to droplets (Figure 5.2d). The size of the portions of film released into the solution varied widely from less than a micrometre to tens of micrometres (Figure 5.3).

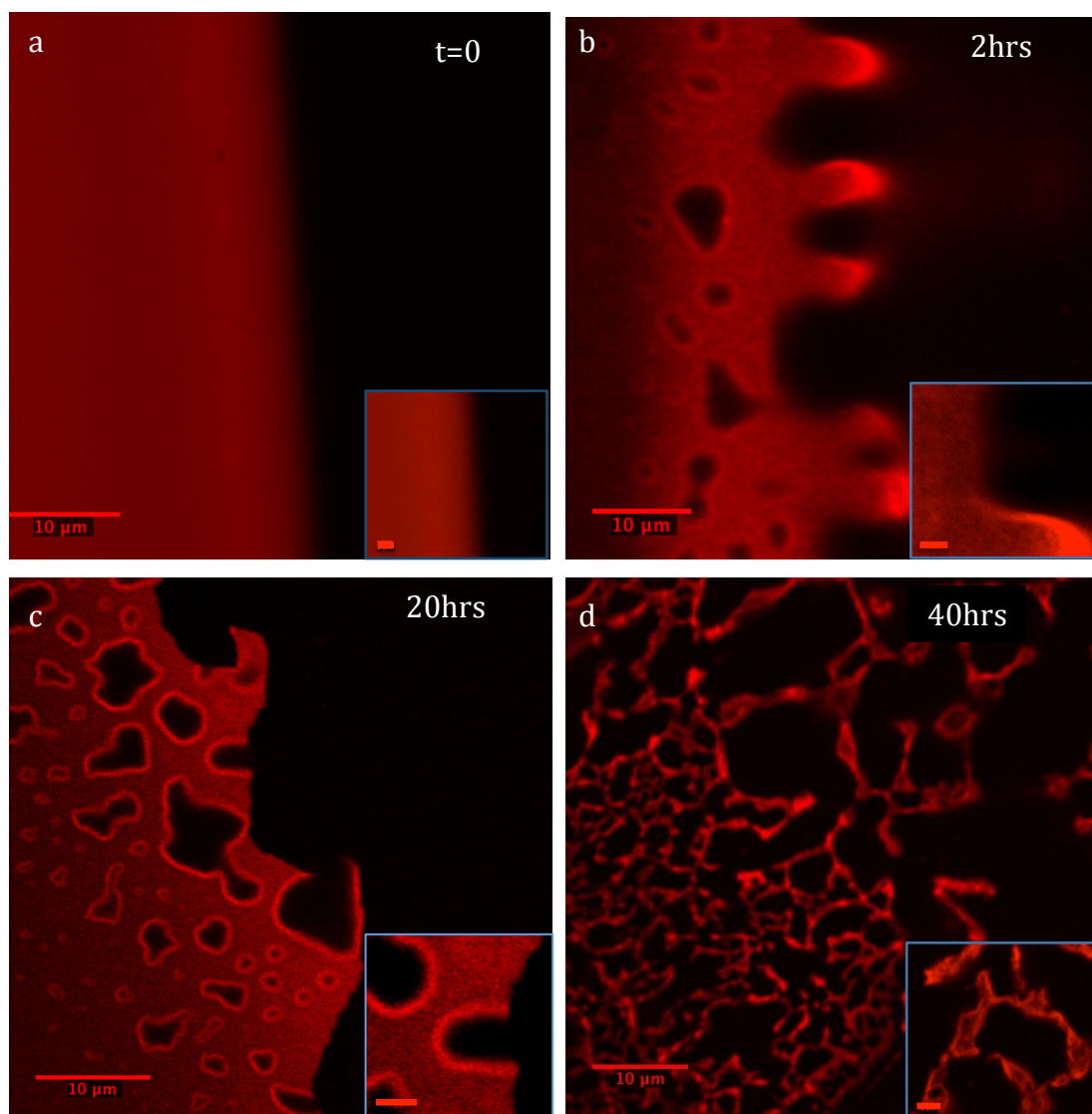


Figure 5.2 Swelling and detachment of a thin film of Rhodamine labelled PMPC-PDPA

A film of Rhodamine labelled polymer before the addition of PBS (a) and 2 hours (b), 20 hours (c) or 40 hours after PBS and a magnetic stirrer were added. The film was imaged using a confocal laser-scanning microscope, image scale bar = 10 µm, smaller inset scale bar = 2 µm.

The local concentration of amphiphilic copolymer in water controls the favourable architecture of the particles (Battaglia and Ryan, 2006b, Battaglia and Ryan, 2005b). High concentrations of copolymer in water favours long-ranged ordered structures called lyotropic crystals. Lyotropic crystals are maintained through the balance between Van der Waals forces, the hydrophobic interaction and the hydrophilic forces that occur at high copolymer concentrations (Lipowsky and Leibler, 1986).

After parts of the film become detached, the local copolymer-water ratio drops, decreasing local Van der Waals forces and resulting in an increase in strong hydration forces that favour the formation of smaller separated structures. Membrane fluctuations allow the membrane to curve into hollow enclosed configurations to prevent the unfavourable interaction of the hydrophobic block with water (Figure 5.4). The combination of energy provided by stirring and the repulsive hydration forces promote the detachment of smaller branched tubular structures and diverse high-genus assemblies. These particles then break up into tubular polymersomes. Finally, through processes of pearling and budding, these tubes break further into smaller tubes and finally spherical polymersomes (Figure 5.4).

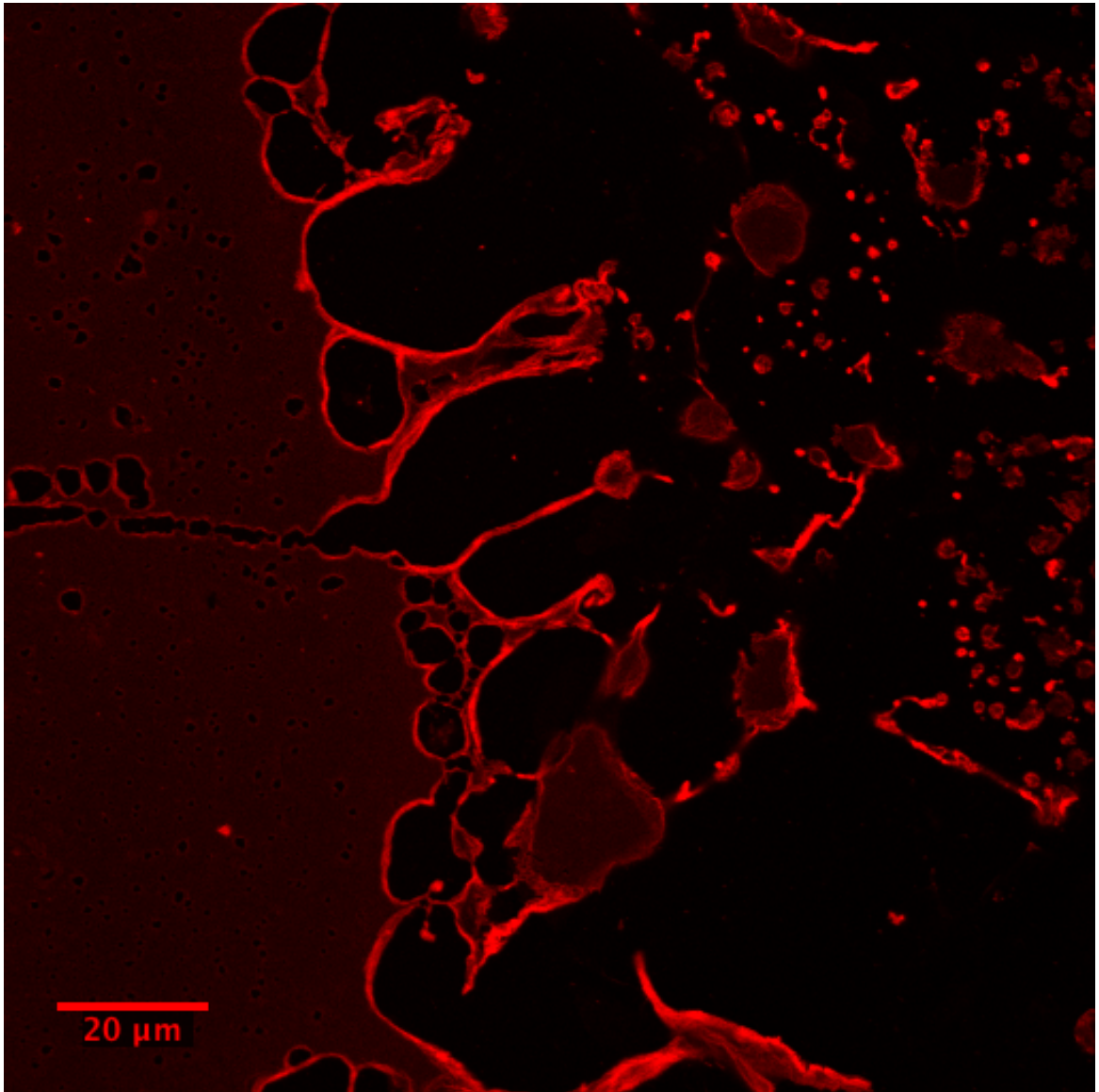


Figure 5.3 Release of components of the polymer film into the solution
A confocal photomicrograph demonstrating the size diversity of components of film released after 40 hours stirring.

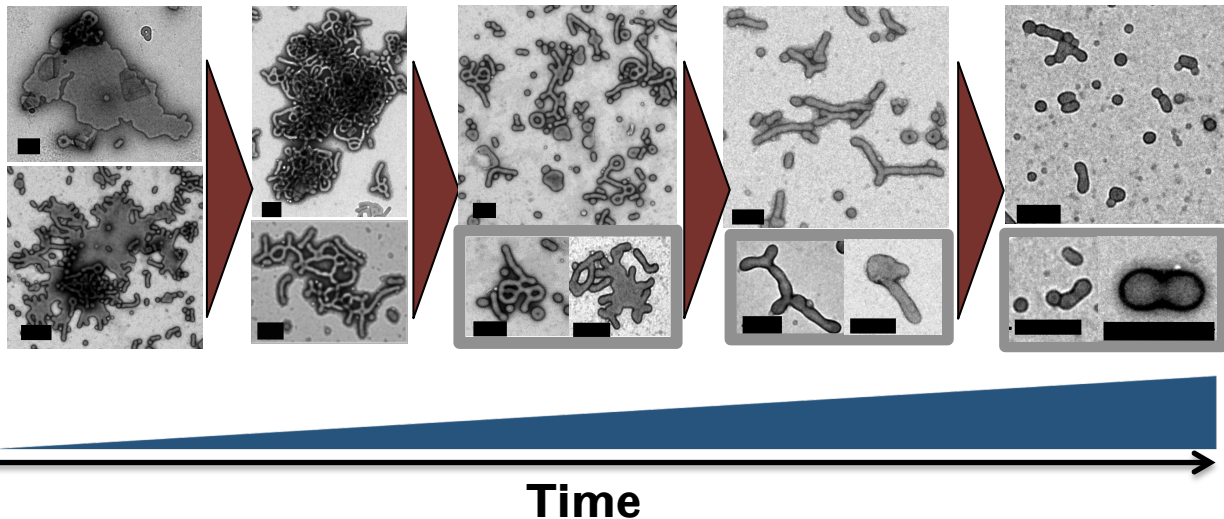


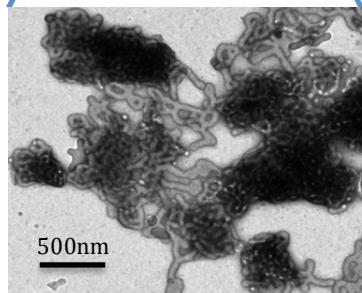
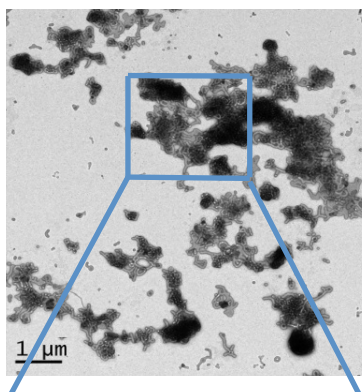
Figure 5.4 Formation of tubular polymersomes and spherical polymersomes from larger structures.

Released pieces of film swell into a continuous tubular network this then breaks into single tubes and small-entangled structures. These break further into smaller tubes that finally pearl and bud into spherical polymersomes, scale bars = 200nm.

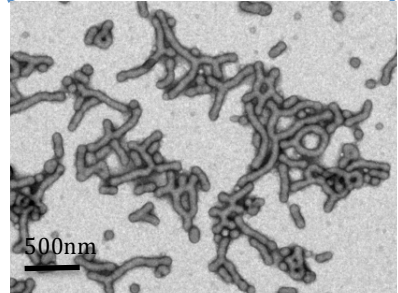
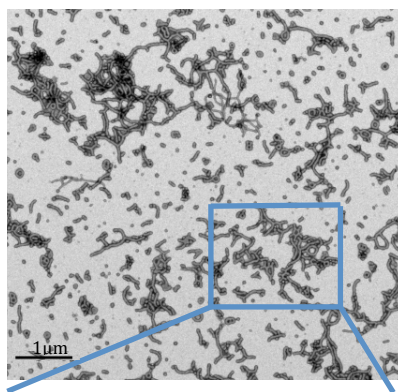
5.2.3 Separation of Tubular Polymersomes

Sections of the swollen film are continuously released until the film has been discharged into the solution. This means at any one time, multiple phases in the transition will co-exist. In order to purify the tubular polymersomes from the other structures the sample was centrifuged at two speeds, separating the particles based on their size and density (Figure 5.5). First, the sample was centrifuged at 2000RCF and the pellet was removed and re-suspended. This fraction contained the large and dense particles from the lyotropic phases. The supernatant was then re-centrifuged at 15000RCF and the pellet was removed and re-suspended, this fraction contained the tubular polymersomes. Those particles that remained in the supernatant were the third fraction containing predominantly smaller, spherical particles.

Lyotropic fraction



Tubular fraction



Spherical fraction

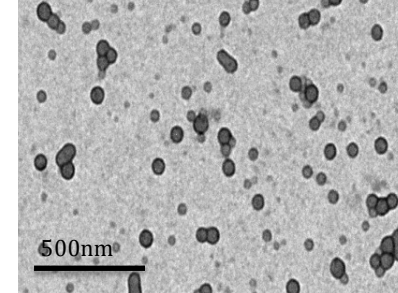
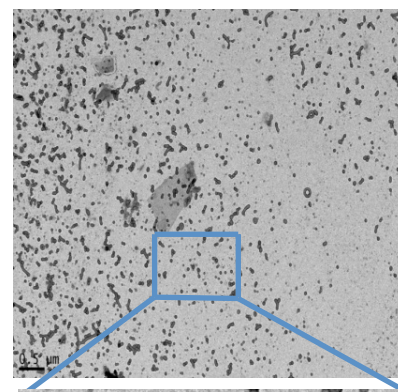


Figure 5.5 Separation of self-assembled structures by centrifugation.

The sample was spun at 2000RCF, the pellet was re-suspended, this fraction contained the lyotropic structure shown in the image on the left. The supernatant was then centrifuged at 15000RCF and the pellet re-suspended, this contained the tubular fraction shown in the central micrograph. The supernatant contained the predominately spherical fraction as shown in the photomicrograph on the right.

By separating the solution into these three fractions it was possible to quantify the relative mass of each fraction using RP-HPLC associated with UV detection (Figure 5.6). In keeping with the model of formation, the lyotropic structures initially form a high percentage of the detached particles. Over time, these begin to disassemble and the number of tubular and spherical polymersomes increases. At week 4 the number of tubular polymersomes reaches its maximum and then decreases, while the amount of spherical polymersomes continues to increase. This maximum signifies the point at which the transition of tubular polymersomes into spherical polymersomes overtakes the number of new tubular polymersomes formed from the lyotropic structures, as the lyotropic fraction is depleted.

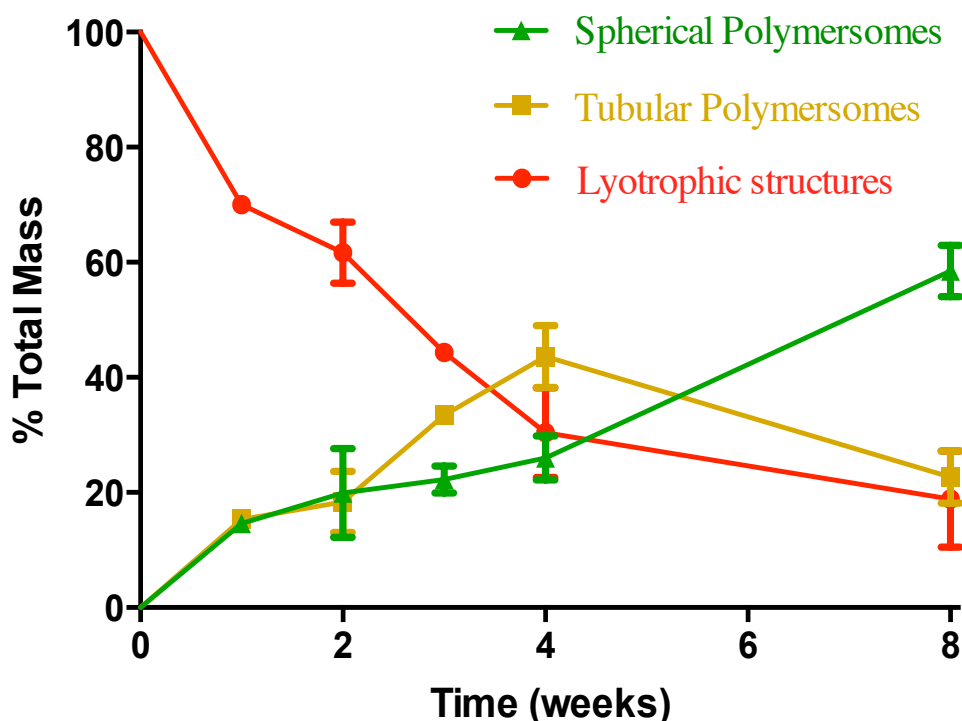


Figure 5.6 Formation of structures over time.

The proportion of the three fractions measured over time, at each time point the fractions were separated by centrifugation and the mass of each fraction was measured using RP-HPLC with UV detection (error bars = SD, n=3).

5.2.4 Tubular Polymersome Internalisation

The uptake kinetics of tubular polymersomes were investigated in primary human neutrophils. Flow cytometry was used to quantify the internalisation of rhodamine-labelled tubular polymersomes in comparison to rhodamine-labelled spherical polymersomes into neutrophils over time. To ensure that any difference between the internalisation of spherical and tubular particles was a result of shape rather than size, the mean diameter of the spherical polymersomes were designed to mimic the diameter and length of the tubular polymersomes (Figure 5.7a).

Spherical polymersomes were formed using pH switch and purified by differential centrifugation using the method described in chapter 4. The tube diameter and length were manually measured using ImageJ software from TEM photomicrographs. As shown in Figure 5.7b, the 60nm and 240nm spherical polymersomes had similar size distributions to the tubular polymersome diameter and length respectively. Neutrophils were incubated with rhodamine-labelled tubular or spherical polymersomes and the fluorescence intensity was measured by flow cytometry. A biphasic uptake profile was observed for the tubular polymersomes (Figure 5.7b). This uptake profile is different from that observed for the spherical polymersomes which show a rapid internalisation followed by a single plateau. The two phase increase in fluorescence for the neutrophils incubated with tubular particles may be explained by an initial binding step, followed by a delayed internalisation.

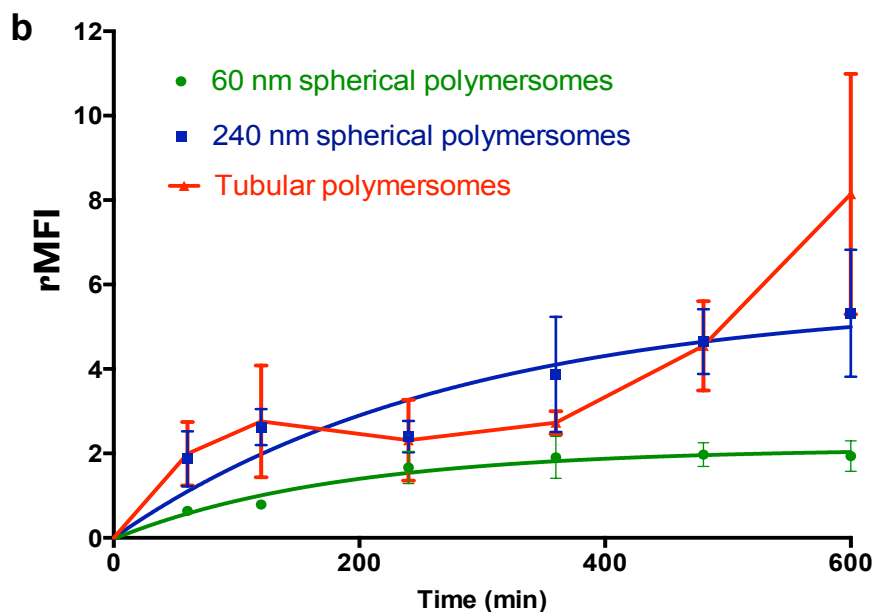
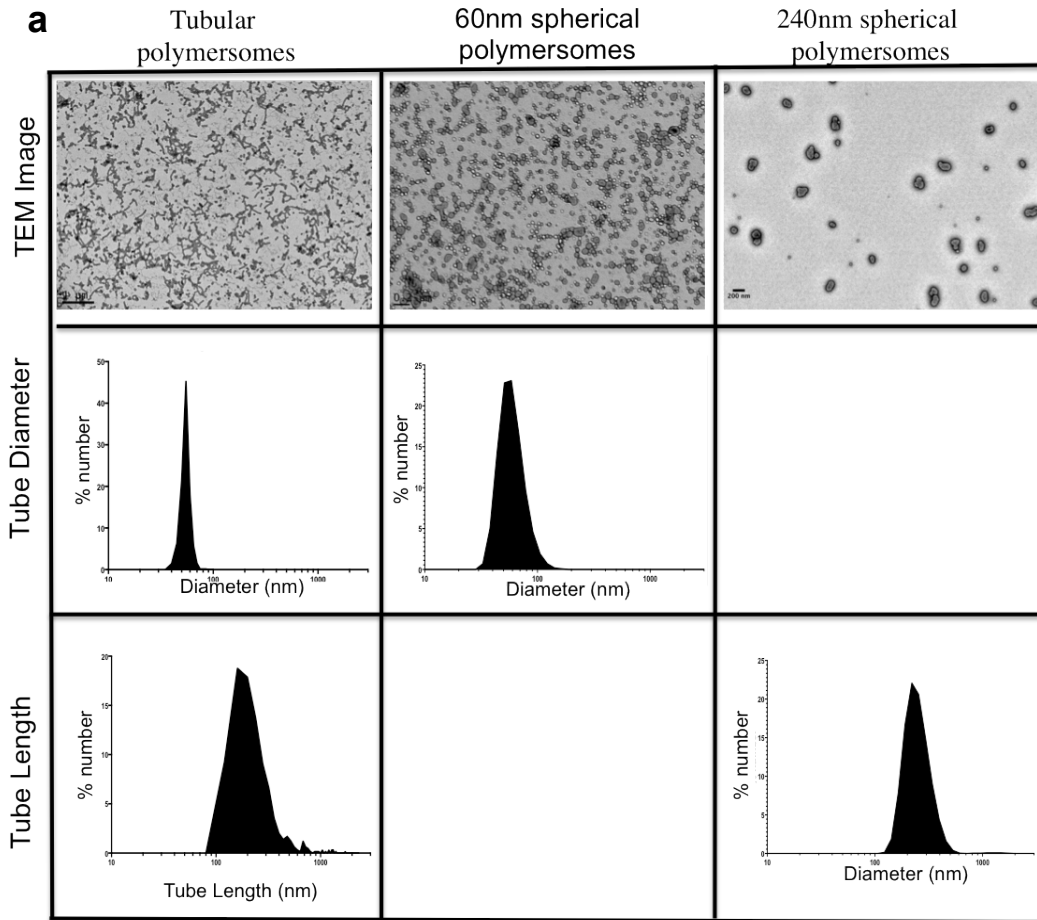


Figure 5.7 Internalisation of tubular polymersomes into neutrophils

(a) The first row shows TEM photomicrographs of rhodamine-labelled tubular polymersomes or spherical polymersomes (scale bars left to right 1 μ m, 200nm, 200nm). Below are histograms of the diameter and length distributions. Histograms of spherical polymersomes were made by DLS and histograms of tubular polymersome length and diameter were measured on ImageJ from TEM photomicrographs. (b) Neutrophil rMFI over time after incubation with rhodamine-labelled spherical or tubular polymersomes as measured by flow cytometry (error bars =SEM, n=3).

Confocal microscopy of neutrophils treated with rhodamine-labelled tubular polymersomes reveals a predominant cell membrane localisation after 5 hours incubation, whereas, after 9 hours the rhodamine signal can be observed within the cells, signifying successful internalisation (Figure 5.8). This was further confirmed by 3D analysis of confocal z-stacks from a single neutrophil (Figure 5.9).

5.2.5 Delivery of BSA into Neutrophils by Tubular Polymersomes

One key advantage of polymersomes compared with solid micelles is their ability to encapsulate hydrophilic molecules within their aqueous lumen. It has previously been shown that the protein bovine serum albumin (BSA) can be efficiently encapsulated within polymersomes by electroporation (Wang et al., 2012). To test the ability of tubular polymersomes to encapsulate and deliver BSA, BSA was labelled with an Alexa-647 fluorophore using a commercially available labelling kit (Invitrogen). PMPC-PDPA tubular polymersomes were formed and purified using the protocol described earlier and mixed with the Alexa-647 labelled BSA. The BSA was encapsulated by electroporation and un-encapsulated BSA was removed using gel permeation chromatography. Using confocal microscopy, free tubular polymersomes encapsulating the fluorescent BSA were visualised (Figure 5.10a) and a clear tubular morphology was observed. The tubular polymersomes were incubated with primary human neutrophils for 9 hours. Confocal microscopy revealed successful intracellular delivery (Figure 5.10b).

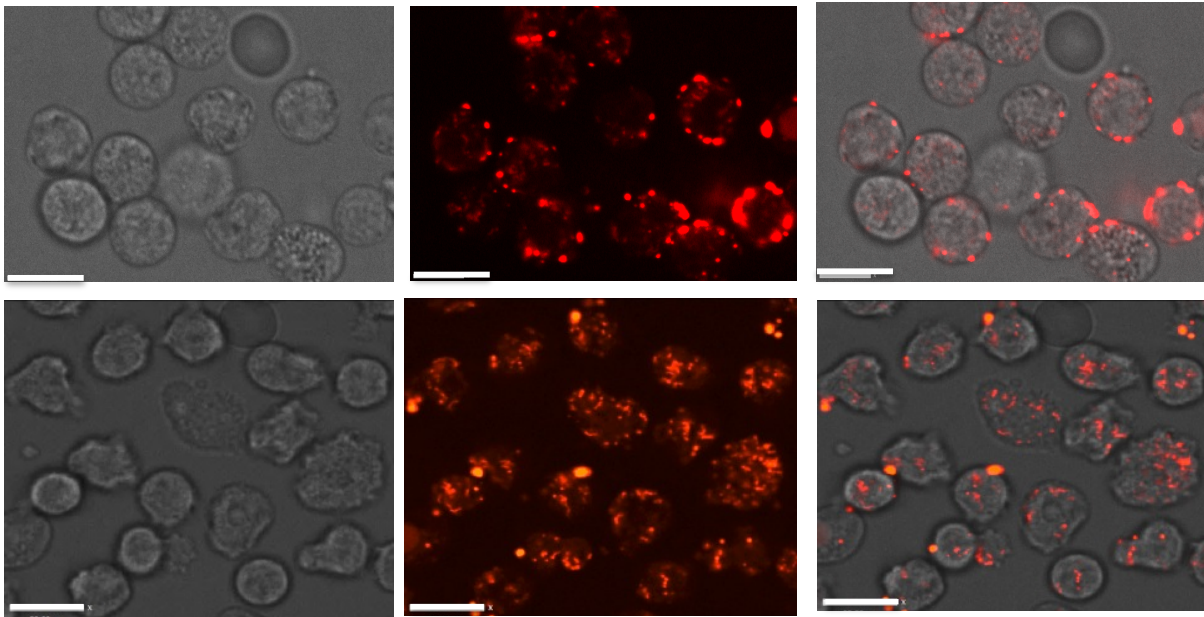


Figure 5.8 Delayed internalisation of tubular polymersomes.

Laser scanning confocal microscopy of neutrophil after 5 hours (upper images) or 9 hours (lower images) incubation with rhodamine labelled tubular polymersomes. Tubular polymersomes are predominantly located on the plasma membrane at 5 hours, but are subsequently internalised by 9 hours incubation, scale bar =8 μm .

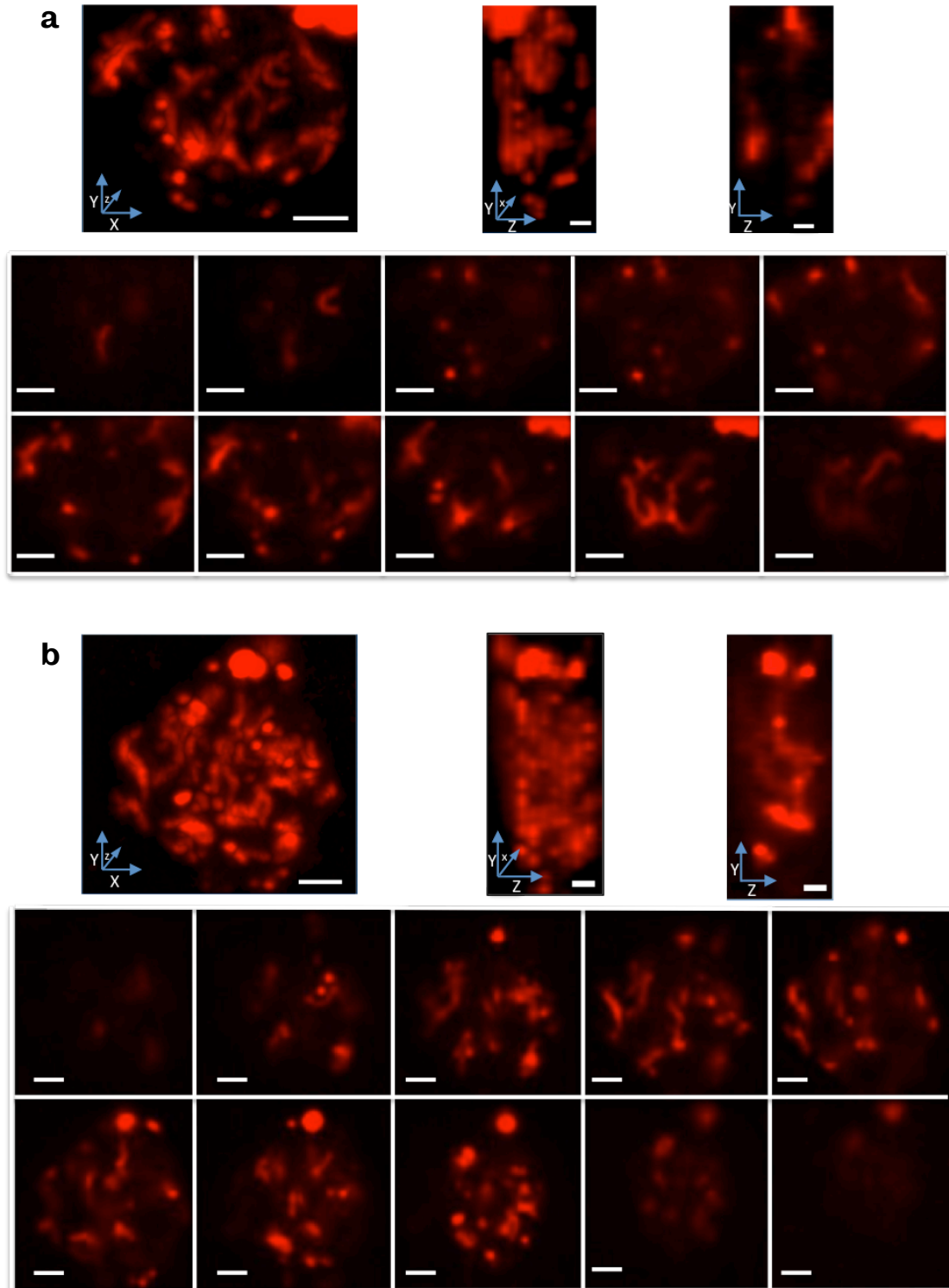


Figure 5.9 Analysis of confocal z-stacks of single neutrophils.

3D analysis of confocal z-stacks of a single neutrophil after 5 hours (a) or 9 hours (b) treatment with rhodamine-labelled tubular polymersomes. The neutrophils are shown in a three-dimensional view at two angles: straight on (left image) and at 90 degrees (central image). The right image shows a single x-slice through the centre of the neutrophil. The lower images in c and d display a montage of the confocal micrographs at the different z-planes. Scale bars= 2 μ m.

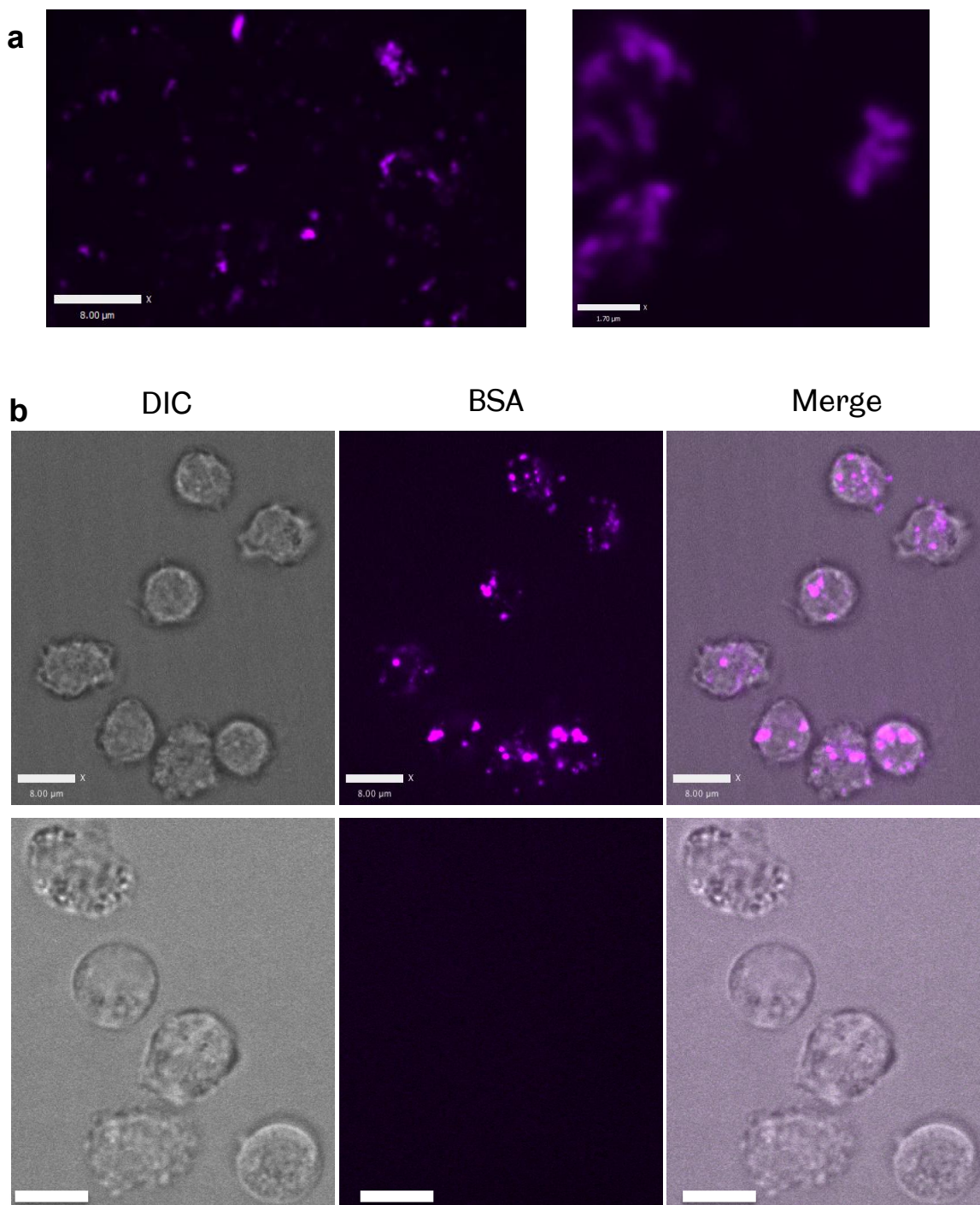


Figure 5.10 Tubular polymersomes encapsulating Alexa-647 labelled BSA.

(a) Confocal micrograph of tubular polymersomes encapsulating Alexa-647 labelled BSA. (b) Confocal micrographs of neutrophils after 9 hours incubation with tubular polymersomes encapsulating BSA (upper image) and a control (lower image). Scale bars= 1.7 μ m for upper right image, all other images were 8 μ m.

5.3 Discussion

5.3.1 Non-Spherical Nanoparticles

A number of studies have demonstrated the formation of non-spherical nanoparticles using various techniques (Grumelard et al., 2004, Reiner et al., 2006, Mitragotri and Lahann, 2009). Rod-like nanoparticles and cylindrical micelles in particular have shown promise in drug delivery for their unique targeting abilities and high circulation times (Kolhar et al., 2013, Geng et al., 2007, Cai et al., 2007, Christian et al., 2009). In this chapter I have explored a novel method of producing and purifying PMPC-PDPA tubular polymersomes and demonstrate that these tubular polymersomes are internalised by human neutrophils.

5.3.2 Internalisation of Tubular Polymersomes

The average diameter of the tubular polymersomes was approximately 60nm, which is within the optimal diameter range that has been determined theoretically and experimentally to induce membrane wrapping (reviewed in (Canton and Battaglia, 2012)). This interaction, coupled with the high avidity of the PMPC polymer for the scavenger receptors may promote the embedding of tubular polymersome within the membrane (Colley et al., 2014b). The exact mechanism by which tubular polymersomes are internalised is not known. The strong interaction with the membrane could result in a local deformation, which may progress to full endocytosis. Alternatively, the attached tubes may be slowly internalised from the natural turnover of the plasma membrane. A similar type of delayed or “frustrated endocytosis”, has been observed for other highly

anisotropic particles (Decuzzi and Ferrari, 2008, Champion and Mitragotri, 2006, Champion and Mitragotri, 2009).

Although shape is known to be an important factor in the design of a nanovector, the majority of engineered nanovectors are spherical. Cylindrical micelles can be formed from amphiphilic block copolymers by controlling the polymer packing parameter (Israelachvili et al., 1976), but these solid structures do not contain an aqueous core that enables the encapsulation of water soluble molecules (Blanzas et al., 2009a). Carbon nanotubes have received a great deal of attention as drug delivery carriers and although visually carbon nanotubes appear similar in structure to tubular polymersomes, they have very different properties (Canton and Battaglia, 2012). In contrast to the “soft” polymer membrane, carbon nanotubes are held together by strong covalent bonds making them stiff and inflexible, and their entry into cells occurs through a “needle-like” penetration of the membrane (Kostarelos et al., 2007, Porter et al., 2007).

The striking effects of polymersome shape on internalisation kinetics that was observed in this chapter highlight opportunities for tubular polymersomes in drug delivery. Despite the large volume of the tubular polymersomes, the amount of tubular polymersomes internalised by the neutrophils at the later time points was surprisingly high. The larger membrane and luminal volumes of tubular polymersomes may allow encapsulation of larger drug loads and provide higher delivery efficiencies.

It is now well known that non-spherical nanoparticles have different internalisation kinetics when compared to their spherical counterparts, which may be in part due to the large energy requirement for endocytosis of particles with high aspect ratios. In particular, the tangent angle at the point of contact between the particle and cell has been shown to play an important role in whether internalisation takes place and upon the rate of internalisation (Decuzzi and Ferrari, 2008, Champion and Mitragotri, 2006, Gratton et al., 2008a). Undoubtedly, the impact of shape on internalisation will also depend on the size, surface chemistry and viscoelastic properties of the particle (Decuzzi and Ferrari, 2008, Decuzzi et al., 2004).

Another intriguing feature of the tubular polymersomes presented here is the long dwelling time at the cell surface before internalisation. Particles with high aspect ratios, such as tubular polymersomes, form more receptor-ligand interactions leading to an increased binding avidity. However, the shape of tubular polymersomes results in higher dislodging forces from shear stress (Decuzzi and Ferrari, 2006, Lee et al., 2009). This means the ability for a tubular polymersome to bind to a cell in the blood stream will also depend strongly on the affinity of the receptor ligand interaction and the density of receptors on the target cell. Recently, the Mitragotri group demonstrated rod shaped particles with attached targeting ligands had higher specificity than spherical particles when injected into mice (Kolhar et al., 2013). This is because weak receptor ligand interactions were more easily influenced by shear induced

unbinding (Kolhar et al., 2013). One could speculate that the high membrane dwelling time of tubular polymersomes observed in this study could result in an even greater probability of shear-induced detachment. Another possibility is that the shape will influence its intracellular fate, particularly if the length of the tube exceeds 500nm, the typical diameter of a mature endosome; but further work is required to elucidate these features in more detail.

Chapter 6: Polymersomes as Intracellular Delivery

Vectors for Human Neutrophils

6.1 Introduction

Neutrophils are the most abundant leukocyte in the human body and play a key role in the neutralisation of invading pathogens. Circulating neutrophils follow chemical gradients to travel towards sites of infection and clear pathogens by phagocytosis. Cytoplasmic granules deliver a cocktail of proteases and reactive oxygen species to the phagosome allowing the neutrophil to digest the pathogen intracellularly. Importantly, if neutrophils sense invading pathogens but are unable to reach them, they degranulate, releasing their degradative contents into the extracellular environment. This process is essential for preventing bacterial escape, but if poorly regulated can be harmful to the host (Nathan and Ding, 2010).

Neutrophils undergo spontaneous apoptosis and are thought to have a short life span of approximately 8 hours in the circulation (Dancey et al., 1976). During apoptosis, neutrophils downregulate receptors on their membrane and upregulate “eat me” signals such as phosphatidylserine, which allow apoptotic neutrophils to be recognised and phagocytosed by macrophages (Fadok et al., 1998a). The phagocytosis of apoptotic neutrophils by macrophages is an important step in inflammation resolution that prompts macrophages to release

anti-inflammatory cytokines such as TGF- β that help resolve inflammation and initiate tissue repair (Fadok et al., 1998b).

Stimulation with survival factors such as granulocyte-macrophage colony-stimulating factor (GM-CSF) delays neutrophil apoptosis, which can lead to excessive tissue damage as observed in multiple disease states such as rheumatoid arthritis and chronic obstructive pulmonary disease (Cascao et al., 2010, Snelgrove et al., 2010, Beeh and Beier, 2006). Glucocorticoids are generally the first line of treatment in chronic inflammatory disease and have proven very effective in treating eosinophil dominated inflammation, but their effectiveness in neutrophil dominated inflammatory diseases is more modest (Haslett et al., 1990).

Promotion of neutrophil apoptosis is a potential therapeutic direction for the treatment of neutrophil dominated inflammatory diseases, but genetic alteration of neutrophils has proven very difficult. This has not only limited our ability to manipulate neutrophils for therapeutic intervention, but has also limited our understanding of the molecular pathways that control neutrophil function. A number of neutrophil transfection techniques have been suggested, but none have become well established (Leuenroth et al., 2000, Sivertson et al., 2007). Cyclin-dependent kinase inhibitors (CDKi), such as the broad spectrum CDKi (R)-roscovitine, have emerged as potent inducers of neutrophil apoptosis. Pioneering work by Rossi and colleagues demonstrated that incubation with (R)-roscovitine led to rapid neutrophil apoptosis, even in the presence of potent

survival factors such as GM-CSF (Rossi et al., 2006). To demonstrate its potential *in vivo*, roscovitine was tested in three inflammatory mouse models including serum transfer arthritis. In all three models roscovitine accelerated inflammatory resolution (Rossi et al., 2006).

Despite the effectiveness of roscovitine in animal models of inflammation, its use clinically may be limited by off-target side effects. In phase I clinical trials reported side effects included nausea, vomiting, hyperkalaemia and liver dysfunctions (Le Tourneau et al., 2010, Benson et al., 2007). In addition, non-selective induction of neutrophil apoptosis could compromise the immune system and leave patients more susceptible to infection. Targeting roscovitine to neutrophils at inflammatory sites using polymersomes may help reduce side effects and improve the therapeutic outcome of roscovitine treatment for inflammatory diseases.

In this chapter PMPC-PDPA polymersomes are explored as a drug delivery vector for neutrophils. The polymersomes are tested for adverse effects on neutrophil viability and cytokine release and their ability to deliver small molecules, antibodies and siRNA is investigated. Finally, roscovitine is encapsulated within polymersomes and its ability to promote neutrophil apoptosis *in vitro* and accelerate inflammatory resolution *in vivo* is explored.

6.2 Results

6.2.1 Neutrophil Viability and Cytokine Release are not Altered by PMPC-PDPA Polymersomes

The use of nanotechnology in medicine has often been limited by concerns of toxicity. Activation of the immune system by nanoparticles can cause local inflammation or lead to life threatening hypersensitivity reactions (Chanan-Khan et al., 2003, Nel et al., 2006). Neutrophils contain a destructive arsenal of degradative enzymes within their granules, which, if released can cause extensive tissue damage. Activation of neutrophils by certain types of nanoparticles has been reported, but the impact of nanoparticles on neutrophils has been poorly studied (Goncalves et al., 2011).

Activation of neutrophils and initiation of their pro-inflammatory response results in the production and release of inflammatory cytokines such as interleukin-8 (IL-8) (Strieter et al., 1992). IL-8 is a potent chemokine that is involved in coordinating the immune response. In order to determine the effect of polymersomes on neutrophil activation, primary human neutrophils were purified from healthy donors and incubated with polymersomes for 4 or 6 hours. Supernatants were extracted and the IL-8 concentration was measured by ELISA. Incubation with polymersomes at a concentration of 1mg/ml had no effect on neutrophil IL-8 release compared with the PBS control (Figure 6.1 a, b). In contrast, the positive control lipopolysaccharide (LPS) activated neutrophils and increased the amount of IL-8 release at both time points.

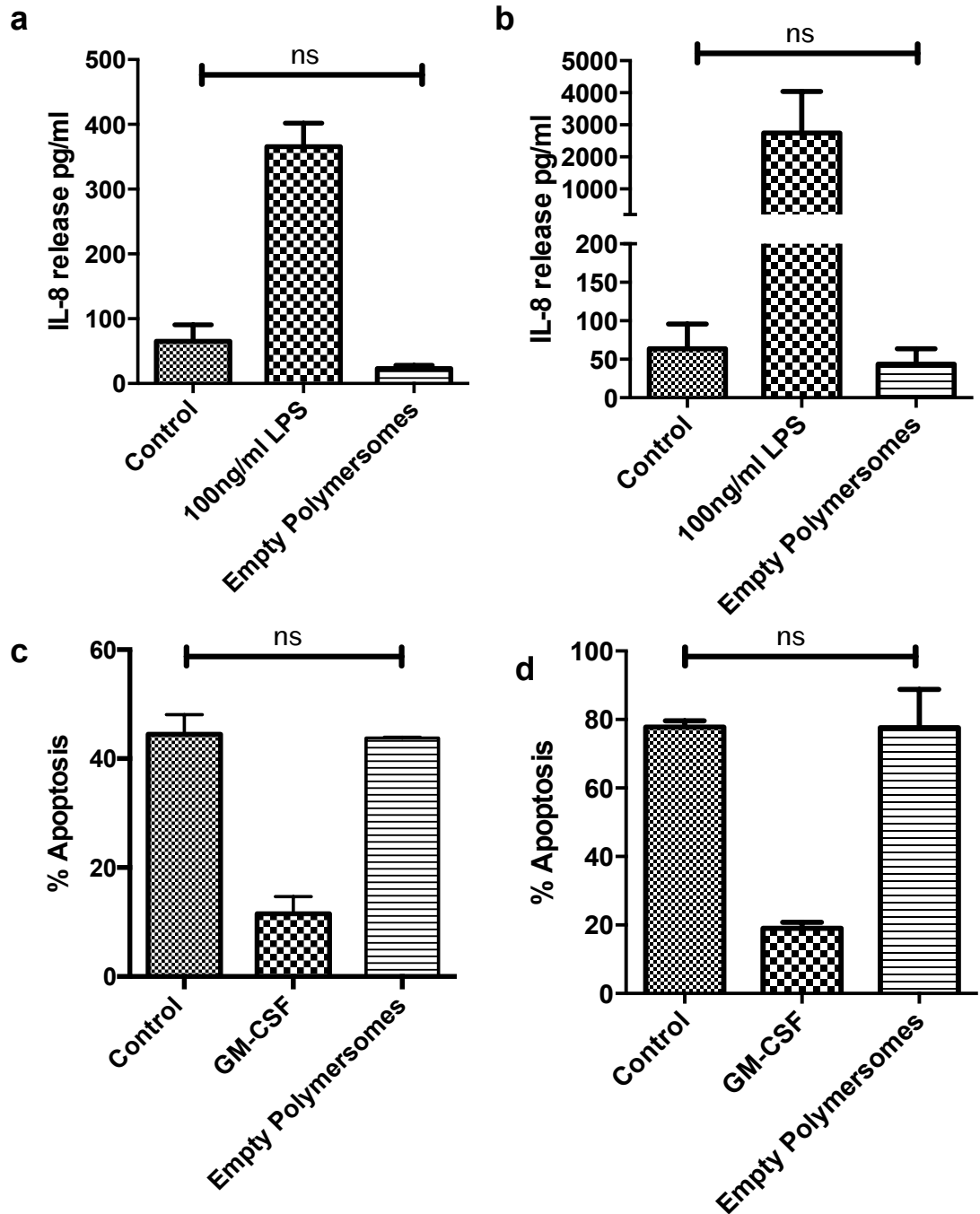


Figure 6.1 Polymersomes have no effect on neutrophil activation or viability.

Interleukin-8 cytokine release of primary human neutrophils was measured using an ELISA after 4 hours (a) or 6 hours (b) incubation with 1 mg/ml polymersomes. The rate of apoptosis was measured after 8 hours (c) or 20 hours (d) incubation with polymersomes. Polymersomes did not significantly differ from the PBS control in all experiments (one-way ANOVA with post Bonferroni's multiple comparison test, error bars = SEM, n=3).

Neutrophils undergo spontaneous apoptosis, but incubation of neutrophils with pro-inflammatory molecules can increase their lifespan. To ensure that polymersomes do not alter neutrophil life span, the rate of neutrophil apoptosis after incubation with 1mg/ml of polymersomes for 8 or 20 hours was measured by observation of nuclear morphology on histochemically stained cytospin preparations according to well accepted protocols (Parker et al., 2009). Treatment with GM-CSF resulted in a reduction in neutrophil apoptosis at both time points, but empty polymersomes had no effect on neutrophil apoptosis counts compared with the PBS control (Figure 6.1c, d).

6.2.2 Polymersome Mediated Delivery of Rhodamine B Octadecyl ester Perchlorate

Our knowledge of neutrophil biology and ability to manipulate them for therapeutic intervention has been restricted by an absence of effective neutrophil vectors. To explore the potential of PMPC-PDPA polymersomes as a neutrophil vector, polymersomes encapsulating the fluorescent dye rhodamine B octadecyl ester perchlorate (rhodamine B) were incubated with human neutrophils. After just 15 minutes incubation, neutrophils displayed an increased fluorescence intensity compared to the control; this demonstrates a rapid uptake of the polymersomes by neutrophils. The neutrophil fluorescence signal continued to rise throughout the experiment (Figure 6.2a).

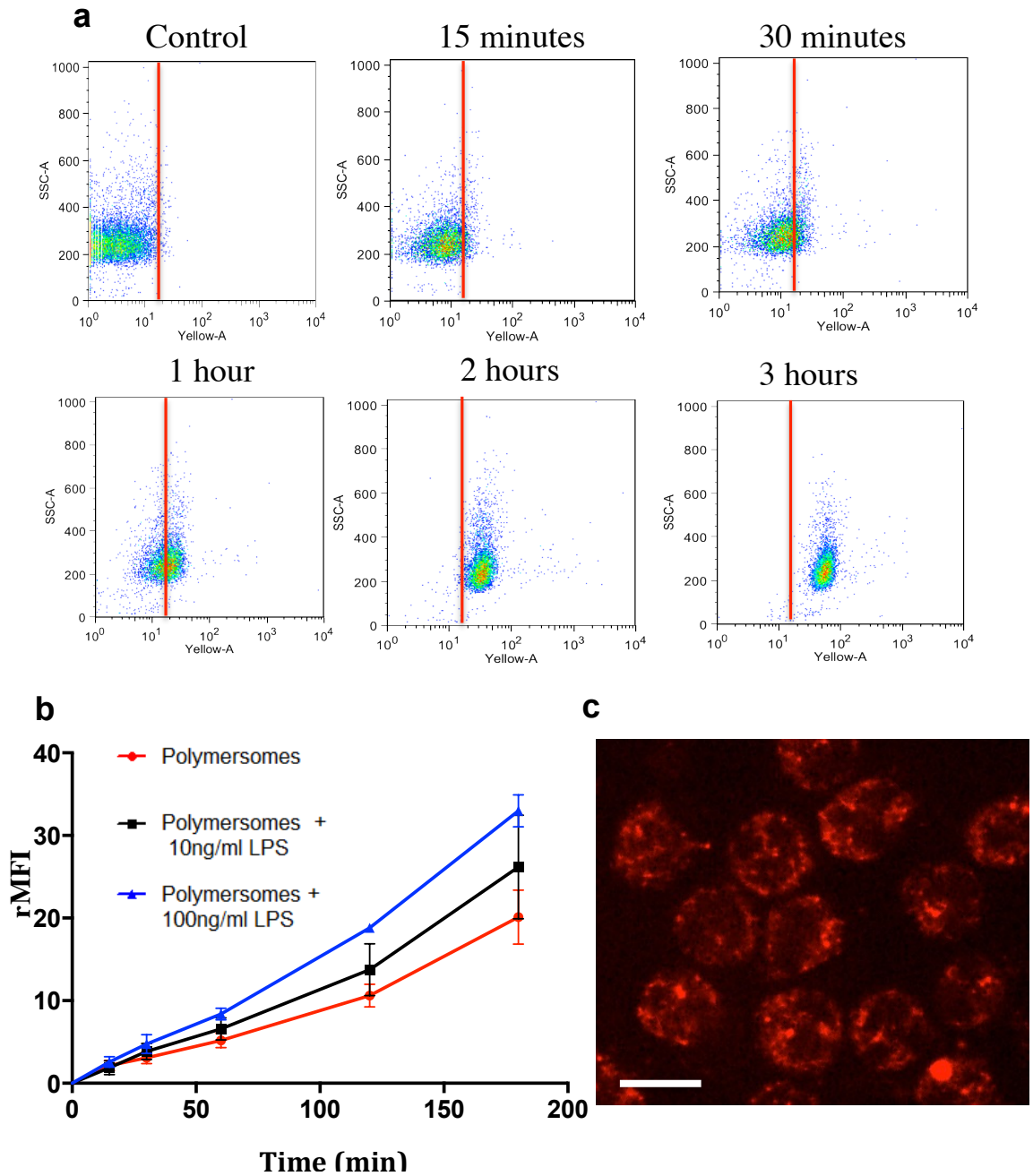


Figure 6.2 Uptake of polymersomes encapsulating rhodamine B by human neutrophils.

(a) Flow cytometry dot plot of primary human neutrophils after incubation with polymersomes encapsulating the fluorescent dye rhodamine B octadecyl ester perchlorate. (b) The fluorescence intensity of neutrophils over time as measured by flow cytometry with or without the prior addition of LPS to activate the neutrophils. Neutrophil fluorescence significantly increased with incubation time ($p < 0.0001$) and upon treatment with LPS ($p < 0.01$) (Two-way ANOVA $n = 3$). (c) A single z-slice confocal photomicrograph of neutrophils after 3 hours incubation with the polymersomes encapsulating rhodamine B., scale bar = $8\mu\text{m}$.

To investigate the effect of neutrophil activation on polymersome internalisation, neutrophils were incubated for 1 hour with lipopolysaccharide at 10ng/ml or 100ng/ml. Polymersomes encapsulating rhodamine B were added to the media and the neutrophil fluorescence intensity was measured at multiple time points by flow cytometry as described above. Using a two way ANOVA it was shown the neutrophil fluorescence intensity significantly increased with time ($p < 0.0001$) and upon treatment with LPS ($P = 0.0029$), indicating a more rapid internalisation of polymersomes in activated cells. A confocal photomicrograph of neutrophils after 3 hours treatment with polymersomes encapsulating rhodamine B is shown in Figure 6.2c. Having established polymersomes could successfully deliver small molecules into neutrophils I then sought to identify which functional cargoes could be successfully delivered.

6.2.3 Polymersome Mediated Delivery of Alexa-647-Labelled siRNA

Small interfering RNAs (siRNA) are double stranded RNA molecules that were discovered in plants as an antiviral defence mechanism for targeting and silencing genes recognised as viral (Hamilton and Baulcombe, 1999). siRNA acts in the RNA interference (RNAi) pathway by assembling with and activating the RNA-induced silencing complex (RISC). The RISC complex binds to the complementary nucleotide sequence resulting in site-specific cleavage and silencing. siRNAs are routinely used in genetic screens and for understanding gene function in a range of cell types. But genetic manipulation of neutrophils by RNA interference (RNAi) has proven challenging because the short life span and

sensitivity of neutrophils to the methods of introducing nucleic acids have prevented the success of mainstream approaches.

The ability of PMPC-PDPA polymersomes to rapidly deliver cargo into neutrophils without effecting their viability or activation may allow them to overcome the shortfalls of other transfection methods. To test this hypothesis Alexa-647 labelled siRNA was encapsulated within polymersomes using pH switch. The polymersomes were then incubated with human neutrophils for 6 hours, before the cells were washed and analysed by flow cytometry or confocal microscopy. Flow cytometry analysis of neutrophils incubated with increasing siRNA concentration demonstrated a dose dependent increase in the neutrophil fluorescence intensity (Figure 6.3a, b). Photomicrographs of neutrophils treated with 40nM siRNA encapsulated within polymersomes are shown in Figure 6.3c. Dispersed fluorescence throughout the cells demonstrates successful cytoplasmic delivery of the siRNA.

Mcl-1 is known to play an important role in neutrophil survival and has a high turnover rate, which makes it an excellent target for siRNA knockdown experiments (Moulding et al., 1998, Moulding et al., 2001). Mcl-1 siRNA was encapsulated within polymersomes by pH switch. Polymersomes encapsulating Mcl-1 were incubated with highly pure human neutrophils for 20 hours in the presence of GM-CSF. Following incubation, the rate of neutrophil apoptosis was assessed and RNA was extracted for analysis by reverse transcription polymerase chain reaction (RT-PCR).

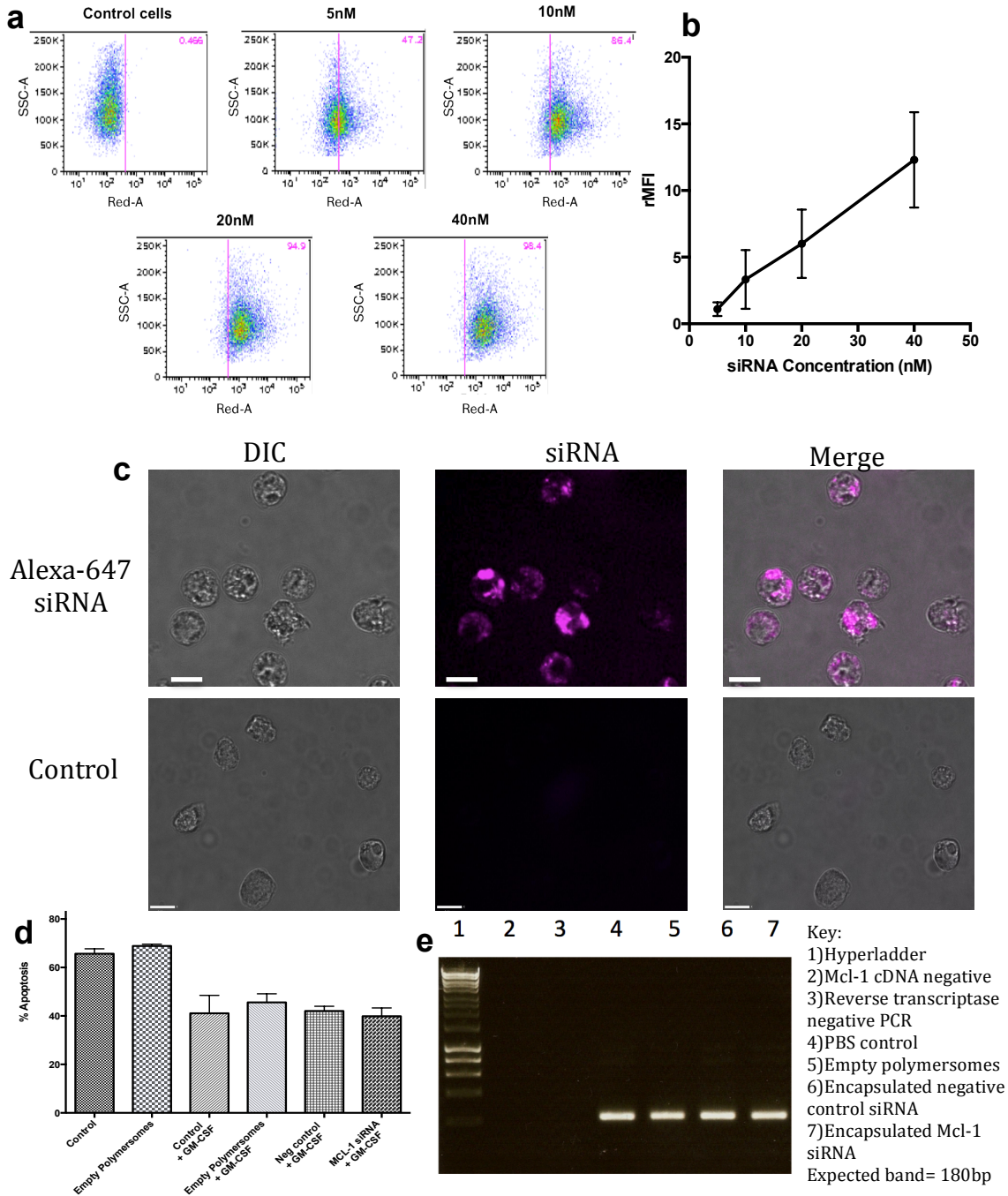


Figure 6.3. Delivery of siRNA into live human neutrophils.

(a) Flow cytometry dot plots of neutrophils incubated with polymersomes encapsulating Alexa-647 labelled siRNA for 6 hours. (b) A line graph of neutrophil rMFI after treatment with polymersomes encapsulating siRNA with final siRNA concentrations of 5, 10, 20 or 40nM (error bars = SEM, n=2). (c) Confocal photomicrographs of neutrophils incubated with 40nM of Alexa-647 siRNA loaded, polymersomes, scale bar = 8µm. (d) Neutrophil apoptosis rates after incubation for 20 hours with polymersomes encapsulating Mcl-1 siRNA at a final concentration of 10nM of siRNA, and 1mg/ml of polymer (error bars = SEM, n=3). (e) PCR analysis of neutrophil Mcl-1 RNA.

Despite the successful siRNA delivery demonstrated in the microscopy experiments, polymersome mediated delivery of Mcl-1 siRNA failed to increase the rate of neutrophil apoptosis (Figure 6,3 d). The unsuccessful knockdown of Mcl-1 was confirmed by RT-PCR, which demonstrated that neutrophil Mcl-1 levels were no different from the controls.

6.2.4 Polymersome Mediated Delivery of Antibodies

Direct delivery of antibodies into neutrophils may allow a more rapid intervention by inhibiting the intracellular targets after binding to their functional epitopes. To explore the ability of polymersomes to deliver antibodies into neutrophils, α -tubulin targeting antibodies were fluorescently labelled with the Alexa-647 tag using a commercially available kit. The fluorescent antibodies were then encapsulated within spherical polymersomes using pH switch and incubated with human neutrophils for 6 hours prior to analysis by confocal microscopy. α -tubulin was chosen as a target because a clear labelling of the microtubule network would demonstrate successful epitope binding. As shown in Figure 6.4, the antibody was successfully delivered intracellularly, but the fluorescent signal was predominantly localised to distinct foci within the cell.

Large cargo such as antibodies may be less efficiently released from endosomes after polymersome internalisation. TEM studies on human fibroblasts have demonstrated that approximately 30% of gold labelled antibodies are retained within the endolysosomal compartment (Canton et al., 2013). The volume of the

endosomes and lysosomes is relatively low compared to the entire cell volume, this means the concentration of antibody within the compartment will be high, which may hinder the visualisation of the released antibody. To reduce the signal from the endolysosomal compartment the fluorescence quencher trypan blue was co-encapsulated with the α -tubulin antibody. As shown in Figure 6.4, the addition of trypan blue resulted in a more diffuse signal in the neutrophils, demonstrating endosomal release of some of the polymersome cargo, however, the fluorescence staining still did not appear to label the microtubule network.

Many commercial antibodies available for immunocytochemistry are designed to target fixed antigens; therefore, antibodies delivered into live cells using polymersomes may have a lower affinity for the un-fixed antigen. Alternatively, the targeting epitope may be less accessible without the addition of a permeabilising detergent and the absence of a blocking step may further reduce the targeting efficiency of the antibody.

To explore whether a different neutrophil epitope was preserved, the experiment was repeated using a Brilliant Violet-labelled antibody targeting a γ -tubulin epitope. To improve the image quality, the neutrophils were adhered to the glass-imaging dish by coating the dish with fibrinogen, preventing the neutrophils from moving excessively during microscopy. A confocal photomicrograph of neutrophils after 6 hours incubation with γ -tubulin encapsulating polymersomes is displayed as an intensity plot, with weak signal shown in blue and strong signal in red. As shown in Figure 6.5 the antibody was

present throughout the cytoplasm of the neutrophil but regions of high intensity were commonly observed, suggesting centriole targeting (the predominant location of γ -tubulin).

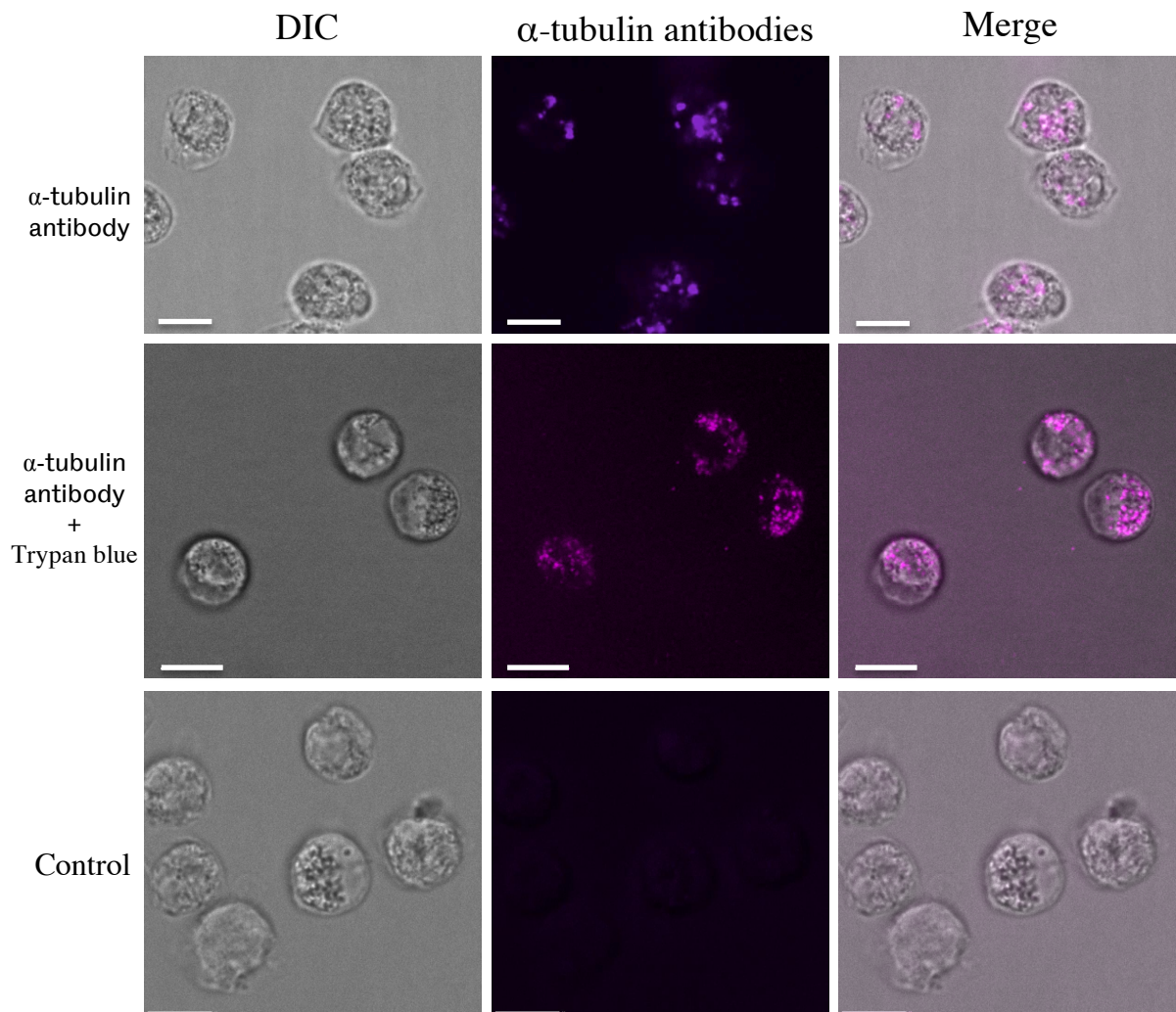


Figure 6.4 Intracellular delivery of alexa-647 labelled α -tubulin targeting antibodies into human neutrophils

Confocal micrographs of human neutrophils after 6 hours incubation with polymersomes encapsulating an alexa-647 labelled α -tubulin targeting antibody or a PBS treated control. Scale bar =8 μ m.

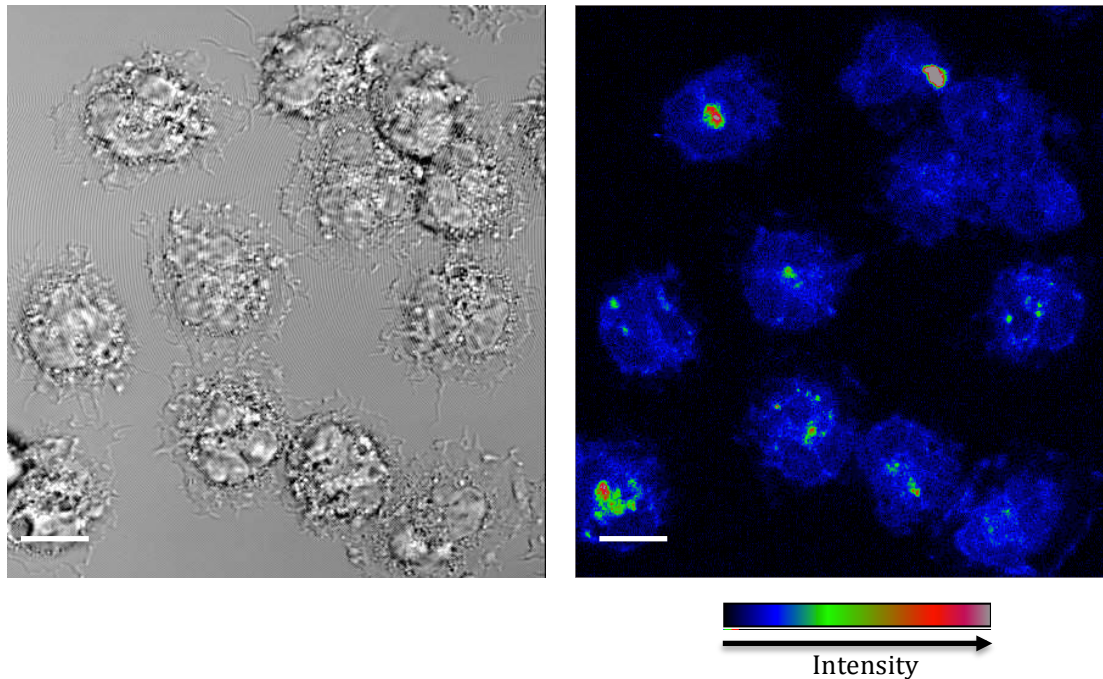


Figure 6.5 Polymersome delivery of brilliant violet γ -tubulin targeting antibody into neutrophils.

Neutrophils were adhered to an imaging dish by coating the glass with fibrinogen. Adhered neutrophils were incubated with polymersomes encapsulating a brilliant violet-labelled γ -tubulin targeting antibody and trypan blue for 6 hours before visualisation by laser scanning confocal microscopy. The fluorescence image (right) is displayed as an intensity projection with regions of low fluorescence intensity shown in blue and high intensity is shown in red. The left image shows the DIC. Scale bar = $8\mu\text{m}$.

6.2.5 Encapsulation of (R)-Roscovitine to Promote Neutrophil

Apoptosis

Neutrophil apoptosis and subsequent clearance by macrophages is an important step in inflammation resolution (Savill et al., 1989). But an abundance of survival factors can delay constitutive neutrophil apoptosis in patients with chronic inflammatory diseases. The broad-spectrum cyclin-dependent kinase inhibitor (CDKi) (R)-roscovitine down regulates the survival protein Mcl-1 leading to neutrophil apoptosis even in the presence of survival factors (Leitch et al., 2010). However, off-target side effects in clinical trials have limited its

clinical use and non-selective neutrophil apoptosis may leave patients susceptible to infection.

Encapsulation of roscovitine within polymersomes may help improve their uptake into neutrophils and reduce off-target side effects. To test this hypothesis roscovitine was encapsulated within polymersomes using the film-rehydration method. A thin film was prepared containing 2mg of roscovitine and 18mg of PMPC-PDPA. 2ml of PBS was added to the film and this was left stirring for 4 weeks. Free roscovitine was subsequently removed using gel permeation chromatography. To explore the effect of particle shape on roscovitine delivery, polymersomes were purified using differential centrifugation. As described in Chapter 5, large lyotropic structures were initially removed and the particles were purified by size and density into tubular and spherical polymersomes (Figure 6.6).

To measure the concentration of encapsulated roscovitine and the final concentration of polymer after purification, polymersomes were disassembled by lowering the pH to 6 through the addition of 1M HCL and then the concentration of polymer and roscovitine was analysed using HPLC with UV detection. The concentration of polymer and roscovitine was measured for the roscovitine loaded tubular and spherical polymersomes (Table 6.1).

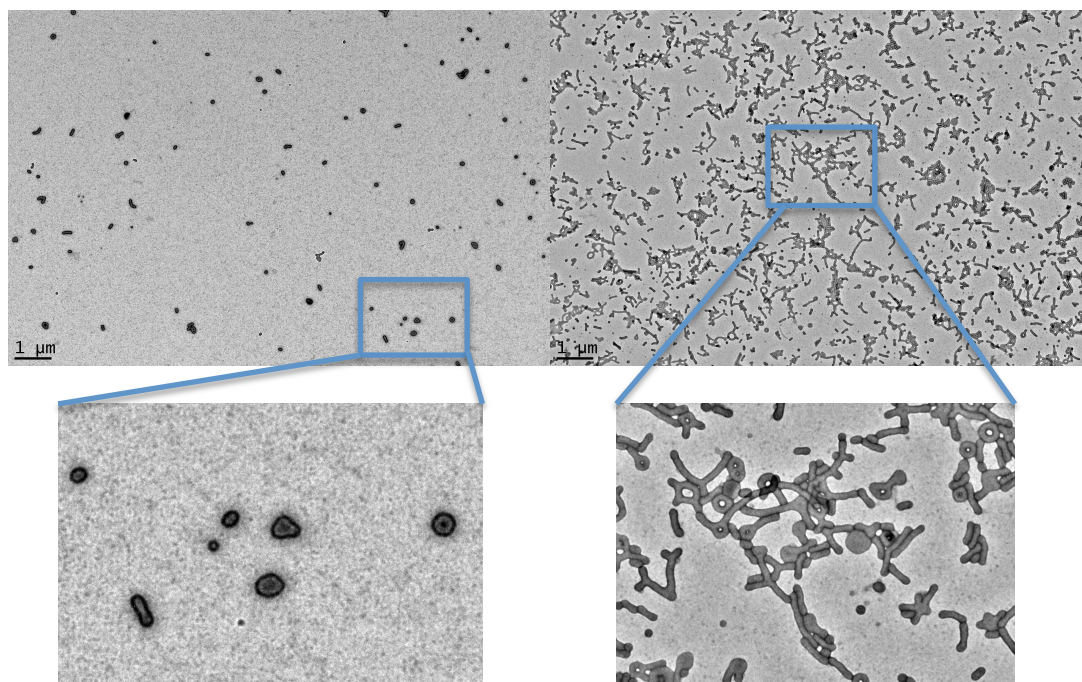


Figure 6.6 Purification of (R)-roscovitine polymersomes by shape.

TEM micrographs of (R)-roscovitine polymersomes formed using the film rehydration method. Using differential centrifugation particles were separated into fractions containing predominantly spherical structures (left) and tubular structures (right).

Having shown roscovitine could be successfully encapsulated within polymersomes, the ability of roscovitine polymersomes to induce human neutrophil apoptosis was tested *in vitro*. Human neutrophils treated with the pro-inflammatory survival cytokine GM-CSF were incubated for 8 hours with tubular or spherical polymersomes encapsulating roscovitine, or free roscovitine. Neutrophil viability was assessed with annexin V and propidium iodide staining and analysed by flow cytometry (Figure 6.7).

	Polymer Concentration (mg/ml)	Roscovitine concentration (mg/ml)
Tubular polymersomes	4.73	0.51
Spherical polymersomes	5.70	0.10

Table 6.1 Polymer and roscovitine concentrations for tubular polymersomes and spherical polymersomes as measured by RP-HPLC.

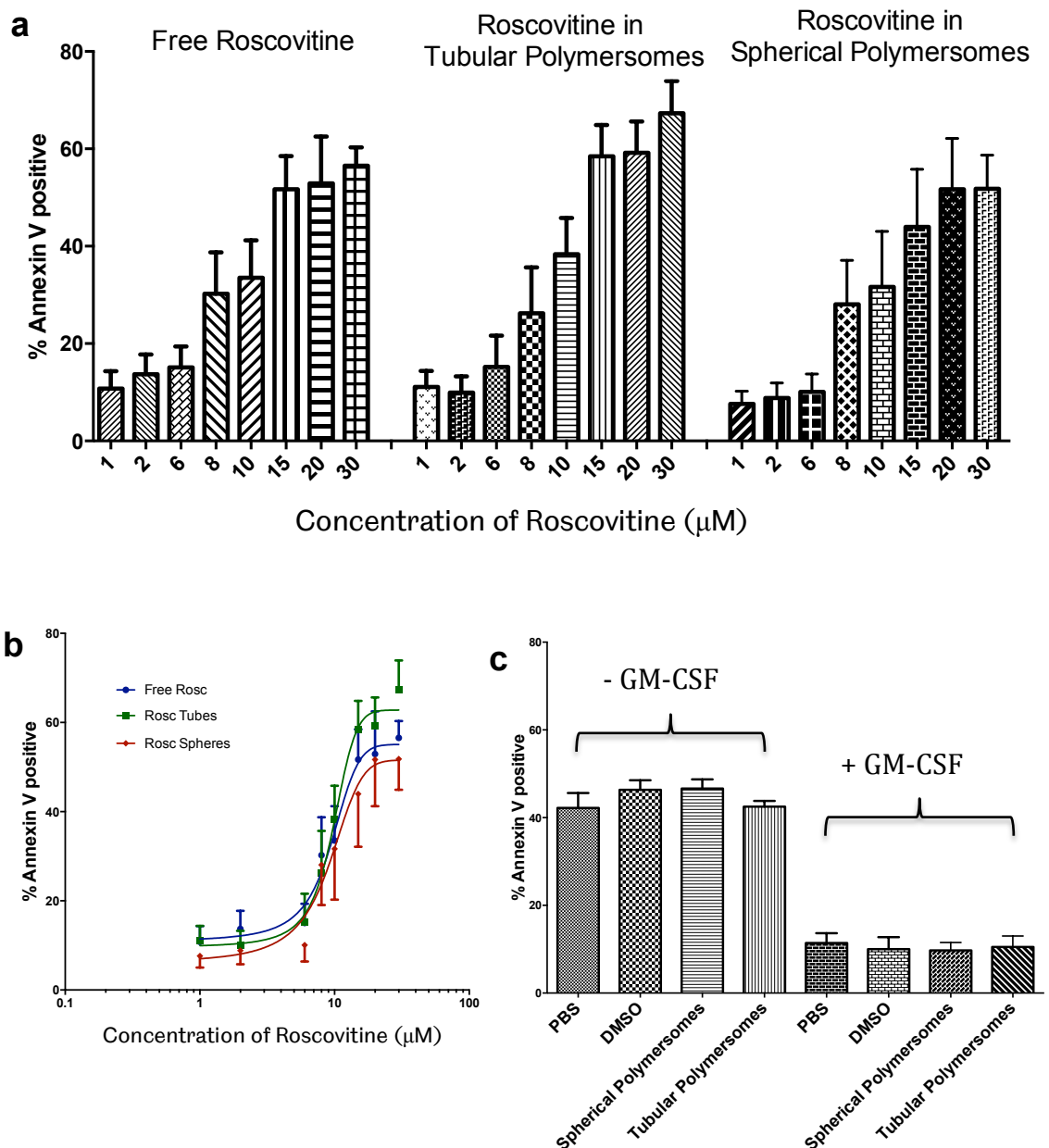


Figure 6.7 Roscovitine encapsulated within polymersomes promotes neutrophil apoptosis in vitro.

Spherical and tubular polymersomes encapsulating roscovitine or free roscovitine were incubated with human neutrophils for 8 hours in the presence of the survival cytokine GM-CSF. Neutrophils were then stained with alexa-647 annexin V and propidium iodide and viability was assessed by flow cytometry. The percentage of annexin V positive neutrophils after 8 hours incubation with free or encapsulated roscovitine is displayed as a bar chart (a) or a line graph (b). Treatment with roscovitine significantly increased neutrophil apoptosis in all 3 groups ($P < 0.0001$) but encapsulation within tubular polymersomes or spherical polymersomes did not significantly affect the apoptosis rates compared with free roscovitine (two way ANOVA, $n=4$, error bars show SEM). (c) A bar graph of the controls without roscovitine after 8 hours treatment with or without GM-CSF (error bars = SEM, $n=4$).

Treatment with roscovitine resulted in a dose dependent increase in the rate of apoptosis in all three groups, but encapsulation of roscovitine within tubular or spherical polymersomes had no significant effect on the rate of neutrophil apoptosis compared with free roscovitine. This shows that both tubular polymersomes and spherical polymersomes can successfully deliver functional roscovitine into human neutrophils at a rate similar to the diffusion of free roscovitine. Although encapsulated roscovitine had a similar effect to free roscovitine *in vitro*, polymersomes may enable roscovitine to be delivered more efficiently to neutrophils *in vivo*.

6.2.6 Encapsulated (R)-Roscovitine Promotes Inflammation Resolution in an *in vivo* Zebrafish Model

To test the ability of roscovitine polymersomes to enhance inflammation resolution *in vivo*, a model of inflammation in the zebrafish larvae was employed. In this model neutrophils are tracked using a zebrafish line that labels neutrophils with GFP under the control of the neutrophil specific myeloid peroxidase promoter (Bennett et al., 2001, Renshaw et al., 2006). Transection of the caudal fin induces a local inflammatory response that is tracked and quantified by manual counting of neutrophils at the site of injury (Renshaw et al., 2006). Neutrophils are recruited to the injury site with maximal numbers occurring at approximately 6 hours post injury (hpi). After 6 hours, the number of neutrophils gradually declines and by 24 hours the number returns to baseline levels signifying inflammation resolution.

By incubating zebrafish with anti-inflammatory compounds and counting neutrophils in the tail region at 12hpij, the ability of these compounds to speed up inflammation resolution can be measured and quantified. This has led to the discovery of novel pro-resolving therapeutics in compound screens (Robertson et al., 2014a) and helped to elucidate the mechanism of anti-inflammatory compounds (Burgon et al., 2014).

To compare the ability of encapsulated roscovitine and free roscovitine to promote inflammation resolution *in vivo*, mpx:GFP zebrafish were injured by tail transection and good responders were treated at 4hpij with free roscovitine, roscovitine encapsulated in tubular polymersomes, roscovitine encapsulated in spherical polymersomes, or their controls. At 12hpij the neutrophils at the site of injury were counted under a fluorescence microscope to determine if the treatments improved the speed of inflammation resolution. As shown in Figure 6.8, spherical polymersomes encapsulating roscovitine significantly reduced the number of neutrophils at the site of injury at 12hpij compared with the free roscovitine or control groups. Roscovitine loaded tubular polymersomes also reduced the number of neutrophils at the site of injury compared with the free roscovitine or the untreated control groups, but was not significantly lower than the empty tubular polymersomes. These results demonstrate that roscovitine encapsulated in polymersomes can speed up inflammation resolution *in vivo* significantly better than the free drug.

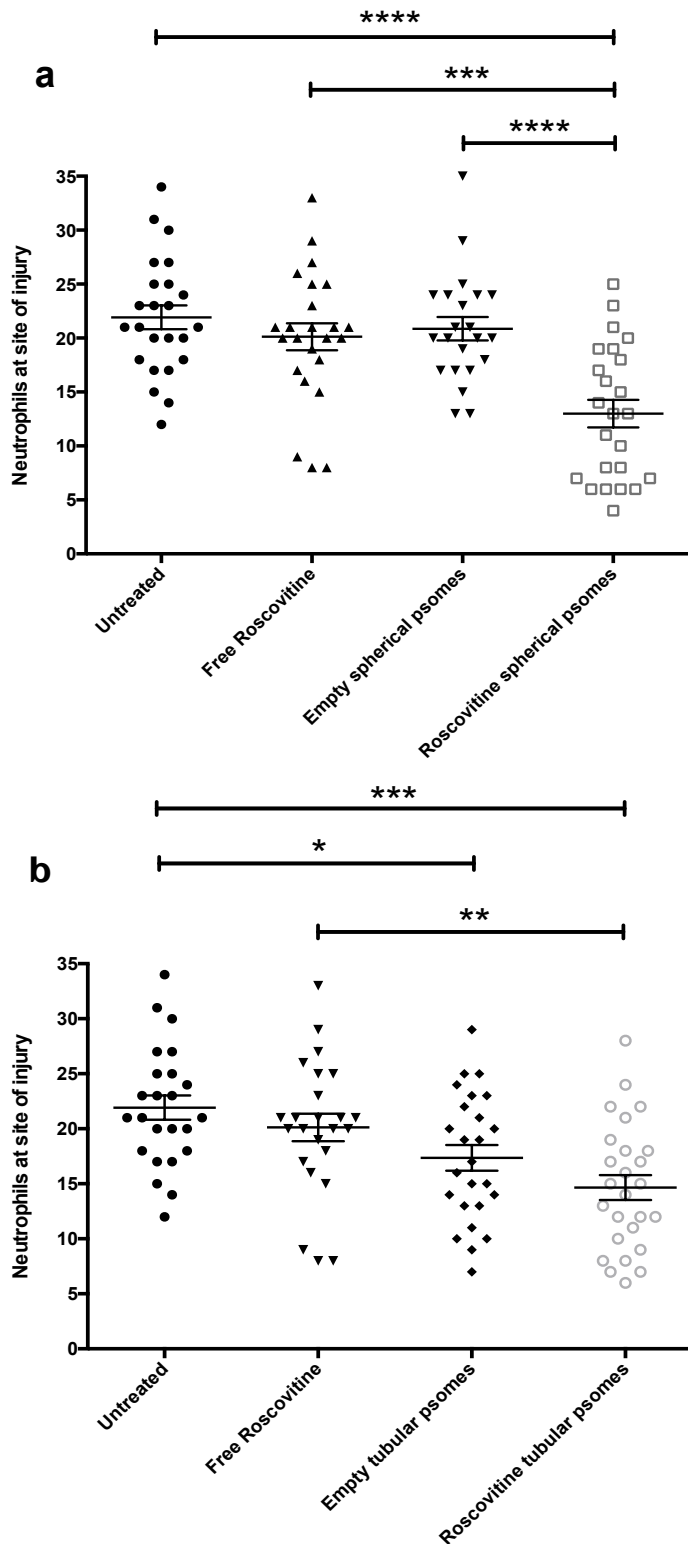


Figure 6.8. Encapsulation of roscovitine within polymersomes improves inflammation resolution in vivo.

3-day post fertilisation zebrafish larvae (mpx:GFP) were subject to tail injury by transection of the tail end. 4 hours post injury they were treated with roscovitine encapsulated in spherical polymersomes (a), roscovitine encapsulated within tubular polymersomes (b) or their indicated controls. Neutrophil numbers at the site of injury were assessed at 12 hours post injury (one way ANOVA with Bonferroni's post hoc comparison, * $P < 0.05$, ** $P < 0.01$, *** $P < 0.001$, **** $P < 0.0001$. Lines represent the mean and error bars = SEM, $n = 3$).

6.3 Discussion

Neutrophils have proven very difficult cells to manipulate and no commercially available vector exists that enables the efficient intracellular delivery of cargo within their short life span and without compromising their viability. In this chapter I have investigated PMPC-PDPA polymersomes as an intracellular delivery vector for neutrophils demonstrating that the polymersomes do not induce human neutrophil cytokine release or alter their rates of constitutive apoptosis. I go on to show that polymersomes can deliver a range of cargo into neutrophils, including functional roscovitine that promoted neutrophil apoptosis *in vitro* and sped up inflammation resolution *in vivo*.

6.3.1 Polymersomes do not Alter Neutrophil Viability or Induce Cellular Activation

Neutrophil numbers are carefully regulated to prevent unnecessary damage to host tissues (Summers et al., 2010). A successful neutrophil vector must be able to deliver their cargo intracellularly without inducing cell death, or neutrophil activation. Polymersomes had no effect on the rate of neutrophil apoptosis, or on their cytokine release. This result is in keeping with the high biocompatibility of PMPC-PDPA polymersomes that has been previously demonstrated on a range of cell types (Massignani et al., 2009).

The ability of PMPC-PDPA polymersomes to deliver cargo into neutrophils without detrimental effects may be attributed to a number of features. Firstly, the neutral charge of the polymersome membrane prevents unspecific

interactions between polymersomes and cellular components. Cationic nanoparticles, which are widely used as reagents for delivering nucleic acids *in vitro*, can activate leukocytes through TLR4 (Kedmi et al., 2010). In fact lipoplex, the most studied non-viral nucleic acid vector, causes systemic inflammation and toxicity when injected into mice (Elouahabi et al., 2003) (Baatz et al., 2001). Another non-fouling property of these polymersomes can be attributed to the highly hydrophilic PMPC block, it has been estimated that each MPC monomer is solvated by up to 24 water molecules (Blanazs et al., 2011). This makes the polymersomes highly resistant to protein adhesion.

6.3.2 Polymersome Delivery of Fluorescent Cargo into Neutrophils

Polymersomes encapsulating fluorescent rhodamine B were internalised rapidly into human neutrophils with an increase in neutrophil fluorescence apparent after just 15 minutes incubation. As neutrophils are short-lived cells, rapid intracellular delivery is essential to allow functional effects to occur within the neutrophil lifespan. It is likely that the rapid internalisation of polymersomes is mediated through a high binding affinity for their target receptors. It has previously been shown that the class B scavenger receptors, scavenger receptors B1 and B2 (SR-BI/SRBII) and CD36 are essential for the internalisation of PMPC-PDPA polymersomes into a number of cell types (Colley et al., 2014a). Indeed CD36 and SR-BI/SRBII are expressed by neutrophils (Murphy et al., 2011, Koprassch et al., 2004), but further experiments are needed to confirm their role in polymersome internalisation.

Interestingly, activation of neutrophils with lipopolysaccharide resulted in a significant increase in the rate of polymersome internalisation. Activated neutrophils upregulate surface receptors from intracellular granules allowing them to respond quickly to invading pathogens (Bainton et al., 1987). An up-regulation of the polymersome target receptors would result in an increased rate of polymersome binding and endocytosis (Decuzzi and Ferrari, 2006).

6.3.3 Polymersome Mediated Delivery of siRNA and Antibodies into Human Neutrophils

Neutrophil dominated inflammatory diseases could be treated by promoting neutrophil apoptosis through genetic manipulation or protein transduction, however, despite a number of attempts, neutrophils have proved to be very difficult cells to transfect. Successful knockdown of Mcl-1 in human neutrophils has been reported through the simple addition of Mcl-1 targeting oligonucleotides to the cell media (Leuenroth et al., 2000, Sivertson et al., 2007). Yet oligonucleotides do not readily pass through the cell membrane and other groups, including our own, have failed to reproduce this effect (Renshaw and Rossi personal communications). A number of other reports have described successful neutrophil transduction using viral vectors (Dick et al., 2009, Johnson et al., 2006, Gardiner et al., 2002). Manipulating neutrophils using viral vectors has great potential in deciphering molecular mechanisms of neutrophil function (Dick et al., 2009), but viruses activate neutrophils and may be rapidly cleared *in vivo*. Other methods used to deliver molecules into neutrophils include transactivator of transcription (TAT)-fusion proteins (Gao et al., 2007, Uriarte et

al., 2011, Alvarado-Kristensson et al., 2004), electroporation techniques (Johnson et al., 2006, Tamassia et al., 2008) and BioPORTER lipid vesicles (Rane et al., 2003), but these techniques often lack efficiency and none have become well established in the neutrophil community.

In this study polymersomes successfully delivered fluorescent siRNA into human neutrophils as assessed by flow cytometry and confocal microscopy. But the knockdown of Mcl-1 with encapsulated siRNA was unsuccessful. The reason for this is unclear. It is possible that the quantity of siRNA delivered was insufficient; indeed many nucleic acid vectors require final siRNA concentrations higher than the 10nM used in this study. Future studies should optimise the encapsulation protocol in order to improve the encapsulation efficiency of siRNA so that higher concentrations can be delivered.

The intracellular delivery of antibodies offers another approach for manipulating cellular processes by targeting intracellular epitopes. Unlike genetic manipulation, antibodies offer the ability to target molecular machinery rapidly. Antibodies may be engineered to target functional groups on active intracellular proteins rendering them ineffective, or alternatively, intracellular antibodies may be useful in live imaging for deciphering intracellular processes. A small number of publications have demonstrated intracellular antibody delivery using liposomes (Rahmanzadeh et al., 2010), viral vectors (Kondo et al., 2008), micro-needles (Li et al., 2009) and electroporation (Baron et al., 2000)

but these techniques are impractical in neutrophils due to their short life spans and sensitivity to activation.

Fluorescent α -tubulin targeting antibodies were successfully delivered into neutrophils *in vitro* using PMPC-PDPA polymersomes. Confocal microscopy of neutrophils highlighted distinct foci within the cell, but these were less apparent when the fluorescence quencher trypan blue was co-encapsulated within the polymersomes. This is consistent with previous studies that demonstrate reduced labelling of endosomes and lysosomes in human dermal fibroblasts after co-encapsulation of trypan blue (Lewis et al., 2009).

Antibodies for intracellular imaging are often designed for fixed epitopes and involve antigen retrieval through invasive methods such as heat shock. The poor labelling of α -tubulin may represent a reduced affinity for the unfixed epitope or an inability to reach the epitope. When the experiment was repeated with a fluorescent γ -tubulin targeting antibody, an improved targeting specificity was observed. In fact, this antibody also been shown to successfully bind to its epitope when delivered using polymersomes into a number of other cell types including human dermal fibroblasts, further supporting that this antibody remains functional in live cells (Canton et al., 2013). Further experiments will be necessary to determine the potency of delivered antibodies in inhibiting intracellular proteins such as Mcl-1.

6.3.4 Polymersome Delivery of Roscovitine Drives Neutrophil Apoptosis

Roscovitine encapsulated in both tubular polymersomes and spherical polymersomes promoted neutrophil apoptosis *in vitro* in a dose dependent manner. The ability of encapsulated roscovitine to promote neutrophil apoptosis was not significantly different to that of free roscovitine. This suggests that the mass of roscovitine delivered into neutrophils using polymersomes is similar to the mass of free roscovitine that enters cells by simple diffusion. Surprisingly, tubular polymersomes were able to deliver enough roscovitine within 8 hours to promote neutrophil apoptosis, despite the delay in their internalisation (see chapter 5). The hydrophobic drug roscovitine may be able to diffuse from bound tubular polymersomes into the cell interior. Alternatively, the relatively large volume of tubular polymersomes may be sufficient to deliver enough roscovitine into the cells despite the delay in internalisation.

Clinically, the delivery of roscovitine in polymersomes offers a number of advantages compared with the free drug. Firstly, the higher uptake of polymersomes into activated neutrophils may improve the targeting of neutrophils at inflamed sites with less effect on resting neutrophils. Secondly, the leaky vasculature surrounding inflamed tissue results in the passive accumulation of nanoparticles (Bader, 2012). This has been exploited for the delivery of anti-inflammatory compounds or imaging agents in the diagnosis and treatment of rheumatoid arthritis (Ishihara et al., 2009, Koning et al., 2006, Williams et al., 1987, Vanniasinghe et al., 2009). Finally, improved polymersome

targeting can be achieved by functionalising the polymersome corona with ligands or antibodies (Broz et al., 2005).

6.3.5 Roscovitine Polymersomes Enhance Inflammation Resolution in an *in vivo* Zebrafish Model

Zebrafish provide an excellent model for studying the innate immune system. The transparent embryos contain neutrophils and macrophages, which can be fluorescently labelled by transgenesis. By 3dpf the innate immune system is fully functional allowing its role in infection and inflammation to be understood in the absence of the adaptive immune system that does not mature until 1 month post fertilisation (Willett et al., 1997). The zebrafish has been instrumental in the study of neutrophil biology, leading to a number of discoveries in the field, including the role of neutrophil reverse migration in inflammation resolution (Mathias et al., 2006, Elks et al., 2011). Zebrafish tail fin transection results in sterile inflammation characterised by neutrophil recruitment peaking at 6hpij and neutrophil resolution by 24hpij (Renshaw et al., 2006). This provides a relatively cheap, rapid and effective method for testing the potency of anti-inflammatory compounds in promoting inflammation resolution (Wang et al., 2014, Robertson et al., 2014a).

Using the zebrafish tail transection model, it was shown that roscovitine encapsulated within tubular polymersomes or spherical polymersomes promoted inflammation resolution significantly quicker than the free drug. Unexpectedly, zebrafish treated with empty tubular polymersomes showed a

small improvement in inflammation resolution compared with the untreated control. This could be caused by a number of mechanisms; for instance, the high dwelling time of the tubular polymersomes on the neutrophil membrane may impede the contact of pro-inflammatory mediators resulting in a suppression of neutrophil activation. Further research will be necessary to confirm this effect. Free roscovitine alone did not significantly reduce neutrophil numbers at the injury site compared with the untreated control, although the mean number of neutrophils was slightly lower. The improvement of encapsulated roscovitine compared with the free drug suggests that polymersomes were more efficient at delivering the drug into zebrafish neutrophils than could be achieved by simple diffusion.

These results agree with previous studies that have demonstrated polymersomes are able to successfully deliver molecules through tissues. For instance, recently it was demonstrated that polymersomes can successfully deliver molecules through *ex vivo* human skin, and were able to deliver molecules to the central core of a multicellular tumour spheroid (Pegoraro et al., 2014, Colley et al., 2014b). It is likely the improved ability of roscovitine polymersomes to deliver molecules across tissues increased their ability to reach the neutrophils in the zebrafish tail. These results highlight the possibility of using roscovitine encapsulated within polymersomes for treating inflammatory skin diseases such as psoriasis or severe eczema.

Chapter 7: Treating Intracellular *Staphylococcus aureus* Infection with Encapsulated Antibiotics

7.1 Introduction

The great variety and severity of *Staphylococcus aureus* (*S. aureus*) disease demonstrates the versatility of this human pathogen. Colonisation of a third of the population enables *S. aureus* to maintain its ubiquity within our environment and predisposes colonised individuals to infection (Weidenmaier et al., 2004). The complexity of *S. aureus* infection makes the disease challenging to treat, and persistent or recurrent infections are common even after intervention with active antibiotics (Chang et al., 2003).

One of the most devastating *S. aureus* diseases is blood stream infection, which is associated with a mortality rate of approximately 30%. Upon entering the bloodstream, *S. aureus* is capable of infecting almost any organ and metastatic infections in the heart valves and bones are particularly common. Metastatic infections are associated with the formation of pus filled abscesses and the destruction of vital tissue.

Although *S. aureus* is not traditionally considered an intracellular pathogen, increasing evidence demonstrates *S. aureus* can internalise and survive within host cells (Garzoni and Kelley, 2009). Up-regulation of virulence factors involved in capsule development, oxidative stress and the neutralisation of

antimicrobials, enable *S. aureus* to resist destruction once engulfed by professional phagocytes (Voyich et al., 2005). Survival within phagocytes, particularly neutrophils, may not only reduce *S. aureus* killing, but also facilitate *S. aureus* dissemination and tissue infection (Thwaites and Gant, 2011). In fact, *S. aureus* mutants that cannot survive within neutrophils cause far fewer disseminated and lethal infections (Voyich et al., 2005) and the transfer of neutrophils containing intracellular *S. aureus* into naïve mice, is sufficient for *S. aureus* to establish infection (Gresham et al., 2000).

The zebrafish has emerged as a powerful model for studying *S. aureus* infection (Prajnsnar et al., 2008). In this model *S. aureus* injected into the circulation are quickly engulfed by neutrophils and macrophages and the infection is slowly resolved, or escalates and overwhelms the fish. Overwhelming infections are linked to the formation of tissue abscesses, which grow and are eventually fatal. Importantly, this model revealed that zebrafish infected with a mixed inoculum of two *S. aureus* strains, have an output population of bacteria that is often asymmetrically distributed, with one of the two strains predominating (Prajnsnar et al., 2012). This population skewing was dependent on the presence of myeloid cells, suggesting that *S. aureus* infection can be dispersed and then seeded by host phagocytes (Prajnsnar et al., 2012). Analysis of abscess formation in the kidneys of mice was also shown to be predominantly clonal (McVicker et al., 2014).

Intracellular persistence of *S. aureus* might not only facilitate their dissemination into tissues, but also protect them from extracellular antibiotics. For these reasons, targeting intracellular bacteria may remove *S. aureus* bacteraemia more rapidly, reducing the risk of tissue abscesses and relapsing infections. In this chapter I explore the potential of PMPC-PDPA polymersomes to encapsulate antibiotics and deliver them into phagocytes to treat intracellular *S. aureus* infection.

7.2 Results

7.2.1 Encapsulation of Antibiotics within Polymersomes

To explore polymersomes as a drug vector in the treatment of intracellular *S. aureus* infection, four different antibiotics were encapsulated by either pH switch or film rehydration: vancomycin, lysostaphin, gentamicin and rifampicin. Following antibiotic encapsulation, free drug was removed using gel permeation chromatography.

To ensure the polymersomes were optimal for the delivery of antibiotics into neutrophils, they were designed and purified to have average diameters of approximately 150-200nm (Figure 7.1). This diameter range, as demonstrated in Chapter 4, is thought to be most effective at delivering cargo into neutrophils. TEM photomicrographs of polymersomes after purification formed using the pH switch or film rehydration method are shown in Figure 7.1a. The size range measured by DLS, was similar for all polymersome samples regardless of antibiotic cargo.

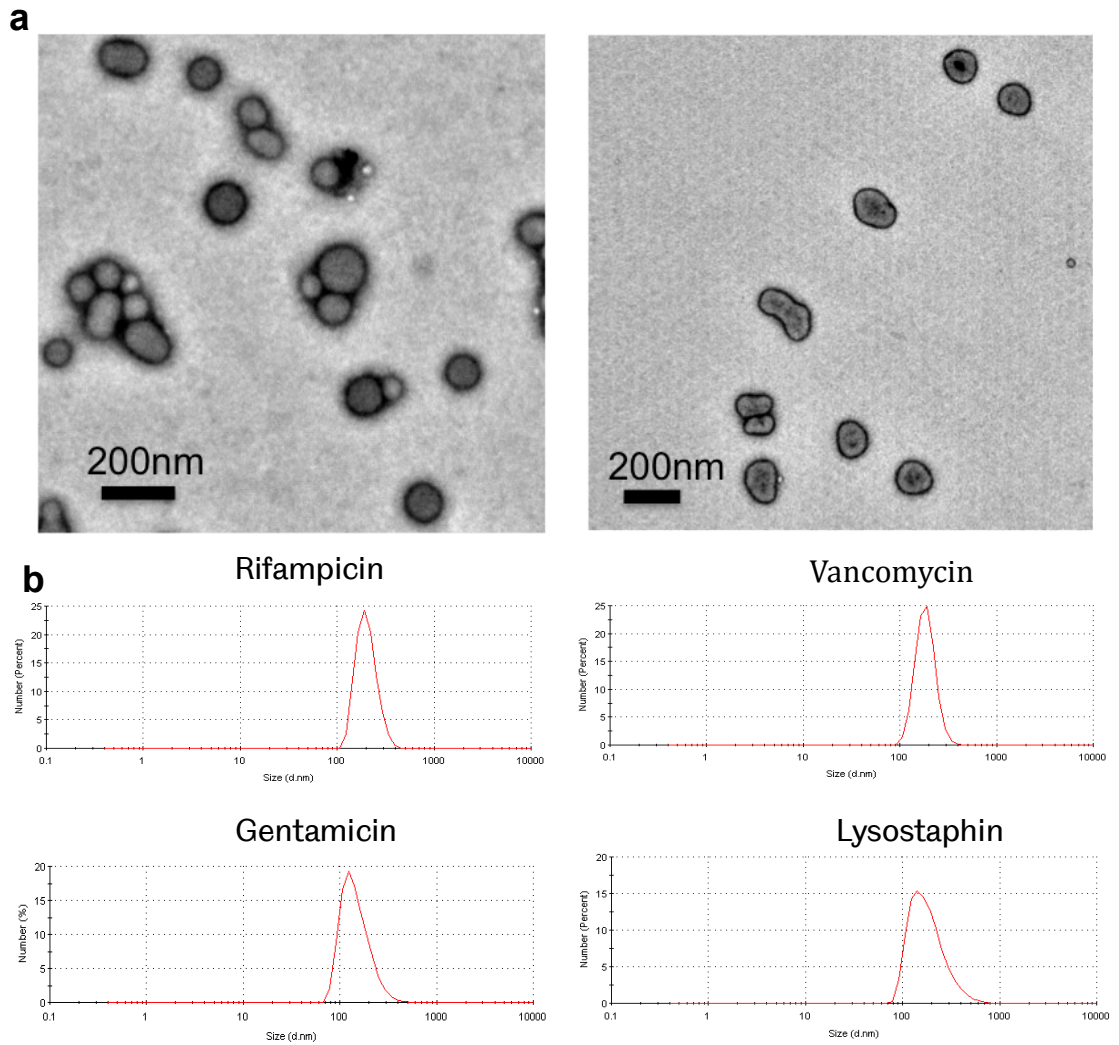


Figure 7.1 Purification of polymersomes to the optimum size range. Polymersomes encapsulating antibiotics were purified to the optimal size range for neutrophil internalisation. (a) Representative photomicrographs of polymersomes formed by film rehydration (left) or pH switch (right). (b) Size histograms for each polymersome sample as measured by DLS.

After polymersome formation and purification, the concentration of encapsulated antibiotics was measured. Rifampicin has a high absorbance at the lower end of the visible spectrum enabling its concentration to be calculated by visible spectroscopy at 475nm. Gentamicin has a poor UV/visible absorbance, therefore its concentration was quantified using a previously described method that utilises the reaction between gentamicin amino groups and fluorescent o-phthaldialdehyde (OPA) (Gubernator et al., 2006). This allowed gentamicin quantification by fluorimetry. The quantification of encapsulated vancomycin and lysostaphin was achieved using RP-HPLC with associated UV detection.

The calculated concentrations of encapsulated antibiotics within 10mg/ml of polymersomes are displayed below in Table 7.1. Lysostaphin is an antibacterial enzyme so encapsulation was not attempted using the film rehydration method, where prolonged stirring times at room temperature could lead to protein degradation. Similarly, rifampicin was not encapsulated by pH switch because this hydrophobic antibiotic must first be resuspended in an organic solvent, which may interfere with polymersome formation. The quantity of antibiotic encapsulated within polymersomes varied widely between the different antibiotics tested. The highest load was seen for rifampicin, which is most likely a result of the drug hydrophobicity.

7.2.2 Polymersome Mediated Intracellular Delivery of Antibiotics to Treat Intracellular *S. aureus* infection in THP-1 Macrophages.

To study the ability of antibiotic loaded polymersomes to treat intracellular *S. aureus* infection, a macrophage infection model developed by Jamil Jubrail was employed. This model utilises THP-1 monocytes a cell line derived from an acute monocytic leukaemia patient. THP-1 cells were differentiated into macrophages using phorbol-12-myristate-13-acetate (PMA) and infected with *S. aureus* at a multiplicity of infection (MOI) of 5 for 6 hours. The cells were then washed and gentamicin added to the media to remove extracellular *S. aureus*. The macrophages were then treated with polymersomes encapsulating an antibiotic, empty polymersomes with the free antibiotic, or the free antibiotic alone. At 6.5 hours, 22 hours and 46 hours post infection (hpif), macrophages were lysed, plated on agar and the number of viable colonies counted.

Antibiotic	Final concentration by pH switch ($\mu\text{g/ml}$)	Final concentration by film rehydration ($\mu\text{g/ml}$)
Vancomycin	0.266	3.11
Gentamicin	15	12
Lysostaphin	4	n/a
Rifampicin	n/a	375

Table 7.1. Concentration of encapsulated antibiotics in 10mg/ml of polymersomes after encapsulation by pH switch or film rehydration.

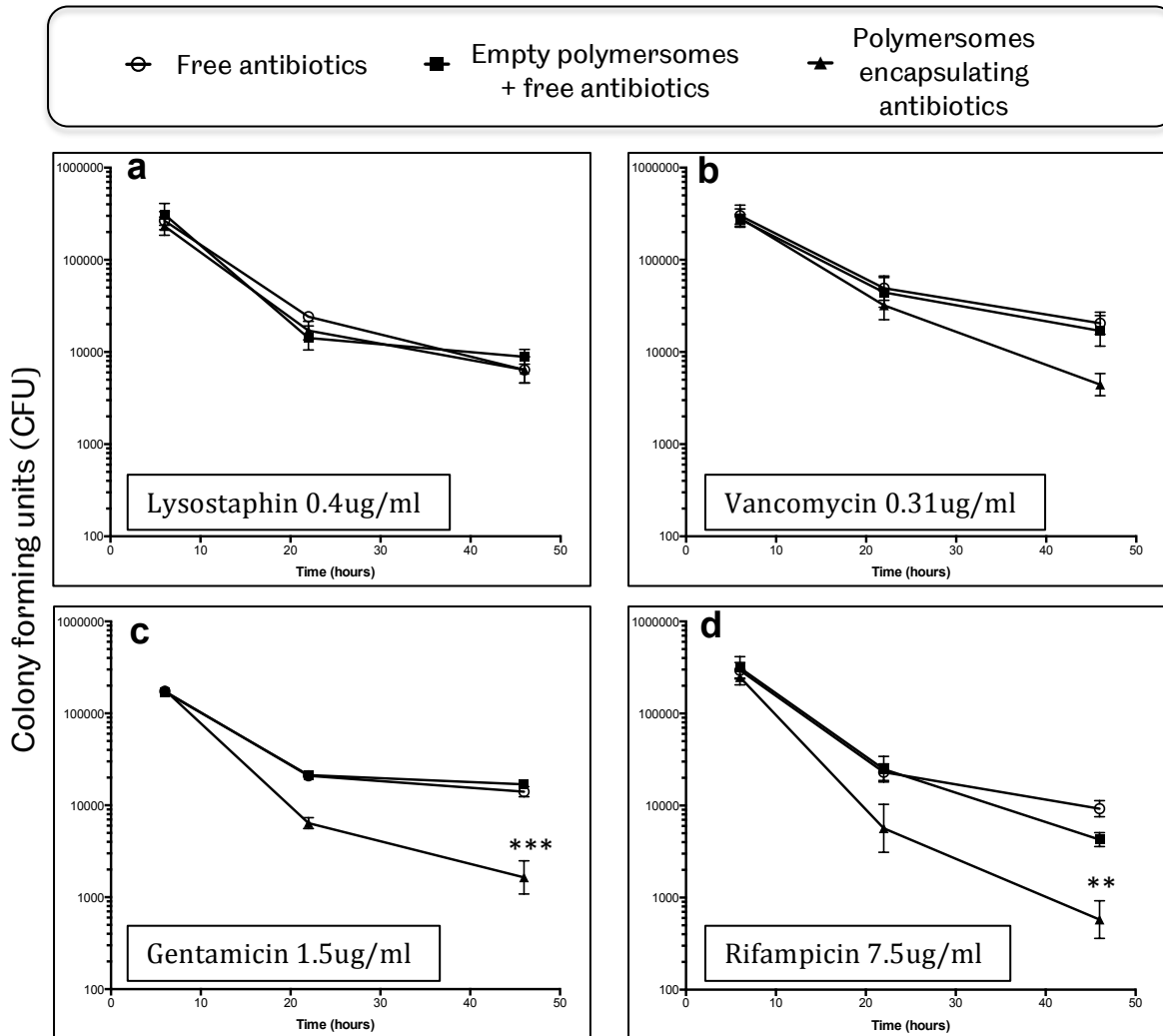


Figure 7.2. Intracellular delivery of antibiotics into THP-1 macrophages.

THP-1 macrophages were infected with *S. aureus* (MOI of 5) for 6 hours. Following infection, gentamicin was added to the media to kill extracellular bacteria. Macrophages were treated with polymersomes encapsulating lysostaphin (a), vancomycin (b), gentamicin (c) or rifampicin (d) or their controls of free drug or free drug with empty polymersomes. At 6 hours, 22 hours and 46 hours macrophages were lysed and plated on a BHI agar plate for bacterial colonies to be counted (One way ANOVA ** P<0.01, ***P<0.001, error bars = SEM, n=3).

After 6 hours incubation, macrophages efficiently phagocytose *S. aureus*, with intracellular burdens of approximately 200000 colony forming units (CFU). Treatment with encapsulated lysostaphin had no effect compared with the free drug (Figure 7.2a). Treatment with encapsulated vancomycin resulted in a lower infectious burden at 46 hours compared with the controls, but this did not reach statistical significance (Figure 7.2b).

Treatment with encapsulated gentamicin or rifampicin resulted in a significant reduction in the intracellular *S. aureus* burden, with a 9 fold and 16 fold reduction respectively compared with the free antibiotic after 46 hours infection (Figure 7.2c, d). The effect of encapsulated gentamicin on the number of bacterial CFU after 46 hours infection was dose dependent (Figure 7.3). These results demonstrate polymersome-mediated delivery of gentamicin and rifampicin was more effective at killing intracellular *S. aureus* than the free antibiotic *in vitro*.

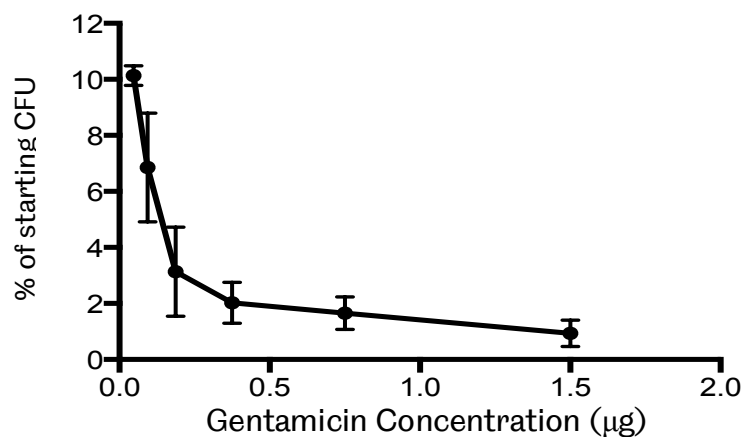


Figure 7.3. Encapsulated gentamicin reduced intracellular *S. aureus* burden in a dose dependent manner.

Macrophages were incubated with gentamicin encapsulating polymersomes for 46 hours at 6 doses. The results are normalised to the initial number of CFU before treatment (error bars= SEM, n=3).

7.2.3 Polymersome Mediated Intracellular Delivery into Zebrafish

Phagocytes

As discussed in the previous chapter, zebrafish provide an excellent *in vivo* model for visualising phagocytes due to their transparency in the larval stages and their amenability to genetic manipulation. These features have also allowed researchers to study the mechanisms of host-pathogen interactions at the cellular level and understand their roles in immune function and disease (Renshaw and Trede, 2012). Zebrafish larvae can be infected by either incubation with pathogens (Davis et al., 2002) or more commonly through microinjections of a controlled dose (Davis and Ramakrishnan, 2009, Prajsnar et al., 2008).

Injecting zebrafish larvae into the yolk sac circulation valley delivers molecules into the blood stream in a manner analogous to mammalian intravenous injection (Prajsnar et al., 2008). To investigate the final location of circulating polymersomes, rhodamine-labelled polymersomes were injected into the circulation valley of 2 day post fertilisation (dpf) zebrafish larvae. After 2 hours incubation zebrafish larvae were then mounted in agar and imaged by fluorescence microscopy. Zebrafish experiments were performed in collaboration with Doctor Tomasz Prajsnar, who assisted with all zebrafish injections in this chapter.

Fluorescence microscopy revealed rhodamine-labelled polymersomes were readily internalised by a subset of cells that appeared in and near the circulation

(Figure 7.4). It has previously been shown that PMPC-PDPA polymersomes are not internalised by red blood cells, which do not have active endocytosis mechanisms (Massignani et al., 2009), suggesting these cells were circulating leukocytes, most likely neutrophils or macrophages.

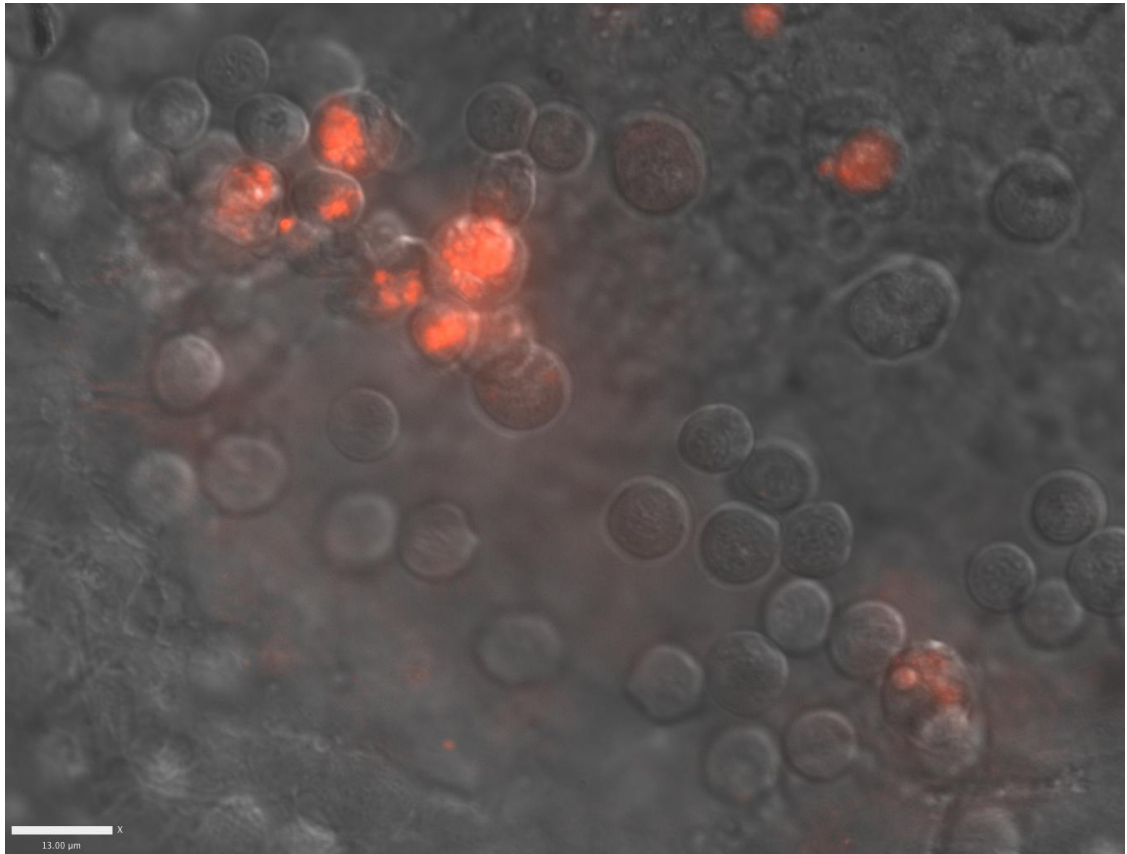


Figure 7.4. Internalisation of rhodamine-labelled polymersomes by circulating cells in the zebrafish embryo.

1nl of rhodamine-labelled polymersomes (5mg/ml) were injected into the circulation valley of 2dpf zebrafish larvae. After 2 hours incubation zebrafish were mounted in agar and imaged by fluorescence microscopy, scale bar = 13μm.

To confirm polymersomes were internalised by phagocytes, the experiment was repeated with a transgenic zebrafish line (*mpx:GFP*, *fms:mCherry*), whose macrophages express mCherry under the *fms* promoter and neutrophils

express GFP under the tissue specific *mpx* promoter. The *fms* promoter is also expressed in pigment containing cells called xanthophores, but as xanthophores are static cells they can be differentiated from motile macrophages.

Polymersomes encapsulating a far-red dye (BODIPY TR ceramide) were injected into the circulation valley of 2dpf zebrafish larvae and imaged by confocal microscopy 12 hours later. Figure 7.5 shows a confocal photomicrograph of the zebrafish tail region. The polymersome cargo co-localised with a number of neutrophils and macrophages demonstrating successful polymersome internalisation by these cells. A blue arrow in Figure 7.5a highlights an unlabelled cell with internalised polymersomes. A short time lapse movie demonstrated the cell was motile, suggesting it was a leukocyte (Figure 7.5b). As this transgenic line does not label macrophages with 100% efficiency it is likely this cell was an unlabelled macrophage.

After demonstrating polymersomes can deliver their cargo into zebrafish neutrophils and macrophages, the ability to deliver polymersomes into infected phagocytes was explored. Polymersomes were made by pH switch with rhodamine-conjugated PMPC-PDPA. CFP-labelled *S. aureus* was injected into 2dpf zebrafish embryos followed by the rhodamine-labelled polymersomes 2 hours later. As shown in Figure 7.6, *S. aureus* and polymersomes were internalised by the same phagocytes in the zebrafish circulation.

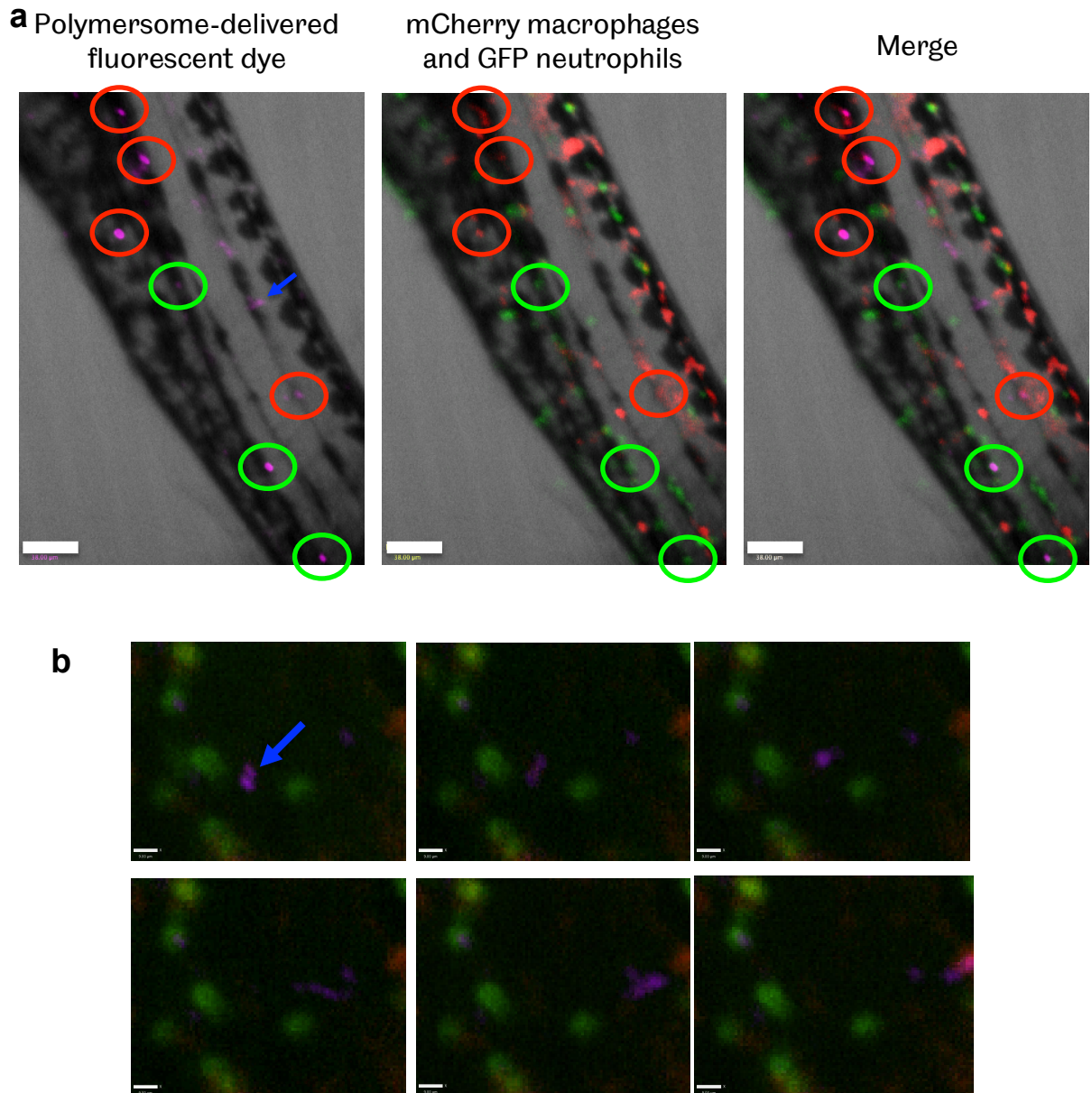


Figure 7.5 In vivo imaging of polymersome internalisation by zebrafish neutrophils and macrophages

(a) 2dpf transgenic zebrafish embryo *Tg(mpx:GFP)i114 x Tg(fms:GAL4.VP16)i186*, with macrophages labelled red and neutrophils labelled green, were injected with 1nl of polymersomes encapsulating a far red fluorescent dye (2mg/ml) (purple). The zebrafish were then imaged by confocal microscopy 12 hours later. The far-red fluorescent dye co-localised with macrophages (red circles), or neutrophils (green circles). The blue arrow indicates a cell that has no mCherry or GFP signal (scale bar=50µm). (b) High magnification of cell highlighted in (a) with a blue arrow. This cell was followed by time-lapse microscopy, revealing the cell was motile (scale bar=9µm).

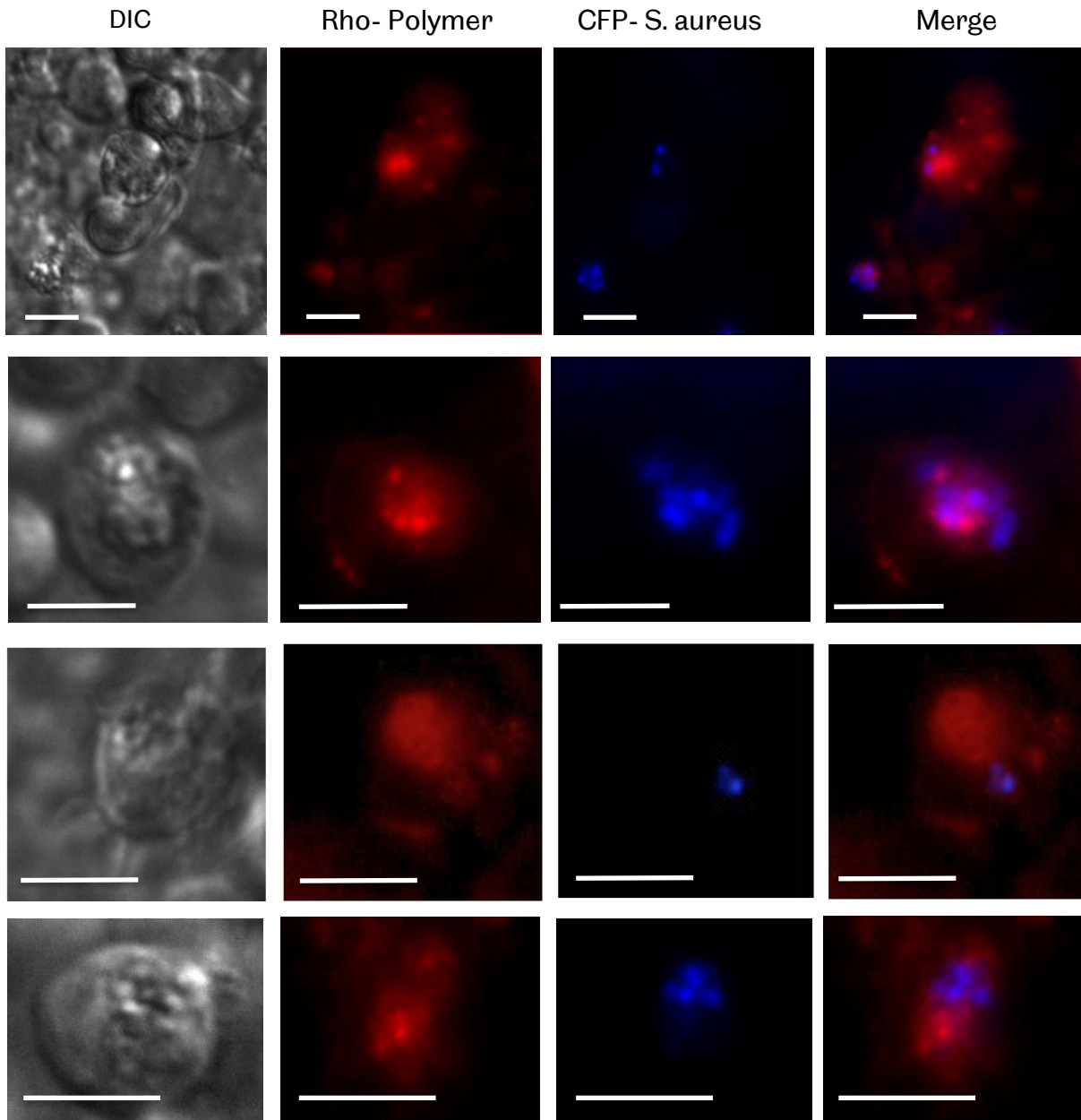


Figure 7.6 In vivo imaging of zebrafish phagocytes after injection of CFP-labelled *S. aureus* and rhodamine-labelled polymersomes.

Zebrafish embryos were injected 2 dpf with CFP-labelled *S. aureus* followed by an injection of rhodamine-labelled polymersomes 1 hour later. Zebrafish were imaged by fluorescence microscopy 2 hour later (scale bar = 8 μ m).

The delivery of antibiotics into a cell may not be sufficient to kill intracellular *S. aureus* if the delivered cargo does not reach the same intracellular compartment. To compare the intracellular location of polymersome cargo with intracellular *S. aureus*, lysostaphin was fluorescently labelled with an alexa-647 fluorophore. Fluorescent lysostaphin was encapsulated within polymersomes by pH switch and 2dpf zebrafish were injected with GFP-labelled *S. aureus* followed by lysostaphin polymersomes 1 hour later. 2 hours after treatment zebrafish were imaged by confocal microscopy.

Figure 7.7 shows four z-slices of a single z-stack from the circulation valley of a zebrafish embryo. All observed phagocytes with intracellular *S. aureus* also contained lysostaphin delivered intracellularly by the polymersomes. A good co-localisation is seen between the lysostaphin and the *S. aureus*; in fact, lysostaphin appeared most concentrated in the cellular compartments that contained the *S. aureus* bacteria. As discussed in the previous chapter, after polymersome disassembly within the early endosome, some polymersome cargo remains within the endolysosomal pathway. It is likely that the high degree of co-localisation between the *S. aureus* and the lysostaphin corresponded to a high concentration of both within the phagosome.

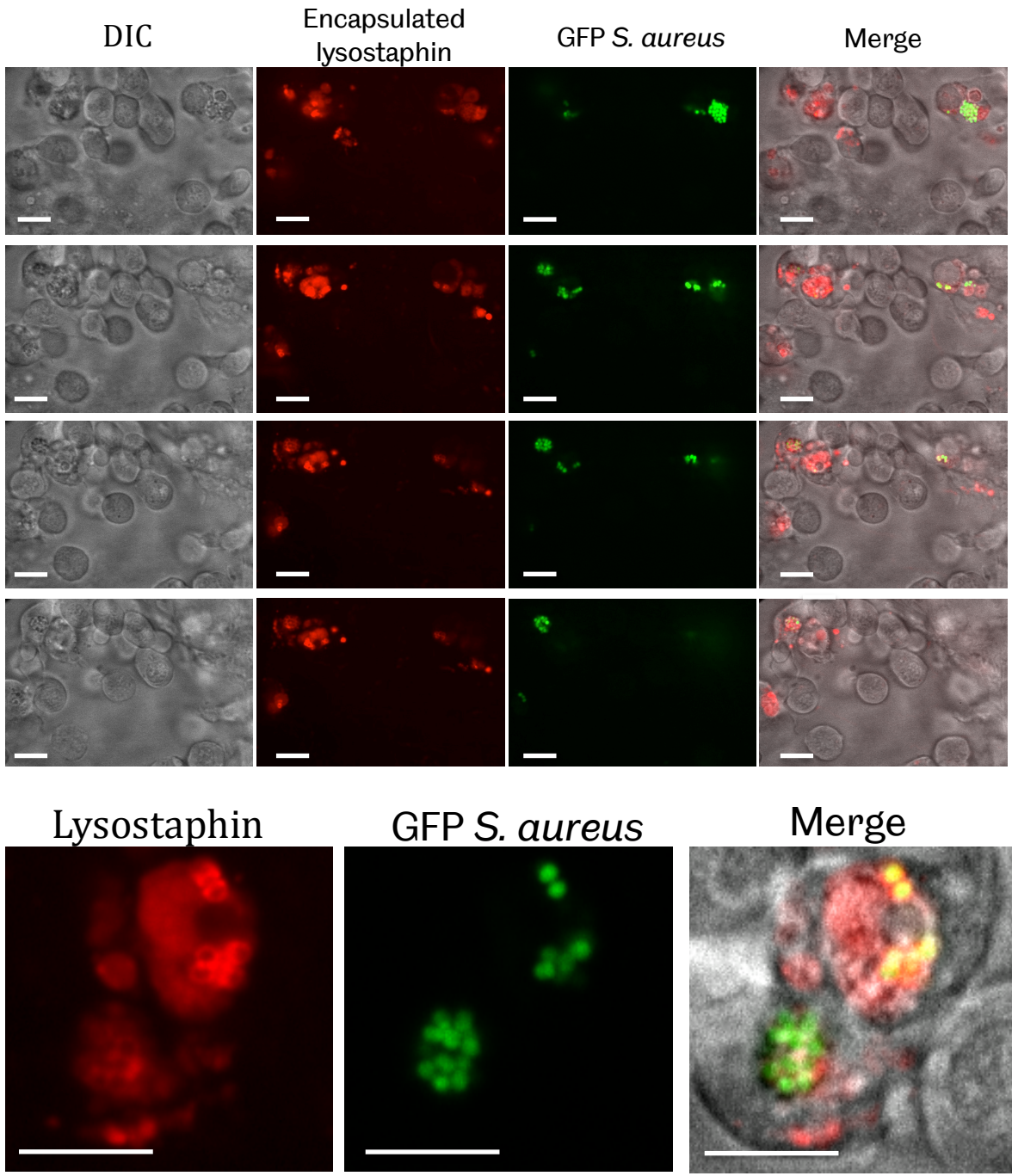


Figure 7.7 Polymersome cargo co-localised with *S. aureus* in infected phagocytes.

Zebrafish embryos 2dpf were injected with GFP-labelled *S. aureus* followed by an injection of polymersomes encapsulating alexa-647 labelled lysostaphin 1 hour later. 2 hours after polymersome injection zebrafish were mounted on agar and imaged by confocal microscopy. Good co-localisation was observed between *S. aureus* and delivered lysostaphin. Below the z-stack is a cropped high magnification image from the same z-stack, scale bars=8µm.

7.2.4 Intracellular Delivery of Antibiotics in an *in vivo* Model of *S. aureus* Infection

To explore the benefits of the intracellular delivery of antibiotics *in vivo*, an established zebrafish infection model was employed (Prajsnar et al., 2008). In this model zebrafish receive an injection of 1200CFU of *S. aureus* into their circulation, which are readily internalised by phagocytes. The infection is slowly resolved or escalates and overwhelms the fish. Zebrafish begin to succumb to life-threatening infections after approximately 40 hours post infection (hpif), so this timepoint was used as an output to determine the extent of zebrafish infection (Prajsnar et al., 2008).

To compare the effect of encapsulated antibiotics and free antibiotics to treat *S. aureus* infection, zebrafish embryos (2dpf) were injected with *S. aureus* followed by a second injection of gentamicin loaded polymersomes 20 hours later. Leaving the infected zebrafish for 20 hours before treatment helps to mimic the clinical scenario, where antibiotics are often given some time after the initial infection. Following treatment, zebrafish were left for a further 20 hours (40hpif) before they were homogenised, diluted and plated on brain-heart infusion (BHI) agar. Agar plates were incubated at 37°C overnight before viable colonies were counted to determine bacterial burden.

Zebrafish treated with gentamicin loaded polymersomes were compared with zebrafish treated with empty polymersomes and free gentamicin, or free gentamicin only. In this preliminary study only two log₁₀ dilutions were

performed, which resulted in a limit of detection of 400000CFU, but zebrafish with bacterial burdens above this limit have become overwhelmed from the infection. Surprisingly, zebrafish groups treated with polymersomes suffered from a greater number of overwhelming infections (Figure 7.8). This indicates the polymersomes were impairing the ability of zebrafish to deal with the bacterial infection. It is possible that excess polymersomes were competing with *S. aureus* for internalisation by the circulating phagocytes. This would reduce the clearance of *S. aureus* from the blood stream.

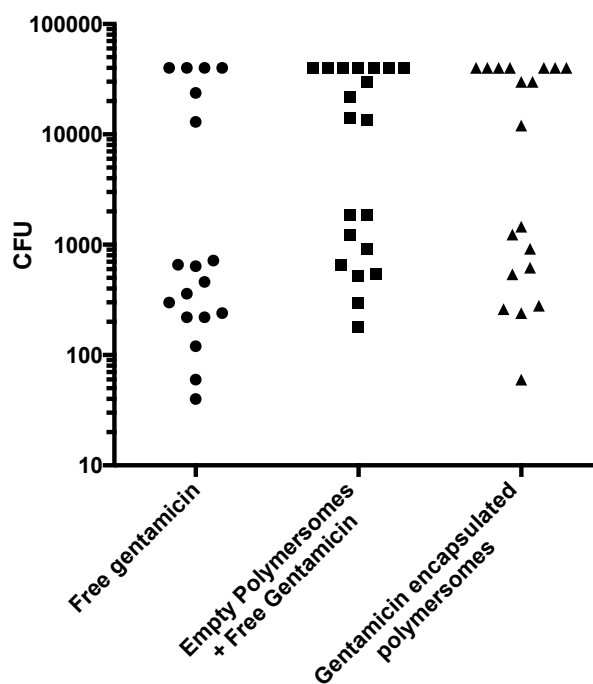


Figure 7.8. Intracellular delivery of gentamicin in an in vivo *S. aureus* infection model.

Zebrafish embryos 2dpf were injected with 1200CFU of *S. aureus* followed by a second injection 20 hours later with gentamicin loaded polymersomes, empty polymersomes with free gentamicin, or free gentamicin alone (1 nl at 30ug/ml gentamicin and 10mg/ml polymer). Zebrafish were then left for 20 hours before zebrafish were homogenised and plated on BHI agar for viable colony counts.

The optimal concentration of polymer would enable polymersomes to quickly deliver antibiotics into zebrafish without excess free polymersomes remaining within the circulation. To measure the degree to which polymersomes were internalised by circulating phagocytes or remain circulating within the bloodstream, rhodamine-labelled polymersomes were injected into zebrafish 2dpf at five different concentrations. At each concentration, the fluorescence intensity from the circulation and from phagocytes was measured by fluorescence microscopy and normalised to the intensity of the un-injected control fish.

As shown in Figure 7.9, the fluorescence intensity from the phagocytes and the circulation was dependent on the concentration of polymer injected. Polymersomes with concentrations higher than 0.5mg/ml had fluorescence intensities in the circulation greater than the control, suggesting excess polymersomes were left in the circulation and not yet internalised. The fluorescence intensity from the phagocytes also increased with rising polymer concentrations up to 1mg/ml. Interestingly, the fluorescence intensity from the phagocytes in zebrafish treated with 1mg/ml is similar to zebrafish treated with higher concentrations, whereas, the fluorescence intensity from the circulation was substantially less than in fish treated with higher polymer concentrations. Therefore, treatment with 1mg/ml may enable sufficient intracellular delivery of antibiotics into circulating phagocytes, while minimising the presence of free polymersomes in the circulation.

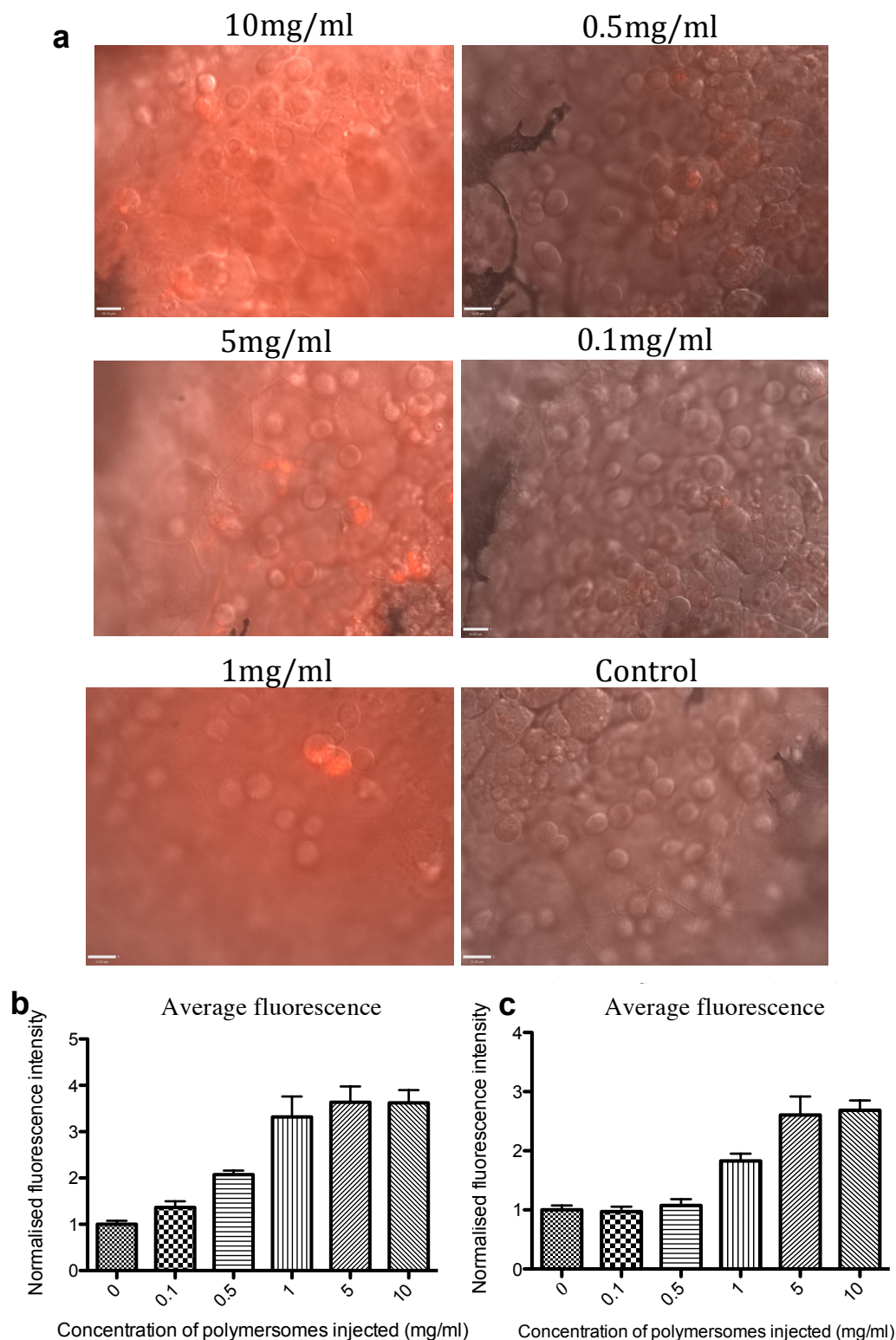


Figure 7.9. Optimisation of polymer concentration for uptake into circulating phagocytes.

Zebrafish embryos 2dpf were injected with rhodamine-labelled polymersomes at five different concentrations, or left un-injected as a control. Zebrafish were imaged by fluorescence microscopy and average rhodamine signal calculated from six different phagocytes or six different points in the blood (n=3) (a). The results are plotted in bar charts showing the average fluorescence intensity from the phagocytes at each concentration (b) or the average fluorescence intensity from the circulation (c)(error bars =SD, n=3).

Informed by the dose optimisation experiment, zebrafish were infected in accordance with the previous infection protocol and treated with 1 mg/ml of gentamicin loaded polymersomes or the equivalent controls (Figure 7.10a). Zebrafish treated with polymersomes did not show more overwhelming infections compared with the free gentamicin group, suggesting that the lower dose was not affecting the ability of zebrafish to deal with the *S. aureus* infection (Figure 7.10a). The group of zebrafish receiving gentamicin loaded polymersomes had a lower burden of infection compared with the control groups, demonstrating the intracellular delivery of antibiotics was beneficial in this model, although the encapsulated gentamicin group did not perform significantly better than the free gentamicin control.

The delivery of antibiotics intracellularly using polymersomes enables bacteria to be killed within the cell, but will not kill extracellular bacteria. Overwhelming infections occur when bacteria escape phagocytes and form abscesses, whereas, when bacteria are maintained intracellularly within phagocytes the number of bacteria will be kept below the initial injection volume. In Figure 7.10b the bacterial CFU for each group is displayed for the fish with bacterial burdens lower than the number of bacteria in the initial injection (1200CFU), where bacteria were maintained intracellularly. In this graph zebrafish treated with gentamicin loaded polymersomes had significantly less viable bacteria than the free gentamicin group, suggesting the polymersomes were delivering the gentamicin and killing the bacteria intracellularly.

The zebrafish infection model was repeated with polymersomes encapsulating lysostaphin or vancomycin and their controls. Consistent with the *in vitro* experiments, there was no significant difference between the encapsulated antibiotics compared with the control groups (Figure 7.11)

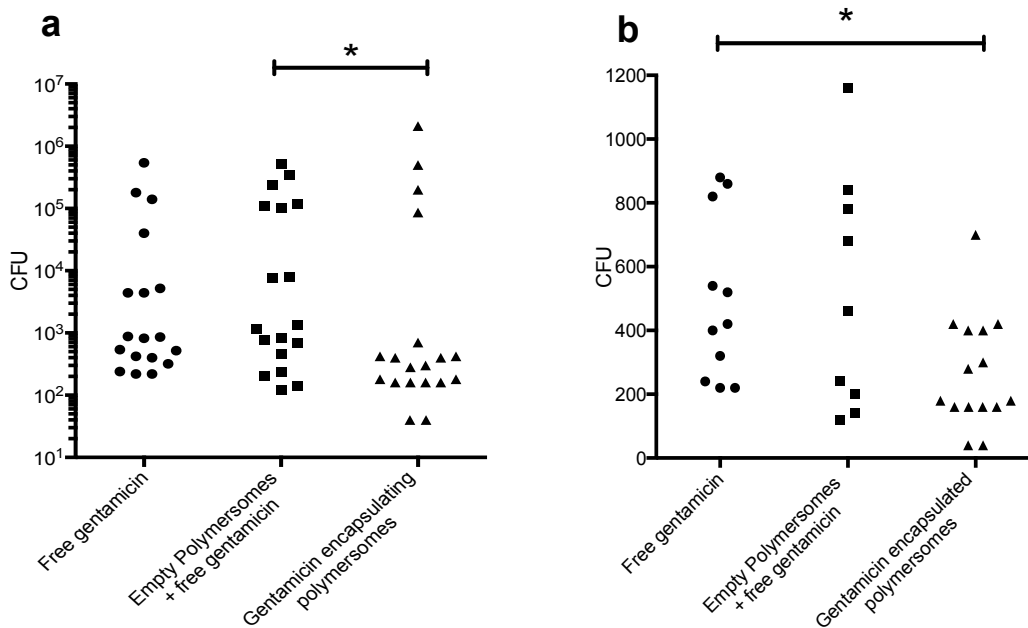


Figure 7.10. Intracellular delivery of gentamicin in an in vivo *S. aureus* infection model at a polymer concentration of 1mg/ml.

(a) Zebrafish embryos 2dpf were injected with *S. aureus* followed by a second injection 20 hours later with gentamicin encapsulated within polymersomes, empty polymersomes with free gentamicin, or free gentamicin alone (1nl at 3ug/ml gentamicin and 1mg/ml polymer). Zebrafish were then left for 20 hours before they were homogenised and plated on agar for viable colony counts. (b) The total number of CFU in zebrafish with bacterial burdens lower than the starting dose (1200CFU) (Kruskal-Wallis test with Dunn's multiple comparison *P<0.05).

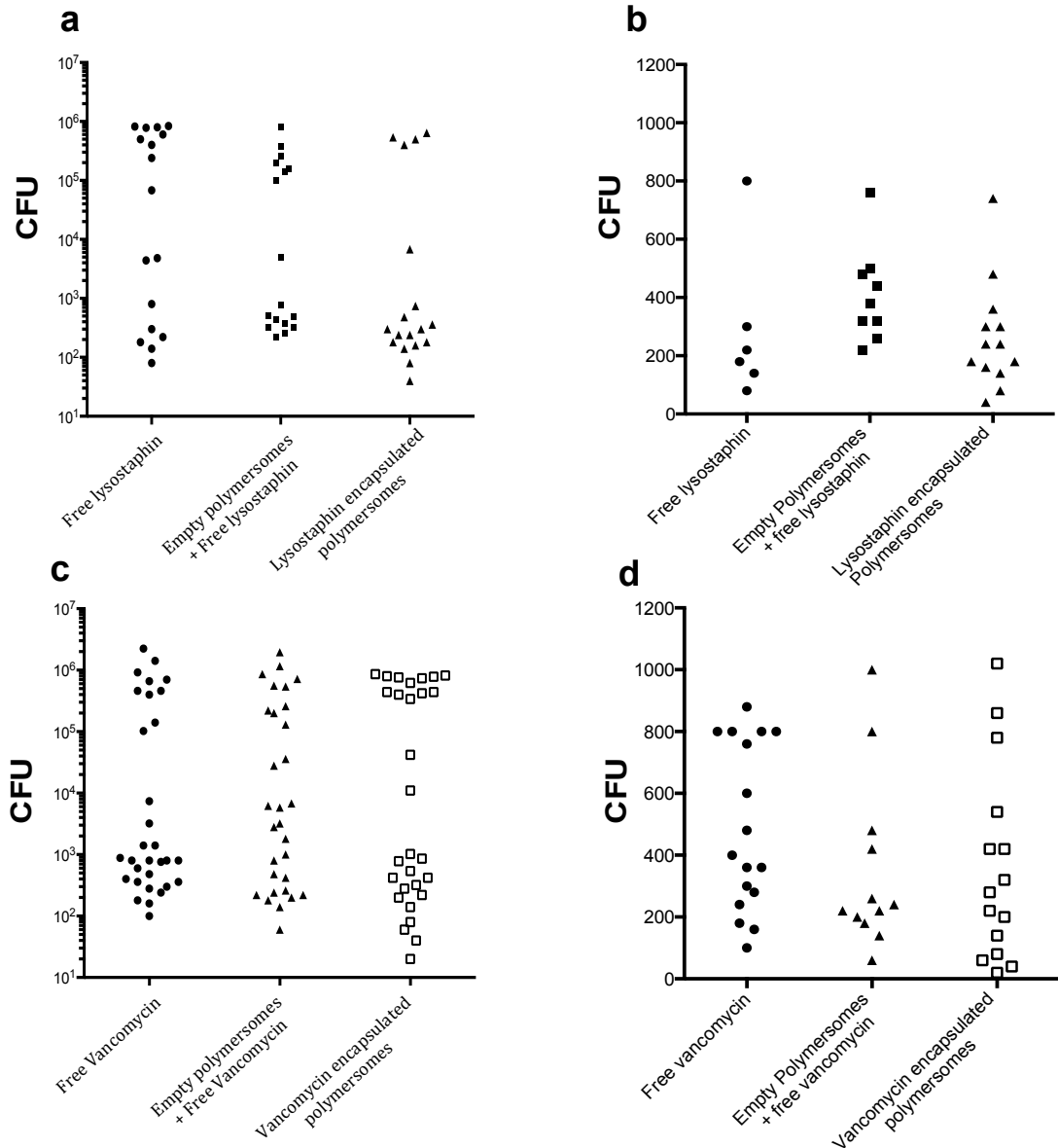


Figure 7.11. Intracellular delivery of lysostaphin and vancomycin in an in vivo *S. aureus* infection model at a polymer concentration of 1mg/ml.

Zebrafish embryos 2dpf were injected with *S. aureus* followed by a second 1nl injection 20 hours later with vancomycin (0.31 μ g/ml) or lysostaphin (0.4 μ g/ml) encapsulated within polymersomes or their equivalent controls. Zebrafish were left for 20 hours before being homogenised and plated on agar for viable colony counts. Graphs show the total number of CFU after treatment with lysostaphin (a) or vancomycin (c) and the number of CFU in zebrafish with bacterial burdens lower than the starting dose (1200CFU) for lysostaphin (b) or vancomycin (d). Results are not significant (Kruskal-Wallis test with Dunn's multiple comparison).

Finally, the potency of rifampicin-loaded polymersomes was tested in the zebrafish infection model. Polymersomes encapsulating rifampicin significantly reduced the burden of *S. aureus* infection in zebrafish compared with the controls, both when all zebrafish were measured (Figure 7.12a), or in only those zebrafish where bacteria was maintained below the initial infection dose (Figure 7.12b). These results demonstrate that rifampicin delivered intracellularly is a more effective treatment than the free drug in reducing the burden of *S. aureus* infection.

To determine the effect of rifampicin polymersomes on zebrafish survival, zebrafish were infected and treated with the same infection protocol. Fish were checked at multiple time points and the number of surviving fish was recorded up to 70 hours post treatment (or 90hpf). All zebrafish treated with rifampicin showed high survival rates with a 91% survival rate in zebrafish treated with free rifampicin and a 96% survival in those treated with empty polymersomes and free rifampicin or rifampicin loaded polymersomes.

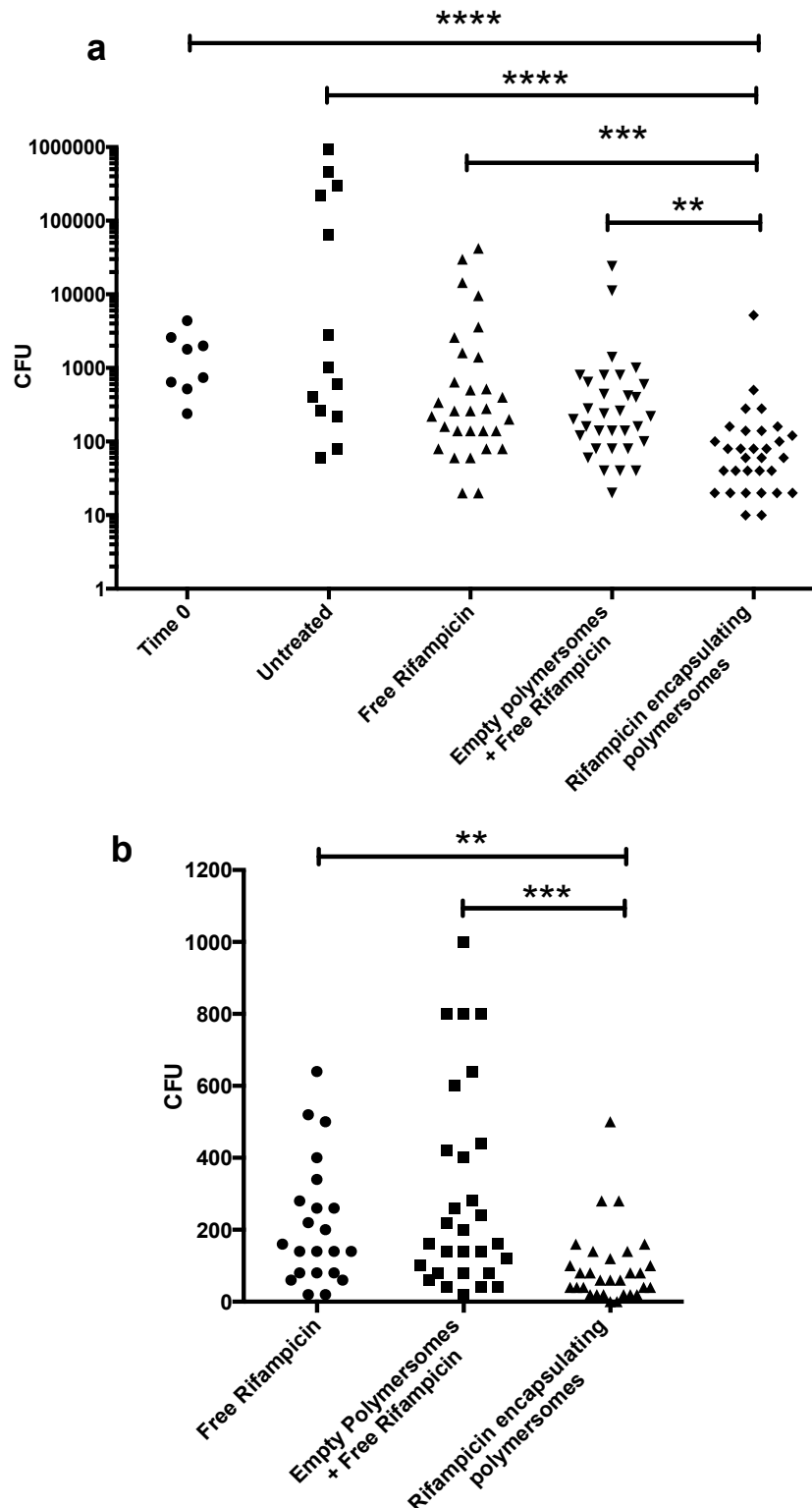


Figure 7.12. Polymersome mediated intracellular delivery of rifampicin in vivo in *S. aureus* infected zebrafish embryos.

Zebrafish embryos 2dpf were injected with *S. aureus* followed by a second injection 20 hours later with rifampicin (37.5 μ g/ml) encapsulated within polymersomes or controls. Zebrafish were then left for 20 hours before being homogenised and plated on BHI agar for viable colony counts. Graphs show the total number of CFU after treatment (a) and the number of CFU in zebrafish with bacterial burdens lower than the starting dose only (b) (Kruskal-Wallis test with Dunn's multiple comparison **P<0.01 ***P<0.001)

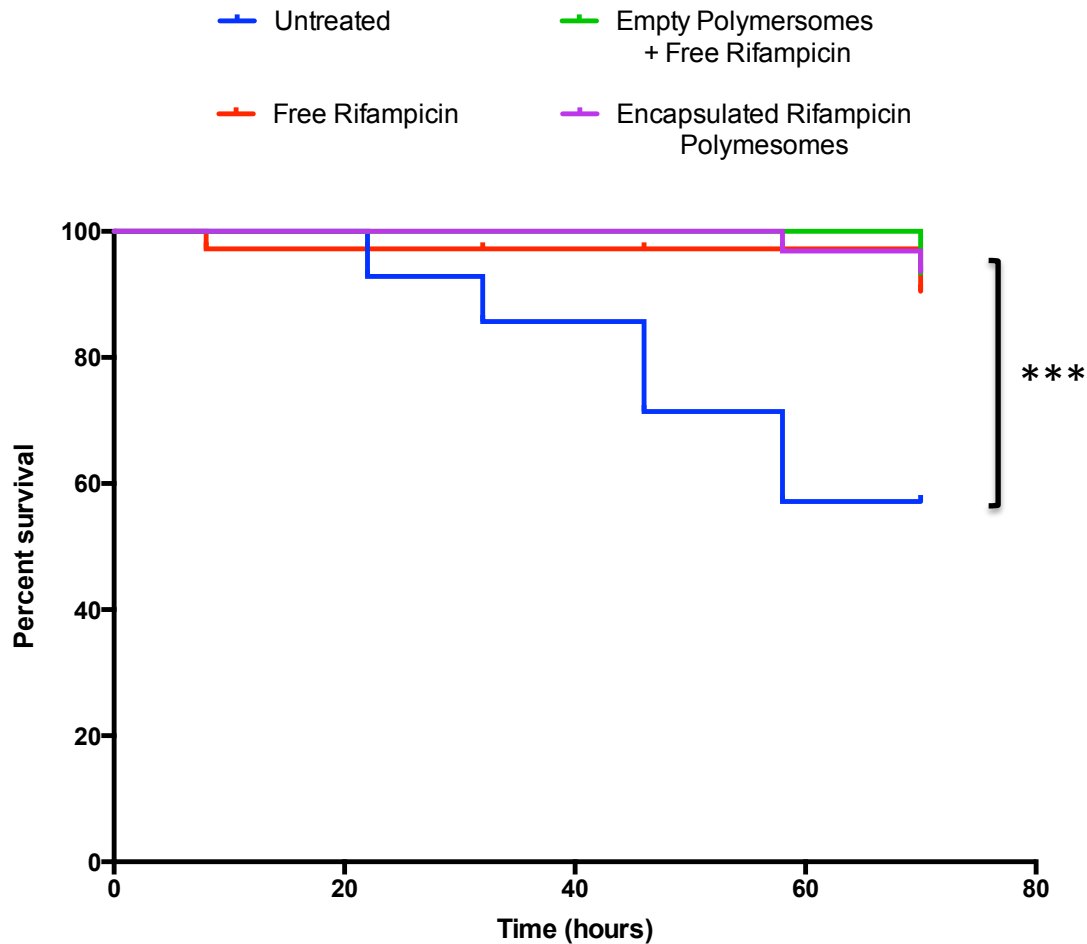


Figure 7.13. Zebrafish survival after *S. aureus* infection and treatment with encapsulated rifampicin.

Zebrafish embryos 2dpf were injected with *S. aureus* followed by a second injection 20 hours later with rifampicin ($37.5\mu\text{g/ml}$) encapsulated within polymersomes, empty polymersomes and free rifampicin, free rifampicin alone or untreated. Fish were checked at multiple time points and the number of surviving fish was recorded (** $P < 0.001$ log rank (Mantel-Cox) test).

7.3 Discussion

S. aureus is the most common cause of blood stream bacterial infection. Early intervention with antibiotics reduces the risk of metastatic infection, but where bacteria persist, disseminated infection can be life threatening. It is now clear that *S. aureus* can survive intracellularly for prolonged periods of time in neutrophils (Melly et al., 1960, Rogers and Tompsett, 1952, Kapral and Shayegani, 1959, Gresham et al., 2000), mononuclear phagocytes (Kapral and Shayegani, 1959, Kubica et al., 2008) and a number of other non-professional phagocytes and cell lines (reviewed in (Garzoni and Kelley, 2009)).

Intracellular survival of *S. aureus*, particularly in neutrophils, is linked with recurrent and disseminated infection (Bosse et al., 2005, Thwaites and Gant, 2011, Chang et al., 2003). Recurrence or persistence of *S. aureus* is particularly common following blood stream infection and is associated with significant morbidity and mortality (Chang et al., 2003). Once *S. aureus* penetrates the blood stream it can infect almost any organ (Khatib et al., 2006), but deletion of gene regulators involved in intracellular survival reduces the number of disseminated and fatal infections (Voyich et al., 2009, Heyer et al., 2002). Clinical reports are also starting to highlight a role for neutrophils in *S. aureus* dissemination in humans. Large clinical studies have shown that neutropenic patients are less likely to develop blood stream *S. aureus* infections, and where bacteraemia does occur, patients have a greater chance of survival, fewer symptoms of sepsis and have a reduced risk of developing metastatic infections (Venditti et al., 2003, Velasco et al., 2006).

In this chapter I have investigated the potential of PMPC-PDPA polymersomes to deliver antibiotics into phagocytes to treat intracellular infection. I have shown that polymersomes can encapsulate a range of antibiotics to varying degrees and demonstrated that antibiotics can be delivered into phagocytes to reduce the intracellular *S. aureus* burden *in vitro* and *in vivo*.

7.3.1 Polymersome Mediated Delivery of Antibiotics to Kill Intracellular *S. aureus* in THP-1 Monocyte Derived Macrophages

After phagocytosis of *S. aureus* by macrophages, bacteria can survive intracellularly for a number of days (Kubica et al., 2008). For this reason, monocyte derived macrophages have emerged as an excellent model for measuring intracellular killing of *S. aureus* by antibiotics. In particular, THP-1 monocyte derived macrophages are a highly reproducible cell model and share many of the characteristics of primary human macrophages (Auwerx, 1991). THP-1 monocyte derived macrophages have been utilised to measure the intracellular bactericidal effects of a range of antibiotics, which have shown the intracellular activities of antibiotics are always lower than that observed extracellularly (Barcia-Macay et al., 2006b, Barcia-Macay et al., 2006a, Lemaire et al., 2005, Carryn et al., 2003). In fact, many antibiotics tested showed very little intracellular killing. Antibiotics that did have significant intracellular bactericidal effects were highly dependent on the extracellular concentration and the duration of cell exposure.

In this chapter, THP-1 monocyte derived macrophages have been employed as a model for studying the intracellular bactericidal effects of intracellular antibiotics delivered using polymersomes. This work was done in collaboration with Jamil Jubrail who previously established and optimised the macrophage infection model. After treatment with polymersomes, the intracellular killing varied widely depending on the encapsulated antibiotic; the greatest reduction in viable *S. aureus* was demonstrated with the rifampicin polymersomes.

The intracellular bactericidal effect of an antibiotic depends on the concentration within the cell and the intracellular minimum bactericidal concentration (MBC). The concentration of encapsulated antibiotic varied widely between the four antibiotics tested. The dose-response curve for encapsulated gentamicin demonstrated that the intracellular killing is highly dependent on the delivered dose. It is possible that the low encapsulation of vancomycin and lysostaphin prevented the antibiotic reaching intracellular bactericidal concentrations. Another important consideration is the activity of the antibiotics in the intracellular environment. For instance, gentamicin is known to be less active against intraphagocytic *S. aureus* due to the higher MBC at low pH (Baudoux et al., 2007), whereas, rifampicin remains highly active at low pH (Barcia-Macay et al., 2006b).

For the delivered antibiotic to be effective intracellularly it must also reach the same intracellular location as the internalised bacteria. When cells are treated with free antibiotics, aminoglycosides such as gentamicin are thought to have a

predominantly lysosomal localisation within cells, whereas, a number of other antibiotics such as the fluoroquinolones are predominantly located within the cytosol (Carryn et al., 2003). The chemical properties of the antibiotics may also influence their cellular distribution when delivered into the cells using polymersomes. For instance, the hydrophobicity of rifampicin could enable it to diffuse more readily throughout the entire phagocytes enabling the bacteria to be killed throughout the cell.

7.3.2 Intracellular Delivery into Phagocytes *in vivo*

After establishing that delivered antibiotics can reduce the burden of intracellular *S. aureus* infection *in vitro*, it was then sought to determine whether this method could improve the outcome of *S. aureus* infection *in vivo*. For the polymersomes to be effective in treating intracellular *S. aureus* infection they must be able to efficiently deliver cargo into infected phagocytes. Using a transgenic zebrafish line it was shown that polymersomes injected into the circulation of zebrafish embryos were internalised by both neutrophils and macrophages. Subsequently injection of CFP-labelled *S. aureus*, followed by rhodamine-labelled polymersomes demonstrated that polymersomes were internalised by infected phagocytes.

Having demonstrated polymersomes were internalised by infected zebrafish phagocytes, fluorescent lysostaphin was encapsulated and delivered into *S. aureus* infected zebrafish to determine whether the antibiotics co-localised with the *S. aureus* in the infected phagocytes. Strikingly confocal microscopy

revealed a high local co-localisation of intracellular *S. aureus* with lysostaphin, with the concentration of lysostaphin appearing greatest in subcellular regions containing the *S. aureus* bacteria. This demonstrates that polymersomes can deliver antibiotics into the same intracellular compartments as *S. aureus* in infected phagocytes.

Despite demonstrating that lysostaphin could be delivered into infected phagocytes, lysostaphin was the only antibiotic to show no intracellular bactericidal activity *in vitro*. Lysostaphin is an antibacterial enzyme that acts by cleaving pentaglycin bridges in the *S. aureus* cell wall. It is a membrane impermeable enzyme and so its intracellular activity has not been described. It is possible the low pH or degradative enzymes within the phagosome could inactivate the enzyme, which repressed its effect intracellularly. But further research is required to confirm this.

7.3.3 Polymersome Mediated Intracellular Delivery of Antibiotics in an *in vivo S. aureus* Infection Model

A model of *S. aureus* infection in zebrafish embryos has been developed in the Renshaw research group, which has helped delineate the importance of phagocytes in the pathogenesis of *S. aureus* infection (Prajsnar et al., 2008). In this model *S. aureus* injected into the zebrafish embryo circulation is quickly engulfed by neutrophils and macrophages, and the infection is slowly resolved, or escalates and overwhelms the fish. In those fish that succumb to an

overwhelming infection, bacterial growth is linked to the formation of one or more abscesses, commonly around the heart (Prajsnar et al., 2008).

In one study, zebrafish infected with a mixed inoculum of two *S. aureus* strains differing only in their resistance marker or fluorescence marker, revealed the output population of bacteria was commonly asymmetrically distributed, with one of the two strains predominating (Prajsnar et al., 2012). This observation was dependent on the presence of phagocytes. This indicates that some abscesses can originate from a single cell founder and phagocytes act as the intracellular reservoir for *S. aureus* survival and dissemination.

To explore the ability of polymersomes encapsulating antibiotics to treat *S. aureus* infection, zebrafish embryos were infected with *S. aureus* followed by treatment with the encapsulated antibiotics 20 hours later. Initial experiments showed an increased number of overwhelming infections, suggesting that the presence of polymersomes was interfering with the ability of the phagocytes to clear bacteria. As scavenger receptors are important in the phagocytosis of non-opsonised *S. aureus* (Philips et al., 2005), excess polymersomes may compete with *S. aureus* for receptors, resulting in a decreased rate of phagocytosis. Subsequent imaging studies demonstrated an excess of uninternalised polymersomes within the bloodstream at higher concentrations and therefore the dose of polymersomes was reduced to 1mg/ml in further experiments.

Encapsulated vancomycin, lysostaphin, gentamicin and rifampicin were tested in the zebrafish infection model at a polymer concentration of 1mg/ml. In agreement with the *in vitro* data, encapsulated lysostaphin and vancomycin had no significant effect on the zebrafish infectious burden, whereas, treatment with encapsulated gentamicin showed a small improvement compared to controls. Zebrafish treated with encapsulated rifampicin showed the greatest improvement, with very low numbers of viable *S. aureus* recovered at the end of the experiment.

When tested in a survival model of *S. aureus* infection, treatment with both free and encapsulated rifampicin resulted in great improvement in zebrafish survival. Treatment with encapsulated rifampicin resulted in a 96% survival and zebrafish treated with free rifampicin had a 91% survival rate compared with the 57% survival in the untreated group. This highlights the importance of intracellular bacteria in the infection process, as it demonstrates that treatment with intracellular rifampicin is sufficient to significantly reduce the *S. aureus* burden. Additionally, the reduction in intracellular bacteria in surviving fish may reduce the likelihood of recurrent infection. Future experiments should explore the ability of encapsulated rifampicin to reduce bacterial relapse in long-term infection models and combine free rifampicin with encapsulated rifampicin to explore the benefits of the joint treatment, which may act synergistically to eliminate both intracellular and extracellular bacteria.

Collectively, these results suggest that the delivery of rifampicin into infected phagocytes may provide an effective treatment for *S. aureus* infection. In particular, these experiments suggest that the intracellular delivery of rifampicin helps to eliminate the intracellular burden of infection more readily, which may result in a reduction in recurrent infections and enable bacteria to be eliminated on shorter courses of antibiotics.

Chapter 8: Final Discussion and Future Perspectives

8.1 Optimisation of Polymersome Size

Initial experiments explored methods for separating pre-formed PMPC-PDPA polymersomes into separate size fractions. When polymersomes of different sizes were incubated with neutrophils, those with an average diameter of 190nm were the most efficient at delivering cargo. To compare the effect of polymersome size on internalisation into other cell types, Maria Milagros Avila Olias in the Battaglia research group repeated this size experiment in the oral carcinoma cancer cell line FaDu, demonstrating a very similar trend to the results observed in this thesis. The receptor-ligand ratio is known to influence the rate of internalisation and the optimal particle diameter for membrane wrapping (Gao et al., 2005, Yuan and Zhang, 2010), therefore it would be interesting to measure the expression of scavenger receptors on neutrophils, FaDu cells and other mammalian cells and to compare their receptor expression with the rate of polymersome internalisation of a range of polymersome sizes.

It is worth noting that the size also has a great effect on the biodistribution and tissue extravasation of nanoparticles. Therefore the optimum size of polymersomes *in vivo* will also depend on a number of other factors such as the route of administration, and the properties and location of the target tissue. Future studies focusing on the biodistribution of different sized PMPC-PDPA polymersomes could greatly enhance our ability to target specific diseases.

8.2 Tubular Polymersomes

Despite the importance of nanoparticle shape, the majority of vectors used in drug delivery have been spherical. In this thesis tubular polymersomes were formed during film rehydration by exploiting the transition between large lyotropic structures and dispersed spherical polymersomes. These tubular polymersomes rapidly adhered to the neutrophil membrane, but internalisation was delayed. Again this experiment was repeated in FaDu cells by Maria Milagros Avila Olias, which also demonstrated a delay in tubular polymersome internalisation (Robertson et al., 2014b). The exact mechanism by which this occurs is unclear, it is possible that the unusual shape of tubular polymersomes alters the mechanism of endocytosis. Interestingly, when analysing the uptake by confocal microscopy, the morphology of some tubular particles seem to remain intact within the cell. This may suggest that they are trafficked to an intracellular compartment that is not acidified. Alternatively, some tubular polymersomes may be too long to be delivered to an endosome, which are thought to be only up to 500nm in diameter. More research should focus on the mechanisms of endocytosis of different sizes and shapes of PMPC-PDPA polymersomes.

Another interesting observation during this study was the higher drug loads in tubular polymersomes compared with spherical polymersomes. Guy Yealland in the Battaglia research group has also observed that tubular PMPC-PDPA polymersomes encapsulate higher concentrations of the hydrophobic drug

ursolic acid. Higher drug loads could improve the efficiency of drug delivery and reduce the mass of polymer required to deliver the same volume of drug.

It is anticipated that tubular PMPC-PDPA polymersomes will have very different properties to their spherical counterparts *in vivo*. As mentioned in the results section filomicelles, otherwise known as cylindrical micelles, which have a similar shape to the tubular polymersomes presented here, have greater circulation times than spherical micelles (Geng et al., 2007). This has led to their use as ligand targeted drug carriers, because their longer circulation times and improved binding selectivity enable them to target specific cells or tissues more efficiently (Shuvaev et al., 2011, Oltra et al., 2013, Kolhar et al., 2013). These groups used cylindrical micelles made with the hydrophilic block PEG and ligands were conjugated to the PEG block to target the particles to a specific location.

In this thesis tubular polymersomes were made with the hydrophilic block PMPC, which appears to have a high affinity for cell surface class B scavenger receptors and hence acts itself as a ligand for cell receptors (Colley et al., 2014b). As the class B scavenger receptors are widely expressed by mammalian cells, PMPC-PDPA polymersomes are internalised by many different cell types. However, the rate of internalisation varies depending on the cell type, which is thought to correlate with the expression of these scavenger receptors. When the uptake of PMPC-PDPA polymersomes was compared across a number of different cells macrophages internalised the polymersomes most readily

(Canton, unpublished data), which are known to have high expression of scavenger receptors. Circulating tubular PMPC-PDPA polymersomes may adhere more specifically to cells with a high expression of the class B scavenger receptors because particles with high aspect ratios are known to be more easily detached under shear forces so greater adhesion strength is required for particle binding (Kolhar et al., 2013).

8.3 Polymersome as Intracellular Delivery Vectors for Neutrophils

Despite the abundance of drug delivery vectors available, neutrophils have proven very difficult cells to manipulate. In this thesis I have demonstrated that PMPC-PDPA polymersomes can deliver fluorescent dyes, nucleic acids, antibodies and the CDKi (R)-roscovitine into neutrophils. Roscovitine loaded polymersomes were able to promote human neutrophil apoptosis *in vitro* and speed up inflammation resolution in an *in vivo* zebrafish model of neutrophil inflammation. Recently, the Rossi research group has demonstrated that the CDKi AT7519 can promote neutrophil apoptosis with even greater potency than roscovitine (EC_{50} of 61nM compared with 5 μ M for roscovitine) (Lucas et al., 2014). They found that AT7519 lowered the level of the anti-apoptotic protein Mcl-1 in macrophages, but did not drive macrophage apoptosis or impair the ability of macrophages to clear apoptotic neutrophils. This finding is very important for this thesis, as polymersomes are readily internalised by macrophages and macrophage apoptosis could exacerbate inflammation by reducing the clearance of apoptotic neutrophils.

The Rossi group also found AT7519 treatment did not impair the resolution of lung *E.coli* infection in mice, in fact, it appeared to speed up the clearance of the bacterium, with lung bacterial counts lower following AT7519 treatment (Lucas et al., 2014). This suggests CDKi mediated neutrophil apoptosis does not weaken the immune response to infection, but these results should be repeated in other organs and with different pathogens. If the CKDi's do not cause significant immune suppression, then they may be effective in treating inflammatory disease with secondary bacterial infection. The inflammatory skin diseases psoriasis and atopic eczema are commonly linked with *S. aureus* skin infection, which can cause severe symptoms. Encapsulation of CDKi's such as AT7519 within PMPC-PDPA may enable the drug to be delivered through the skin to treat the inflammation without compromising the clearance of the bacterial infection. Co-encapsulation of a CDKi with an antibiotic may be synergistic in the treatment of both components of the disease.

8.4 Polymersome Mediated Delivery of Antibiotics to Treat Intracellular *S. aureus* Infection

In Chapter 7 antibiotics were encapsulated within polymersomes and used to treat intracellular *S. aureus* infection. The highest antibiotic load was observed with rifampicin, due to the drug hydrophobicity. However, despite the lower encapsulation of gentamicin, gentamicin loaded polymersomes still reduced the infectious burden *in vitro* and *in vivo*. Gentamicin influx and efflux across cell membranes is very slow, therefore intracellular delivery will result in the drug

accumulating within the cell. This might explain why a significant reduction in the intracellular *S. aureus* burden was observed despite the low concentration (Van Bambeke et al., 2006). Remarkably, the amount of gentamicin administered in the zebrafish experiment (based on a zebrafish embryo mass of 250 μ g) was over 500 times lower than the amount administered to humans (12 μ g/kg compared with 7mg/kg). Considering that gentamicin has been associated with significant nephrotoxicity, enabling the antibiotic to be administered at lower doses would be advantageous (Cosgrove et al., 2009). Additionally, some antibiotics are not brought forward by pharmaceutical companies because of limitations in the drug solubility, biodistribution or toxicity, which could be improved with polymersomes.

Treatment with encapsulated rifampicin in the zebrafish infection model significantly reduced the *S. aureus* burden compared with the free drug. This result suggests encapsulated antibiotics could clear *S. aureus* from the body more rapidly than the free drug. If polymersomes encapsulating antibiotics can completely remove *S. aureus* more rapidly, then this would enable patients to be treated on shorter courses of antibiotics and would reduce the incidence of recurring infections, which are very common following *S. aureus* bacteraemia and associated with high morbidity and mortality.

Rapid removal of *S. aureus* from patients treated with encapsulated antibiotics may also minimise the development of antibiotic resistance. Exposure to antibiotics is the key driving force for the development of resistance. Low

concentrations of antibiotics can produce small stepwise mutations, so aggressive high dose therapies may be beneficial. Recent work in the Renshaw and Foster research groups have shown sub-curative doses of antibiotics, which have no effect on the growth or survival of *S. aureus*, increase the ratio of pre-existing resistant bacteria (McVicker et al., 2014). This means exposing *S. aureus* to low concentrations of antibiotics *in vivo* will benefit the resistant bacteria even if the antibiotic dose is so low that it does not affect the growth of the susceptible bacteria. Polymersomes may allow the bacteria to be killed more rapidly intracellularly without exposing them to sub-optimal concentrations of antibiotics that can speed up the formation of drug resistant strains.

Even in the face of active antibiotics *S. aureus* bacteraemia remains a global health burden. With these bacteria rapidly developing resistance to all our available treatments we desperately need to explore new methods for minimising the conditions that favour resistant strains and to utilise the antibiotics we have available to kill the bacteria most effectively. The results in this thesis provide more evidence that intracellular infection is an important component of *S. aureus* bacteraemia progression and supports further research into therapies that target infected phagocytes.

8.5 Limitations

In this thesis, knockdown of neutrophil Mcl-1 at the RNA level using siRNA was unsuccessful, but the reason for this is not known. It is possible that the siRNA was degraded during preparation or within the cell, or that the low

concentration of siRNA prevented efficient knockdown. Due to the expense of siRNA and the time required to perform the experiment, I was not able to optimize the siRNA delivery. Improved encapsulation efficiency may be achieved by conjugating a molecule to the siRNA that improves its interaction with the polymer. Cholesterol-siRNA conjugates have been used for targeting siRNA to the liver *in vivo* and our group has shown that cholesterol is encapsulated with high efficiency (Yealland personal communications); therefore, cholesterol conjugation may improve the siRNA encapsulation efficiency.

Neutrophils are sensitive cells and are very easily activated by foreign molecules. They can also be activated during purification and cell culture, so good technique is needed to work with these cells. Therefore it was surprising that the PMPC-PDPA polymersomes had no effect on neutrophil life span or IL-8 release. IL-8 is the most studied neutrophil cytokine. Following neutrophil activation high concentrations of IL-8 are expelled from pre-formed granules and additional IL-8 is produced by de-novo synthesis (Pellme et al., 2006). This makes IL-8 a robust readout for neutrophil activation, however, in order to completely rule out low levels of activation more cytokine ELISAs could be employed and membrane markers for neutrophil activation could be accessed by flow cytometry. For instance, upregulation of adhesion molecules, including CD11b, are associated with neutrophil priming (van Eeden et al., 1999).

As mentioned previously, the lack of neutrophil activation may be linked to the hydration of the PMPC block that prevents unspecific interactions with the cell.

The zwitterionic nature of this block gives PMPC a net neutral charge, which prevents it from binding to charged molecules and proteins, but still allows it to interact strongly with water molecules. For hydrated polymers, resistance to protein absorption is known to correlate with grafting density and the degree of hydration (Feng et al., 2007).

Although the polymersomes did not appear to affect neutrophil activation in this thesis, it is possible that the increase in endocytosis events may in itself affect gene expression, even if the polymersomes are not directly detrimental to the cells. Our group has previously found using a PCR array on HeLa cells that polymersomes do not upregulate pro-inflammatory genes such as NF- κ B and IL-6 (unlike lipofectmine), but they do upregulate interferon regulatory factors (Patikarnmonthon, unpublished communication). Interestingly they showed that polymersomes also upregulated interferon stimulated exonuclease gene 20kDa (ISG20), which can cleave both single- and double-stranded exogenous DNA (Espert et al., 2004). Upregulation of exonucleases as part of an antiviral response may explain why siRNA did not successfully knockdown its target mRNA in this thesis. An improved encapsulation efficiency may allow siRNA to be delivered in fewer polymersomes and reduce the upregulation of exonucleases within the cell.

Our group has shown that PMPC-PDPA polymersomes are biocompatible in both *in vitro* experiments and *in vivo* animal models; however, an important consideration is the long-term accumulation of the polymer in the body. Many

nanoparticle formulations accumulate in the liver, which may have long-term detrimental consequences. Biodegradable polymers have been developed to help combat this, and our group is researching methods of formulating biodegradable PMPC-PDPA polymers, although it is important to note that biodegradable polymers have their own disadvantages; they often have poor shelf lives and can be more permeable to encapsulated molecules. Metabolites of biodegradable polymers need to be thoroughly tested, as these can also be a source of toxicity (Singh and Ramarao, 2013).

The zebrafish model of *S. aureus* infection allows high numbers of animals to be tested within a single experiment and has lower ethical and monetary costs than mammalian models. Nonetheless, the model does have some limitations. In this model zebrafish embryos were injected at 30 and 50 hours post fertilization, but the liver is not fully formed until about 5 days post fertilization. Therefore, these studies should be repeated in mammalian models where the liver has fully matured.

8.6 Conclusions

In this thesis I have explored PMPC-PDPA polymersomes as intracellular delivery vectors for the treatment of neutrophil dominated infectious and inflammatory diseases. The project began by forming and purifying polymersomes of different sizes and shapes and exploring their ability to encapsulate and deliver molecules into neutrophils. I found that spherical polymersomes could deliver cargo most effectively with a diameter of 190nm. Tubular polymersomes were formed by

film rehydration and purified using centrifugation. Flow cytometry and confocal microscopy studies revealed that the tubular polymersomes were also internalised by neutrophils, but their uptake was delayed at the plasma membrane.

Polymersomes were able to encapsulate and deliver a range of cargo into human neutrophils including antibodies, nucleic acids, fluorescent dyes and other small molecules. (R)-roscovitine loaded polymersomes enhanced inflammation resolution in an *in vivo* assay of neutrophilic inflammation. Finally antibiotics were encapsulated to treat intracellular *S. aureus* infection. Rifampicin loaded polymersomes significantly reduced the number of intracellular bacteria in THP-1 macrophages and improved the bacterial burden in a zebrafish model of *S. aureus* infection. Together these findings improve our understanding of the physical properties of polymersomes that influence their internalisation and these results have important consequences for the study and treatment of neutrophilic inflammation and *S. aureus* infection.

References

- ABRAHAM, E. P. & CHAIN, E. 1940. An enzyme from bacteria able to destroy penicillin. *Nature*, 146, 837-837.
- ABRAHAM, E. P., CHAIN, E., FLETCHER, C. M., GARDNER, A., HEATLEY, N., JENNINGS, M. & FLOREY, H. W. 1941. Further observations on penicillin. *The Lancet*, 238, 177-189.
- AKINC, A. & BATTAGLIA, G. 2013. Exploiting Endocytosis for Nanomedicines. *Cold Spring Harbor Perspectives in Biology*, 5.
- ALBANESE, A., TANG, P. S. & CHAN, W. C. W. 2012. The Effect of Nanoparticle Size, Shape, and Surface Chemistry on Biological Systems. *Annual Review of Biomedical Engineering, Vol 14*, 14, 1-16.
- ALONZO, F., III & TORRES, V. J. 2013. Bacterial Survival Amidst an Immune Onslaught: The Contribution of the Staphylococcus aureus Leukotoxins. *Plos Pathogens*, 9.
- ALVARADO-KRISTENSSON, M., MELANDER, F., LEANDERSSON, K., R $\sqrt{\partial}$ NNSTRAND, L., WERNSTEDT, C. & ANDERSSON, T. 2004. p38-MAPK signals survival by phosphorylation of caspase-8 and caspase-3 in human neutrophils. *The Journal of experimental medicine*, 199, 449-458.
- AMULIC, B., CAZALET, C., HAYES, G. L., METZLER, K. D. & ZYCHLINSKY, A. 2012. Neutrophil Function: From Mechanisms to Disease. *Annual Review of Immunology, Vol 30*, 30, 459-489.
- ANWAR, S., PRINCE, L. R., FOSTER, S. J., WHYTE, M. K. B. & SABROE, I. 2009. The rise and rise of Staphylococcus aureus: laughing in the face of granulocytes. *Clinical and Experimental Immunology*, 157, 216-224.
- ARIEL, A., FREDMAN, G., SUN, Y.-P., KANTARCI, A., VAN DYKE, T. E., D LUSTER, A. & SERHAN, C. N. 2006. Apoptotic neutrophils and T cells sequester chemokines during immune response resolution through modulation of CCR5 expression. *Nature Immunology*, 7, 1209-1216.
- ASHCROFT, G. S., LEI, K., JIN, W., LONGENECKER, G., KULKARNI, A. B., GREENWELL-WILD, T., HALE-DONZE, H., MCGRADY, G., SONG, X.-Y. & WAHL, S. M. 2000. Secretory leukocyte protease inhibitor mediates non-redundant functions necessary for normal wound healing. *Nature Medicine*, 6, 1147-1153.
- AUWERX, J. 1991. THE HUMAN LEUKEMIA-CELL LINE, THP-1 - A MULTIFACETED MODEL FOR THE STUDY OF MONOCYTE-MACROPHAGE DIFFERENTIATION. *Experientia*, 47, 22-31.
- BAATZ, J. E., ZOU, Y. & KORFHAGEN, T. R. 2001. Inhibitory effects of tumor necrosis factor-alpha on cationic lipid-mediated gene delivery to airway cells in vitro. *Biochimica Et Biophysica Acta-Molecular Basis of Disease*, 1535, 100-109.
- BADER, R. A. 2012. The development of targeted drug delivery systems for rheumatoid arthritis treatment. *Rheumatoid Arthritis - Treatment, Dr. Andrew Lemmey (Ed.)*, ISBN: 978-953-307-850-2, InTech, DOI: 10.5772/26155, 111-132.
- BAINTON, D. F., MILLER, L. J., KISHIMOTO, T. K. & SPRINGER, T. A. 1987. LEUKOCYTE ADHESION RECEPTORS ARE STORED IN PEROXIDASE-

- NEGATIVE GRANULES OF HUMAN-NEUTROPHILS. *Journal of Experimental Medicine*, 166, 1641-1653.
- BANTEL, H., SINHA, B., DOMSCHKE, W., PETERS, G., SCHULZE-OSTHOFF, K. & JANICKE, R. U. 2001. alpha-toxin is a mediator of Staphylococcus aureus-induced cell death and activates caspases via the intrinsic death pathway independently of death receptor signaling. *Journal of Cell Biology*, 155, 637-647.
- BARCIA-MACAY, M., LEMAIRE, S., MINGEOT-LECLERCQ, M.-P., TULKENS, P. M. & VAN BAMBEKE, F. 2006a. Evaluation of the extracellular and intracellular activities (human THP-1 macrophages) of telavancin versus vancomycin against methicillin-susceptible, methicillin-resistant, vancomycin-intermediate and vancomycin-resistant Staphylococcus aureus. *Journal of Antimicrobial Chemotherapy*, 58, 1177-1184.
- BARCIA-MACAY, M., SERAL, C., MINGEOT-LECLERCQ, M. P., TULKENS, P. M. & VAN BAMBEKE, F. 2006b. Pharmacodynamic evaluation of the intracellular activities of antibiotics against Staphylococcus aureus in a model of THP-1 macrophages. *Antimicrobial Agents and Chemotherapy*, 50, 841-851.
- BARON, S., POAST, J., RIZZO, D., MCFARLAND, E. & KIEFF, E. 2000. Electroporation of antibodies, DNA, and other macromolecules into cells: a highly efficient method. *Journal of Immunological Methods*, 242, 115-126.
- BATTAGLIA, G. & RYAN, A. J. 2005a. Bilayers and interdigitation in block copolymer vesicles. *Journal of the American Chemical Society*, 127, 8757-8764.
- BATTAGLIA, G. & RYAN, A. J. 2005b. The evolution of vesicles from bulk lamellar gels. *Nature materials*, 4, 869-76.
- BATTAGLIA, G. & RYAN, A. J. 2006a. Neuron-like tubular membranes made of diblock copolymer amphiphiles. *Angewandte Chemie-International Edition*, 45, 2052-2056.
- BATTAGLIA, G. & RYAN, A. J. 2006b. Pathways of polymeric vesicle formation. *Journal of Physical Chemistry B*, 110, 10272-10279.
- BATTAGLIA, G., TOMAS, S. & RYAN, A. J. 2007. Lamellarsomes: metastable polymeric multilamellar aggregates. *Soft Matter*, 3, 470-475.
- BAUDOUX, P., BLES, N., LEMAIRE, S., MINGEOT-LECLERCQ, M.-P., TULKENS, P. M. & VAN BAMBEKE, F. 2007. Combined effect of pH and concentration on the activities of gentamicin and oxacillin against Staphylococcus aureus in pharmacodynamic models of extracellular and intracellular infections. *Journal of Antimicrobial Chemotherapy*, 59, 246-253.
- BEEH, K. M. & BEIER, J. 2006. Handle with care: targeting neutrophils in chronic obstructive pulmonary disease and severe asthma? *Clinical and Experimental Allergy*, 36, 142-157.
- BENNETT, C. M., KANKI, J. P., RHODES, J., LIU, T. X., PAW, B. H., KIERAN, M. W., LANGENAU, D. M., DELAHAYE-BROWN, A., ZON, L. I., FLEMING, M. D. & LOOK, A. T. 2001. Myelopoiesis in the zebrafish, Danio rerio. *Blood*, 98, 643-651.
- BENSON, C., WHITE, J., DE BONO, J., O'DONNELL, A., RAYNAUD, F., CRUICKSHANK, C., MCGRATH, H., WALTON, M., WORKMAN, P., KAYE, S., CASSIDY, J., GIANELLA-BORRADORI, A., JUDSON, I. & TWELVES, C. 2007. A phase I trial of the selective oral cyclin-dependent kinase inhibitor seliciclib (CYC202; R-

- Roscovitine), administered twice daily for 7 days every 21 days. *British Journal of Cancer*, 96, 29-37.
- BEYER, K., POETSCHKE, C., PARTECKE, L. I., VON BERNSTORFF, W., MAIER, S., BROEKER, B. M. & HEIDECHE, C.-D. 2014. TRAIL Induces Neutrophil Apoptosis and Dampens Sepsis-Induced Organ Injury in Murine Colon Ascendens Stent Peritonitis. *Plos One*, 9.
- BHOWMIK, A., SEEMUNGAL, T. A. R., SAPSFORD, R. J. & WEDZICHA, J. A. 2000. Relation of sputum inflammatory markers to symptoms and lung function changes in COPD exacerbations. *Thorax*, 55, 114-120.
- BIANCHI, M. E. 2007. DAMPs, PAMPs and alarmins: all we need to know about danger. *Journal of Leukocyte Biology*, 81, 1-5.
- BLANAZS, A., ARMES, S. P. & RYAN, A. J. 2009a. Self-Assembled Block Copolymer Aggregates: From Micelles to Vesicles and their Biological Applications. *Macromolecular Rapid Communications*, 30, 267-277.
- BLANAZS, A., MASSIGNANI, M., BATTAGLIA, G., ARMES, S. P. & RYAN, A. J. 2009b. Tailoring Macromolecular Expression at Polymersome Surfaces. *Advanced Functional Materials*, 19, 2906-2914.
- BLANAZS, A., WARREN, N. J., LEWIS, A. L., ARMES, S. P. & RYAN, A. J. 2011. Self-assembly of double hydrophilic block copolymers in concentrated aqueous solution. *Soft Matter*, 7, 6399-6403.
- BORREGAARD, N. 2010. Neutrophils, from Marrow to Microbes. *Immunity*, 33, 657-670.
- BOSSE, M. J., GRUBER, H. E. & RAMP, W. K. 2005. Internalization of bacteria by osteoblasts in a patient with recurrent, long-term osteomyelitis - A case report. *Journal of Bone and Joint Surgery-American Volume*, 87A, 1343-1347.
- BRATTON, D. L. & HENSON, P. M. 2011. Neutrophil clearance: when the party is over, clean-up begins. *Trends in immunology*, 32, 350-357.
- BRINKMANN, V., REICHARD, U., GOOSMANN, C., FAULER, B., UHLEMANN, Y., WEISS, D. S., WEINRAUCH, Y. & ZYCHLINSKY, A. 2004. Neutrophil extracellular traps kill bacteria. *Science*, 303, 1532-1535.
- BRINKMANN, V. & ZYCHLINSKY, A. 2007. Beneficial suicide: why neutrophils die to make NETs. *Nature Reviews Microbiology*, 5, 577-582.
- BRINKMANN, V. & ZYCHLINSKY, A. 2012. Neutrophil extracellular traps: Is immunity the second function of chromatin? *Journal of Cell Biology*, 198, 773-783.
- BRIONES, E., COLINO, C. I. & LANA O, J. M. 2008. Delivery systems to increase the selectivity of antibiotics in phagocytic cells. *Journal of Controlled Release*, 125, 210-227.
- BROZ, P., BENITO, S. M., SAW, C., BURGER, P., HEIDER, H., PFISTERER, M., MARSCH, S., MEIER, W. & HUNZIKER, P. 2005. Cell targeting by a generic receptor-targeted polymer nanocontainer platform. *Journal of Controlled Release*, 102, 475-488.
- BURTON, J., ROBERTSON, A. L., SADIKU, P., WANG, X., HOOPER-GREENHILL, E., PRINCE, L. R., WALKER, P., HOGGETT, E. E., WARD, J. R., FARROW, S. N., ZUERCHER, W. J., JEFFREY, P., SAVAGE, C. O., INGHAM, P. W., HURLSTONE, A. F., WHYTE, M. K. B. & RENSHAW, S. A. 2014. Serum and Glucocorticoid-Regulated Kinase 1 Regulates Neutrophil Clearance during Inflammation Resolution. *Journal of Immunology*, 192, 1796-1805.

- CAI, S. S., VIJAYAN, K., CHENG, D., LIMA, E. M. & DISCHER, D. E. 2007. Micelles of different morphologies - Advantages of worm-like filomicelles of PEO-PCL in paclitaxel delivery. *Pharmaceutical Research*, 24, 2099-2109.
- CAMPS, M., RUCKLE, T., JI, H., ARDISSONE, V., RINTELEN, F., SHAW, J., FERRANDI, C., CHABERT, C., GILLIERON, C., FRANCON, B., MARTIN, T., GRETENER, D., PERRIN, D., LEROY, D., VITTE, P. A., HIRSCH, E., WYMAN, M. P., CIRILLO, R., SCHWARZ, M. K. & ROMMEL, C. 2005. Blockade of PI3K gamma suppresses joint inflammation and damage in mouse models of rheumatoid arthritis. *Nature Medicine*, 11, 936-943.
- CANTON, I. & BATTAGLIA, G. 2012. Endocytosis at the nanoscale. *Chemical Society Reviews*, 41, 2718-2739.
- CANTON, I., MASSIGNANI, M., PATIKARNMONTHON, N., CHIERICO, L., ROBERTSON, J., RENSHAW, S. A., WARREN, N. J., MADSEN, J. P., ARMES, S. P., LEWIS, A. L. & BATTAGLIA, G. 2013. Fully synthetic polymer vesicles for intracellular delivery of antibodies in live cells. *Faseb Journal*, 27, 98-108.
- CARRYN, S., CHANTEUX, H., SERAL, C., MINGEOT-LECLERCQ, M. P., VAN BAMBEKE, F. & TULKENS, P. M. 2003. Intracellular pharmacodynamics of antibiotics. *Infectious Disease Clinics of North America*, 17, 615-+.
- CASCAO, R., ROSARIO, H. S., SOUTO-CARNEIRO, M. M. & FONSECA, J. E. 2010. Neutrophils in rheumatoid arthritis: More than simple final effectors. *Autoimmunity Reviews*, 9, 531-535.
- CELSUS, A. C. & BROCA, P. 1876. *De medicina*, G. Masson.
- CHAMPION, J. A. & MITRAGOTRI, S. 2006. Role of target geometry in phagocytosis. *Proceedings of the National Academy of Sciences of the United States of America*, 103, 4930-4934.
- CHAMPION, J. A. & MITRAGOTRI, S. 2009. Shape Induced Inhibition of Phagocytosis of Polymer Particles. *Pharmaceutical Research*, 26, 244-249.
- CHANAN-KHAN, A., SZEBENI, J., SAVAY, S., LIEBES, L., RAFIQUE, N. M., ALVING, C. R. & MUGGIA, F. M. 2003. Complement activation following first exposure to pegylated liposomal doxorubicin (Doxil): possible role in hypersensitivity reactions. *Annals of Oncology*, 14, 1430-1437.
- CHANG, F. Y., PEACOCK, J. E., MUSER, D. M., TRIPLETT, P., MACDONALD, B. B., MYLOTTE, J. M., O'DONNELL, A., WAGENER, M. M. & YU, V. L. 2003. Staphylococcus aureus bacteremia - Recurrence and the impact of antibiotic treatment in a prospective multicenter study. *Medicine*, 82, 333-339.
- CHAUDHURI, A., BATTAGLIA, G. & GOLESTANIAN, R. 2011. The effect of interactions on the cellular uptake of nanoparticles. *Physical Biology*, 8.
- CHEUNG, A. L., BAYER, A. S., ZHANG, G. Y., GRESHAM, H. & XIONG, Y. Q. 2004. Regulation of virulence determinants in vitro and in vivo in Staphylococcus aureus. *Fems Immunology and Medical Microbiology*, 40, 1-9.
- CHITHRANI, B. D. & CHAN, W. C. W. 2007. Elucidating the mechanism of cellular uptake and removal of protein-coated gold nanoparticles of different sizes and shapes. *Nano Letters*, 7, 1542-1550.
- CHITHRANI, B. D., GHAZANI, A. A. & CHAN, W. C. W. 2006. Determining the size and shape dependence of gold nanoparticle uptake into mammalian cells. *Nano Letters*, 6, 662-668.
- CHOI, H. S., LIU, W., MISRA, P., TANAKA, E., ZIMMER, J. P., IPE, B. I., BAWENDI, M. G. & FRANGIONI, J. V. 2007. Renal clearance of quantum dots. *Nature Biotechnology*, 25, 1165-1170.

- CHOW, J. C., YOUNG, D. W., GOLENBOCK, D. T., CHRIST, W. J. & GUSOVSKY, F. 1999. Toll-like receptor-4 mediates lipopolysaccharide-induced signal transduction. *Journal of Biological Chemistry*, 274, 10689-10692.
- CHRISTIAN, D. A., CAI, S. S., GARBUZENKO, O. B., HARADA, T., ZAJAC, A. L., MINKO, T. & DISCHER, D. E. 2009. Flexible Filaments for in Vivo Imaging and Delivery: Persistent Circulation of Filomicelles Opens the Dosage Window for Sustained Tumor Shrinkage. *Molecular Pharmaceutics*, 6, 1343-1352.
- CLOHESSY, J. G., ZHUANG, J., DE BOER, J., GIL-GIL, G. & BRADY, H. J. 2006. Mcl-1 interacts with truncated Bid and inhibits its induction of cytochrome c release and its role in receptor-mediated apoptosis. *Journal of Biological Chemistry*, 281, 5750-5759.
- CLOHESSY, J. G., ZHUANG, J. G. & BRADY, H. J. M. 2004. Characterisation of Mcl-1 cleavage during apoptosis of haematopoietic cells. *British Journal of Haematology*, 125, 655-665.
- COLGAN, S. P., SERHAN, C. N., PARKOS, C. A., DELPARCER, C. & MADARA, J. L. 1993. LIPOXIN A(4) MODULATES TRANSMIGRATION OF HUMAN NEUTROPHILS ACROSS INTESTINAL EPITHELIAL MONOLAYERS. *Journal of Clinical Investigation*, 92, 75-82.
- COLLEY, H. E., HEARNDEN, V., AVILA-OLIAS, M., CECCHIN, D., CANTON, I., MADSEN, J., MACNEIL, S., WARREN, N., HU, K. & MCKEATING, J. A. 2014a. Polymersome-mediated delivery of combination anti-cancer therapy to head and neck cancer cells: 2D and 3D in vitro evaluation. *Molecular pharmaceutics*.
- COLLEY, H. E., HEARNDEN, V., AVILA-OLIAS, M., CECCHIN, D., CANTON, I., MADSEN, J., MACNEIL, S., WARREN, N., HU, K., MCKEATING, J. A., ARMES, S. P., MURDOCH, C., THORNHILL, M. H. & BATTAGLIA, G. 2014b. Polymersome-Mediated Delivery of Combination Anticancer Therapy to Head and Neck Cancer Cells: 2D and 3D in Vitro Evaluation. *Molecular Pharmaceutics*, 11, 1176-1188.
- COOPER, M. D. & ALDER, M. N. 2006. The evolution of adaptive immune systems. *Cell*, 124, 815-822.
- COSGROVE, S. E., VIGLIANI, G. A., CAMPION, M., FOWLER, V. G., JR., ABRUTYN, E., COREY, G. R., LEVINE, D. P., RUPP, M. E., CHAMBERS, H. F., KARCHMER, A. W. & BOUCHER, H. W. 2009. Initial Low-Dose Gentamicin for Staphylococcus aureus Bacteremia and Endocarditis Is Nephrotoxic. *Clinical Infectious Diseases*, 48, 713-721.
- COX, G. 1996. IL-10 enhances resolution of pulmonary inflammation in vivo by promoting apoptosis of neutrophils. *American Journal of Physiology-Lung Cellular and Molecular Physiology*, 271, L566-L571.
- COX, G., GAULDIE, J. & JORDANA, M. 1992. BRONCHIAL EPITHELIAL CELL-DERIVED CYTOKINES (G-CSF AND GM-CSF) PROMOTE THE SURVIVAL OF PERIPHERAL-BLOOD NEUTROPHILS INVITRO. *American Journal of Respiratory Cell and Molecular Biology*, 7, 507-513.
- CUCONATI, A., MUKHERJEE, C., PEREZ, D. & WHITE, E. 2003. DNA damage response and MCL-1 destruction initiate apoptosis in adenovirus-infected cells. *Genes & development*, 17, 2922-2932.
- DANCEY, J. T., DEUBELBEISS, K. A., HARKER, L. A. & FINCH, C. A. 1976. NEUTROPHIL KINETICS IN MAN. *Journal of Clinical Investigation*, 58, 705-715.

- DAVIES, M. J. 2011. Myeloperoxidase-derived oxidation: mechanisms of biological damage and its prevention. *Journal of clinical biochemistry and nutrition*, 48, 8.
- DAVIES, P., BAILEY, P. J., GOLDENBERG, M. M. & FORDHUTCHINSON, A. W. 1984. THE ROLE OF ARACHIDONIC-ACID OXYGENATION PRODUCTS IN PAIN AND INFLAMMATION. *Annual Review of Immunology*, 2, 335-357.
- DAVIS, J. M., CLAY, H., LEWIS, J. L., GHORI, N., HERBOMEL, P. & RAMAKRISHNAN, L. 2002. Real-time visualization of Mycobacterium-macrophage interactions leading to initiation of granuloma formation in zebrafish embryos. *Immunity*, 17, 693-702.
- DAVIS, J. M. & RAMAKRISHNAN, L. 2009. The Role of the Granuloma in Expansion and Dissemination of Early Tuberculous Infection. *Cell*, 136, 37-49.
- DE HAAS, C. J. C., VELDKAMP, K. E., PESCHEL, A., WEERKAMP, F., VAN WAMEL, W. J. B., HEEZIUS, E., POPPELIER, M., VAN KESSEL, K. P. M. & VAN STRIJP, J. A. G. 2004. Chemotaxis inhibitory protein of Staphylococcus aureus, a bacterial antiinflammatory agent. *Journal of Experimental Medicine*, 199, 687-695.
- DECUZZI, P. & FERRARI, M. 2006. The adhesive strength of non-spherical particles mediated by specific interactions. *Biomaterials*, 27, 5307-5314.
- DECUZZI, P. & FERRARI, M. 2008. The receptor-mediated endocytosis of nonspherical particles. *Biophysical Journal*, 94, 3790-3797.
- DECUZZI, P., LEE, S., DECUZZI, M. & FERRARI, M. 2004. Adhesion of microfabricated particles on vascular endothelium: A parametric analysis. *Annals of Biomedical Engineering*, 32, 793-802.
- DELEO, F. R. & CHAMBERS, H. F. 2009. Reemergence of antibiotic-resistant Staphylococcus aureus in the genomics era. *Journal of Clinical Investigation*, 119, 2464-2474.
- DEROUE, M., THOMAS, L., CROSS, A., MOOTS, R. J. & EDWARDS, S. W. 2004. Granulocyte macrophage colony-stimulating factor signaling and proteasome inhibition delay neutrophil apoptosis by increasing the stability of Mcl-1. *Journal of Biological Chemistry*, 279, 26915-26921.
- DESAI, M. P., LABHASETWAR, V., WALTER, E., LEVY, R. J. & AMIDON, G. L. 1997. The mechanism of uptake of biodegradable microparticles in Caco-2 cells is size dependent. *Pharmaceutical Research*, 14, 1568-1573.
- DI STEFANO, A., CAPELLI, A., LUSUARDI, M., BALBO, P., VECCHIO, C., MAESTRELLI, P., MAPP, C. E., FABBRI, L. M., DONNER, C. F. & SAETTA, M. 1998. Severity of airflow limitation is associated with severity of airway inflammation in smokers. *American Journal of Respiratory and Critical Care Medicine*, 158, 1277-1285.
- DICK, E. P., PRINCE, L. R., PRESTWICH, E. C., RENSHAW, S. A., WHYTE, M. K. B. & SABROE, I. 2009. Pathways regulating lipopolysaccharide-induced neutrophil survival revealed by lentiviral transduction of primary human neutrophils. *Immunology*, 127, 249-255.
- DIMITROV, D. S. 2004. Virus entry: Molecular mechanisms and biomedical applications. *Nature Reviews Microbiology*, 2, 109-122.
- DIMOVA, R., SEIFERT, U., POULIGNY, B., FORSTER, S. & DOBEREINER, H. G. 2002. Hyperviscous diblock copolymer vesicles. *European Physical Journal E*, 7, 241-250.
- DING, Q., HE, X., HSU, J.-M., XIA, W., CHEN, C.-T., LI, L.-Y., LEE, D.-F., LIU, J.-C., ZHONG, Q., WANG, X. & HUNG, M.-C. 2007. Degradation of Mcl-1 by beta-

- TrCP mediates glycogen synthase kinase 3-induced tumor suppression and chemosensitization. *Molecular and Cellular Biology*, 27, 4006-4017.
- DISCHER, B. M., WON, Y. Y., EGE, D. S., LEE, J. C. M., BATES, F. S., DISCHER, D. E. & HAMMER, D. A. 1999. Polymersomes: Tough vesicles made from diblock copolymers. *Science*, 284, 1143-1146.
- DUFORT, S., SANCEY, L. & COLL, J. L. 2011. Physico-chemical parameters that govern nanoparticles fate also dictate rules for their molecular evolution. *Advanced Drug Delivery Reviews*.
- DUMONT, A. L., NYGAARD, T. K., WATKINS, R. L., SMITH, A., KOZHAYA, L., KREISWIRTH, B. N., SHOPSIN, B., UNUTMAZ, D., VOYICH, J. M. & TORRES, V. J. 2011. Characterization of a new cytotoxin that contributes to *Staphylococcus aureus* pathogenesis. *Molecular Microbiology*, 79, 814-825.
- DZHAGALOV, I., ST. JOHN, A. & HE, Y.-W. 2007. The antiapoptotic protein Mcl-1 is essential for the survival of neutrophils but not macrophages. *Blood*, 109, 1620-1626.
- EDWARDS, A. M., POTTS, J. R., JOSEFSSON, E. & MASSEY, R. C. 2010. *Staphylococcus aureus* Host Cell Invasion and Virulence in Sepsis Is Facilitated by the Multiple Repeats within FnBPA. *Plos Pathogens*, 6.
- EL KEBIR, D., JOZSEF, L., KHREISS, T., PAN, W., PETASIS, N. A., SERHAN, C. N. & FILEP, J. G. 2007. Aspirin-triggered lipoxins override the apoptosis-delaying action of serum amyloid A in human neutrophils: A novel mechanism for resolution of inflammation. *Journal of Immunology*, 179, 616-622.
- EL KEBIR, D., JOZSEF, L., PAN, W. & FILEP, J. G. 2008. Myeloperoxidase delays neutrophil apoptosis through CD11b/CD18 integrins and prolongs inflammation. *Circulation Research*, 103, 352-359.
- EL KEBIR, D., JOZSEF, L., PAN, W., WANG, L., PETASIS, N. A., SERHAN, C. N. & FILEP, J. G. 2009. 15-Epi-lipoxin A(4) Inhibits Myeloperoxidase Signaling and Enhances Resolution of Acute Lung Injury. *American Journal of Respiratory and Critical Care Medicine*, 180, 311-319.
- ELKS, P. M., VAN EEDEN, F. J., DIXON, G., WANG, X., REYES-ALDASORO, C. C., INGHAM, P. W., WHYTE, M. K. B., WALMSLEY, S. R. & RENSHAW, S. A. 2011. Activation of hypoxia-inducible factor-1 alpha (Hif-1 alpha) delays inflammation resolution by reducing neutrophil apoptosis and reverse migration in a zebrafish inflammation model. *Blood*, 118, 712-722.
- ELLIS, T. N. & BEAMAN, B. L. 2004. Interferon-gamma activation of polymorphonuclear neutrophil function. *Immunology*, 112, 2-12.
- ELOUAHABI, A., FLAMAND, V., OZKAN, S., PAULART, F., VANDENBRANDEN, M., GOLDMAN, M. & RUYSSCHAERT, J. M. 2003. Free cationic Liposomes inhibit the inflammatory response to cationic Lipid-DNA complex injected intravenously and enhance its Transfection efficiency. *Molecular Therapy*, 7, 81-88.
- ESPERT, L., REY, C., GONZALEZ, L., DEGOLS, G., CHELBI-ALIX, M. K., MECHTI, N. & GONGORA, C. 2004. The exonuclease ISG20 is directly induced by synthetic dsRNA via NF-kB and IRF1 activation. *Oncogene*, 23, 4636-4640.
- FADOK, V. A., BRATTON, D. L., FRASCH, S. C., WARNER, M. L. & HENSON, P. M. 1998a. The role of phosphatidylserine in recognition of apoptotic cells by phagocytes. *Cell Death and Differentiation*, 5, 551-562.
- FADOK, V. A., BRATTON, D. L., KONOWAL, A., FREED, P. W., WESTCOTT, J. Y. & HENSON, P. M. 1998b. Macrophages that have ingested apoptotic cells in

- vitro inhibit proinflammatory cytokine production through autocrine/paracrine mechanisms involving TGF-beta, PGE2, and PAF. *Journal of Clinical Investigation*, 101, 890-898.
- FARDET, L., KASSAR, A., CABANE, J. & FLAHAULT, A. 2007. Corticosteroid-induced adverse events in adults - Frequency, screening and prevention. *Drug Safety*, 30, 861-881.
- FAURSCHOU, M. & BORREGAARD, N. 2003. Neutrophil granules and secretory vesicles in inflammation. *Microbes and Infection*, 5, 1317-1327.
- FAUSTINO, L., FONSECA, D., FLORSHEIM, E., RESENDE, R., LEPIQUE, A., FAQUIM-MAURO, E., GOMES, E., SILVA, J., YAGITA, H. & RUSSO, M. 2014. Tumor necrosis factor-related apoptosis-inducing ligand mediates the resolution of allergic airway inflammation induced by chronic allergen inhalation. *Mucosal immunology*.
- FENG, W., NIEH, M.-P., ZHU, S., HARROUN, T. A., KATSARAS, J. & BRASH, J. L. 2007. Characterization of protein resistant, grafted methacrylate polymer layers bearing oligo (ethylene glycol) and phosphorylcholine side chains by neutron reflectometry. *Biointerphases*, 2, 34-43.
- FILEP, J. G. & EL KEBIR, D. 2009. Neutrophil Apoptosis: A Target for Enhancing the Resolution of Inflammation. *Journal of Cellular Biochemistry*, 108, 1039-1046.
- FOSTER, T. J. 2005. Immune evasion by Staphylococci. *Nature Reviews Microbiology*, 3, 948-958.
- FOSTER, T. J., GEOGHEGAN, J. A., GANESH, V. K. & HOEOEK, M. 2014. Adhesion, invasion and evasion: the many functions of the surface proteins of Staphylococcus aureus. *Nature Reviews Microbiology*, 12, 49-62.
- FOWLER, V. G., JR., ALLEN, K. B., MOREIRA, E. D., JR., MOUSTAFA, M., ISGRO, F., BOUCHER, H. W., COREY, G. R., CARMELI, Y., BETTS, R., HARTZEL, J. S., CHAN, I. S. F., MCNEELY, T. B., KARTSONIS, N. A., GURIS, D., ONORATO, M. T., SMUGAR, S. S., DINUBILE, M. J. & SOBANJO-TER MEULEN, A. 2013. Effect of an Investigational Vaccine for Preventing Staphylococcus aureus Infections After Cardiothoracic Surgery A Randomized Trial. *Jama-Journal of the American Medical Association*, 309, 1368-1378.
- FRANCOIS, S., EL BENNA, J., DANG, P. M. C., PEDRUZZI, E., GOUGEROT-POCIDALO, M. A. & ELBIM, C. 2005. Inhibition of neutrophil apoptosis by TLR agonists in whole blood: Involvement of the phosphoinositide 3-Kinase/Akt and NF-kappa B signaling pathways, leading to increased levels of Mcl-1, Al, and phosphorylated bad. *Journal of Immunology*, 174, 3633-3642.
- FURZE, R. C. & RANKIN, S. M. 2008. Neutrophil mobilization and clearance in the bone marrow. *Immunology*, 125, 281-288.
- GAO, H. J., SHI, W. D. & FREUND, L. B. 2005. Mechanics of receptor-mediated endocytosis. *Proceedings of the National Academy of Sciences of the United States of America*, 102, 9469-9474.
- GAO, X.-P., ZHU, X., FU, J., LIU, Q., FREY, R. S. & MALIK, A. B. 2007. Blockade of class IA phosphoinositide 3-kinase in neutrophils prevents NADPH oxidase activation-and adhesion-dependent inflammation. *Journal of Biological Chemistry*, 282, 6116-6125.
- GARDINER, E. M., PESTONJAMASP, K. N., BOHL, B. P., CHAMBERLAIN, C., HAHN, K. M. & BOKOCH, G. M. 2002. Spatial and temporal analysis of Rac activation during live neutrophil chemotaxis. *Current biology*, 12, 2029-2034.

- GARZONI, C. & KELLEY, W. L. 2009. Staphylococcus aureus: new evidence for intracellular persistence. *Trends in Microbiology*, 17, 59-65.
- GENG, Y., DALHAIMER, P., CAI, S., TSAI, R., TEWARI, M., MINKO, T. & DISCHER, D. E. 2007. Shape effects of filaments versus spherical particles in flow and drug delivery. *Nature Nanotechnology*, 2, 249-255.
- GERNEZ, Y., TIROUVANZIAM, R. & CHANEZ, P. 2010. Neutrophils in chronic inflammatory airway diseases: can we target them and how? *European Respiratory Journal*, 35, 467-469.
- GODA, T. & ISHIHARA, K. 2006. Soft contact lens biomaterials from bioinspired phospholipid polymers. *Expert Review of Medical Devices*, 3, 167-174.
- GODSON, C., MITCHELL, S., HARVEY, K., PETASIS, N. A., HOGG, N. & BRADY, H. R. 2000. Cutting edge: Lipoxins rapidly stimulate nonphlogistic phagocytosis of apoptotic neutrophils by monocyte-derived macrophages. *Journal of Immunology*, 164, 1663-1667.
- GOLDRICK, B. 2002. First Reported Case of VRSA in the United States: An alarming development in microbial resistance. *AJN The American Journal of Nursing*, 102, 17.
- GOLPON, H. A., FADOK, V. A., TARASEVICIENE-STEWART, L., SCERBAVICIUS, R., SAUER, C., WELTE, T., HENSON, P. M. & VOELKEL, N. F. 2004. Life after corpse engulfment: phagocytosis of apoptotic cells leads to VEGF secretion and cell growth. *Faseb Journal*, 18, 1716-+.
- GONCALVES, D. M., DE LIZ, R. & GIRARD, D. 2011. Activation of neutrophils by nanoparticles. *The Scientific World Journal*, 11, 1877-1885.
- GRATTON, S. E. A., NAPIER, M. E., ROPP, P. A., TIAN, S. & DESIMONE, J. M. 2008a. Microfabricated Particles for Engineered Drug Therapies: Elucidation into the Mechanisms of Cellular Internalization of PRINT Particles. *Pharmaceutical Research*, 25, 2845-2852.
- GRATTON, S. E. A., ROPP, P. A., POHLHAUS, P. D., LUFT, J. C., MADDEN, V. J., NAPIER, M. E. & DESIMONE, J. M. 2008b. The effect of particle design on cellular internalization pathways. *Proceedings of the National Academy of Sciences of the United States of America*, 105, 11613-11618.
- GRAY, C., LOYNES, C. A., WHYTE, M. K. B., CROSSMAN, D. C., RENSHAW, S. A. & CHICO, T. J. A. 2011. Simultaneous intravital imaging of macrophage and neutrophil behaviour during inflammation using a novel transgenic zebrafish. *Thrombosis and Haemostasis*, 105, 811-819.
- GREEN, P. F. & LIMARY, R. 2001. Block copolymer thin films: pattern formation and phase behavior. *Advances in Colloid and Interface Science*, 94, 53-81.
- GRESHAM, H. D., LOWRANCE, J. H., CAVER, T. E., WILSON, B. S., CHEUNG, A. L. & LINDBERG, F. P. 2000. Survival of Staphylococcus aureus inside neutrophils contributes to infection. *Journal of Immunology*, 164, 3713-3722.
- GRUMELARD, J., TAUBERT, A. & MEIER, W. 2004. Soft nanotubes from amphiphilic ABA triblock macromonomers. *Chemical Communications*, 1462-1463.
- GUBERNATOR, J., DRULIS-KAWA, Z. & KOZUBEK, A. 2006. A simple and sensitive fluorometric method for determination of gentamicin in liposomal suspensions. *International Journal of Pharmaceutics*, 327, 104-109.
- HACHICHA, M., POULIOT, M., PETASIS, N. A. & SERHAN, C. N. 1999. Lipoxin (LX)A(4) and aspirin-triggered 15-epi-LXA(4) inhibit tumor necrosis factor 1 alpha-initiated neutrophil responses and trafficking: Regulators of a cytokine-chemokine axis. *Journal of Experimental Medicine*, 189, 1923-1929.

- HAGER, M., COWLAND, J. B. & BORREGAARD, N. 2010. Neutrophil granules in health and disease. *Journal of Internal Medicine*, 268, 25-34.
- HALLETT, M. B. & LLOYDS, D. 1995. NEUTROPHIL PRIMING - THE CELLULAR SIGNALS THAT SAY AMBER BUT NOT GREEN. *Immunology Today*, 16, 264-268.
- HAMDY, S., HADDADI, A., SHAYEGANPOUR, A., ALSHAMSAN, A., ALIABADI, H. M. & LAVASANIFAR, A. 2011. The Immunosuppressive Activity of Polymeric Micellar Formulation of Cyclosporine A: In Vitro and In Vivo Studies. *Aaps Journal*, 13, 159-168.
- HAMILTON, A. J. & BAULCOMBE, D. C. 1999. A species of small antisense RNA in posttranscriptional gene silencing in plants. *Science*, 286, 950-952.
- HAN, J., GOLDSTEIN, L. A., GASTMAN, B. R., FROELICH, C. J., YIN, X. M. & RABINOWICH, H. 2004. Degradation of Mcl-1 by granzyme B - Implications for Bim-mediated mitochondrial apoptotic events. *Journal of Biological Chemistry*, 279, 22020-22029.
- HARRO, C. D., BETTS, R. F., HARTZEL, J. S., ONORATO, M. T., LIPKA, J., SMUGAR, S. S. & KARTSONIS, N. A. 2012. The immunogenicity and safety of different formulations of a novel *Staphylococcus aureus* vaccine (V710): Results of two Phase I studies. *Vaccine*, 30, 1729-1736.
- HASLETT, C., SAVILL, J. & MEAGHER, L. 1990. MACROPHAGE RECOGNITION OF SENESCENT GRANULOCYTES. *Biochemical Society Transactions*, 18, 225-227.
- HAYWARD, J. A. & CHAPMAN, D. 1984. BIOMEMBRANE SURFACES AS MODELS FOR POLYMER DESIGN - THE POTENTIAL FOR HEMOCOMPATIBILITY. *Biomaterials*, 5, 135-142.
- HEYER, G., SABA, S., ADAMO, R., RUSH, W., SOONG, G., CHEUNG, A. & PRINCE, A. 2002. *Staphylococcus aureus* agr and sarA functions are required for invasive infection but not inflammatory responses in the lung. *Infection and Immunity*, 70, 127-133.
- HIRAMATSU, K., HANAOKI, H., INO, T., YABUTA, K., OGURI, T. & TENOVER, F. C. 1997. Methicillin-resistant *Staphylococcus aureus* clinical strain with reduced vancomycin susceptibility. *Journal of Antimicrobial Chemotherapy*, 40, 135-136.
- HIRSIGER, S., SIMMEN, H.-P., WERNER, C. L., WANNER, G. A. & RITTIRSCH, D. 2012. Danger Signals Activating the Immune Response after Trauma. *Mediators of Inflammation*.
- HUNTER, A. C. & MOGHIMI, S. M. 2010. Cationic carriers of genetic material and cell death: A mitochondrial tale. *Biochimica Et Biophysica Acta-Bioenergetics*, 1797, 1203-1209.
- IMBULUZQUETA, E., LEMAIRE, S., GAMAZO, C., ELIZONDO, E., VENTOSA, N., VECIANA, J., VAN BAMBEKE, F. & BLANCO-PRIETO, M. J. 2012. Cellular pharmacokinetics and intracellular activity against *Listeria monocytogenes* and *Staphylococcus aureus* of chemically modified and nanoencapsulated gentamicin. *Journal of Antimicrobial Chemotherapy*, 67, 2158-2164.
- ISHIDA, T., ICHIKAWA, T., ICHIHARA, M., SADZUKA, Y. & KIWADA, H. 2004. Effect of the physicochemical properties of initially injected liposomes on the clearance of subsequently injected PEGylated liposomes in mice. *Journal of Controlled Release*, 95, 403-412.

- ISHIHARA, K., NOMURA, H., MIHARA, T., KURITA, K., IWASAKI, Y. & NAKABAYASHI, N. 1998. Why do phospholipid polymers reduce protein adsorption? *Journal of Biomedical Materials Research*, 39, 323-330.
- ISHIHARA, T., KUBOTA, T., CHOI, T. & HIGAKI, M. 2009. Treatment of Experimental Arthritis with Stealth-Type Polymeric Nanoparticles Encapsulating Betamethasone Phosphate. *Journal of Pharmacology and Experimental Therapeutics*, 329, 412-417.
- ISRAELACHVILI, J. N., MITCHELL, D. J. & NINHAM, B. W. 1976. THEORY OF SELF-ASSEMBLY OF HYDROCARBON AMPHIPHILES INTO MICELLES AND BILAYERS. *Journal of the Chemical Society-Faraday Transactions II*, 72, 1525-1568.
- JAIN, R. K. & STYLIANOPOULOS, T. 2010. Delivering nanomedicine to solid tumors. *Nature Reviews Clinical Oncology*, 7, 653-664.
- JAIN, S. & BATES, F. S. 2004. Consequences of nonergodicity in aqueous binary PEO-PB micellar dispersions. *Macromolecules*, 37, 1511-1523.
- JEVONS, M. P., COE, A. W. & PARKER, M. T. 1963. METHICILLIN RESISTANCE IN STAPHYLOCOCCI. *Lancet*, 1, 904-&.
- JEVONS, M. P., ROLINSON, G. N. & KNOX, R. 1961. CELBENIN-RESISTANT STAPHYLOCOCCI. *British Medical Journal*, 1, 124-&.
- JIANG, W., KIM, B. Y. S., RUTKA, J. T. & CHAN, W. C. W. 2008. Nanoparticle-mediated cellular response is size-dependent. *Nature Nanotechnology*, 3, 145-150.
- JOHNSON, J. L., ELLIS, B. A., MUNAFO, D. B., BRZEZINSKA, A. A. & CATZ, S. D. 2006. Gene transfer and expression in human neutrophils. The phox homology domain of p47phox translocates to the plasma membrane but not to the membrane of mature phagosomes. *BMC immunology*, 7, 28.
- KAKIZAWA, Y. & KATAOKA, K. 2002. Block copolymer micelles for delivery of gene and related compounds. *Advanced Drug Delivery Reviews*, 54, 203-222.
- KAPRAL, F. A. & SHAYEGANI, M. G. 1959. INTRACELLULAR SURVIVAL OF STAPHYLOCOCCI. *Journal of Experimental Medicine*, 110, 123-138.
- KAWAI, T. & AKIRA, S. 2010. The role of pattern-recognition receptors in innate immunity: update on Toll-like receptors. *Nature Immunology*, 11, 373-384.
- KEDMI, R., BEN-ARIE, N. & PEER, D. 2010. The systemic toxicity of positively charged lipid nanoparticles and the role of Toll-like receptor 4 in immune activation. *Biomaterials*, 31, 6867-6875.
- KEMPE, S., KESTLER, H., LASAR, A. & WIRTH, T. 2005. NF-kappa B controls the global pro-inflammatory response in endothelial cells: evidence for the regulation of a pro-atherogenic program. *Nucleic Acids Research*, 33, 5308-5319.
- KHATIB, R., JOHNSON, L. B., FAKIH, M. G., RIEDERER, K., KHOSROVANEH, A., TABRIZ, M. S., SHARMA, M. & SAEED, S. 2006. Persistence in Staphylococcus aureus bacteremia: Incidence, characteristics of patients and outcome. *Scandinavian Journal of Infectious Diseases*, 38, 7-14.
- KIRBY, W. M. M. 1944. Extraction of a highly potent penicillin inactivator from penicillin resistant staphylococci. *Science*, 99, 452-453.
- KLUYTMANS, J., VANBELKUM, A. & VERBRUGH, H. 1997. Nasal carriage of Staphylococcus aureus: Epidemiology, underlying mechanisms, and associated risks. *Clinical Microbiology Reviews*, 10, 505-&.
- KOLACZKOWSKA, E. & KUBES, P. 2013. Neutrophil recruitment and function in health and inflammation. *Nat Rev Immunol*, 13, 159-75.

- KOLHAR, P., ANSELMO, A. C., GUPTA, V., PANT, K., PRABHAKARPANDIAN, B., RUOSLAHTI, E. & MITRAGOTRI, S. 2013. Using shape effects to target antibody-coated nanoparticles to lung and brain endothelium. *Proc Natl Acad Sci U S A*, 110, 10753-8.
- KONDO, Y., FUSHIKIDA, K., FUJIEDA, T., SAKAI, K., MIYATA, K., KATO, F. & KATO, M. 2008. Efficient delivery of antibody into living cells using a novel HVJ envelope vector system. *Journal of Immunological Methods*, 332, 10-17.
- KONING, G. A., SCHIFFELERS, R. M., WAUBEN, M. H. M., KOK, R. J., MASTROBATTISTA, E., MOLEMA, G., TEN HAGEN, T. L. M. & STORM, G. 2006. Targeting of angiogenic endothelial cells at sites of inflammation by dexamethasone phosphate-containing RGD peptide liposomes inhibits experimental arthritis. *Arthritis and Rheumatism*, 54, 1198-1208.
- KOPPRASCH, S., PIETZSCH, J., WESTENDORF, T., KRUSE, H. J. & GRASSLER, J. 2004. The pivotal role of scavenger receptor CD36 and phagocyte-derived oxidants in oxidized low density lipoprotein-induced adhesion to endothelial cells. *International Journal of Biochemistry & Cell Biology*, 36, 460-471.
- KOSTARELOS, K., LACERDA, L., PASTORIN, G., WU, W., WIECKOWSKI, S., LUANGSIVILAY, J., GODEFROY, S., PANTAROTTO, D., BRIAND, J. P., MULLER, S., PRATO, M. & BIANCO, A. 2007. Cellular uptake of functionalized carbon nanotubes is independent of functional group and cell type. *Nature Nanotechnology*, 2, 108-113.
- KUBICA, M., GUZIK, K., KOZIEL, J., ZAREBSKI, M., RICHTER, W., GAJKOWSKA, B., GOLDA, A., MACIAG-GUDOWSKA, A., BRIX, K., SHAW, L., FOSTER, T. & POTEMPA, J. 2008. A Potential New Pathway for Staphylococcus aureus Dissemination: The Silent Survival of S. aureus Phagocytosed by Human Monocyte-Derived Macrophages. *Plos One*, 3.
- LAWSON, M. A. & MAXFIELD, F. R. 1995. CA²⁺ AND CALCINEURIN-DEPENDENT RECYCLING OF AN INTEGRIN TO THE FRONT OF MIGRATING NEUTROPHILS. *Nature*, 377, 75-79.
- LE TOURNEAU, C., FAIVRE, S., LAURENCE, V., DELBALDO, C., VERA, K., GIRRE, V., CHIAO, J., ARMOUR, S., FRAME, S., GREEN, S. R., GIANELLA-BORRADORI, A., DIERAS, V. & RAYMOND, E. 2010. Phase I evaluation of seliciclib (R-roscovitine), a novel oral cyclin-dependent kinase inhibitor, in patients with advanced malignancies. *European Journal of Cancer*, 46, 3243-3250.
- LEE, A., WHYTE, M. K. B. & HASLETT, C. 1993. INHIBITION OF APOPTOSIS AND PROLONGATION OF NEUTROPHIL FUNCTIONAL LONGEVITY BY INFLAMMATORY MEDIATORS. *Journal of Leukocyte Biology*, 54, 283-288.
- LEE, J.-S., STOEVA, S. I. & MIRKIN, C. A. 2006. DNA-induced size-selective separation of mixtures of gold nanoparticles. *Journal of the American Chemical Society*, 128, 8899-8903.
- LEE, S. Y., FERRARI, M. & DECUZZI, P. 2009. Shaping nano-/micro-particles for enhanced vascular interaction in laminar flows. *Nanotechnology*, 20.
- LEE, T. H., HORTON, C. E., KYANAUNG, U., HASKARD, D., CREA, A. E. G. & SPUR, B. W. 1989. LIPOXIN-A4 AND LIPOXIN-B4 INHIBIT CHEMOTACTIC RESPONSES OF HUMAN-NEUTROPHILS STIMULATED BY LEUKOTRIENE-B4 AND N-FORMYL-L-METHIONYL-L-LEUCYL-L-PHENYLALANINE. *Clinical Science*, 77, 195-203.

- LEITCH, A. E., HASLETT, C. & ROSSI, A. G. 2009. Cyclin-dependent kinase inhibitor drugs as potential novel anti-inflammatory and pro-resolution agents. *British Journal of Pharmacology*, 158, 1004-1016.
- LEITCH, A. E., LUCAS, C. D., MARWICK, J. A., DUFFIN, R., HASLETT, C. & ROSSI, A. G. 2012. Cyclin-dependent kinases 7 and 9 specifically regulate neutrophil transcription and their inhibition drives apoptosis to promote resolution of inflammation. *Cell Death and Differentiation*, 19, 1950-1961.
- LEITCH, A. E., RILEY, N. A., SHELDRAKE, T. A., FESTA, M., FOX, S., DUFFIN, R., HASLETT, C. & ROSSI, A. G. 2010. The cyclin-dependent kinase inhibitor Roscovitine down-regulates Mcl-1 to override pro-inflammatory signalling and drive neutrophil apoptosis. *European Journal of Immunology*, 40, 1127-1138.
- LEMAIRE, S., VAN BAMBEKE, F., MINGEOT-LECLERCQ, M. P. & TULKENS, P. M. 2005. Activity of three beta-lactams (ertapenem, meropenem and ampicillin) against intraphagocytic *Listeria monocytogenes* and *Staphylococcus aureus*. *Journal of Antimicrobial Chemotherapy*, 55, 897-904.
- LEUENROTH, S. J., GRUTKOSKI, P. S., AYALA, A. & SIMMS, H. H. 2000. The loss of Mcl-1 expression in human polymorphonuclear leukocytes promotes apoptosis. *Journal of Leukocyte Biology*, 68, 158-166.
- LEVY, B. D., DE SANCTIS, G. T., DEVCHAND, P. R., KIM, E., ACKERMAN, K., SCHMIDT, B. A., SZCZEKLIK, W., DRAZEN, J. M. & SERHAN, C. N. 2002. Multi-pronged inhibition of airway hyper-responsiveness and inflammation by lipoxin A4. *Nature Medicine*, 8, 1018-1023.
- LEWIS, A. L. 2000. Phosphorylcholine-based polymers and their use in the prevention of biofouling. *Colloids and Surfaces B-Biointerfaces*, 18, 261-275.
- LEWIS, A. L., BATTAGLIA, G. & MASSIGNANI, M. 2009. Intracellular antibody delivery. Google Patents.
- LEWIS, A. L., TOLHURST, L. A. & STRATFORD, P. W. 2002. Analysis of a phosphorylcholine-based polymer coating on a coronary stent pre- and post-implantation. *Biomaterials*, 23, 1697-1706.
- LI, G., BADKAR, A., NEMA, S., KOLLI, C. S. & BANGA, A. K. 2009. In vitro transdermal delivery of therapeutic antibodies using maltose microneedles. *International Journal of Pharmaceutics*, 368, 109-115.
- LILES, W. C., KIENER, P. A., LEDBETTER, J. A., ARUFFO, A. & KLEBANOFF, S. J. 1996. Differential expression of Fas (CD95) and Fas ligand on normal human phagocytes: Implications for the regulation of apoptosis in neutrophils. *Journal of Experimental Medicine*, 184, 429-440.
- LIMARY, R. & GREEN, P. F. 1999. Dewetting instabilities in thin block copolymer films: Nucleation and growth. *Langmuir*, 15, 5617-5622.
- LIPOWSKY, R. & LEIBLER, S. 1986. UNBINDING TRANSITIONS OF INTERACTING MEMBRANES. *Physical Review Letters*, 56, 2541-2544.
- LOEFFLER, B., HUSSAIN, M., GRUNDMEIER, M., BRUECK, M., HOLZINGER, D., VARGA, G., ROTH, J., KAHL, B. C., PROCTOR, R. A. & PETERS, G. 2010. *Staphylococcus aureus* Panton-Valentine Leukocidin Is a Very Potent Cytotoxic Factor for Human Neutrophils. *Plos Pathogens*, 6.
- LOMAS, H., CANTON, I., MACNEIL, S., DU, J., ARMES, S. P., RYAN, A. J., LEWIS, A. L. & BATTAGLIA, G. 2007. Biomimetic pH Sensitive Polymersomes for Efficient DNA Encapsulation and Delivery. *Advanced Materials*, 19, 4238-4243.

- LOMAS, H., DU, J., CANTON, I., MADSEN, J., WARREN, N., ARMES, S. P., LEWIS, A. L. & BATTAGLIA, G. 2010. Efficient Encapsulation of Plasmid DNA in pH-Sensitive PMPC-PDPA Polymersomes: Study of the Effect of PDPA Block Length on Copolymer-DNA Binding Affinity. *Macromolecular bioscience*, 10, 513-530.
- LOMAS, H., MASSIGNANI, M., ABDULLAH, K. A., CANTON, I., LO PRESTI, C., MACNEIL, S., DU, J., BLANAZS, A., MADSEN, J., ARMES, S. P., LEWIS, A. L. & BATTAGLIA, G. 2008. Non-cytotoxic polymer vesicles for rapid and efficient intracellular delivery. *Faraday discussions*, 139, 143-59; discussion 213-28, 419-20.
- LOPEZ, A. F., WILLIAMSON, D. J., GAMBLE, J. R., BEGLEY, C. G., HARLAN, J. M., KLEBANOFF, S. J., WALTERSDORPH, A., WONG, G., CLARK, S. C. & VADAS, M. A. 1986. RECOMBINANT HUMAN GRANULOCYTE-MACROPHAGE COLONY-STIMULATING FACTOR STIMULATES INVITRO MATURE HUMAN NEUTROPHIL AND EOSINOPHIL FUNCTION, SURFACE-RECEPTOR EXPRESSION, AND SURVIVAL. *Journal of Clinical Investigation*, 78, 1220-1228.
- LOPRESTI, C., LOMAS, H., MASSIGNANI, M., SMART, T. & BATTAGLIA, G. 2009. Polymersomes: nature inspired nanometer sized compartments. *Journal of Materials Chemistry*, 19, 3576-3590.
- LORD, B. I., BRONCHUD, M. H., OWENS, S., CHANG, J., HOWELL, A., SOUZA, L. & DEXTER, T. M. 1989. THE KINETICS OF HUMAN GRANULOPOIESIS FOLLOWING TREATMENT WITH GRANULOCYTE COLONY-STIMULATING FACTOR INVIVO. *Proceedings of the National Academy of Sciences of the United States of America*, 86, 9499-9503.
- LOTZ, S., AGA, E., WILDE, I., VAN ZANDBERGEN, G., HARTUNG, T., SOLBACH, W. & LASKAY, T. 2004. Highly purified lipoteichoic acid activates neutrophil granulocytes and delays their spontaneous apoptosis via CD14 and TLR2. *Journal of Leukocyte Biology*, 75, 467-477.
- LU, F., WU, S.-H., HUNG, Y. & MOU, C.-Y. 2009. Size Effect on Cell Uptake in Well-Suspended, Uniform Mesoporous Silica Nanoparticles. *Small*, 5, 1408-1413.
- LUCAS, C. D., DORWARD, D. A., TAIT, M. A., FOX, S., MARWICK, J. A., ALLEN, K. C., ROBB, C. T., HIRANI, N., HASLETT, C., DUFFIN, R. & ROSSI, A. G. 2014. Downregulation of Mcl-1 has anti-inflammatory pro-resolution effects and enhances bacterial clearance from the lung. *Mucosal Immunology*, 7, 857-868.
- MADSEN, J., CANTON, I., WARREN, N. J., THEMISTOU, E., BLANAZS, A., USTBAS, B., TIAN, X., PEARSON, R., BATTAGLIA, G., LEWIS, A. L. & ARMES, S. P. 2013. Nile Blue-Based Nanosized pH Sensors for Simultaneous Far-Red and Near-Infrared Live Bioimaging. *Journal of the American Chemical Society*, 135, 14863-14870.
- MADSEN, J., WARREN, N. J., ARMES, S. P. & LEWIS, A. L. 2011. Synthesis of Rhodamine 6G-Based Compounds for the ATRP Synthesis of Fluorescently Labeled Biocompatible Polymers. *Biomacromolecules*, 12, 2225-2234.
- MAJNO, G. 1991. *The healing hand: man and wound in the ancient world*, Harvard University Press.
- MARTIN, C., BURDON, P. C., BRIDGER, G., GUTIERREZ-RAMOS, J.-C., WILLIAMS, T. J. & RANKIN, S. M. 2003. Chemokines acting via CXCR2 and CXCR4 control the

- release of neutrophils from the bone marrow and their return following senescence. *Immunity*, 19, 583-593.
- MASSIGNANI, M., CANTON, I., SUN, T., HEARNDEN, V., MACNEIL, S., BLANAZS, A., ARMES, S. P., LEWIS, A. & BATTAGLIA, G. 2010. Enhanced Fluorescence Imaging of Live Cells by Effective Cytosolic Delivery of Probes. *Plos One*, 5.
- MASSIGNANI, M., LOPRESTI, C., BLANAZS, A., MADSEN, J., ARMES, S. P., LEWIS, A. L. & BATTAGLIA, G. 2009. Controlling Cellular Uptake by Surface Chemistry, Size, and Surface Topology at the Nanoscale. *Small*, 5, 2424-2432.
- MATHIAS, J. R., PERRIN, B. J., LIU, T.-X., KANKI, J., LOOK, A. T. & HUTTENLOCHER, A. 2006. Resolution of inflammation by retrograde chemotaxis of neutrophils in transgenic zebrafish. *Journal of Leukocyte Biology*, 80, 1281-1288.
- MATUTEBELLO, G., LILES, W. C., RADELLA, F., STEINBERG, K. P., RUZINSKI, J. T., JONAS, M., CHI, E. Y., HUDSON, L. D. & MARTIN, T. R. 1997. Neutrophil apoptosis in the acute respiratory distress syndrome. *American Journal of Respiratory and Critical Care Medicine*, 156, 1969-1977.
- MAYA, S., INDULEKHA, S., SUKHITHASRI, V., SMITHA, K. T., NAIR, S. V., JAYAKUMAR, R. & BISWAS, R. 2012. Efficacy of tetracycline encapsulated O-carboxymethyl chitosan nanoparticles against intracellular infections of *Staphylococcus aureus*. *International Journal of Biological Macromolecules*, 51, 392-399.
- MCCLUE, S. J., BLAKE, D., CLARKE, R., COWAN, A., CUMMINGS, L., FISCHER, P. M., MACKENZIE, M., MELVILLE, J., STEWART, K., WANG, S. D., ZHELEV, N., ZHELEVA, D. & LANE, D. P. 2002. In vitro and in vivo antitumor properties of the cyclin dependent kinase inhibitor CYC202 (R-roscovitine). *International Journal of Cancer*, 102, 463-468.
- MCGRATH, E. E., MARRIOTT, H. M., LAWRIE, A., FRANCIS, S. E., SABROE, I., RENSHAW, S. A., DOCKRELL, D. H. & WHYTE, M. K. B. 2011. TNF-related apoptosis-inducing ligand (TRAIL) regulates inflammatory neutrophil apoptosis and enhances resolution of inflammation. *Journal of Leukocyte Biology*, 90, 855-865.
- MCLOUGHLIN, R. M., LEE, J. C., KASPER, D. L. & TZIANABOS, A. O. 2008. IFN-gamma regulated chemokine production determines the outcome of *Staphylococcus aureus* infection. *Journal of Immunology*, 181, 1323-1332.
- MCLOUGHLIN, R. M., SOLINGA, R. M., RICH, J., ZALESKI, K. J., COCCHIARO, J. L., RISLEY, A., TZIANABOS, A. O. & LEE, J. C. 2006. CD4(+) T cells and CXC chemokines modulate the pathogenesis of *Staphylococcus aureus* wound infections. *Proceedings of the National Academy of Sciences of the United States of America*, 103, 10408-10413.
- MCCMAHON, H. T. & BOUCROT, E. 2011. Molecular mechanism and physiological functions of clathrin-mediated endocytosis. *Nature Reviews Molecular Cell Biology*, 12, 517-533.
- MCVICKER, G., PRAJSNAR, T. K., WILLIAMS, A., WAGNER, N. L., BOOTS, M., RENSHAW, S. A. & FOSTER, S. J. 2014. Clonal Expansion during *Staphylococcus aureus* Infection Dynamics Reveals the Effect of Antibiotic Intervention. *Plos Pathogens*, 10.
- MEDZHITOV, R. 2007. Recognition of microorganisms and activation of the immune response. *Nature*, 449, 819-826.

- MEDZHITOV, R., PRESTONHURLBURT, P. & JANEWAY, C. A. 1997. A human homologue of the Drosophila Toll protein signals activation of adaptive immunity. *Nature*, 388, 394-397.
- MELLY, M. A., THOMISON, J. B. & ROGERS, D. E. 1960. FATE OF STAPHYLOCOCCI WITHIN HUMAN LEUKOCYTES. *Journal of Experimental Medicine*, 112, 1121-&.
- MILLER, J. B., HARRIS, J. M. & HOBBIE, E. K. 2014. Purifying Colloidal Nanoparticles through Ultracentrifugation with Implications for Interfaces and Materials. *Langmuir*.
- MITRAGOTRI, S. & LAHANN, J. 2009. Physical approaches to biomaterial design. *Nature Materials*, 8, 15-23.
- MOELLERING, R. C., JR. 1998. The specter of glycopeptide resistance: Current trends and future considerations. *American Journal of Medicine*, 104, 3S-6S.
- MORJARIA, J. B., MALERBA, M. & POLOSA, R. 2010. Biologic and pharmacologic therapies in clinical development for the inflammatory response in COPD. *Drug Discovery Today*, 15, 396-405.
- MORO, T., TAKATORI, Y., ISHIHARA, K., KONNO, T., TAKIGAWA, Y., MATSUSHITA, T., CHUNG, U. I., NAKAMURA, K. & KAWAGUCHI, H. 2004. Surface grafting of artificial joints with a biocompatible polymer for preventing periprosthetic osteolysis. *Nature Materials*, 3, 829-836.
- MOULDING, D. A., AKGUL, C., DEROUET, M., WHITE, M. R. H. & EDWARDS, S. W. 2001. Bcl-2 family expression in human neutrophils during delayed and accelerated apoptosis. *Journal of Leukocyte Biology*, 70, 783-792.
- MOULDING, D. A., QUAYLE, J. A., HART, C. A. & EDWARDS, S. W. 1998. Mcl-1 expression in human neutrophils: Regulation by cytokines and correlation with cell survival. *Blood*, 92, 2495-2502.
- MOYNAGH, P. N. 2005. TLR signalling and activation of IRFs: revisiting old friends from the NF-kappa B pathway. *Trends in Immunology*, 26, 469-476.
- MURPHY, A. J., WOOLLARD, K. J., SUHARTOYO, A., STIRZAKER, R. A., SHAW, J., SVIRIDOV, D. & CHIN-DUSTING, J. P. F. 2011. Neutrophil Activation Is Attenuated by High-Density Lipoprotein and Apolipoprotein A-I in In Vitro and In Vivo Models of Inflammation. *Arteriosclerosis Thrombosis and Vascular Biology*, 31, 1333-U221.
- MURRAY, J., BARBARA, J. A. J., DUNKLEY, S. A., LOPEZ, A. F., VANOSTADE, X., CONDLIFFE, A. M., DRANSFIELD, I., HASLETT, C. & CHILVERS, E. R. 1997. Regulation of neutrophil apoptosis by tumor necrosis factor-alpha: Requirement for TNFR55 and TNFR75 for induction of apoptosis in vitro. *Blood*, 90, 2772-2783.
- NAKAI, T., KANAMORI, T., SANDO, S. & AOYAMA, Y. 2003. Remarkably size-regulated cell invasion by artificial viruses. saccharide-dependent self-aggregation of glycoviruses and its consequences in glycoviral gene delivery. *Journal of the American Chemical Society*, 125, 8465-8475.
- NATHAN, C. 2002. Points of control in inflammation. *Nature*, 420, 846-852.
- NATHAN, C. 2006. Neutrophils and immunity: challenges and opportunities. *Nature Reviews Immunology*, 6, 173-182.
- NATHAN, C. & DING, A. 2010. Nonresolving Inflammation. *Cell*, 140, 871-882.
- NEL, A., XIA, T., MADLER, L. & LI, N. 2006. Toxic potential of materials at the nanolevel. *Science*, 311, 622-627.

- NEL, A. E., MAEDLER, L., VELEGOL, D., XIA, T., HOEK, E. M. V., SOMASUNDARAN, P., KLAESSIG, F., CASTRANOVA, V. & THOMPSON, M. 2009. Understanding biophysicochemical interactions at the nano-bio interface. *Nature Materials*, 8, 543-557.
- NORDENFELT, P. & TAPPER, H. 2011. Phagosome dynamics during phagocytosis by neutrophils. *Journal of Leukocyte Biology*, 90, 271-284.
- NURNBERGER, T. & BRUNNER, F. 2002. Innate immunity in plants and animals: emerging parallels between the recognition of general elicitors and pathogen-associated molecular patterns. *Current Opinion in Plant Biology*, 5, 318-324.
- NUSSLEIN-VOLHARD, C. & DAHM, R. 2002. *Zebrafish*, Oxford University Press.
- OLTRA, N. S., SWIFT, J., MAHMUD, A., RAJAGOPAL, K., LOVERDE, S. M. & DISCHER, D. E. 2013. Filomicelles in nanomedicine - from flexible, fragmentable, and ligand-targetable drug carrier designs to combination therapy for brain tumors. *Journal of Materials Chemistry B*, 1, 5177-5185.
- OSAKI, F., KANAMORI, T., SANDO, S., SERA, T. & AOYAMA, Y. 2004. A quantum dot conjugated sugar ball and its cellular uptake on the size effects of endocytosis in the subviral region. *Journal of the American Chemical Society*, 126, 6520-6521.
- OTTO, M. 2010. Basis of Virulence in Community-Associated Methicillin-Resistant *Staphylococcus aureus*. *Annual Review of Microbiology*, Vol 64, 2010, 64, 143-162.
- OWEN, C. A. & CAMPBELL, E. J. 1999. The cell biology of leukocyte-mediated proteolysis. *Journal of Leukocyte Biology*, 65, 137-150.
- PARKER, L. C., PRINCE, L. R., BUTTLE, D. J. & SABROE, I. 2009. The Generation of Highly Purified Primary Human Neutrophils and Assessment of Apoptosis in Response to Toll-Like Receptor Ligands. *Toll-Like Receptors: METHODS AND PROTOCOLS*, 517, 191-204.
- PARTON, R. G. & DEL POZO, M. A. 2013. Caveolae as plasma membrane sensors, protectors and organizers. *Nature Reviews Molecular Cell Biology*, 14, 98-112.
- PEARSON, R. T., WARREN, N. J., LEWIS, A. L., ARMES, S. P. & BATTAGLIA, G. 2013. Effect of pH and Temperature on PMPC-PDPA Copolymer Self-Assembly. *Macromolecules*, 46, 1400-1407.
- PEGORARO, C., CECCHIN, D., GRACIA, L. S., WARREN, N., MADSEN, J., ARMES, S. P., LEWIS, A., MACNEIL, S. & BATTAGLIA, G. 2013. Enhanced drug delivery to melanoma cells using PMPC-PDPA polymersomes. *Cancer Letters*, 334, 328-337.
- PEGORARO, C., CECCHIN, D., MADSEN, J., WARREN, N., ARMES, S. P., MACNEIL, S., LEWIS, A. & BATTAGLIA, G. 2014. Translocation of flexible polymersomes across pores at the nanoscale. *Biomaterials Science*, 2, 680-692.
- PELKMANS, L. & HELENIUS, A. 2002. Endocytosis via caveolae. *Traffic*, 3, 311-320.
- PELLME, S., MORGELIN, M., TAPPER, H., MELLQVIST, U.-H., DAHLGREN, C. & KARLSSON, A. 2006. Localization of human neutrophil interleukin-8 (CXCL-8) to organelle (s) distinct from the classical granules and secretory vesicles. *Journal of Leukocyte Biology*, 79, 564-573.
- PESCHEL, A. 2002. How do bacteria resist human antimicrobial peptides? *Trends in Microbiology*, 10, 179-186.

- PHILIPS, J. A., RUBIN, E. J. & PERRIMON, N. 2005. Drosophila RNAi screen reveals CD36 family member required for mycobacterial infection. *Science*, 309, 1251-1253.
- PILLAY, J., DEN BRABER, I., VRISEKOOOP, N., KWAST, L. M., DE BOER, R. J., BORGHANS, J. A. M., TESSELAAR, K. & KOENDERMAN, L. 2010. In vivo labeling with (H₂O)-H-2 reveals a human neutrophil lifespan of 5.4 days. *Blood*, 116, 625-627.
- PINHO, V., RUSSO, R. D. C., AMARAL, F. A., DE SOUSA, L. P., BARSANTE, M. M., DE SOUZA, D. G., ALVES-FILHO, J. C., CARA, D. C., HAYFLICK, J. S., ROMMEL, C., RUCKLE, T., ROSSI, A. G. & TEIXEIRA, M. M. 2007. Tissue- and stimulus-dependent role of phosphatidylinositol 3-kinase Isoforms for neutrophil recruitment induced by chemoattractants in vivo. *Journal of Immunology*, 179, 7891-7898.
- PORTER, A. E., GASS, M., MULLER, K., SKEPPER, J. N., MIDGLEY, P. A. & WELLAND, M. 2007. Direct imaging of single-walled carbon nanotubes in cells. *Nature Nanotechnology*, 2, 713-717.
- PRABHA, S., ZHOU, W. Z., PANYAM, J. & LABHASETWAR, V. 2002. Size-dependency of nanoparticle-mediated gene transfection: studies with fractionated nanoparticles. *International Journal of Pharmaceutics*, 244, 105-115.
- PRAJSNAR, T. K., CUNLIFFE, V. T., FOSTER, S. J. & RENSHAW, S. A. 2008. A novel vertebrate model of Staphylococcus aureus infection reveals phagocyte-dependent resistance of zebrafish to non-host specialized pathogens. *Cellular microbiology*, 10, 2312-2325.
- PRAJSNAR, T. K., HAMILTON, R., GARCIA-ÉLARA, J., MCVICKER, G., WILLIAMS, A., BOOTS, M., FOSTER, S. J. & RENSHAW, S. A. 2012. A privileged intraphagocyte niche is responsible for disseminated infection of Staphylococcus aureus in a zebrafish model. *Cellular microbiology*, 14, 1600-1619.
- PRIEST, N. K., RUDKIN, J. K., FEIL, E. J., VAN DEN ELSEN, J. M. H., CHEUNG, A., PEACOCK, S. J., LAABEI, M., LUCKS, D. A., RECKER, M. & MASSEY, R. C. 2012. From genotype to phenotype: can systems biology be used to predict Staphylococcus aureus virulence? *Nature Reviews Microbiology*, 10, 791-797.
- PRINCE, L. R., GRAHAM, K. J., CONNOLLY, J., ANWAR, S., RIDLEY, R., SABROE, I., FOSTER, S. J. & WHYTE, M. K. 2012. Staphylococcus aureus induces eosinophil cell death mediated by Æ±-hemolysin. *Plos One*, 7, e31506.
- PROCTOR, R. A. 2012. Is there a future for a Staphylococcus aureus vaccine? *Vaccine*, 30, 2921-2927.
- QUE, Y. A., HAEFLIGER, J. A., PIROTH, L., FRANCOIS, P., WIDMER, E., ENTENZA, J. M., SINHA, B., HERRMANN, M., FRANCIOLI, P., VAUDAUX, P. & MOREILLON, P. 2005. Fibrinogen and fibronectin binding cooperate for valve infection and invasion in Staphylococcus aureus experimental endocarditis. *Journal of Experimental Medicine*, 201, 1627-1635.
- RAHMANZADEH, R., RAI, P., CELLI, J. P., RIZVI, I., BARON-LUEHR, B., GERDES, J. & HASAN, T. 2010. Ki-67 as a Molecular Target for Therapy in an In vitro Three-Dimensional Model for Ovarian Cancer. *Cancer Research*, 70, 9234-9242.

- RANDIS, T. M., PURI, K. D., ZHOU, H. & DIACOVO, T. G. 2008. Role of PI3K delta and PI3K gamma in inflammatory arthritis and tissue localization of neutrophils. *European Journal of Immunology*, 38, 1215-1224.
- RANE, M. J., PAN, Y., SINGH, S., POWELL, D. W., WU, R., CUMMINS, T., CHEN, Q., MCLEISH, K. R. & KLEIN, J. B. 2003. Heat shock protein 27 controls apoptosis by regulating Akt activation. *Journal of Biological Chemistry*, 278, 27828-27835.
- REDDY, S. T., VAN DER VLIES, A. J., SIMEONI, E., ANGELI, V., RANDOLPH, G. J., O'NEILL, C. P., LEE, L. K., SWARTZ, M. A. & HUBBELL, J. A. 2007. Exploiting lymphatic transport and complement activation in nanoparticle vaccines. *Nature Biotechnology*, 25, 1159-1164.
- REINER, J. E., WELLS, J. M., KISHORE, R. B., PFEFFERKORN, C. & HELMERSON, K. 2006. Stable and robust polymer nanotubes stretched from polymersomes. *Proc Natl Acad Sci U S A*, 103, 1173-7.
- REJMAN, J., OBERLE, V., ZUHORN, I. S. & HOEKSTRA, D. 2004. Size-dependent internalization of particles via the pathways of clathrin- and caveolae-mediated endocytosis. *Biochemical Journal*, 377, 159-169.
- REN, Y., XIE, Y., JIANG, G. P., FAN, J. Q., YEUNG, J., LI, W., TAM, P. K. H. & SAVILL, J. 2008. Apoptotic cells protect mice against lipopolysaccharide-induced shock. *Journal of Immunology*, 180, 4978-4985.
- RENSHAW, S. A., LOYNES, C. A., TRUSHELL, D. M. I., ELWORTHY, S., INGHAM, P. W. & WHYTE, M. K. B. 2006. A transgenic zebrafish model of neutrophilic inflammation. *Blood*, 108, 3976-3978.
- RENSHAW, S. A., PARMAR, J. S., SINGLETON, V., ROWE, S. J., DOCKRELL, D. H., DOWER, S. K., BINGLE, C. D., CHILVERS, E. R. & WHYTE, M. K. B. 2003. Acceleration of human neutrophil apoptosis by TRAIL. *Journal of Immunology*, 170, 1027-1033.
- RENSHAW, S. A. & TREDE, N. S. 2012. A model 450 million years in the making: zebrafish and vertebrate immunity. *Disease Models & Mechanisms*, 5, 38-47.
- RICHARDS, M. K., LIU, F. L., IWASAKI, H., AKASHI, K. & LINK, D. C. 2003. Pivotal role of granulocyte colony-stimulating factor in the development of progenitors in the common myeloid pathway. *Blood*, 102, 3562-3568.
- ROBERTSON, A. L., HOLMES, G. R., BOJARCZUK, A. N., BURGON, J., LOYNES, C. A., CHIMEN, M., SAWTELL, A. K., HAMZA, B., WILLSON, J., WALMSLEY, S. R., ANDERSON, S. R., COLES, M. C., FARROW, S. N., SOLARI, R., JONES, S., PRINCE, L. R., IRIMIA, D., RAINGER, G. E., KADIRKAMANATHAN, V., WHYTE, M. K. B. & RENSHAW, S. A. 2014a. A Zebrafish Compound Screen Reveals Modulation of Neutrophil Reverse Migration as an Anti-Inflammatory Mechanism. *Science Translational Medicine*, 6.
- ROBERTSON, J. D., YEALLAND, G., AVILA-OLIAS, M., CHERICO, L., BANDMANN, O., RENSHAW, S. A. & BATTAGLIA, G. 2014b. pH-Sensitive Tubular Polymersomes: Formation and Applications in Cellular Delivery. *ACS nano*, 8, 4650-61.
- ROGERS, D. E. & TOMPSETT, R. 1952. THE SURVIVAL OF STAPHYLOCOCCI WITHIN HUMAN LEUKOCYTES. *Journal of Experimental Medicine*, 95, 209-&.
- ROOIJAKKERS, S. H. M., RUYKEN, M., ROOS, A., DAHA, M. R., PRESANIS, J. S., SIM, R. B., VAN WAMEL, W. J. B., VAN KESSEL, K. P. M. & VAN STRIJP, J. A. G. 2005. Immune evasion by a staphylococcal complement inhibitor that acts on C3 convertases. *Nature Immunology*, 6, 920-927.

- ROSSI, A. G., SAWATZKY, D. A., WALKER, A., WARD, C., SHELDRAKE, T. A., RILEY, N. A., CALDICOTT, A., MARTINEZ-LOSA, M., WALKER, T. R., DUFFIN, R., GRAY, M., CRESCENZI, E., MARTIN, M. C., BRADY, H. J., SAVILL, J. S., DRANSFIELD, I. & HASLETT, C. 2006. Cyclin-dependent kinase inhibitors enhance the resolution of inflammation by promoting inflammatory cell apoptosis. *Nature Medicine*, 12, 1056-1064.
- SABROE, I., JONES, E. C., USHER, L. R., WHYTE, M. K. B. & DOWER, S. K. 2002. Toll-like receptor (TLR)2 and TLR4 in human peripheral blood granulocytes: A critical role for monocytes in leukocyte lipopolysaccharide responses. *Journal of Immunology*, 168, 4701-4710.
- SAITOH, T., KOMANO, J., SAITOH, Y., MISAWA, T., TAKAHAMA, M., KOZAKI, T., UEHATA, T., IWASAKI, H., OMORI, H., YAMAOKA, S., YAMAMOTO, N. & AKIRA, S. 2012. Neutrophil Extracellular Traps Mediate a Host Defense Response to Human Immunodeficiency Virus-1. *Cell Host & Microbe*, 12, 109-116.
- SAKAI-KATO, K., OTA, S., HYODO, K., ISHIHARA, H., KIKUCHI, H. & KAWANISHI, T. 2011. Size separation and size determination of liposomes. *Journal of Separation Science*, 34, 2861-2865.
- SALGADO-PABON, W. & SCHLIEVERT, P. M. 2014. Models matter: the search for an effective *Staphylococcus aureus* vaccine. *Nature Reviews Microbiology*.
- SAVERYMUTTU, S., PETERS, A., KESHAVARZIAN, A., REAVY, H. & LAVENDER, J. 1985. The kinetics of 111indium distribution following injection of 111indium labelled autologous granulocytes in man. *British journal of haematology*, 61, 675-685.
- SAVILL, J. S., WYLLIE, A. H., HENSON, J. E., WALPORT, M. J., HENSON, P. M. & HASLETT, C. 1989. MACROPHAGE PHAGOCYTOSIS OF AGING NEUTROPHILS IN INFLAMMATION - PROGRAMMED CELL-DEATH IN THE NEUTROPHIL LEADS TO ITS RECOGNITION BY MACROPHAGES. *Journal of Clinical Investigation*, 83, 865-875.
- SAWATZKY, D. A., WILLOUGHBY, D. A., COLVILLE-NASH, P. R. & ROSSI, A. G. 2006. The involvement of the apoptosis-modulating proteins ERK 1/2, Bcl-X-L and Bax in the resolution of acute inflammation in vivo. *American Journal of Pathology*, 168, 33-41.
- SCHWAB, L., GORONCY, L., PALANIYANDI, S., GAUTAM, S., TRIANTAFYLLOPOULOU, A., MOCSAI, A., REICHARDT, W., KARLSSON, F. J., RADHAKRISHNAN, S. V., HANKE, K., SCHMITT-GRAEFF, A., FREUDENBERG, M., VON LOEWENICH, F. D., WOLF, P., LEONHARDT, F., BAXAN, N., PFEIFER, D., SCHMAH, O., SCHOENLE, A., MARTIN, S. F., MERTELSMANN, R., DUYSER, J., FINKE, J., PRINZ, M., HENNEKE, P., HAECKER, H., HILDEBRANDT, G. C., HAECKER, G. & ZEISER, R. 2014. Neutrophil granulocytes recruited upon translocation of intestinal bacteria enhance graft-versus-host disease via tissue damage. *Nature Medicine*, 20, 648-654.
- SENGUPTA, S. 2014. Clinical translational challenges in nanomedicine. *Mrs Bulletin*, 39, 259-264.
- SERHAN, C. N. & CHIANG, N. 2013. Resolution phase lipid mediators of inflammation: agonists of resolution. *Current Opinion in Pharmacology*, 13, 632-640.
- SERHAN, C. N. & SAVILL, J. 2005. Resolution of inflammation: The beginning programs the end. *Nature Immunology*, 6, 1191-1197.

- SERVANT, G., WEINER, O. D., HERZMARK, P., BALLA, T., SEDAT, J. W. & BOURNE, H. R. 2000. Polarization of chemoattractant receptor signaling during neutrophil chemotaxis. *Science*, 287, 1037-1040.
- SHARMA, A. & KHANNA, R. 1998. Pattern formation in unstable thin liquid films. *Physical Review Letters*, 81, 3463-3466.
- SHERIDAN, J. P., MARSTERS, S. A., PITTI, R. M., GURNEY, A., SKUBATCH, M., BALDWIN, D., RAMAKRISHNAN, L., GRAY, C. L., BAKER, K., WOOD, W. I., GODDARD, A. D., GODOWSKI, P. & ASHKENAZI, A. 1997. Control of TRAIL-induced apoptosis by a family of signaling and decoy receptors. *Science*, 277, 818-821.
- SHI, J., GILBERT, G. E., KOKUBO, Y. & OHASHI, T. 2001. Role of the liver in regulating numbers of circulating neutrophils. *Blood*, 98, 1226-1230.
- SHUVAEV, V. V., ILIES, M. A., SIMONE, E., ZAITSEV, S., KIM, Y., CAI, S., MAHMUD, A., DZIUBLA, T., MURO, S., DISCHER, D. E. & MUZYKANTOV, V. R. 2011. Endothelial Targeting of Antibody-Decorated Polymeric Filomicelles. *ACS Nano*, 5, 6991-6999.
- SINGH, R. P. & RAMARAO, P. 2013. Accumulated Polymer Degradation Products as Effector Molecules in Cytotoxicity of Polymeric Nanoparticles. *Toxicological Sciences*, 136, 131-143.
- SIVERTSON, K. L., SEEDS, M. C., LONG, D. L., PEACHMAN, K. K. & BASS, D. A. 2007. The differential effect of dexamethasone on granulocyte apoptosis involves stabilization of Mcl-1L in neutrophils but not in eosinophils. *Cellular Immunology*, 246, 34-45.
- SMART, T., LOMAS, H., MASSIGNANI, M., FLORES-MERINO, M. V., PEREZ, L. R. & BATTAGLIA, G. 2008. Block copolymer nanostructures. *Nano Today*, 3, 38-46.
- SMITH, T. L., PEARSON, M. L., WILCOX, K. R., CRUZ, C., LANCASTER, M. V., ROBINSON-DUNN, B., TENOVER, F. C., ZERVOS, M. J., BAND, J. D., WHITE, E., JARVIS, W. R. & GLYCOPEPTIDE INTERMEDIATE, S. 1999. Emergence of vancomycin resistance in *Staphylococcus aureus*. *New England Journal of Medicine*, 340, 493-501.
- SNELGROVE, R. J., JACKSON, P. L., HARDISON, M. T., NOERAGER, B. D., KINLOCH, A., GAGGAR, A., SHASTRY, S., ROWE, S. M., SHIM, Y. M., HUSSELL, T. & BLALOCK, J. E. 2010. A Critical Role for LTA(4)H in Limiting Chronic Pulmonary Neutrophilic Inflammation. *Science*, 330, 90-94.
- SOUSA, L. P., LOPES, F., SILVA, D. M., TAVARES, L. P., VIEIRA, A. T., REZENDE, B. M., CARMO, A. F., RUSSO, R. C., GARCIA, C. C., BONJARDIM, C. A., ALESSANDRI, A. L., ROSSI, A. G., PINHO, V. & TEIXEIRA, M. M. 2010. PDE4 inhibition drives resolution of neutrophilic inflammation by inducing apoptosis in a PKA-PI3K/Akt-dependent and NF-kappa B-independent manner. *Journal of Leukocyte Biology*, 87, 895-904.
- SPAAN, A. S. N., SUREWAARD, B. G., NIJLAND, R. & VAN STRIJP, J. A. 2013. Neutrophils Versus *Staphylococcus aureus*: A Biological Tug of War*. *Annual review of microbiology*, 67, 629-650.
- STEWART, S. & LIU, G. 2000. Block copolymer nanotubes. *Angewandte Chemie*, 112, 348-352.
- STRIETER, R. M., KASAHARA, K., ALLEN, R. M., STANDIFORD, T. J., ROLFE, M. W., BECKER, F. S., CHENSUE, S. W. & KUNKEL, S. L. 1992. CYTOKINE-INDUCED

- NEUTROPHIL-DERIVED INTERLEUKIN-8. *American Journal of Pathology*, 141, 397-407.
- SUMMERS, C., RANKIN, S. M., CONDLIFFE, A. M., SINGH, N., PETERS, A. M. & CHILVERS, E. R. 2010. Neutrophil kinetics in health and disease. *Trends in Immunology*, 31, 318-324.
- SURATT, B. T., YOUNG, S. K., LIEBER, J., NICK, J. A., HENSON, P. M. & WORTHEN, G. S. 2001. Neutrophil maturation and activation determine anatomic site of clearance from circulation. *American Journal of Physiology-Lung Cellular and Molecular Physiology*, 281, L913-L921.
- SWANSON, J. A. 2008. Shaping cups into phagosomes and macropinosomes. *Nature Reviews Molecular Cell Biology*, 9, 639-649.
- SWEENEY, S. F., WOHRLE, G. H. & HUTCHISON, J. E. 2006. Rapid purification and size separation of gold nanoparticles via diafiltration. *Journal of the American Chemical Society*, 128, 3190-3197.
- TAKANO, T., FIORE, S., MADDOX, J. F., BRADY, H. R., PETASIS, N. A. & SERHAN, C. N. 1997. Aspirin-triggered 15-epi-lipoxin A(4) (LXA(4)) and LXA(4) stable analogues are potent inhibitors of Acute inflammation: Evidence for anti-inflammatory receptors. *Journal of Experimental Medicine*, 185, 1693-1704.
- TAMASSIA, N., LE MOIGNE, V., ROSSATO, M., DONINI, M., MCCARTNEY, S., CALZETTI, F., COLONNA, M., BAZZONI, F. & CASSATELLA, M. A. 2008. Activation of an immunoregulatory and antiviral gene expression program in poly (I: C)-transfected human neutrophils. *The Journal of Immunology*, 181, 6563-6573.
- TANFORD, C. 1980. *The Hydrophobic Effect: Formation of Micelles and Biological Membranes 2d Ed*, J. Wiley.
- THORBURN, A. 2004. Death receptor-induced cell killing. *Cellular Signalling*, 16, 139-144.
- THWAITES, G. E. & GANT, V. 2011. Are bloodstream leukocytes Trojan Horses for the metastasis of Staphylococcus aureus? *Nature Reviews Microbiology*, 9, 215-222.
- TOFTS, P. S., CHEVASSUT, T., CUTAJAR, M., DOWELL, N. G. & PETERS, A. M. 2011. Doubts concerning the recently reported human neutrophil lifespan of 5.4 days. *Blood*, 117, 6050-6052.
- UEDA, T., OSHIDA, H., KURITA, K., ISHIHARA, K. & NAKABAYASHI, N. 1992. PREPARATION OF 2-METHACRYLOYLOXYETHYL PHOSPHORYLCHOLINE COPOLYMERS WITH ALKYL METHACRYLATES AND THEIR BLOOD COMPATIBILITY. *Polymer Journal*, 24, 1259-1269.
- URBAN, C. F., REICHARD, U., BRINKMANN, V. & ZYCHLINSKY, A. 2006. Neutrophil extracellular traps capture and kill Candida albicans yeast and hyphal forms. *Cellular Microbiology*, 8, 668-676.
- URIARTE, S. M., RANE, M. J., LUERMAN, G. C., BARATI, M. T., WARD, R. A., NAUSEEF, W. M. & MCLEISH, K. R. 2011. Granule exocytosis contributes to priming and activation of the human neutrophil respiratory burst. *The Journal of Immunology*, 187, 391-400.
- VALEVA, A., WALEV, I., PINKERNELL, M., WALKER, B., BAYLEY, H., PALMER, M. & BHAKDI, S. 1997. Transmembrane beta-barrel of staphylococcal alpha-toxin forms in sensitive but not in resistant cells. *Proceedings of the National Academy of Sciences of the United States of America*, 94, 11607-11611.

- VAN BAMBEKE, F., BARCIA-MACAY, M., LEMAIRE, S. & TULKENS, P. M. 2006. Cellular pharmacodynamics and pharmacokinetics of antibiotics: Current views and perspectives. *Current Opinion in Drug Discovery & Development*, 9, 218-230.
- VAN EEDEN, S. F., KLUT, M. E., WALKER, B. A. & HOGG, J. C. 1999. The use of flow cytometry to measure neutrophil function. *Journal of immunological methods*, 232, 23-43.
- VAN OERS, M. C. M., RUTJES, F. & VAN HEST, J. C. M. 2013. Tubular Polymersomes: A Cross-Linker-Induced Shape Transformation. *Journal of the American Chemical Society*, 135, 16308-16311.
- VANDENESCH, F., LINA, G. & HENRY, T. 2012. Staphylococcus aureus hemolysins, bi-component leukocidins, and cytolytic peptides: a redundant arsenal of membrane-damaging virulence factors? *Frontiers in Cellular and Infection Microbiology*, 2.
- VANNIASINGHE, A. S., BENDER, V. & MANOLIOS, N. 2009. The Potential of Liposomal Drug Delivery for the Treatment of Inflammatory Arthritis. *Seminars in Arthritis and Rheumatism*, 39, 182-196.
- VELASCO, E., BYINGTON, R., MARTINS, C. A. S., SCHIRMER, M., DIAS, L. M. C. & GONCALVES, V. 2006. Comparative study of clinical characteristics of neutropenic and non-neutropenic adult cancer patients with bloodstream infections. *European Journal of Clinical Microbiology & Infectious Diseases*, 25, 1-7.
- VENDITTI, M., FALCONE, M., MICOZZI, A., CARFAGNA, P., TAGLIETTI, F., SERRA, P. F. & MARTINO, P. 2003. Staphylococcus aureus bacteremia in patients with hematologic malignancies: a retrospective case-control study. *Haematologica*, 88, 923-930.
- VOYICH, J. A., BRAUGHTON, K. R., STURDEVANT, D. E., WHITNEY, A. R., SAID-SALIM, B., PORCELLA, S. F., LONG, R. D., DORWARD, D. W., GARDNER, D. J., KREISWIRTH, B. N., MUSSER, J. M. & DELEO, F. R. 2005. Insights into mechanisms used by Staphylococcus aureus to avoid destruction by human neutrophils. *Journal of Immunology*, 175, 3907-3919.
- VOYICH, J. M., VUONG, C., DEWALD, M., NYGAARD, T. K., KOCIANOVA, S., GRIFFITH, S., JONES, J., IVERSON, C., STURDEVANT, D. E., BRAUGHTON, K. R., WHITNEY, A. R., OTTO, M. & DELEO, F. R. 2009. The SaeR/S Gene Regulatory System Is Essential for Innate Immune Evasion by Staphylococcus aureus. *Journal of Infectious Diseases*, 199, 1698-1706.
- WALMSLEY, S. R., PRINT, C., FARAHI, N., PEYSSONNAUX, C., JOHNSON, R. S., CRAMER, T., SOBOLEWSKI, A., CONDLIFFE, A. M., COWBURN, A. S., JOHNSON, N. & CHILVERS, E. R. 2005. Hypoxia-induced neutrophil survival is mediated by HIF-1 alpha-dependent NF-kappa B activity. *Journal of Experimental Medicine*, 201, 105-115.
- WANG, L., CHIERICO, L., LITTLE, D., PATIKARNMONTHON, N., YANG, Z., AZZOUZ, M., MADSEN, J., ARMES, S. P. & BATTAGLIA, G. 2012. Encapsulation of Biomacromolecules within Polymersomes by Electroporation. *Angewandte Chemie International Edition*.
- WANG, X., ROBERTSON, A. L., LI, J., CHAI, R. J., HAISHAN, W., SADIKU, P., OGRYZKO, N. V., EVERETT, M., YOGANATHAN, K., LUO, H. R., RENSHAW, S. A. & INGHAM, P. W. 2014. Inhibitors of neutrophil recruitment identified using

- transgenic zebrafish to screen a natural product library. *Disease Models & Mechanisms*, 7, 163-169.
- WANG, Y., CHEN, C.-L. & IJIMA, M. 2011. Signaling mechanisms for chemotaxis. *Development Growth & Differentiation*, 53, 495-502.
- WAYAKANON, K., THORNHILL, M. H., DOUGLAS, C. W. I., LEWIS, A. L., WARREN, N. J., PINNOCK, A., ARMES, S. P., BATTAGLIA, G. & MURDOCH, C. 2013. Polymersome-mediated intracellular delivery of antibiotics to treat *Porphyromonas gingivalis*-infected oral epithelial cells. *FASEB journal : official publication of the Federation of American Societies for Experimental Biology*, 27, 4455-65.
- WEI, M. C., ZONG, W.-X., CHENG, E. H.-Y., LINDSTEN, T., PANOUTSAKOPOULOU, V., ROSS, A. J., ROTH, K. A., MACGREGOR, G. R., THOMPSON, C. B. & KORSMEYER, S. J. 2001. Proapoptotic BAX and BAK: a requisite gateway to mitochondrial dysfunction and death. *Science*, 292, 727-730.
- WEIDENMAIER, C., KOKAI-KUN, J. F., KRISTIAN, S. A., CHANTURIYA, T., KALBACHER, H., GROSS, M., NICHOLSON, G., NEUMEISTER, B., MOND, J. J. & PESCHEL, A. 2004. Role of teichoic acids in *Staphylococcus aureus* nasal colonization, a major risk factor in nosocomial infections. *Nature Medicine*, 10, 243-245.
- WEISS, S. J., KLEIN, R., SLIVKA, A. & WEI, M. 1982. Chlorination of taurine by human neutrophils: evidence for hypochlorous acid generation. *Journal of Clinical Investigation*, 70, 598.
- WENZEL, R. P. & PERL, T. M. 1995. THE SIGNIFICANCE OF NASAL CARRIAGE OF STAPHYLOCOCCUS-AUREUS AND THE INCIDENCE OF POSTOPERATIVE WOUND-INFECTION. *Journal of Hospital Infection*, 31, 13-24.
- WHITE, J. R., LEE, J. M., YOUNG, P. R., HERTZBERG, R. P., JUREWICZ, A. J., CHAIKIN, M. A., WIDDOWSON, K., FOLEY, J. J., MARTIN, L. D., GRISWOLD, D. E. & SARAU, H. M. 1998. Identification of a potent, selective non-peptide CXCR2 antagonist that inhibits interleukin-8-induced neutrophil migration. *Journal of Biological Chemistry*, 273, 10095-10098.
- WILLETT, C. E., ZAPATA, A. G., HOPKINS, N. & STEINER, L. A. 1997. Expression of zebrafish rag genes during early development identifies the thymus. *Developmental Biology*, 182, 331-341.
- WILLIAMS, B. D., OSULLIVAN, M. M., SAGGU, G. S., WILLIAMS, K. E., WILLIAMS, L. A. & MORGAN, J. R. 1987. SYNOVIAL ACCUMULATION OF TECHNETIUM LABELED LIPOSOMES IN RHEUMATOID-ARTHRITIS. *Annals of the Rheumatic Diseases*, 46, 314-318.
- WINKELSTEIN, J. A., MARINO, M. C., JOHNSTON, R. B., BOYLE, J., CURNUTTE, J., GALLIN, J. I., MALECH, H. L., HOLLAND, S. M., OCHS, H., QUIE, P., BUCKLEY, R. H., FOSTER, C. B., CHANOCK, S. J. & DICKLER, H. 2000. Chronic granulomatous disease - Report on a national registry of 368 patients. *Medicine*, 79, 155-169.
- WITKO-SARSAT, V., PEDERZOLI-RIBEIL, M., HIRSH, E., SOZZANI, S. & CASSATELLA, M. A. 2011. Regulating neutrophil apoptosis: new players enter the game. *Trends in Immunology*, 32, 117-124.
- WRIGHT, H. L., MOOTS, R. J., BUCKNALL, R. C. & EDWARDS, S. W. 2010. Neutrophil function in inflammation and inflammatory diseases. *Rheumatology*, 49, 1618-1631.

- WRIGHT, H. L., MOOTS, R. J. & EDWARDS, S. W. 2014. The multifactorial role of neutrophils in rheumatoid arthritis. *Nature Reviews Rheumatology*.
- XIA, T., KOVOCHICH, M., LIONG, M., ZINK, J. I. & NEL, A. E. 2008. Cationic polystyrene nanosphere toxicity depends on cell-specific endocytic and mitochondrial injury pathways. *Acs Nano*, 2, 85-96.
- YANG, L., FROIO, R. M., SCIUTO, T. E., DVORAK, A. M., ALON, R. & LUSCINSKAS, F. W. 2005. ICAM-1 regulates neutrophil adhesion and transcellular migration of TNF-alpha-activated vascular endothelium under flow. *Blood*, 106, 584-592.
- YIPP, B. G., PETRI, B., SALINA, D., JENNE, C. N., SCOTT, B. N. V., ZBYTNUIK, L. D., PITTMAN, K., ASADUZZAMAN, M., WU, K., MEIJNDERT, H. C., MALAWISTA, S. E., CHEVANCE, A. D. B., ZHANG, K., CONLY, J. & KUBES, P. 2012. Infection-induced NETosis is a dynamic process involving neutrophil multitasking in vivo. *Nature Medicine*, 18, 1386-+.
- YONEYAMA, M., KIKUCHI, M., NATSUKAWA, T., SHINOBU, N., IMAIZUMI, T., MIYAGISHI, M., TAIRA, K., AKIRA, S. & FUJITA, T. 2004. The RNA helicase RIG-I has an essential function in double-stranded RNA-induced innate antiviral responses. *Nature Immunology*, 5, 730-737.
- YU, K. & EISENBERG, A. 1998. Bilayer morphologies of self-assembled crew-cut aggregates of amphiphilic PS-b-PEO diblock copolymers in solution. *Macromolecules*, 31, 3509-3518.
- YU, X., ACEHAN, D., M $\sqrt{\text{C}}\text{N}\sqrt{\text{C}}\text{TRET}$, J.-F. O., BOOTH, C. R., LUDTKE, S. J., RIEDL, S. J., SHI, Y., WANG, X. & AKEY, C. W. 2005. A structure of the human apoptosome at 12.8 $\sqrt{\text{O}}$ resolution provides insights into this cell death platform. *Structure*, 13, 1725-1735.
- YUAN, H. & ZHANG, S. 2010. Effects of particle size and ligand density on the kinetics of receptor-mediated endocytosis of nanoparticles. *Applied Physics Letters*, 96.
- ZHANG, Q., RAOOF, M., CHEN, Y., SUMI, Y., SURSAL, T., JUNGER, W., BROHI, K., ITAGAKI, K. & HAUSER, C. J. 2010. Circulating mitochondrial DAMPs cause inflammatory responses to injury. *Nature*, 464, 104-U115.
- ZHAO, Y., SUN, X., ZHANG, G., TREWYN, B. G., SLOWING, I. I. & LIN, V. S. Y. 2011. Interaction of Mesoporous Silica Nanoparticles with Human Red Blood Cell Membranes: Size and Surface Effects. *Acs Nano*, 5, 1366-1375.
- ZWAAL, R. F. A., COMFURIUS, P. & VANDEENEN, L. L. M. 1977. MEMBRANE ASYMMETRY AND BLOOD-COAGULATION. *Nature*, 268, 358-360.